SCHOOL OF
CIVIL ENGINEERING

INDIANA
DEPARTMENT OF TRANSPORTATION

JOINT HIGHWAY RESEARCH PROJECT

FHWA/IN/JHRP-96/2
Final Report

# USE OF COAL COMBUSTION RESIDUES AND WASTE FOUNDRY SANDS IN FLOWABLE FILL

S. T. Bhat and
C. W. Lovell

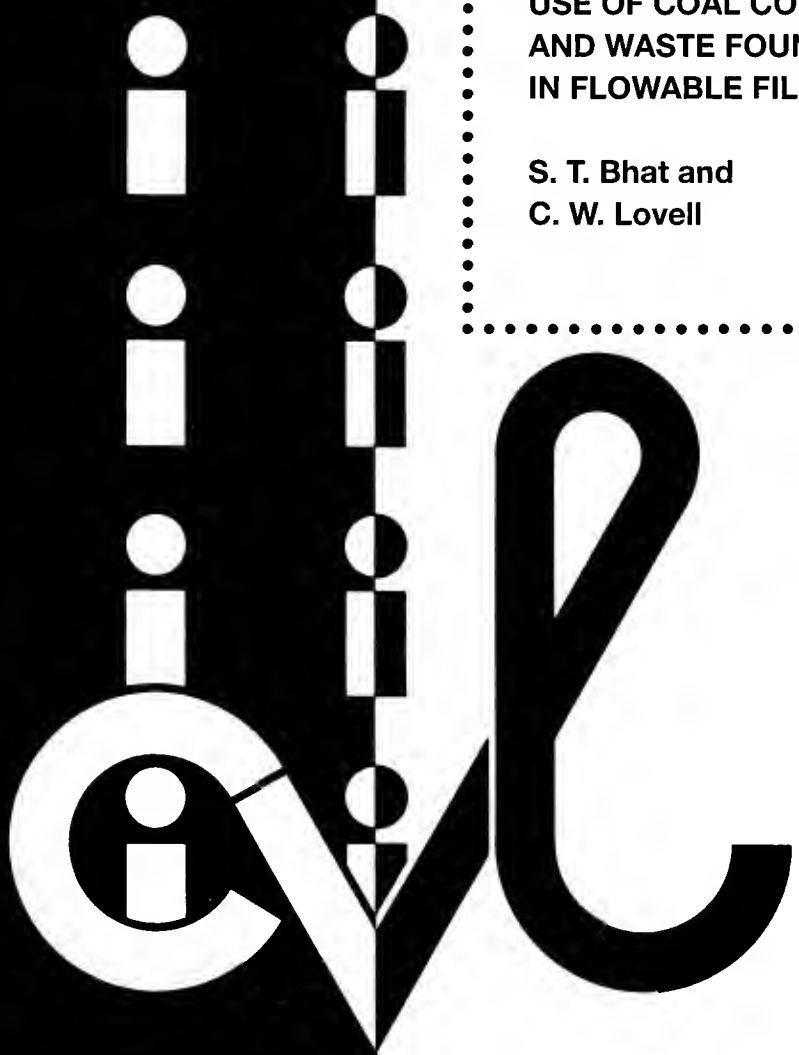

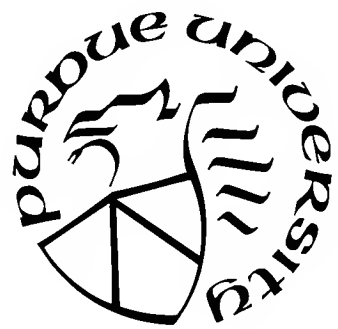


PURDUE UNIVERSITY

FINAL REPORT

# Use of Coal Combustion Residues and Foundry Sands in Flowable Fill

by

Subrahmanya T. Bhat

Graduate Research Assistant

and

C.W. Lovell

Research Engineer

Joint Highway Research Project
Project Number: C-3-63-6V
File number: 6-14-22

Prepared as part of an investigation conducted by the Joint Highway Research Project
Engineering Experiment Station, Purdue University

Funded by

Indiana Department of Transportation and Federal Highway Administration
Indiana Cast Metals Association
C.W. Lovell and Associates, Inc.



School of Civil Engineering
Purdue University
West Lafayette, IN 47907
May 1996

## ACKNOWLEDGEMENT

The authors wish to acknowledge the help provided by Dr. Tommy E. Nantung and David E. Ward, Division of Research, INDOT. Special thanks are extended to Janet Lovell and Joe Walters for their help in laboratory studies. The financial support by Indiana Department of Transportation, Indiana Cast Metals Association and C. W. Lovell and Associates is gratefully acknowledged.

# TABLE OF CONTENTS

# LIST OF TABLES

## LIST OF FIGURES

# IMPLEMENTATION REPORT

The study is directed towards remedying some of the deficiencies in the present state-of-the-art concerning the behavior and design of flowable fill. The focus is on the utilization of waste foundry sand and class F fly ash. The use of waste foundry sand in flowable fill may result in economical mix depending on availability of the material in the near vicinity of the construction site. It is environmentally beneficial as large quantities of environmentally sound waste foundry sands will otherwise be disposed of in waste disposal sites.

The following recommendations are made to INDOT to start implementation of the present research. The recommendations are not necessarily limited to the flowable fills containing WFSs (waste foundry sands), but are applicable to other flowable fills as well.

1. Demonstration projects involving flowable fill using WFS should be arranged. Environmentally sound WFSs from different foundries should be used. The number and location of such projects should be decided by the INDOT. The performance of flowable fill in the field should be closely monitored and compared to the laboratory study carried out in this research. The penetration resistance should be measured during the hardening stage using the field version of the mortar penetrometer.

2. The present specification for flowable fill can be expanded to include WFS as a fine aggregate in flowable fill. Instead of standard mixes, the mix design method suggested in this study may be considered. The walkability criteria using penetration resistance should be used instead of the existing rod method.

3. The bioassay test may be used to screen out potentially hazardous WFSs before using them in flowable fill. However, further study is required before full potential of this method can be utilized. A detailed study on biassay testing of waste foundry sands is being carried out by the environmental group at Purdue University.

# CHAPTER 1. INTRODUCTION

## 1.1 General

Flowable fill is a low strength material consisting of a mix of sand, fly ash, portland cement, and water, that provides an unconfined compressive strength of around 1035 kPa(150 psi). Flowable fill can be used in lieu of conventional compacted soil backfill. Flowable fill may also be known as controlled low strength material(CLSM), lean mix backfill, controlled density fill, or flowable mortar. All these names refer to the same material; however, the most popular name is flowable fill. This relatively new material is becoming increasingly popular due to the inherent advantages associated with its use. There has been continued effort by various agencies, particularly, ready mixed concrete associations, utility companies producing fly ash, in co-operation with the respective Departments of Transportation around the country, to popularize this material; nevertheless, the developments in terms of standards, specifications, test procedures and research are far from satisfactory.

One of the attractions of flowable fill is that it provides an opportunity to use waste materials. Use of waste material in flowable fill serves two purposes: firstly, this may result in an economical mix; secondly, diversion of waste material from landfill to a beneficial use is environmentally beneficial. One such waste material produced in large quantities in Indiana and around the country is waste foundry sand(WFS). The waste foundry sand can be used as a fine aggregate in flowable fill. Since sand is the major component of flowable fill, considerable amount of WFS can be consumed, if the natural sand can be successfully replaced by WFS.

Waste foundry sand is a by-product of the metal casting industry which results from the mold and core making processes. Generally for each ton of good castings shipped, a typical foundry generates around one ton of waste foundry sand(Kennedy and Linne, 1987).

The annual generation of WFS in Indiana alone is at least 500,000 tons. The bulk of this material goes to landfill. The majority of the foundries use the green sand process. The green sand uses natural clay and water to achieve bond strength, and is known to be environmentally non-hazardous in most cases.

Flowable fill produces a mixture that readily flows into place, is self-leveling and is not subject to segregation. Flowability, hardening characteristics, and final strength are the basic considerations for flowable fill. The reason for this is that the parameters influencing the behavior of flowable fill are not properly understood. The object of design should be to produce a dense, less porous material which needs as little cement as possible.

## 1.2 Objectives

This thesis is directed towards remedying some of the deficiencies in the present state-of-the-art concerning the behavior and design of flowable fill. The focus is on the utilization of WFS and class F fly ash. However, the study addresses a much broader perspective so that a unified and rational approach becomes available to understand and predict the behavior of flowable fill in general. The objective is also to answer some of the questions, which need to be answered before flowable fill can be used in many geotechnical applications. Specifically, the objectives pursued are to:

1. develop a rational methodology to design good and economical mixes;
2. understand and model the flow behavior;
3. develop a criteria for evaluating the hardening behavior by correlating penetration resistance with unconfined compressive strength or bearing capacity, and define penetration resistance necessary for walkability;
4. develop a 28-day strength predictive model in order to be able to use this information in a mix design procedure;
5. study the pore structure of hardened flowable fill by mercury intrusion porosimetry technique;

6. understand the stress-strain-strength behavior by conducting drained and undrained triaxial tests;
7. study the permeability characteristics;
8. assess environmental aspect of using WFS in flowable fill by conducting "bioassay" toxicity tests on expressed pore solution; and
9. develop an accelerated strength to predict the 28-day unconfined compressive strength.

## 1.3 Outline of the Thesis

The thesis is organized in ten chapters. A brief outline of each chapter is given below. Chapter 1 outlines the objectives of the thesis. Chapter 2 reviews the developments, applications, and advantages of flowable fill in general. Statistical data on the production and consumption of Coal Combustion By-products both in the United States and the state of Indiana are provided. A broad picture of the foundry industry in the United States, and in the state of Indiana is provided. The process of WFS generation is described. The environmental concern with regard to the use of WFS is briefly discussed. Lastly, the economics are addressed.

Chapter 3 presents the basic physical and chemical properties of the materials, namely, cement, sand, and fly ash used in this research.

Chapter 4 deals with flow behavior of dry sand and fresh flowable fill mix. Flow curves are developed which help understand the mechanics of flow.

Chapter 5 discusses penetration resistance test results using mortar penetrometer. A soil pocket penetrometer is also used to estimate the unconfined compressive strength as the fresh flowable fill hardens. The effect of drainage is studied by introducing geotextile drainage layers. Penetration resistance is correlated with the unconfined compressive strength. Penetration resistance necessary for walkability is defined.

Chapter 6 presents 28-day and 90-day unconfined compressive strength test results. The 28-day compressive strength is correlated with the water/cement ratio. A step by step mix design procedure is described.

Chapter 7 discusses mercury intrusion porosimetry and permeability test results, and bioassay toxicity test results on expressed pore solutions from hardened flowable fill.

Chapter 8 discusses results of consolidated drained and undrained triaxial tests at different confining pressures, and also the Brazilian Tensile Strength test results.

Chapter 9 presents the results of accelerated strength testing using hot water bath. Chapter 10 summarizes and presents conclusions for the present work.

# CHAPTER 2. LITERATURE REVIEW

## 2.1 Introduction

Flowable fill is a low-strength material consisting of a mix of sand and/or fly ash, portland cement and water that provides unconfined compressive strengths ranging from 50 psi to 1200 psi. Flowable fill can be used in lieu of conventional compacted backfill in many applications. This relatively new material is becoming increasingly popular. Most Departments of Transportation have included flowable fill in their specifications.

The history of flowable fill goes back to 1970s when this was a patented material with a name "K-Krete". Flowable fill may also be known as controlled low strength material(CLSM), lean mix backfill, controlled density fill, or flowable mortar. All these names refer to the same material; however, the most popular name is flowable fill.

The object of flowable fill is to produce a mixture that readily flows into place, is self leveling and is not subject to segregation. Flowability, hardening characteristics, and final strength are the basic considerations for flowable fill. There has been continued effort by various agencies, particularly, ready mixed concrete associations, utility companies producing fly ash, in co-operation with respective Departments of Transportation around the country to popularize the use of this material; nevertheless, the developments in terms of standards, specification, test procedures and research, are far from satisfactory.

Flowable fill provides an opportunity to use waste materials. Use of waste material renders two-fold advantages: It may result in an economical mix, and diversion of waste material from landfill to a beneficial use is an obvious environmental benefit.

Waste foundry sand is a waste material that is produced in large quantities in many states of the United States. This material can be used as a fine aggregate in flowable fill. The

quality and constituents of waste foundry sands vary from one foundry to the other, and some are environmentally sound, and others are toxic.

## 2.2 Applications and Advantages

The application for this material truly depends on the imagination of the engineer. The following applications can be noted.

BACKFILL

- Sewer Trenches
- Utility Trenches
- Building Excavations
- Bridge Abutments
- Conduit Trenches

STRUCTURAL FILL

- Road Base
- Mud Jacking
- Foundation Subbase
- Floor Slab Base
- Pipe Bedding
- Retaining Wall Backfill

OTHER USES

- Filling Underground Storage Tanks
- Filling Abandoned Sewers, Wells, Manholes, etc.
- Slope Stabilization
- Soil Erosion Control
- Mud Mats

Case histories involving small as well as large volume applications of flowable fill have been reported in the literature (Krell, 1989, Naik et. al., 1990, Larsen, 1988, 1990, Hennis and Frishette, 1987, Emery and Johnston, 1986, Smith, 1991).

There are several advantages of using flowable fill in place of conventional soil backfill. The main advantage is derived from the fact that there is no need to compact this material. Several advantages of flowable fill when used as a backfill material are listed by Smith (1991).

- Readily available: Using locally available materials, ready mix suppliers can produce flowable fill to meet most project specifications.
- Easy to deliver: Ready mix trucks can deliver specified quantities of flowable fill to the jobsite whenever the material is needed.
- Easy to place: Depending on the type and location of void to be filled, flowable fill can be placed by chute, conveyor, pump, or bucket. Because flowable fill is self-leveling, it needs little or no spreading or compacting. This speeds construction and reduces labor requirements.
- Versatile: Flowable fill mixes can be designed to meet specific requirements.
- Can be excavated: Flowable fill having unconfined compressive strength below 150 psi can be easily excavated with conventional digging equipment.
- Requires less inspection: During placement, soil backfill must be tested after each lift for sufficient compaction. Flowable fill self-compacts consistently and does not need this extensive testing.
- Allows fast return to traffic: Because flowable fill can be placed quickly and can support traffic loads within several hours, it minimizes downtime for pavement repairs.
- Won't settle: Flowable fill does not form voids during placement and won't settle under loading. This advantage is specially significant if the backfill is to be covered by a pavement patch. Soil or granular backfill, if not properly compacted, may settle after a pavement patch is placed and form cracks or dips in the road. It is virtually impossible to perfectly compact the soil around a pipe without leaving voids.

• Reduces excavation costs: Flowable fill allows narrower trenches because it eliminates having to widen trenches to accommodate compaction equipments.

• Improves worker safety: Workers can place flowable fill in a trench without entering the trench, reducing their exposure to possible cave-ins.

• Allows all-weather construction: Flowable fill will displace any standing water left in a trench from rain or melting snow, reducing the need for dewatering pumps. To place flowable fill in cold weather, heat the material using the same methods for heating ready mixed concrete.

• Reduces equipment needs: Unlike soil or granular backfill, flowable fill can be placed without loaders, rollers, or tampers.

• Makes use of waste by-products: Fly ash is a waste by-product. The sand also can be replaced by a waste such as waste foundry sand.

## 2.3 Production and Consumption of CCBs in the United States

Approximately, 87 million tons of Coal Combustion By-Products (CCBs) were produced in the United States in 1990, of which around 22 million tons (i.e. around 25%) were put to use. Table 2.1 illustrates CCBs production and consumption tonnage for 1990 (GAI, 1993). Of all CCBs, fly ash is produced in the highest quantity and most of the fly ash that is consumed goes into production of cement. Virtually, all the Flue gas desulfarization (FGD) material produced is getting stock piled.

## 2.4 Production and Consumption of CCBs in Indiana

Approximately, 6 million tons of CCBs are produced annually in Indiana. Table 2.2 shows the production and consumption of CCBs in Indiana (GAI, 1993). Figure 2.1 shows the fly ash production distribution in Indiana (GAI, 1993). The largest production is concentrated in the southwest corner of Indiana. The largest producers of class F fly ash are

Table 2.1 United States CCBs Production and Consumption in Tons for the Year 1990 (GAI, 1993)

| CCB Catagory | Produced | Utilized | Percent Utilized |
|---|---|---|---|
| Fly Ash | 48,931,722 | 12,420,163 | 25.4 |
| Bottom Ash | 13,705,653 | 5,360,104 | 39.1 |
| Boiler Slag | 5,234,316 | 3,252,220 | 62.1 |
| FGD Material | 18,932,688 | 215,852 | 1.1 |
| Total | 86,804,379 | 21,248,339 | 24.5 |

Table 2.2 Production and Consumption of CCBs in Indiana (tons/year) (GAI, 1993)

| CCB Catagory | Production | Utilization | Percent Utilized |
|---|---|---|---|
| Class C Fly Ash | 437,300 | 237,000 | 54 |
| Class F Fly Ash | 2,754,070 | 57,500 | 2 |
| Bottom Ash | 992,575 | 159,100 | 16 |
| Boiler Slag | 315,190 | 192,300 | 61 |
| FGD Material | 1,531,900 | — | 0 |
| Total | 6,031,035 | 645,900 | 11 |

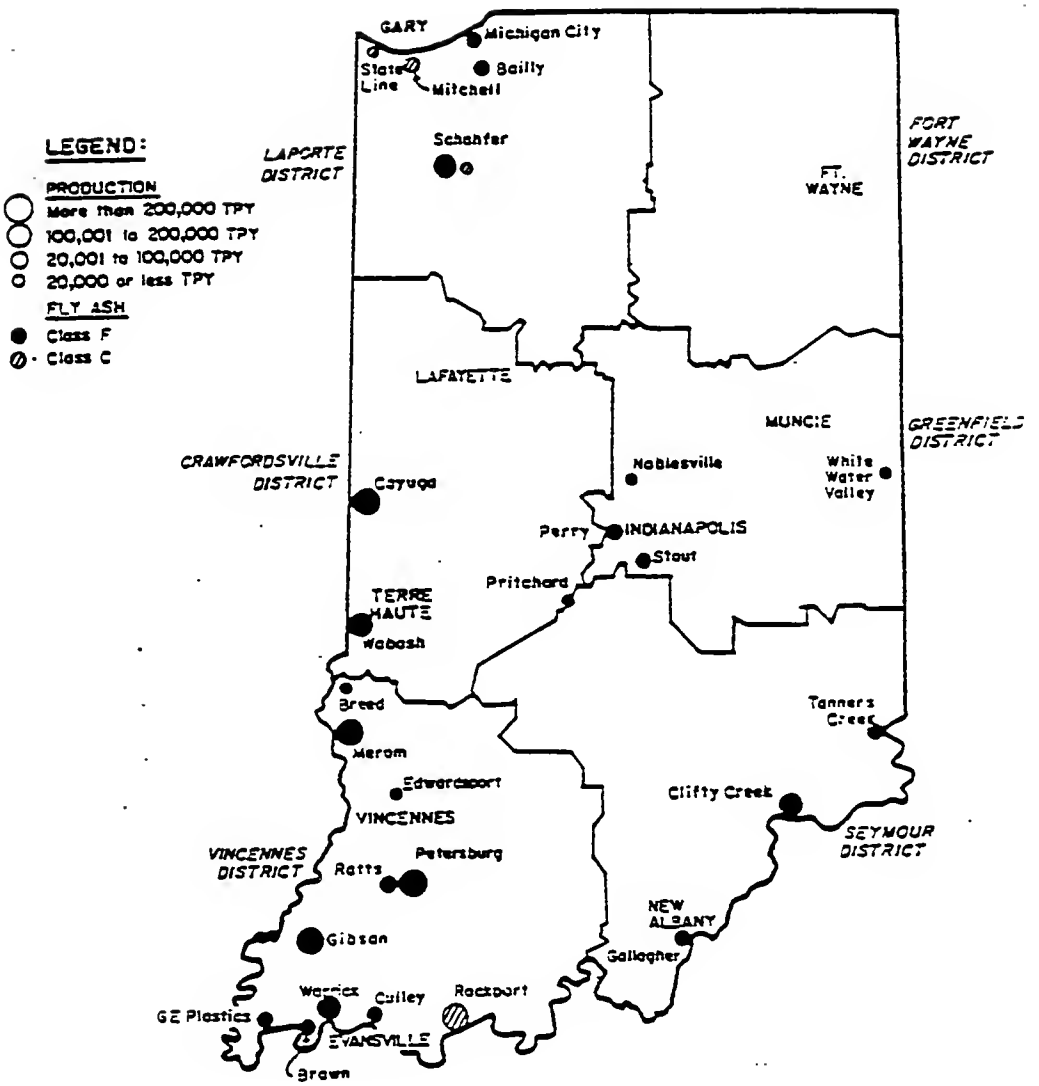


Figure 2.1 Fly Ash Production Distribution in Indiana (GAI, 1993)

the Gibson, Petersburg and Merom Power Stations. The Rockport station produces the largest quantity of class C fly ash.

## 2.5 Properties and Tests

The ACI Committee 229 (1994) reports the desirable properties and tests for flowable fill. These are based on limited research, and need further consideration. There is no standard mix design procedure for flowable fill. The important properties of flowable fill are flowability, hardening characteristics and compressive strength of hardened flowable fill. To allow excavatability, the unconfined compressive strength is to be restricted to 1035 kPa (150 psi).

The flowability is measured by a 7.6 cm × 15.2 cm (3 in. × 6 in.) open ended cylinder. A spread of 20.3 cm (8 in.) or higher gives good flowability. Penetration resistance test in accordance with ASTM C 403, is suggested to measure hardening time or approximate bearing capacity. However, there is no adequate criterion to determine if a given penetration resistance gives adequate bearing capacity. Nantung(1993) investigated the durability of flowable fill under freeze-thaw conditions, and found that this is not a major problem in flowable fill. He also found that flowable fill has better resilient modulus values compared to soil.

## 2.6 Waste Foundry Sand

The foundry industry is basic to an industrial society. Since the 19th century, it has been an important producer of farm implements, water pipes, and valves. In this century, all power-producing machines, electric motors, internal combustion engines, and steam turbines are made by the foundries from castings. Most of these castings are made in sand molds that either contain organic additives or are bound together by organic polymers. The majority of the foundries do iron castings.

There are two basic sand mixtures used in the casting process, "green sand" and "no-bake" sand. Green sand uses natural clay and water to achieve bond strength while no-bake sand uses synthetic resin to achieve bond strength. The green sand process is the most popular one. The additives and binders in the sand decompose under the heat of molten iron to produce smoke and vapors of unknown composition. The sand is reused in the casting process. However, fresh sand and additives are added to the mix each time to get the required properties. Therefore, a part of the sand after casting is to be thrown out. This is called spent foundry sand or waste foundry sand. The disposal of waste foundry sand is a major concern for the foundry industries. The present disposal cost may vary from $20/ton to $40/ton depending on the area and proximity of land fill. The utilization of this sand for beneficial purposes is the best alternative to disposal. However, the technical and environmental aspect of these applications will have to be addressed before using it for beneficial purposes.

### 2.6.1 Foundry Industry in the United States

In 1976 there were 4517 foundries in the United States. Of these, 1367 were iron foundries (Table 2.3). Presently, the industry is in a state of transition from one that has been labor-intensive to one that is capital-intensive. A density distribution of U.S. iron foundries is given in Figure 2.2. The highest concentration of foundries is in Pennsylvania, Ohio, Michigan, Illinois, Wisconsin, New York, and Indiana, accounting for more than half of the iron-casting capacity of the nation. Two-thirds of the iron foundries are located in metropolitan areas. Out of the total ferrous casting production, gray iron is the major one. Steel, malleable and ductile ferrous castings form only a small portion of total ferrous casting. The major trend in the industry has been the declining use of the cupola for iron melting, with an increase in the use of electric induction furnaces and electric arc furnaces. There is also a continuing trend toward automated casting lines, which adversely affects many smaller foundries. Chemically bound sand is easy to handle on automated equipment. The economic pressure to reduce cost, along with automation, is causing a continual increase in the use of

Table 2.3 Foundries and Iron Foundries in Each State of U.S. as of 1976 (EPA, 1980)

| State | Foundries | Iron Foundries | State | Foundries | Iron Foundries |
|---|---|---|---|---|---|
| Alabama | 90 | 64 | Missouri | 108 | 26 |
| Alaska | 1 | 1 | Montana | 3 | 3 |
| Arizona | 19 | 3 | Nebraska | 24 | 8 |
| Arkansas | 43 | 9 | Nevada | 4 | 2 |
| California | 440 | 8 | New Hampshire | 29 | 8 |
| Colorado | 50 | 12 | New Jersey | 134 | 29 |
| Connecticut | 101 | 20 | New Mexico | 8 | 1 |
| Delaware | 2 | 1 | New York | 282 | 66 |
| D.C. | 2 | 1 | North Carolina | 57 | 27 |
| Florida | 60 | 12 | North Dakato | 3 | 2 |
| Georgia | 44 | 25 | Ohio | 465 | 152 |
| Hawaii | 3 | 2 | Oklahoma | 45 | 22 |
| Idaho | 6 | 4 | Oregon | 54 | 12 |
| Illinois | 333 | 81 | Pennsylvania | 386 | 157 |
| Indiana | 198 | 75 | Rhode Island | 57 | 8 |
| Iowa | 77 | 35 | South Carolina | 29 | 12 |
| Kansas | 57 | 23 | South Dakota | 1 | 1 |
| Kentucky | 30 | 13 | Tennessee | 76 | 40 |
| Louisiana | 24 | 8 | Texas | 175 | 66 |
| Maine | 16 | 8 | Utah | 19 | 12 |
| Maryland | 26 | 10 | Vermont | 4 | 4 |
| Massachusetts | 141 | 43 | Virginia | 48 | 29 |
| Michigan | 351 | 111 | Washington | 53 | 18 |
| Minnesota | 84 | 35 | West Virginia | 28 | 13 |
| Mississippi | 16 | 7 | Wisconsin | 200 | 88 |
| | | | **Total** | **4517** | **1367** |

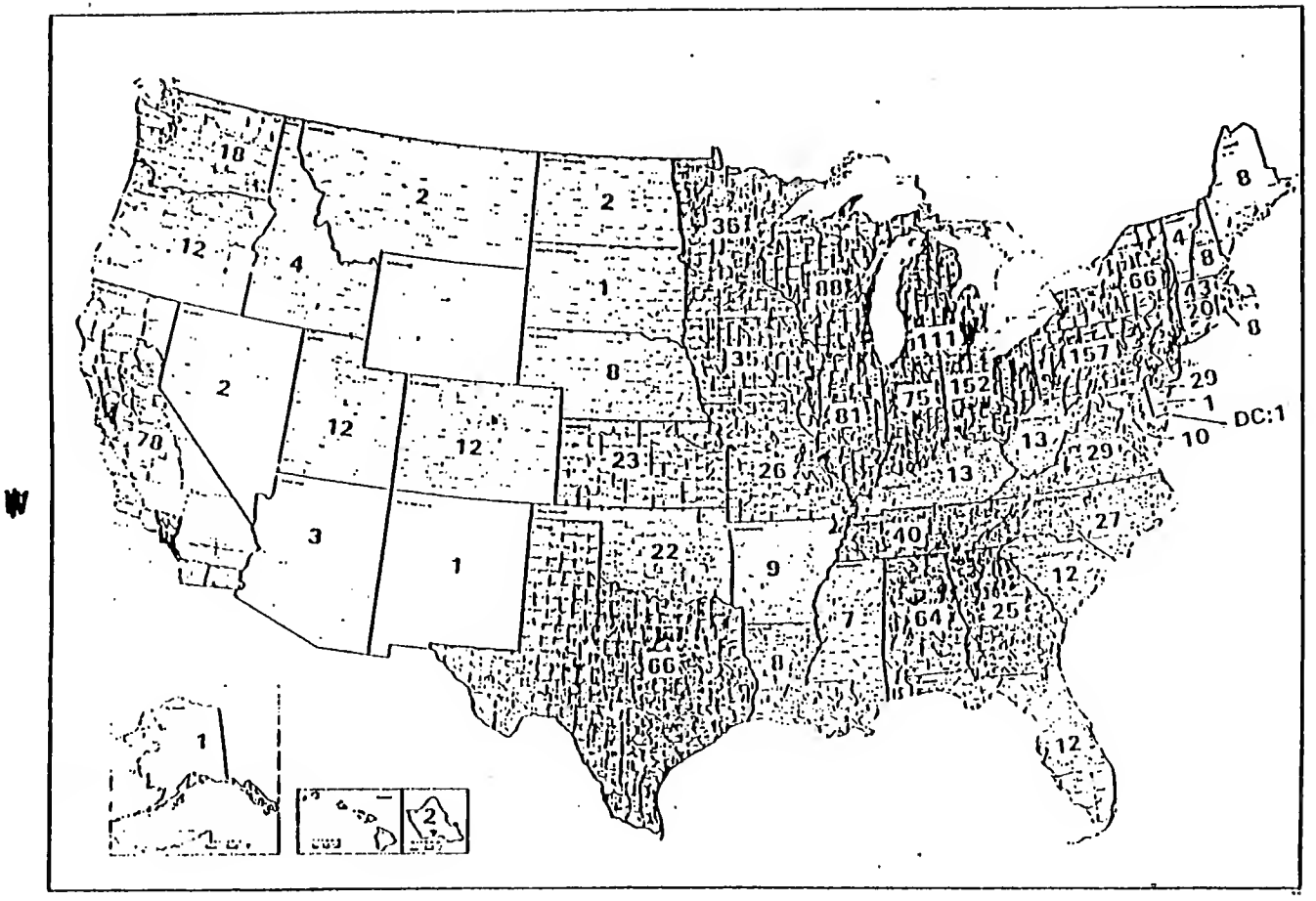


Figure 2.2 Density Distribution of Iron Foundries in the U. S. in 1978 (EPA, 1980)

chemically bound sand. Another major reason for increasing reliance on chemically bound sand is the declining availability of highly skilled labor and the fact that chemically bound sand produces a better product, even with less skilled labor.

### 2.6.2 Foundry Industry in Indiana

There are about 154 foundries in Indiana (Harris, 1992). The information regarding the production of castings, and the amount of waste foundry sand generated in each foundry is not available. Table 2.4 summarizes the information about 30 foundries who are the members of the Indiana Cast Metal Association (INCMA).

### 2.6.3 Waste Sand Generation

#### 2.6.3.1 Basic Process of Casting

There have been great strides in the sophistication of sand casting processes. Nevertheless, the principal processes remain the same. A model is made of wood, metal, or plastic, and placed in a container, which is then packed with sand. Clay and other substances are added to increase the shape holding ability of the sand. After this, the model is removed and the molten metal is poured into the cavity and allowed to cool. Once cool, the mold is broken and discarded leaving a cast iron copy of the desired object. Figure 2.3 presents a graphic presentation of the major operations involved in the foundry industry.

#### 2.6.3.2 Casting Methods: Green Sand and Others

The foundry industry refers to casting methods according to the type of mold used, and sometimes, according to the type of mold binder used. This results in a large number of so-called methods.

Table 2.4 Production of Casting and Waste Foundry Sand in Indiana (INCMA, 1992)

| Type of Metal Cast | Tons per Year |
|---|---|
| Gray Iron | 642,139 |
| Ductile Iron | 63,905 |
| Steel | 47,978 |
| Aluminium | 4608 |
| Copper | 3230 |
| Brass/Bronzes | 2.5 |
| Nickel Base | 50 |
| Stainless Steel | 165 |
| Mn Steel | 280 |
| Type of Molding Sand | Tons Disposed |
| Green Sand | 247,651 |
| Chemically Bonded Sand | 176,610 |
| Shell Mold Sand | 21,783 |

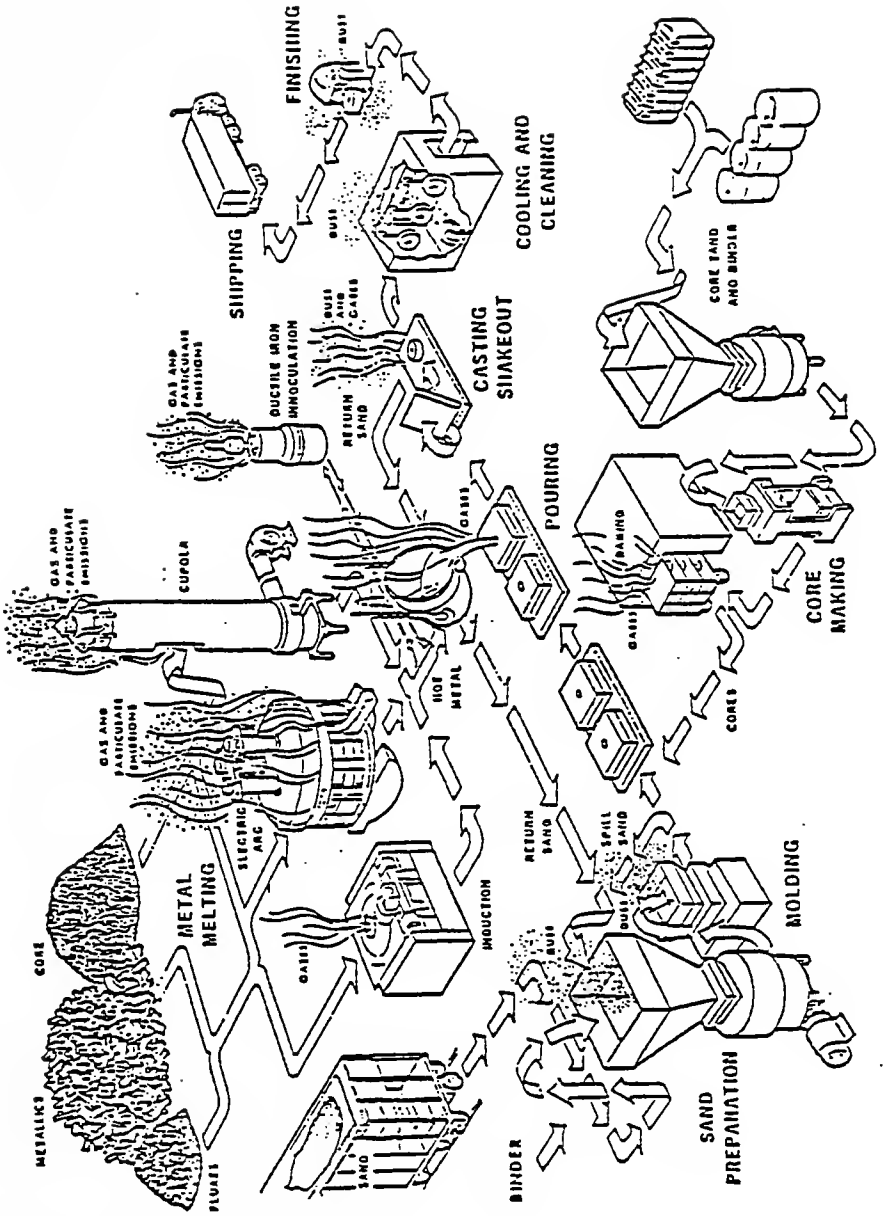


Figure 2.3 Iron Foundry Process Flow Chart (EPA 1980)

Green Sand: Green sand is the original mold type and is still the predominant material in the foundry industry. The term "green sand" is applied when the chief bonding agent is clay, usually western or southern bentonite (montmorillonite). Three to five percent water and organic materials such as sea coal, wood flour and oat hulls, are added in amounts up to 8 percent. The purpose of the organic addition is to cushion the thermal expansion, provide a reducing atmosphere, and promote graphite formation at the sand metal interface to give a better finish to the metal. The addition of carbonaceous materials alleviates "burn-on" or fusing of sand to the casting surface. "Burn-on" is essentially caused by the formation of low melting point iron silicate at the mold-metal interface, as a result of the chemical reaction between silica sand ($SiO_2$) and Wustite (FeO).

The addition of sea coal is very common in sand systems for gray iron, ductile iron and malleable iron castings. Sea coal is a highly volatile bituminous coal, ground to various degrees of fineness. Where molds are cast which contain sea coal, the sand peels more freely from the casting and the cleaning of the castings are more easily accomplished.

The wastes common to this sand system can be grouped into two general catagories; waste sands and emission control residuals. Waste sand is generated in several areas: at shake outs; as floor sweeping in finishing areas; and losses from sand conveying system. This sand has gone through the pouring process and has been subjected to pouring temperatures. Large amounts of waste are also generated from sand screenings. The mold and core "lumps" generated can be a significant quantity depending on the amount of core used in the molding process.

The emission control residuals are produced by wet or dry dust collection systems. The primary emission control residuals from the green sand molding system consists of dusts generated off of mold making , pouring, shake out, return sand lines and those generated from sand and bentonite storage and the sand mixing processes.

Inorganically Bound Molds: The most promising type of inorganic binder is sodium silicate. When this material is mixed with sand, a solid gel is formed as carbon dioxide is blown through the mold. Mold formation is identical to the green sand process and is virtually non-polluting. However, technical difficulties are involved with the binders because

they are too strong and do not weaken from hot metal addition. Therefore, removal of the mold from the metal can be difficult.

Organically Bound Sand: The availability of synthetic resin organic binders has resulted in a large number of mold making techniques, some of which are shell molding, hot box molds, cold set binders, no-bake resins, oils, and full mold process. The details of these processes are given elsewhere in the literature.

Table 2.5 gives the estimated pounds of foundry waste per ton of metal casting produced for various type of metals. It should be noted that there are different sources of solid wastes in a foundry, and all are likely to be disposed of together.

### 2.6.4 Waste Use and Disposal Options

The waste foundry sand can be used or disposed in one of the following ways:

1. Reclamation
2. Disposal, or Treatment and Disposal
3. Beneficial Uses

#### 2.6.4.1 Reclamation

The AFS (American Foundry Men's Society) defines reclamation as "the physical, chemical or thermal treatment of a refractory aggregate to allow its reuse without significantly lowering its original useful properties as required for the application involved". Reclamation is a process to restore a bonded molding or core sand to a condition that enables the sand to be reused in the foundries. The reclamation may be sometimes expensive. However, considering the increasing cost of land fill sites and the environmental concerns, reclamation may be a better option for some foundries. Good(1983) describes various reclamation methods available.

The basic types of reclamation fall into mainly three catagories: thermal, dry attrition scrubbing, and wet attrition scrubbing. In the thermal process, any combustible material

Table 2.5 Estimated Pounds of Foundry Waste per Ton of Metal Casting Produced (Naik et. al., 1994)

| Waste Type | Foundry Type | | | | | |
|---|---|---|---|---|---|---|
| | Malleable | Ductile Iron | Gray Iron | Steel | Aluminium | Brass & Bronze |
| Refractories | 40 | 50 | 80 | 140 | 20 | 40 |
| System Sand | 1250 | 2190 | 670 | 2790 | 280 | 100 |
| Core Sand | 310 | 100 | 30 | 550 | 1370 | 140 |
| Cleaning Room Waste | 60 | 90 | 80 | 270 | 20 | 30 |
| Slag | 100 | 400 | 220 | 350 | -- | -- |
| Coke Ash | -- | 60 | -- | -- | -- | -- |
| Dust Collector Discharge | 20 | -- | 190 | 30 | -- | -- |
| Miscellaneous | 5 | -- | 110 | 5 | 5 | 5 |
| Totals | 1785 | 2890 | 1380 | 4135 | 1695 | 315 |

present in the sand is completely burned leaving only a minute amount of ash which is removed by the dust collection system. Temperatures used are usually between 1000°F and 1500°F.

In the wet attrition scrubbing , impurities are removed partly by washing, and partly by attrition action of sand grain on sand grain. This does an excellent job of removing clay; however, organic coatings are only reduced slightly through the attrition action in the scrubber. Unfortunately, the clays removed in wet reclamation process create sludges, and may be very difficult to dispose of. The economics of this system has resulted in shut-down of many of these units.

In the dry attrition scrubbing, intense attrition action of grain against grain is provided by mechanical or pneumatic means. The dust created by the attrition action is removed by proper dust collection system. If the dust is not removed effectively, it is attracted to the sand grains and will degrade the performance of the reclaimed sand.

2.6.4.2 Disposal, or Treatment and Disposal

Whenever the waste foundry sand is non-hazardous, it can be disposed of in landfills. However, this is not the best option considering the escalating cost of landfill sites. The WFS from ferrous foundries are generally non-hazardous, and those from non-ferrous foundries are most likely to contain cadmium, lead, copper, nickel and zinc. The sands containing hazardous substances will have to be treated before disposal, or stabilized so that the undesirable elements do not leach out from the sand system. Chemical stabilization employs cement or pozzolanic materials that chemically reduce the mobility of metal constituents in the waste, thereby minimizing the tendency for metals to leach from the treated sand. This technology is applicable to wastes containing heavy metals with a high level of suspended solids, low total organic content and low oil and grease content. Hazardous metals from WFS can be sometimes partially recovered using various sophisticated techniques.

2.6.4.3 Beneficial Uses

This is the best option for foundries. However, before WFS is put to beneficial use, firstly the technical feasibility of using this material for a particular application should be proved, and secondly the environmental soundness of this application should be established. The use of WFS in highway embankment construction is a potential high volume application (Javed, 1994). It can be used as a fine aggregate in asphalt concrete (Javed, 1994), and in cement concrete (Naik et. al., 1994).

## 2.7 Environmental Concerns

There is a great deal of concern throughout the country about the environmental issues with regard to the utilization of waste foundry sand for beneficial purposes, involving in the process various bodies- foundry industries, end users such as Departments of Transportation, legislatures, lawers, and academia. The academic and scientific community has the responsibility of establishing a scientific basis and techniques to determine what is hazardous and what is not. One approach is to test the leachate of source material, the other is to see if there is any potential pollution problem around the constructed facility in which WFS is used as a construction material. There are several well known laboratory test procedures for determining the leaching characteristics of wastes: EP toxicity method, TCLP method, AFS method, and ASTM method. The main metals of concern are arsenic, barium, cadmium, chromium, lead, mercury, selenium, and silver. Organics are a great concern because many organic matters are added to sand in foundries. Leaching characteristics of waste foundry sands have been studied in the past (Ham et. al., 1981, 1989, Fahnline and Regan, 1995). These tests are lengthy and expensive. The general opinion is that the green sands do not have to be subjected to so rigorous environmental testing. The application of "bioassay" testing to screen out potentially hazardous green sands is presently being studied by the environmental group at Purdue University (Bastian and Alleman, 1995). (See Appendix )

## 2.8 Economics

The present in-place cost of flowable fill is around $\$40/yd^3$. The material cost of flowable fill is much higher than the material cost of conventional soil backfill. However, when flowable fill is used, there is large saving in labor cost, long term maintainance cost, and saving in time, which makes the flowable fill a better alternative to conventional fill. Brewer and Hurd (1991) have made a cost comparision of conventional fill and flowable fill.

The major component of flowable fill is sand. Any saving in the cost of sand will result in a reduction of overall cost of flowable fill. Waste foundry sand may be obtained free if it is available in the near vicinity.

For the purpose of approximate cost comparision of flowable fills containing clean sand and waste foundry sand, assume that a typical mix with clean sand contains 40 $kg/m^3$ of cement and 1500 $kg/m^3$ of sand. Assuming cost of cement to be \$60/ton (\$66/1000 kg), and cost of sand to be \$4/ton (\$4.4/1000 kg), the material cost of cement and sand in the mix would be \$8.64. Cost of fly ash is not taken into account as both the mixes contain fly ash. Let the clean sand be now replaced by WFS. Assume that the transportation cost of WFS is \$1.50/ton (\$1.65/1000 kg), and that this mix needs 50% more cement (i.e. 60 $kg/m^3$ of cement). The cost of cement and sand in this mix would then be \$6.44. There is obviously a saving in cost when WFS is used as a fine aggregate.

# CHAPTER 3. MATERIALS

## 3.1 Introduction

The ingredients of flowable fill are sand, fly ash, cement, and water. Sand is the major component of flowable fill. Fly ash is added to help flowability. Adding fly ash also serves the purpose of using a waste material for a beneficial purpose. Cement is added to flowable fill for achieving the required strength. Flowable fill provides an opportunity to use marginal materials which do not conform to any standards. For example, sands which do not conform to ASTM C33 standards can very well be used. Since sand is the major component of flowable fill, any saving in the cost of sand will result in an overall economy of flowable fill. Use of a waste material like waste foundry sand would reduce the cost, and also is environmentally beneficial. In this study, three waste foundry sands from ferrous foundries were selected. The ferrous foundry sands are generally benign environmentally; besides, this is the sand produced in the largest quantity in Indiana. A clean concrete sand and a virgin foundry sand were also included to help compare the performance of flowable fills with WFSs and clean sand. Class F fly ashes from two sources in Indiana were used.

## 3.2 Cement

Type I Portland Cement (ASTM-150) supplied by Lone Star Industries at Green Castle, Indiana, was used. The chemical analysis for the cement is shown in Table 3.1.

Table 3.1 Chemical Analysis of Cement

| | |
|---|---|
| Specific gravity | 3.17 |
| Chemical Analysis, % | |
| Silicon Dioxide ($SiO_2$) | 20.7 |
| Aluminium Oxide ($Al_2O_3$) | 5.44 |
| Ferric Oxide ($Fe_2O_3$) | 2.04 |
| Calcium Oxide (CaO) | 64.12 |
| Magnesium Oxide (MgO) | 1.49 |
| Sodium Oxide ($Na_2O$) | 0.09 |
| Potassium Oxide ($K_2O$) | 0.37 |
| Titanium Oxide ($TiO_2$) | - |
| Sulfur Trioxide ($SO_3$) | 2.67 |
| Loss on Ignition, % | 2.07 |

## 3.3 Fly Ash

Fly ashes are broadly classified into two groups based on the calcium content and pozzolanic properties of the fly ash (ASTM C618). Fly ash normally produced from lignite or subbituminous coals is class C fly ash, which has cementitious properties in addition to pozzolanic properties. Fly ash normally produced from anthracite or bituminous coal is class F fly ash which has only pozzolanic properties, and has no self-cementitious characteristics due to the absence of sufficient amount of calcium oxide. Flowable fill with class C fly ash might develop very high strength which is not desirable. On the other hand, when class F fly ash is used, the strength of flowable fill can be controlled by controlling the amount of cement.

The chemical and physical analysis of two class F fly ashes used in this research are given in Table 3.2. The fly ash, SC is from the Unit 18 of Schahfer Station, Northern Indiana Public Service Co., Jasper County, Northern Indiana. The fly ash, GI is from Gibson Station of PSI. The specific gravity of fly ash was determined using pycnometric technique with kerosene as the displacing fluid. The method using kerosene was the procedure specified in ASTM C-188, " Standard Test Method for Density of Hydraulic Cement". The specific gravity of fly ash, SC was 2.36, and that of fly ash, GI was 2.42.

The particle size determination was carried out by the classical Andreasen Pipet Method (Grindrod, 1968). In this procedure, a suspension of particles of 1% by volume was dispersed in water containing 9.8 g/l of dissolved sodium hexametaphosphate dispersing agent by manual shaking, transferred to the Andreasen cylinder, and allowed to settle. The suspension was withdrawn through the pipet from the preset height at designated intervals of time, dried, weighed, and after correcting for dispersing agent weight, calculated as percentage of specified sizes. The limiting particle size at each sampling was determined by Stoke's law. Figure 3.1 shows the particle size distribution for the two fly ashes. The fly ash SC is finer than the fly ash GI.

X-Ray diffraction analyses were carried out using a Siemens D-500 diffractometer using copper radiation. Interpretation of the pattern for the presence of crystalline components is carried out by the usual methods, involving assignment of each of the peaks

Table 3.2 Physical Properties and Chemical Analysis of Fly Ashes

| Description | Fly Ash GI | Fly Ash SC |
|---|---|---|
| Physical Tests | | |
| Fineness passing 45 μm, % | 90 | 100 |
| Specific gravity | 2.42 | 2.36 |
| Chemical Analysis, % | | |
| Silicon Dioxide ($SiO_2$) | 49.34 | 52.04 |
| Aluminium Oxide ($Al_2O_3$) | 20.09 | 20.70 |
| Ferric Oxide ($Fe_2O_3$) | 13.84 | 16.05 |
| Calcium Oxide (CaO) | 1.53 | 4.47 |
| Magnesium Oxide (MgO) | 1.2 | 1.06 |
| Sodium Oxide ($Na_2O$) | 0.91 | 0.94 |
| Potassium Oxide ($K_2O$) | 3.07 | 2.27 |
| Titanium Oxide ($TiO_2$) | 0.97 | 0.98 |
| Sulfur Trioxide ($SO_3$) | - | 1.01 |
| Loss on Ignition, % | 2.80 | 3.13 |

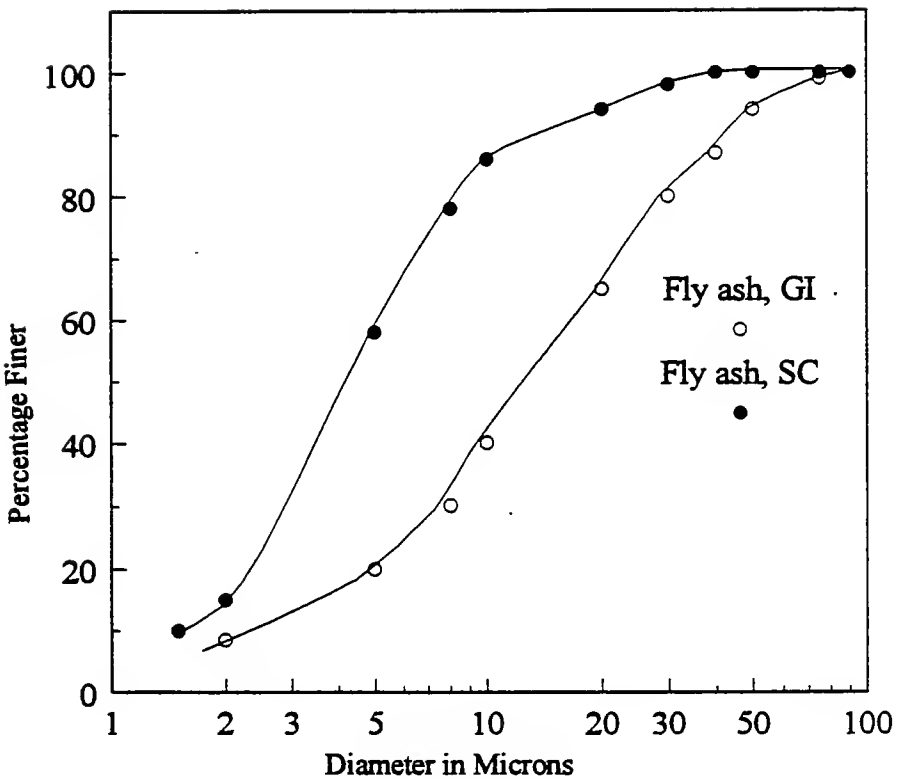


Figure 3.1 Particle Size Distribution for Fly Ashes

present to one (or more) of the crystalline substances which may be present. Figures 3.2 and 3.3 show the x-ray diffraction test results. The main minerals found were Quartz ($SiO_2$), Mullite($Al_6SiO_2O_{13}$), Hematite($Fe_2O_3$) and Magnatite($Fe_3O_4$). In addition to the information on the crystalline components present that is derived from the peak, the x-ray diffraction pattern gives information about the glass present. The glass produces a broad band of intensity that shifts the background upward over a range of $2\theta$ angles that reflects the kind of glass present (Diamond, 1985). The relative intensity of this glass band can be used as a rough measure of the relative amount of glass present in the fly ash, and the angle $2\theta$ at which its maximum occurs provides an indication of the basic structure of the glass. Low calcium fly ashes are known to generally yield band maxima near 23° or 24° $2\theta$ (Cu radiation). This was found to be true for the two class F fly ashes (Figures 3.2 and 3.3).

## 3.4 Sands

Five sands were selected in this study. Sand, R is a river sand which is routinely used in making concrete in the materials laboratory of Purdue University. The sands N, A and G are waste foundry sands from three different foundries in Indiana. Sand, V(N) is a clean virgin sand before using it in the mold making process, and this sand comes out as WFS, N.

### 3.4.1 Water Content

The water content was determined by oven drying the sands for 24 hours. The water contents are shown in Table 3.3. All the sands except WFS, A were dry. The WFS, A had a water content of 10.4%.

### 3.4.2 Gradation

The sands are oven dried before doing dry sieving. Any lumps in the WFS were crushed by hand. The sieve analysis was done in accordance with ASTM C 136. The particle

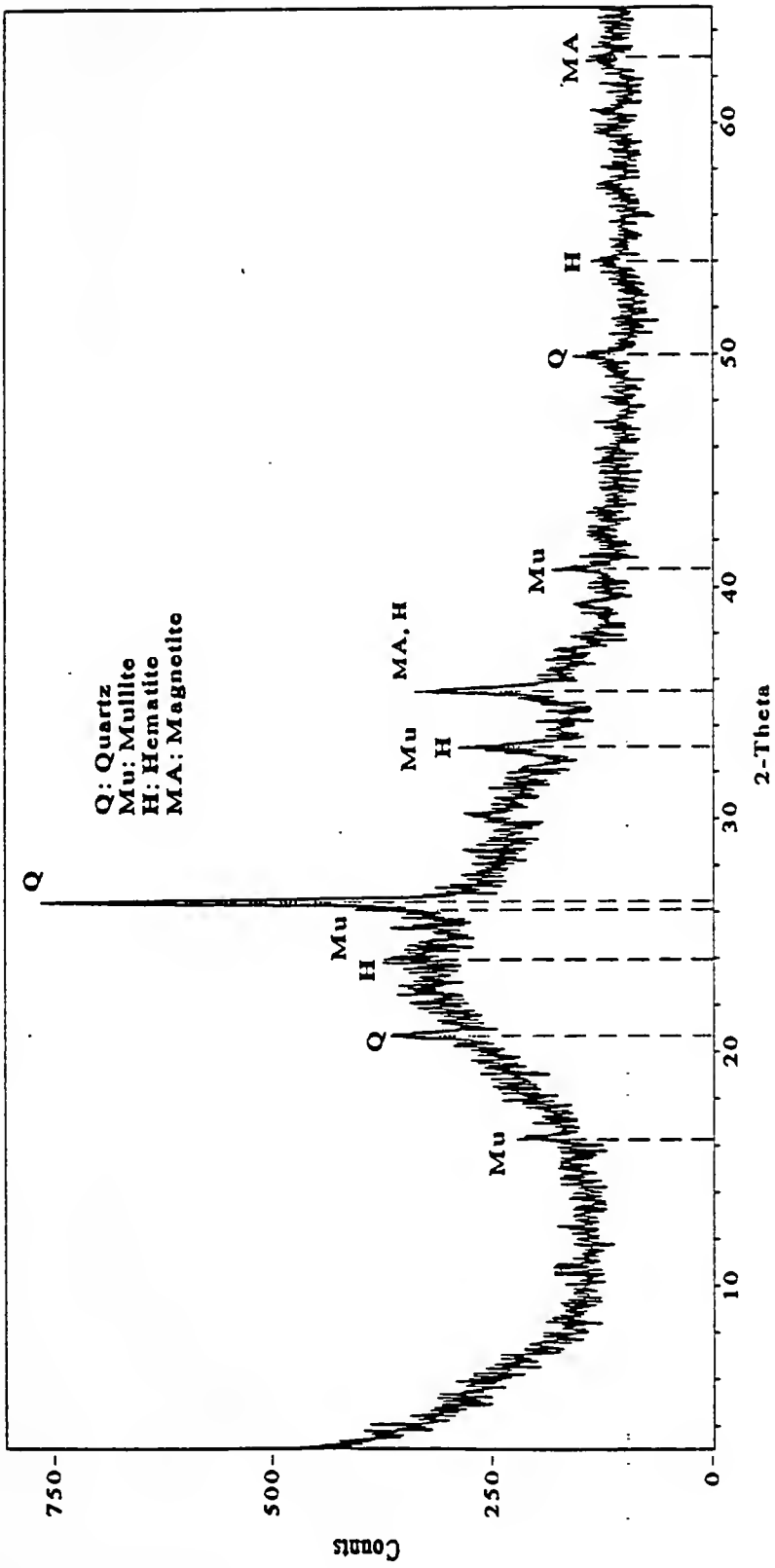


Figure 3.2 X-Ray Diffraction Result for Fly Ash, GI

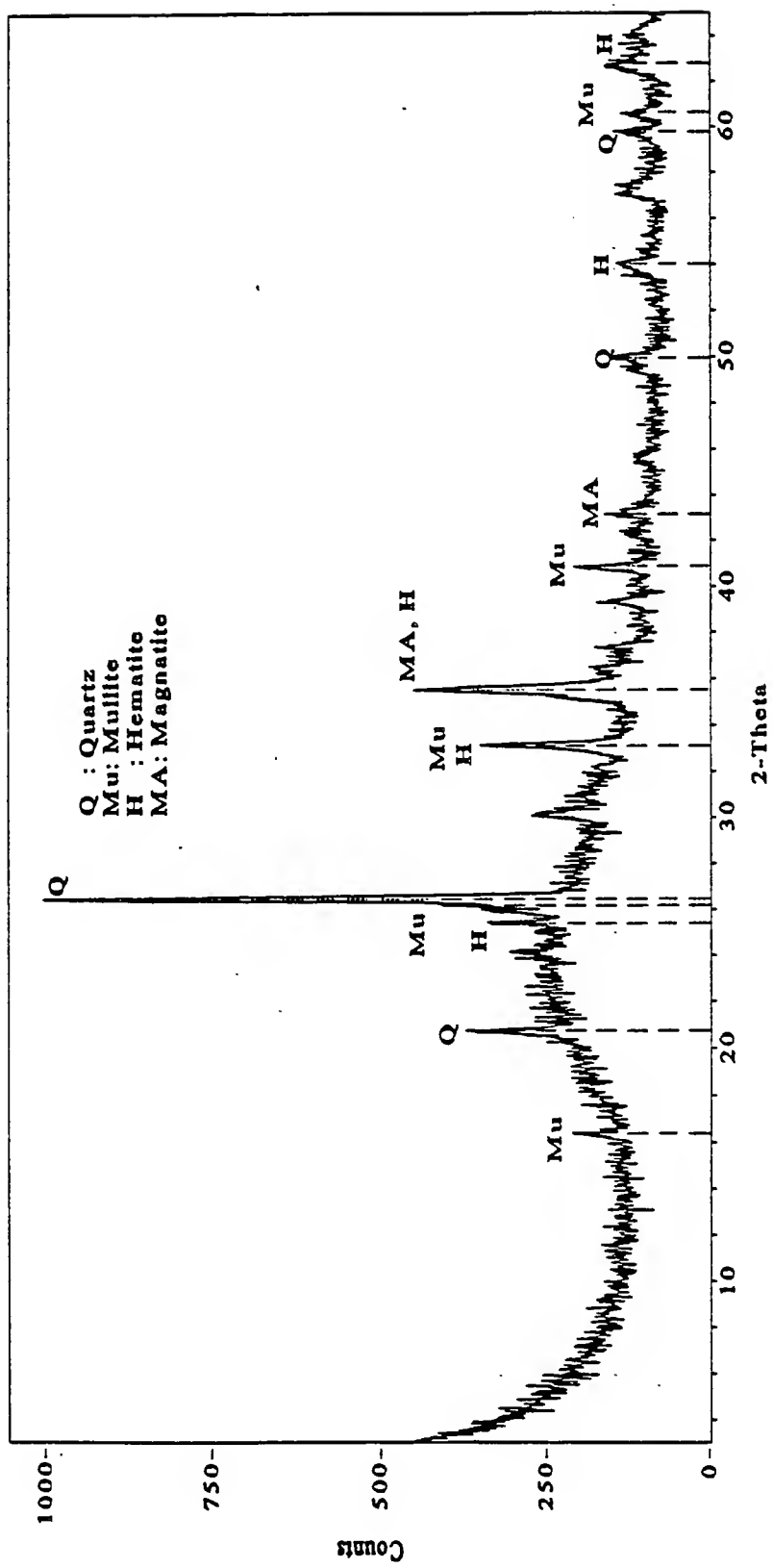


Figure 3.3 X-Ray Diffraction Result for Fly Ash, SC

Table 3.3 Physical Characteristics of Sands

| Identification | Description/Source | $d_{50}$ mm | CU | F.M. | Water Content % | LOI % | Ion Concentration in leachate (mg/liter) $Cl^{-1}$ | $SO_4^{-2}$ |
|---|---|---|---|---|---|---|---|---|
| R | River sand | 0.75 | 2.83 | 2.98 | 0.5 | 6 | N.A. | N.A. |
| V(N) | Virgin foundry sand | 0.32 | 2.24 | 1.5 | 0.25 | 0.1 | N.A. | N.A. |
| N | WFS, source N | 0.36 | 2.41 | 1.57 | 0.9 | 3.8 | 17.6 | 63.9 |
| A | WFS, source A | 0.39 | 6.3 | 1.78 | 10.4 | 7.8 | 60 | 340.2 |
| G | WFS, source G | 0.26 | 5.0 | 1.38 | 1.3 | 2.1 | 9.4 | 120.9 |

Table 3.3 Physical Characteristics of Sands (Continued)

| Identification | Description/Source | $e_{max}$ | $e_{min}$ | $\gamma_{dmax}$ kN/m$^3$ | $\gamma_{dmin}$ kN/m$^3$ | Specific gravity | Bulk sp. gravity (SSD) | Absorption,% |
|---|---|---|---|---|---|---|---|---|
| R | River sand | 0.69 | 0.45 | 18.52 | 15.87 | 2.69 | 2.62 | 1.6 |
| V(N) | Virgin foundry sand | - | - | - | - | 2.66 | 2.64 | 0.5 |
| N | WFS, source N | 0.91 | 0.73 | 14.7 | 13.3 | 2.53 | 2.48 | 1.5 |
| A | WFS, source A | 1.78 | 1.06 | 11.8 | 8.70 | 2.42 | 2.25 | 5.5 |
| G | WFS, source G | 1.01 | 0.67 | 15.0 | 12.4 | 2.50 | 2.45 | 1.6 |

size distribution for all the sands is shown in Figure 3.4. The coefficient of uniformity(CU), $d_{50}$ (50% of the material by weight is finer than this size), and fineness modulus are given in Table 3.3. The river sand, R is a well graded material and conforms to ASTM C33 standard which is the standard specification for concrete aggregates. The WFSs N, A and G are uniformly graded fine sands, and do not conform to ASTM C33 standards. The major portion of these sands lies in between #30(0.6 mm) and #100(0.15mm) sizes. ASTM C33 requires that Fineness Modulus be between 2.3 and 3.1. The Fineness Modulus values for WFSs were all low. Some fine materials, namely, clay and combustible additives such as seacoal are added to the sand in the mold making process. Therefore, some clay size fraction in WFS is to be expected. However, all the material was retained on #200 (75 micron) sieve during dry sieving. The mold is subjected to a high temperature during the metal casting process. It seems that during this process, the binders stick to the sand particles, and do not easily come out. To see if these fine particles get seperated from the sand particles in the presence of water, the sands were soaked in water for 24 hours and washed through the #200 sieve. A quantity of 5 to 10% dry weight of sand passed through #200 sieve. This fraction also contained a lot of carbon particles. Also, the clay in WFS seems to lose much of its plasticity due to high temperature during metal casting.

The virgin sand, V(N) had almost same gradation as its corresponding WFS, N. The addition of binders to sand does not seem to change its gradation significantly.

### 3.4.3 Loss on Ignition (LOI)

To determine Loss on Ignition(LOI), one to two grams of sand is first oven dried at 100°C to constant weight. Then, the sand is cooled in a desicator, and the weight of sand is noted. The dry sand is transferred to a furnace at 750°C for about an hour. The sample is removed from the oven, cooled and weighed. The loss in weight from 100°C to 750°C is taken as Loss on Ignition. Table 3.3 shows LOI test results. The material WFS, A had a high value of LOI of 7.8%. The LOI is generally an indication of carbon content in any material, because the carbon is ignited at high temperature. However, there may be several other

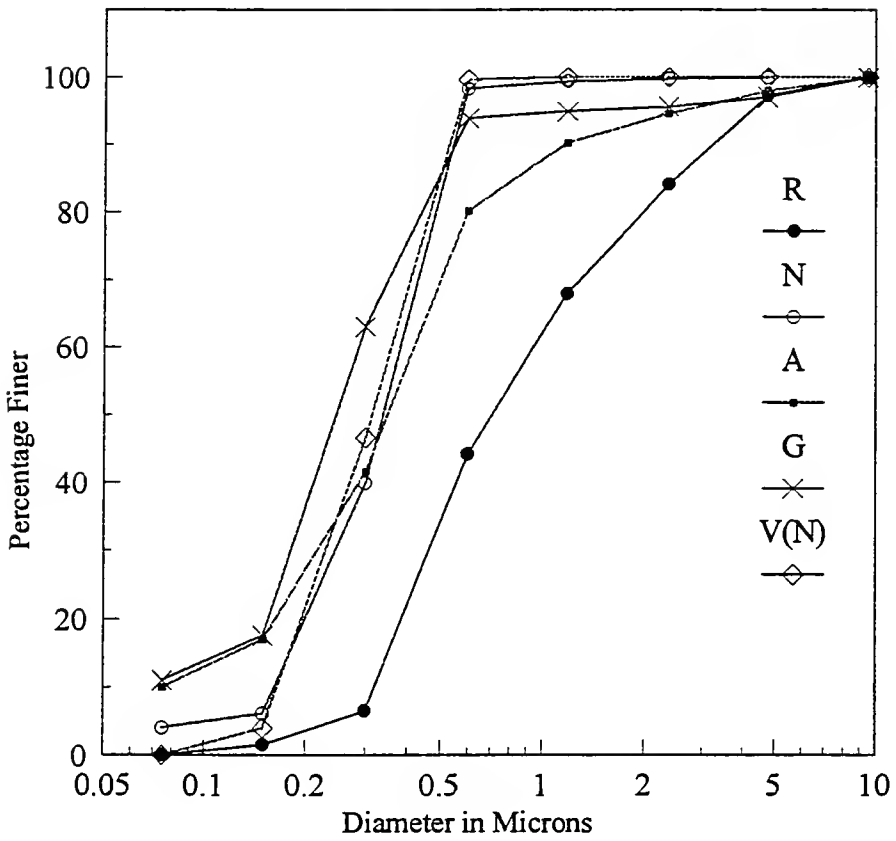


Figure 3.4 Particle Size Distribution for Sands

reactions that take place at 750°C. Surprisingly, the LOI was 6% for the clean river sand, R which did not contain any carbon. The carbonate in the sand must have decomposed giving rise to a loss in weight. Therefore, LOI cannot always be relied upon as a measure of carbon content.

### 3.4.4 Absorption and Specific Gravity

The absorption and specific gravity of sands was determined in accordance with ASTM C128. Absorption is the amount of water necessary to bring the material to saturated-surface-dry (SSD) condition. The SSD condition refers to a state when all the permeable pores in the individual sand grains are filled with water, but there is no excess water on the surface of the grains. The weight of sands in flowable fill mix design was based on the SSD weights. This is logical because the water inside the pores of sands does not contribute to the flowability. The bulk specific gravity is calculated based on the SSD condition. The bulk specific gravity can be used to calculate the bulk volume occupied by sands including intraparticle voids, but excluding interparticle voids. The apparent specific gravity is what is normally referred to as simply "specific gravity". It is called "apparent" on the presumption that there may be always some impenetrable voids left during specific gravity determination.

The absorption and specific gravity test results are shown in Table 3.3. The absorption for all sands including clean sands, except WFS, A was around 1.5%. The WFS, A had a high absorption value of 5.5%. This might be due to the presence of carbon particles. Carbon particles are generally porous and can absorb a lot of water. The specific gravity of WFSs is very low. This may be partly due to the presence of light weight particles like carbon. It is not known if the temperature brings about any change in the specific gravity of sand particles themselves. The low specific gravity of WFSs forms flowable fills with considerably lower unit weights compared to fills with clean sands.

### 3.4.5 Maximum and Minimum Density

Maximum and minimum void ratios ($e_{max}$ and $e_{min}$), and maximum and minimum densities ($\gamma_{dmin}$ and $\gamma_{dmax}$) were determined based on ASTM D 4253 and 4254. The results are shown in Table 3.3.

### 3.4.6 Chloride and Sulfate Ion Concentrations

The leachate from WFS was subjected to ion chromotography to detect the presence of anions in WFSs. The leachate was prepared from 1 solid to 5 water ratio. The chloride and sulfate ions were detected, and the concentrations are shown in Table 3.3.

### 3.4.7 X-Ray Diffraction Analysis

To see if any change in mineralogy has occured in WFS due to high temperature, x-ray diffraction tests were carried out. The results are shown in Figures 3.5 through 3.7. The quartz was the major component in all the sands. Therefore, high temperature in foundries does not destroy the structure of the sands. In WFS, A some montmorillonite was also found.

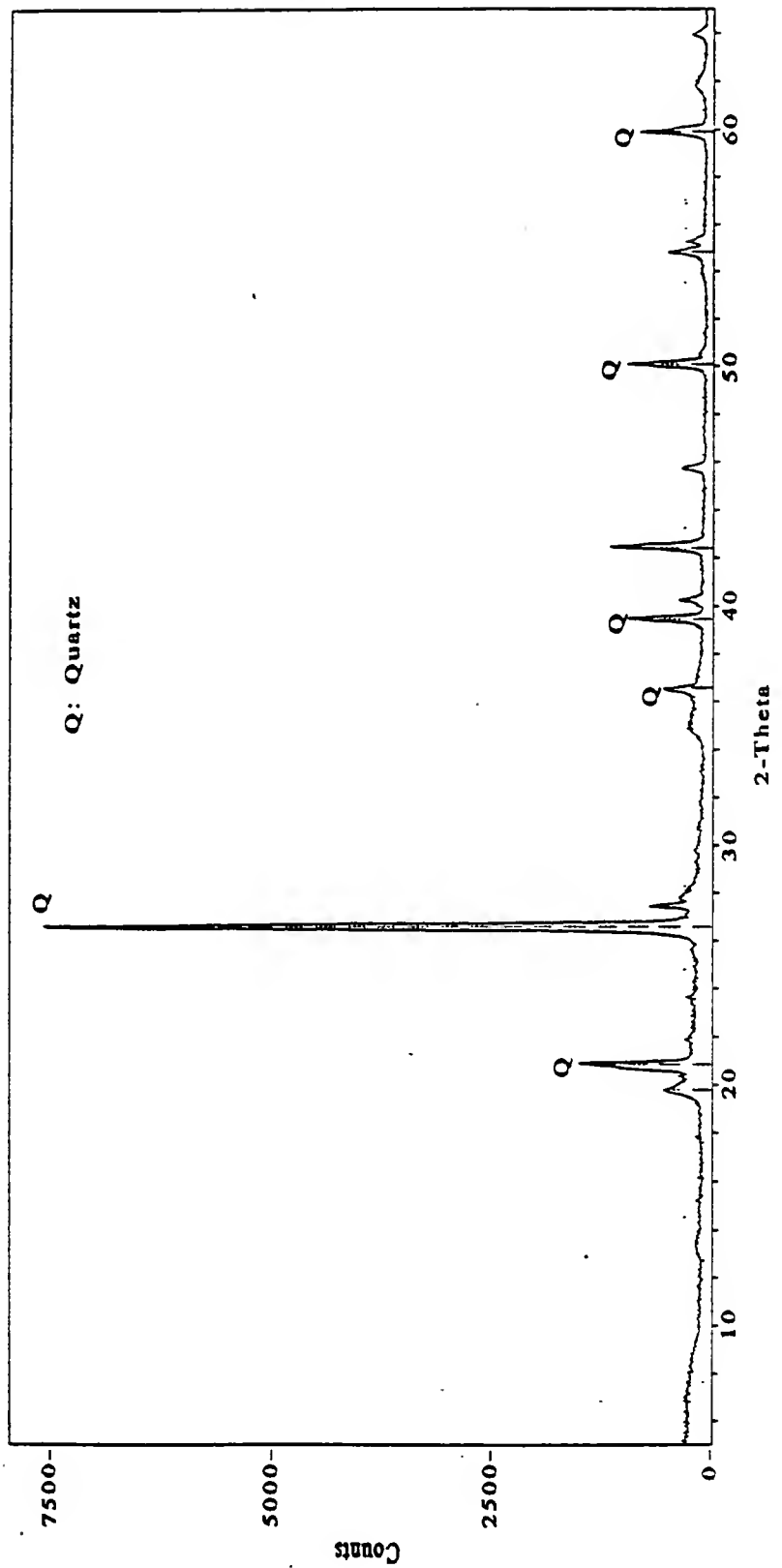


Figure 3.5 X-Ray Diffraction Result for WFS, N

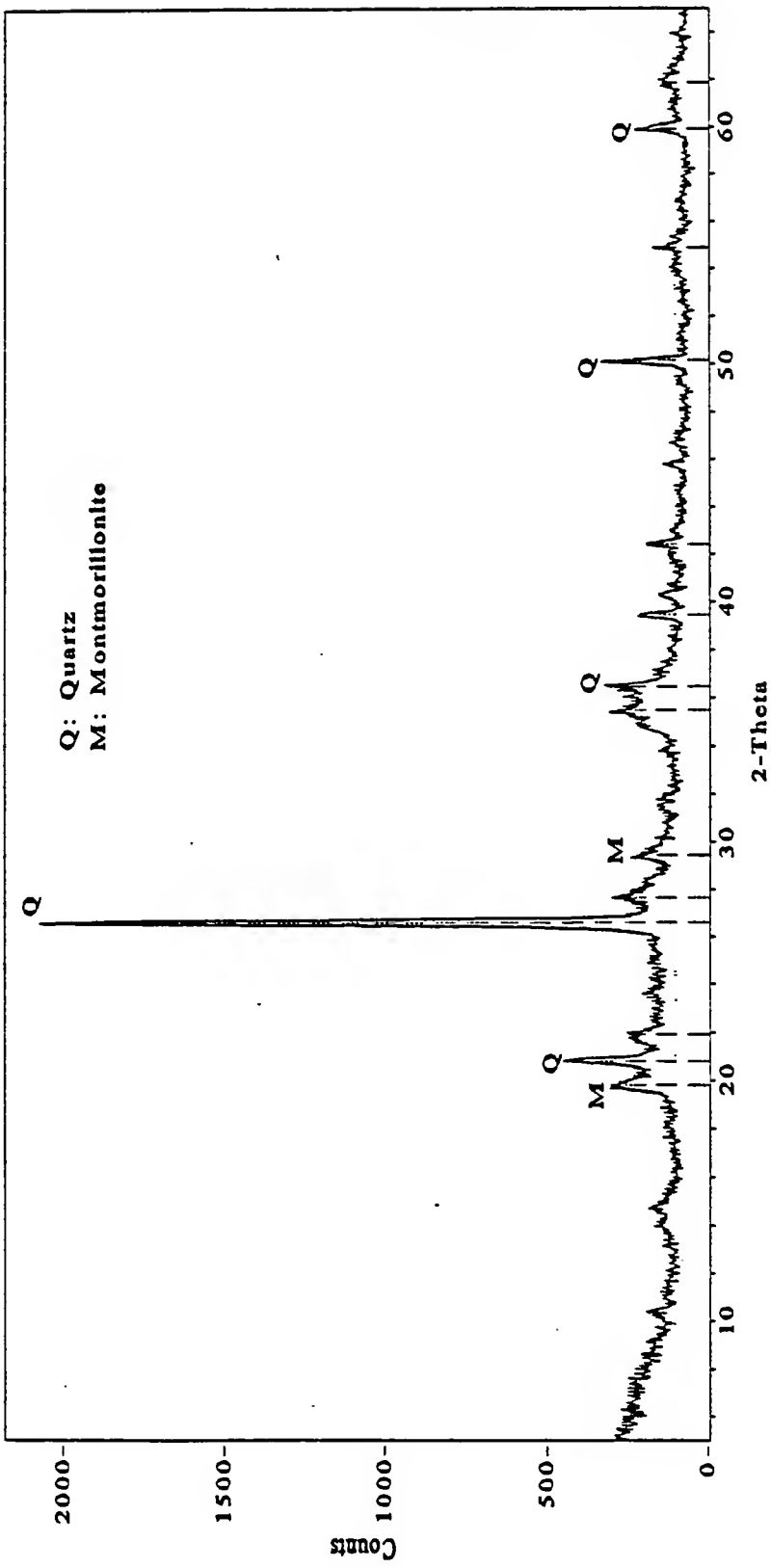


Figure 3.6 X-Ray Diffraction Result for WFS, A

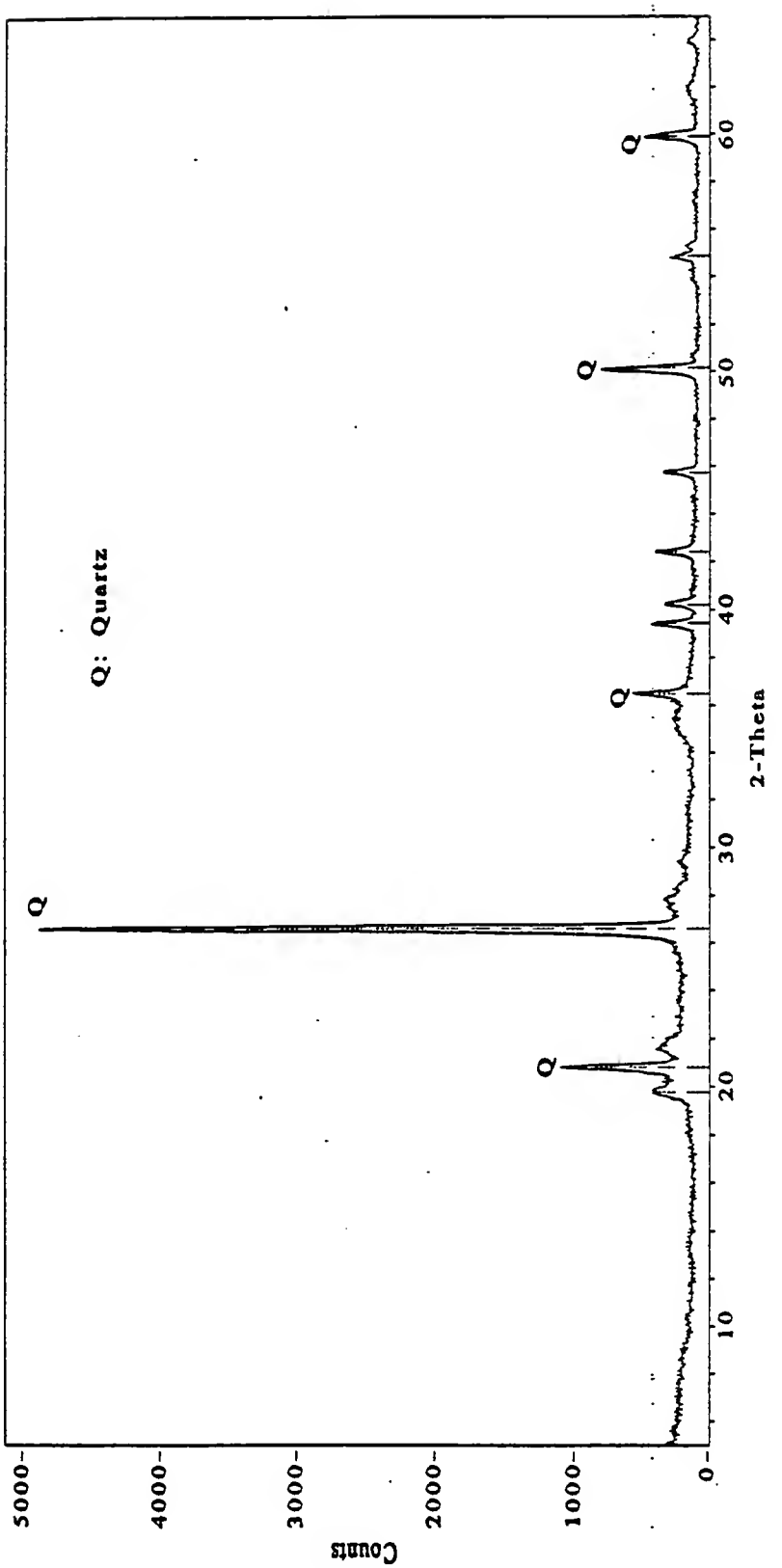


Figure 3.7 X-Ray Diffraction Result for WFS, G

# CHAPTER 4. FLOW BEHAVIOR

## 4.1 Introduction

Flowability is the most important attribute of flowable fill, so much so that the material is named after this attribute. The flowability allows the material to be placed without compaction. When used as a backfill for utility trenches, flowable fill flows around and under the pipes to form a homogeneous support for the pipe, which is not possible when soil backfill is used. It is virtually impossible to compact soil around the pipe. This invariably causes gradual settlement of the surface of the fill over a period of time, leading to costly maintainance. The flowable fill can flow into inaccessible places, for example, an abandoned underground storage tank. These are only examples, and proper flowability is important in every other application.

Flowability does not mean that the material can flow any amount of distance in the field. It depends on the boundary conditions. The flowable fill being poured at the end of a narrow deep trench would flow a longer distance compared to the flowable fill being poured on a level parking lot where the final thickness is intended to be only a few centimeters. The flow also depends on the roughness of the surface on which it flows. If segregation takes place, the solid particles in flowable fill tend to settle, hindering flow. Though the laboratory flow tests do not completely simulate all the field conditions, a simple test has evolved out of the experience of the engineers involved in the application of flowable fill. This test is the Modified Flow Test (ACI Committee 229, 1994), using a 7.6cm × 15.2cm (3 in. × 6 in.) open ended cylinder. In this test, the open ended cylinder is placed on a smooth level surface, and filled with fresh flowable fill. The cylinder is quickly lifted and the average diameter of the circular section of flowable fill formed on the surface is taken as the **spread**. A spread of 20

to 23 cm (8 to 9 in.) or higher is found to give self-levelling characteristics and adequate flow in the field to the flowable fill.

The purpose of adding fly ash to the flowable fill is to facilitate flow. The sand alone can not produce flow because the frictional resistance at particle to particle contact resists flow. Mixing water with sand does not help either, because the sand gets segregated from the water. The presence of fly ash helps retain the water, and also helps flow.

The purpose of this chapter is to introduce a new concept of "flow curves", and to explore how this could advantageously be used in producing a better material. It should be emphasized that the approach to the design of a good flowable fill should be to produce a dense material with as little porosity as practicable, and the state of fresh flowable fill has an important bearing on achieving this goal.

## 4.2 Experimental Program

### 4.2.1 Materials

Five sands, R, N, A, G and V(N), and two class F fly ashes, SC and GI were used in this study. The sand, R is a well graded river sand. The sands, N, A, and G are waste foundry sands (WFSs). The sand, V(N) is a clean virgin sand which comes out as WFS, N after use in the metal casting process. The index properties of sands were given in Chapter 3.

Table 4.1 gives the properties of these sands relevant to this Chapter. Waste foundry sands and virgin foundry sand, V(N) were uniformly graded materials. The WFSs contain small amounts of clay and organic matter. The specific gravity of WFSs is lower compared to that of river sand, R, and virgin sand, V(N).

Table 4.1 Physical Characteristics of Sands

| Ident-ification | Descript-ion/Source | CU | $e_{max}$ | $e_{min}$ | $\gamma_{dmax}$ kN/m$^3$ | $\gamma_{dmin}$ kN/m$^3$ | Specific gravity | Bulk sp. gravity | Absorp-tion,% |
|---|---|---|---|---|---|---|---|---|---|
| R | River sand | 2.83 | 0.69 | 0.45 | 18.52 | 15.87 | 2.69 | 2.62 | 1.6 |
| V(N) | Virgin foundry sand | 2.24 | - | - | - | - | 2.66 | 2.64 | 0.5 |
| N | WFS, source N | 2.41 | 0.91 | 0.73 | 14.7 | 13.3 | 2.53 | 2.48 | 1.5 |
| A | WFS, source A | 6.3 | 1.78 | 1.06 | 11.8 | 8.70 | 2.42 | 2.25 | 5.5 |
| G | WFS, source G | 5.0 | 1.01 | 0.67 | 15.0 | 12.4 | 2.50 | 2.45 | 1.6 |

### 4.2.2 Flow Cone Sand Test

The flow cone sand test was designed by Tobin (1978) to measure relative angularity or roundness of fine aggregate to be used in concrete. It was also intended to quickly estimate the mean particle size. Figure 4.1 shows the flow cone sand test apparatus. Around 1500 ml of the oven dried sand to be tested is passed through a No. 8 (2.36 mm) sieve. Only the portion of the material passing No. 8 sieve is taken for the experiment. The orifice of the flowcone is closed with the left hand finger, and around 1200 ml of the sand is poured into the cone. The finger is then released and the sand is then allowed to flow into the glass jar directly below the orifice. The quantity of sand that is placed in the cone should be sufficient to fill the jar to overflowing. The glass jar is then struck-off level with a straight edge, and the glass jar is weighed. The excess sand in the overflow pan is removed and the overflow pan is returned to its original position. The operator again places his finger beneath the opening in the orifice and empties the contents of the glass jar back into the flow cone. The empty jar is then placed directly under the orifice. The time of flow is then measured with a stopwatch from the instant the finger is released until day-light is observed through the orifice when viewed from above. The same procedure is repeated three times, and the weight and the time measurements are averaged. The average net weight divided by the specific gravity gives the absolute volume or net solids in the jar. The percentage of net solids is obtained by dividing the net solids by the volume of the jar. The volume of the jar in this case was 932 ml. The average time reading is converted to time required for flow of 1000 ml loose volume. The flow rate is expressed as time per unit volume rather than per unit weight, because flow time is found to be independent of specific gravity.

Tobin conducted flow tests on 146 different sands, and the results of the test on separated sizes are shown in Figure 4.2. The straight lines are the average lines for the measured values for each size range. The time of flow is higher for larger size particles. The percentage solid volume indicates the relative angularity. For a given size particles, the time of flow decreases and net solid volume increases as the particles become more rounded. The flow time is directly related to the average particle size which in turn can theoretically be related to fineness modulus (FM). Based on the flow test results on various sands, Tobin

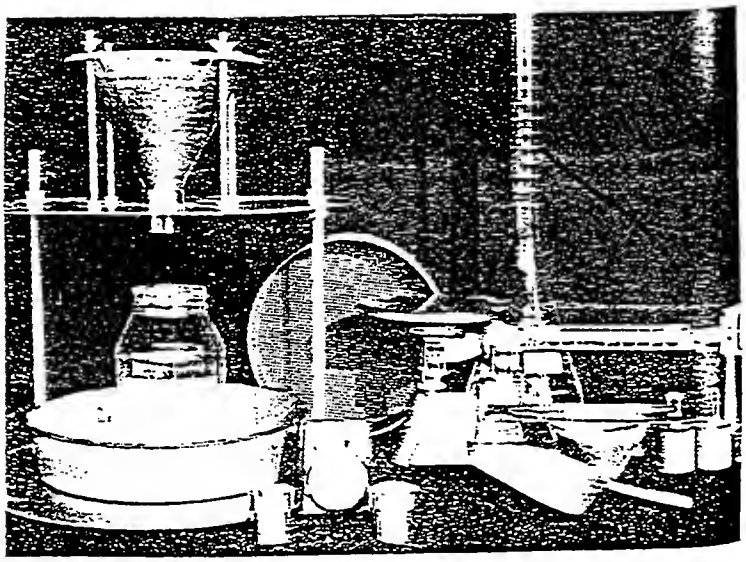

Figure 4.1 Flow Cone Sand Test Apparatus (Tobin, 1978)

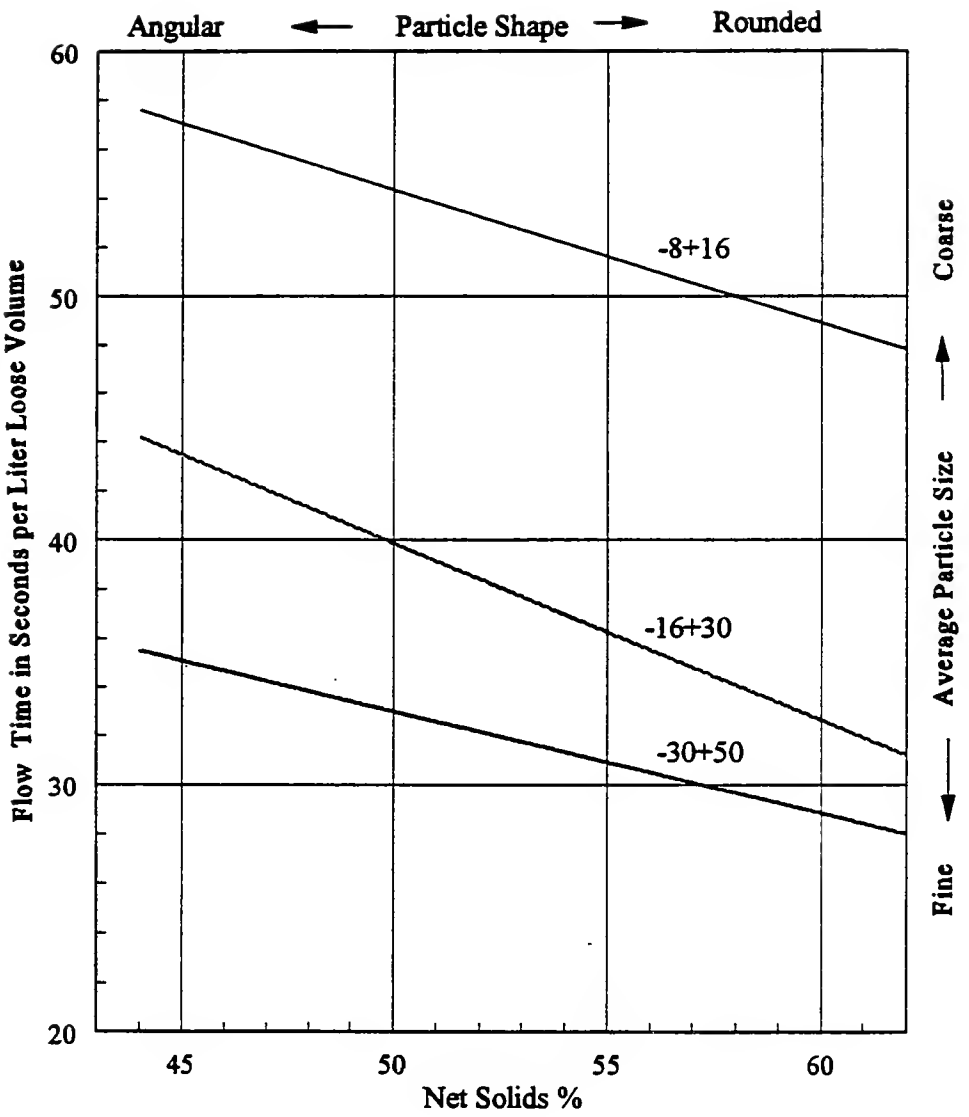


Figure 4.2 Flow Tests on Separated Sand Sizes

developed the fineness modulus lines by interpolation as shown in Figure 4.3. The FM values of 2.91, 2.49, and 2.15 correspond to the coarse, medium, and fine values according to ASTM C33. Flow cone test results below or above these boundary lines would indicate that the material would probably not satisfy ASTM C33 gradation requirements; those below would be too coarse. The vertical dotted lines divide the particle shape into rounded, average, and angular, based upon net solid volume.

### 4.2.3 Flow of Dry Sand-Fly Ash Mixture

To see the effect of fly ash on the flow of dry sand, the mixtures of dry sands with fly ash, GI were allowed to flow through the flow cone. This test was earlier tried by Nantung(1993). The pure sand was first tested in the usual manner. Thus, one jar of loose volume of sand is obtained. This sand is mixed with small amount of known weight of fly ash (around 0.5% to 1% by weight of sand), and then subjected to flow test. The flow time was measured. The weight of bottle along with the sand and fly ash collected in it was also noted. It was observed that the addition of fly ash resulted in denser packing of the sand as indicated by the decrease in level of sand in the jar after it flows through the orifice. The jar is emptied two more times into the flow cone and flow measurements are taken. The procedure is repeated for higher fly ash contents. The addition of fly ash is done to the same fly ash-sand mixture tested in the previous step. Therefore, it is important not to lose any material during each stage of the test. It was observed that as the fly ash content is increased, at some point, the flow through the orifice becomes uneven, and sometimes the mixture completely clogs the orifice.

### 4.2.4 Modified Flow Test for Flowable Fill

Flowability of fresh flowable fill mixture is measured by the modified flow test (ACI Committee 229, 1994) using a 7.6cm × 15.2cm (3 in. × 6 in.) open ended cylinder as shown in Figure 4.4. In this test, the open ended cylinder is placed on a smooth level surface.

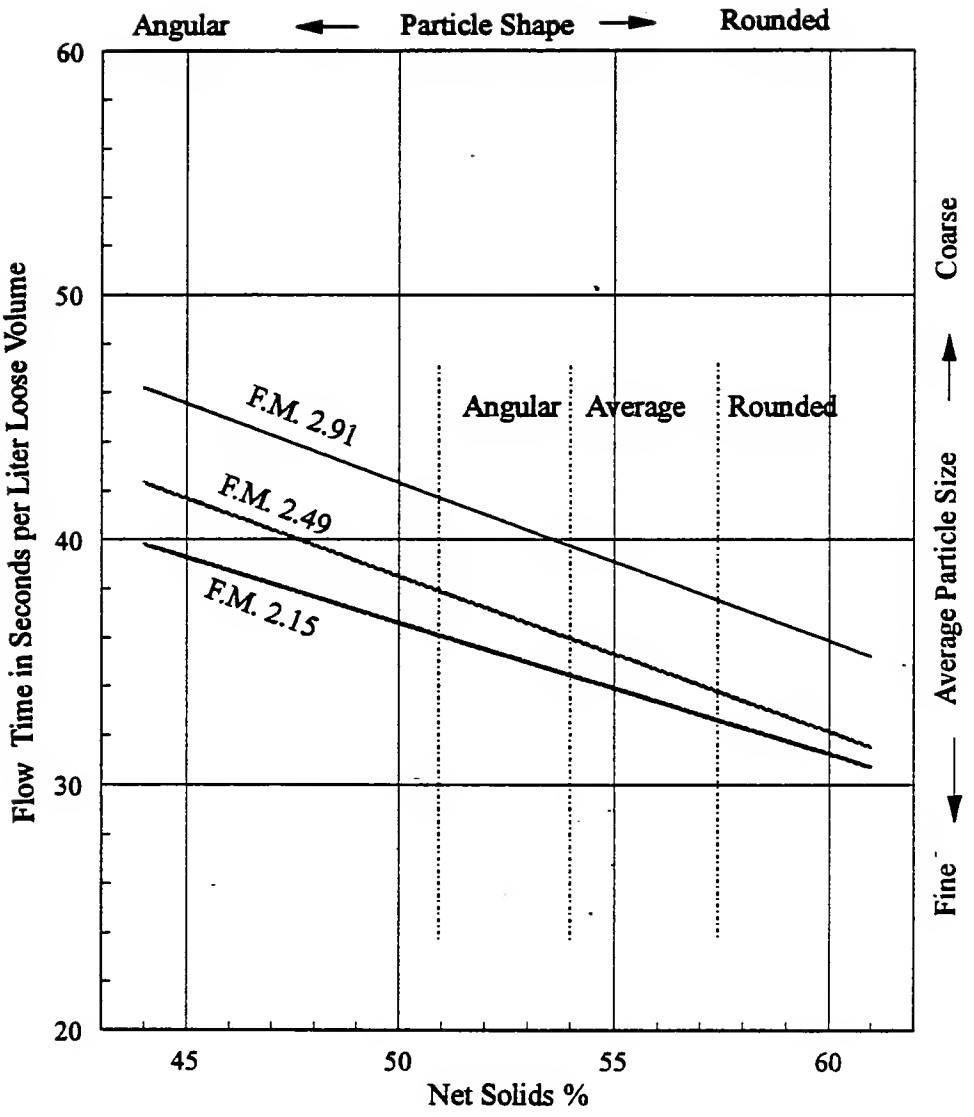


Figure 4.3 Fineness Modulus from Flow Cone Test (Tobin, 1978)

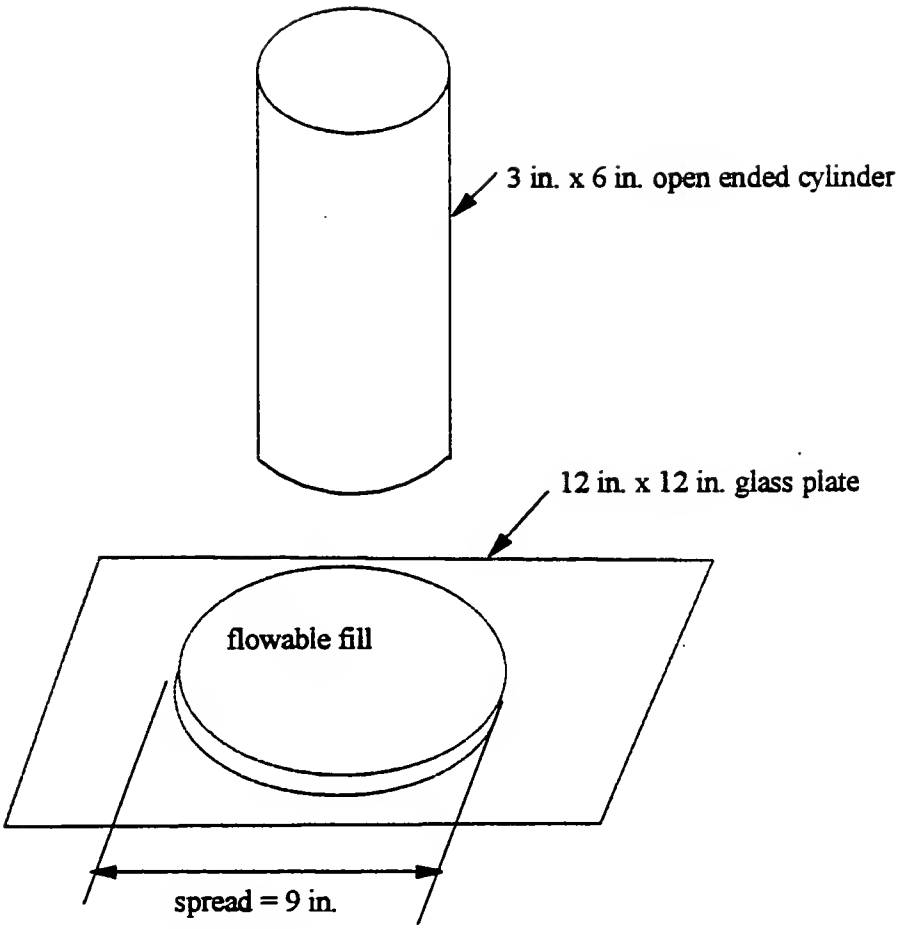


Figure 4.4 Modified Flow Test

Nantung (1993) used a 12 in. × 12 in. smooth glass plate, and the same procedure is adopted in this research. This would reduce the friction between the flowable fill and the surface while it is flowing, and also this ensures consistent results because the roughness and nature of the surface may affect the spread. The cylinder is filled full with fresh flowable fill mix, and the surface is struck off level with a straight edge. Then the cylinder is quickly lifted and the diameter of the circular section of flowable fill formed on the glass plate is taken as the spread. A homogeneous mixture would flow and form a uniform section with equal overall thickness. A spread of 20 to 23cm ( 8 to 9 in.) is found to give self leveling characteristics to the flowable fill, and is also found to give adequate flow during placement in the field.

### 4.2.5 Flow Curve Determination

To draw the flow curve (water-solid ratio vs fly ash content), different proportions of sand, fly ash, cement, and water are to be determined to get a specific flowability. In this study, all flow curves represent 23cm (9 in.) spread. The test involves a trial and error procedure. A portion of typical test data and calculations are shown in Figures 4.5 and 4.6. Approximately, 2000 gm of dry sand is taken. By knowing the absorption of sand, the amount of water necessary to bring it to SSD condition can be calculated. This amount of water is added to the sand. To start with, fly ash equal to around 5 to 10 % by weight of sand is added. For waste foundry sands, a starting point can be with a smaller amount of fly ash. The amount of cement added should be such that the flowable fill with these proportions would have a cement content of around 40 to 60 kg/m$^3$. By knowing the weight and specific gravity of each component, the cement content in a mix per unit final volume (i.e. kg/m$^3$ or lb/yd$^3$ ) can be calculated. A sample calculation is shown in Figure 4.6. It should be noted that the air content in the mix is neglected and that the system is assumed to be completely saturated. Water is added step by step, thoroughly mixing with a spoon, and the flow is measured. If the spread is less than 23cm (9 in.), more water is added, until the spread becomes 23cm (9 in.). The material on the glass plate after measuring the spread is quickly transferred back to the mixing container. Care is taken not to lose any material during this

Sand: R (CONCRETE SAND) Fly Ash: FI
Absorption of Sand: 1.6 %
Dry weight of sand taken = 2000 gm
SSD weight of sand = 2000 × 1.016 = 2032 gm
Amount of water to be added to the dry sand to bring it to SSD= 32 gm

| Sand (SSD)(gm) | Cement (gm) | Fly Ash Added(gm) | water Added(gm) | Spread (in.) | Remarks |
|---|---|---|---|---|---|
| 2032 | 80 | 300 | 200 | | no flow |
| | | – | 100 | | no flow, stiff |
| | | – | 28 | 8 in. | segregates |
| | | 100 | – | 8.5 in. | |
| | | 50 | – | 8 | |
| | | – | 20 | 9 | uniform flow |
| | | 100 | – | 8.5 | |
| | | – | 12.5 | 9 | |
| | | 200 | 60 | 9 | |
| | | 200 | 50.3 | 9 | |
| | | 400 | 100 | – | stiff |
| | | – | 20 | 8.75 | |
| | | – | 20 | 9 | very sticky |
| | | 300 | 60 | 8.5 | |
| | | | 19.7 | 9 | very sticky |
| | | | | | |
| | | | | | |
| | | | | | |
| | | | | | |

Figure 4.5 Typical Laboratory Test for Flow Curve Determination

Sand: R  Fly Ash: Cl

| Sand (SSD) (gm) S | Cement (gm) C | Cumulative Fly Ash Added(gm) F | Cumulative Water Added(gm) W | Spread (in.) | F/(F+S) % | W/(C+F+S) % |
|---|---|---|---|---|---|---|
| 2032 | 80 | 450 | 348 | 9 | 18.1 | 13.6 |
| 2032 | 80 | 550 | 360.5 | 9 | 21.3 | 13.5 |
| 2032 | 80 | 750 | 420.5 | 9 | 27.0 | 14.7 |
| 2032 | 80 | 950 | 470.8 | 9 | 31.9 | 15.4 |
| 2032 | 80 | 1350 | 610.8 | 9 | 39.9 | 17.6 |
| 2032 | 80 | 1650 | 690.5 | 9 | 44.8 | 18.4 |
| | | | | | | |
| | | | | | | |
| | | | | | | |

Note: The cement content in $kg/m^3$ or $lb/yd^3$ goes on reducing in the above mixes as you move down. However, this does not affect flow curve. The cement content may be kept around 40 to 60 $kg/m^3$ for the purpose of flow curve generation. This changes for the actual final mix.

The cement content for the mix in the first row is around 60 $kg/m^3$ which can be calculated as follows:

Total volume of components

$$= \frac{2032}{2.62} + \frac{80}{3.17} + \frac{450}{2.42} + \frac{348}{1} = 1335 \text{ cm}^3$$

$$\text{Cement content} = \frac{80/1000 \text{ kg}}{1335 \times 10^{-6} \text{ m}^3} = 60 \text{ kg/m}^3$$

Figure 4.6 Calculations for Flow Curve Determination

process. This proportion of components yields one point on the flow curve. More fly ash is added to the existing mix producing a stiffer mix. More water is added until a spread of 23cm (9 in.) is produced. This procedure is repeated until sufficient points for the flow curve are obtained. Note that the cement is not added at each stage; therefore, the proportion of cement content in the mix decreases as more fly ash is added. However, this is found not to influence the flow curve.

## 4.3 Results

### 4.3.1 Flow of Sands in Flow Cone

Table 4.2 shows the summary of flow cone sand test results on five dry sands. From the percentage net solids values, percentage voids can be calculated simply by subtracting this value from 100. This value of percentage net voids is the porosity of the sand in that state. By knowing the porosity, the void ratio can be easily calculated. Calculated values of void ratio are shown in Table 4.2. The flow cone test results are also plotted in Figure 4.7. The river sand, R falls close to the ASTM C33 upper bound for gradation. All other sands fall below the ASTM C33 lower boundary indicating that these sands do not conform to the ASTM C33 standard. This was also observed through the actual sieve analysis (Chapter 3). The percentage net solids values in Figure 4.7 indicate the angularity or roundedness of a sand. The higher the percentage net solids value, the more rounded the sand would be. The river sand, R was rounded as indicated by the high percentage net solids value in the flow cone test. On the other hand, waste foundry sands were all angular. The virgin sand, V(N) and WFS, N had almost the same gradation; however, WFS N seems to be slightly more angular than the sand V(N). The WFS A had the lowest value of percentage net solids. Out of the large number of natural sands Tobin tested, no sand had such a low value of percentage net solids value. It seems that the clay coats the waste foundry sand grains, and induces apparent angularity to these sands, and therefore decreases the net solid volume.

Table 4.2 Summary of Flow Cone Sand Test Results

| Sand | Flow Time sec/liter | Net Solids % | Fineness Modulus | | Average Size, mm | | $e_{max}$ for sand | $e_{loose}$ in flow cone test |
|---|---|---|---|---|---|---|---|---|
| | | | -4+0 | -8+0 | -4+0 | -8+0 | | |
| R | 36.77 | 59.5 | 2.98 | 2.57 | 1.34 | 0.81 | 0.69 | 0.68 |
| N | 33.02 | 55.1 | 1.57 | 1.56 | 0.37 | 0.36 | 0.91 | 0.81 |
| A | 35.17 | 43.4 | 1.78 | 1.58 | 0.68 | 0.43 | 1.78 | 1.3 |
| G | 32.95 | 51.2 | 1.38 | 1.18 | 0.54 | 0.29 | 1.01 | 0.95 |
| V(N) | 31.7 | 56.5 | 1.5 | 1.5 | 0.34 | 0.34 | - | 0.77 |

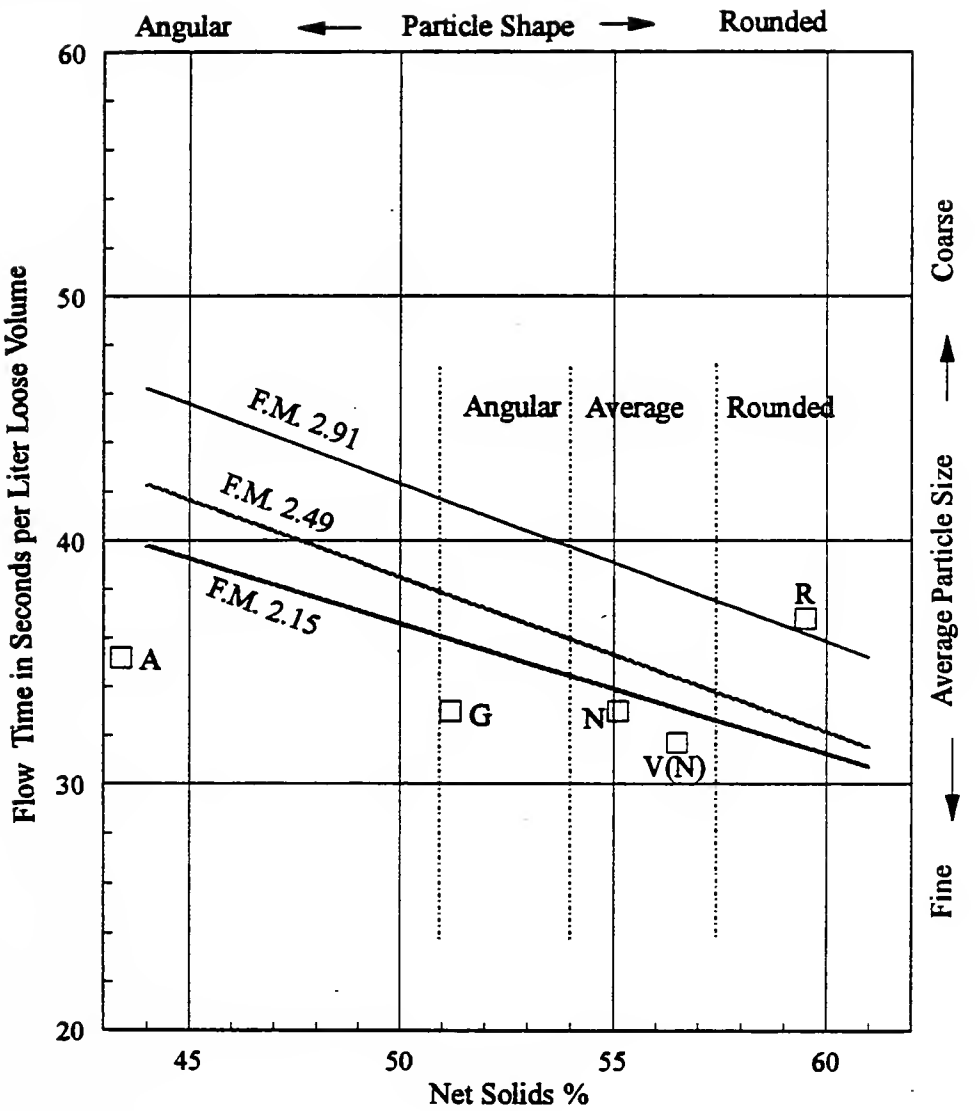


Figure 4.7 Flow Cone Sand Test Results

The void ratio calculated from net solids in Table 4.2 can be compared with the maximum void ratios, $e_{max}$ shown in Table 4.1. The $e_{max}$ represents the loosest possible state for a sand. The $e_{max}$ values were higher than the void ratio of the loose state in flow cone test. However, there is a one to one relation between $e_{max}$ values and void ratios calculated from flow cone tests.

### 4.3.2 Flow of Dry Sand and Fly Ash Mixtures

In Section 4.3.1, the flow behavior of sand in the flow cone was presented. It would be interesting to see how the addition of fly ash to the sand would affect its flow behavior. The dry fly ash alone did not flow well. However, it improves the flow behavior of sand. The variation of flow time of sand-fly ash mixture with the percentage of fly ash in the mixture is shown in Figure 4.8. The fly ash decreases the flow time of sands. Small mostly spherical particles of fly ash particles perhaps act like a ballbearings, and help the sand grains slide past each other quickly and easily. This lubrication effect also helps the sand to achieve a denser packing. This was obvious because the sand-fly ash mixture occupied a smaller total volume in the jar than what the sand alone would occupy during the flow test: The sand alone would fill the jar full; when this sand is mixed with fly ash and let flow, but some space is left at the top of the jar. Therefore, it can be concluded that fly ash apparently decreases the angularity of sand, and induces more apparent roundedness to the sand. Further addition of fly ash in small amounts, further decreases the flow time, and also results in denser packing. The minimum flow time occurs at around 1 to 2 % fly ash content. Further addition of fly ash increases the flow time, and also the loose volume of sand-fly ash mixture starts increasing as indicated by the increasing level of sand-fly ash mixture in the jar. If the addition of fly ash is continued, at some point the sand-fly ash mixture would completely fill the jar. It was also observed that for some sands, fly ash content of more than 3% resulted in a non-uniform flow through the orifice. The flow time data were erratic. In some cases, the orifice was completely clogged stopping the flow altogether. It was also observed that at fly ash contents more than around 2%, segregation of fly ash and sand takes place. The lesson that can be

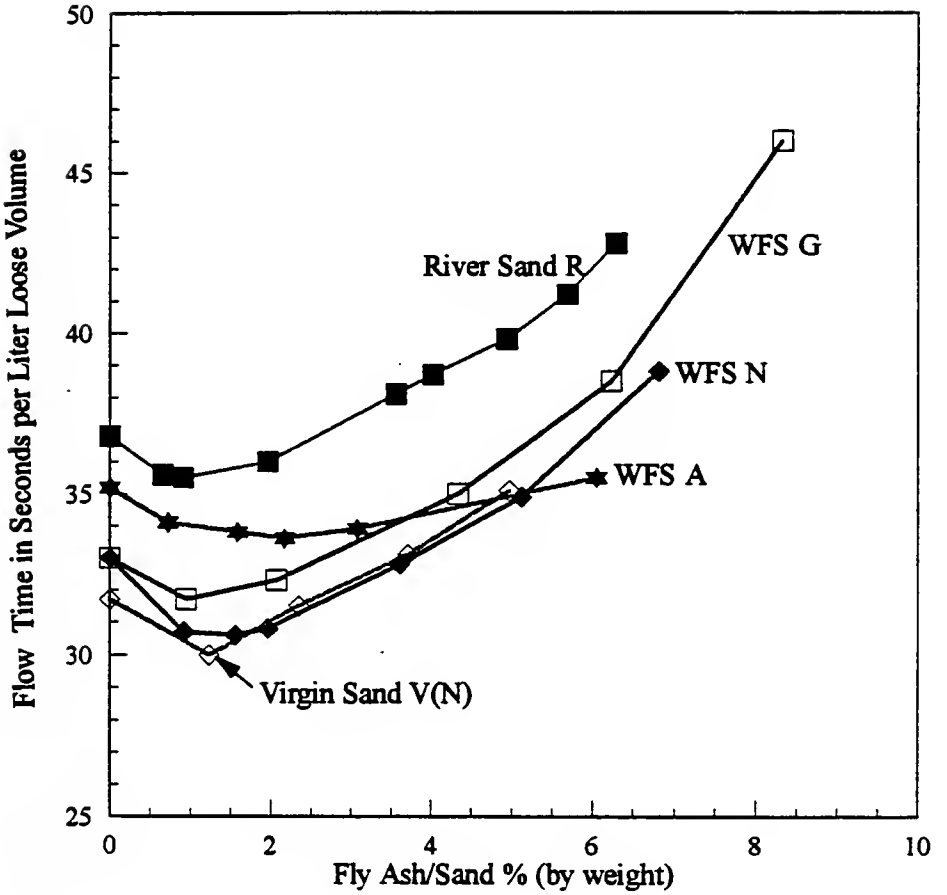


Figure 4.8 Influence of Addition of Fly Ash, GI on Flow Time of Sands in Flow Cone Sand Test

learned from this test is that the fly ash in very small amounts has a lubrication effect on the flow behavior of sand.

### 4.3.3 Flow Behavior of Flowable Fill

The major ingredients of flowable fill are sand, fly ash, and water. The amount of cement is very small. The proportion of fly ash and sand in the mix determines how much water needs to be added to get the required flowability. This relationship between ingredients of flowable fill can be plotted to get a curve such as Figure 4.9 which is called the "***Flow Curve***". The water-solid ratio and fly ash contents are based on the weights of the ingredients. On the other hand, it is possible to represent these parameters based on the volume of the ingredients. However, the difference between these curves was found to be very small; moreover, the parameters based on weights makes it easier to design the mix. Therefore, the parameters are chosen on a weight basis.

Any point on the idealized flow curve in Figure 4.9 gives a water-solid ratio and fly ash content for which the spread in the flow test would be 23cm (9 in.). The effect of increasing fly ash content on flow can be understood as one moves up the flow curve from A through B, C, D to E. The point A represents the minimum amount of fly ash necessary for flow. At any fly ash content below that of point A, the mix would result in segregation and no flow. As some fly ash is added to the mix (say to point B), the water demand (i.e. water-solid ratio necessary to produce 23cm (9 in.) spread in the flow test) decreases. Further addition of fly ash would result in further decrease in water demand until point C is reached, which represents the minimum water demand. Addition of fly ash beyond point C does not help reduce the water demand. On the contrary, it increases the water demand until point E is reached. At point E, the fly ash content is 100% and the water demand is the highest. The fly ash improves flow initially, but larger amounts of fly ash do not necessarily do so. The point of inflection, C where the direction of slope of the flow curve changes represents the minimum water demand, and is called here the "***Point of Minimum Water Demand*** (PMWD)".

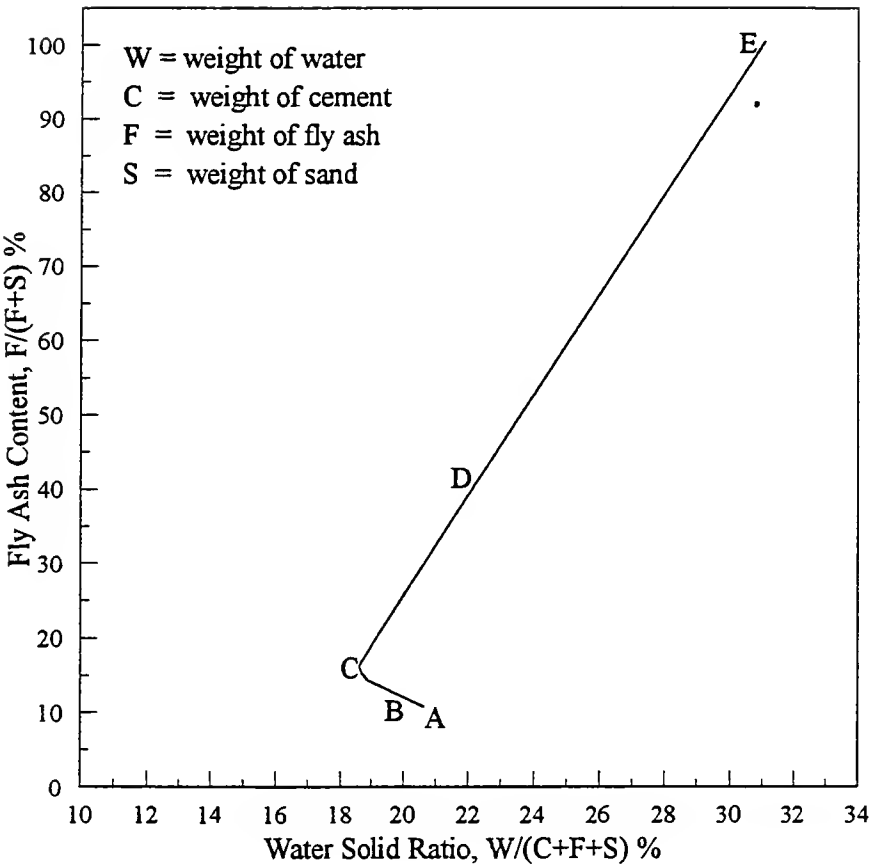


Figure 4.9 An Idealized Flow Curve

The positive effects of fly ash on flow is commonly believed to be the result of the spherical shape of the fly ash particles. This seems to be particularly true for the mixes with low fly ash content (below point C in Figure 4.9). The fly ash particles perhaps swarm around individual sand grains, and act as ballbearings during the flow, thus reducing the frictional resistance of the sand to flow; consequently, the water demand to produce the same flow reduces. However, a different phenomenon controls the flow behavior at high fly ash content (above point C in Figure 4.9). The cement and fly ash particles in a fly ash-cement mixture are found to be in a flocculent state(Helmuth, 1987). This structure of fly ash particles in states of agglomeration results from the interparticle electrostatic forces. These forces also cause a highly viscous suspension. This is what happens at high fly ash contents in flowable fill mixes. The flow now essentially consists of motions of flocs of different sizes and shapes. Thus the advantages of the spherical nature of the fly ash particles are lost. Also, the fineness of fly ash particles increases the total surface area of the particles in the mix. That means more water is needed to coat these particles increasing the water demand. These results suggests that adding a small amount of dispersing agent might help reducing water demand in the mixes containing high percentages of fly ash.

The flowability test using the 7.6cm × 15.2cm(3 in.× 6 in.) cylinder seems to be too simple a test compared to flow cone tests in which time of flow is taken as the measure of flowability. However, the difficulty with the flow cone tests is that results are affected by the maximum size of the aggregate. The cylinder flow test is independent of such effects, as the diameter of the cylinder is very large compared to the maximum particle size in the flowable fill mixes. In the cylinder flow test, when the cylinder is filled, the material inside possesses a certain amount of potential energy equal to the weight of the material multiplied by the average height (equal to half the height) of the cylinder. When the cylinder is lifted, the potential energy in the material gets dissipated during the flow in two ways: the frictional resistance between the flowing material and the glass plate, and the viscous forces within the body of the flowing material. Increasing the water content helps reduce this viscous force. Small amount of fly ash (between points A and C in Figure 4.9) as noted earlier, act as ballbearings and reduce the frictional resistance. The viscosity of the mix containing small

amount of fly ash is low. Thus, small amount of fly ash helps reduce the water demand to produce the same spread. However, at high fly ash contents (above point C in Figure 4.9), viscous forces dominate the flow, and therefore more water needs to be added to reduce the viscosity. Thus the fine aggregate with higher specific gravity have higher potential energy; and therefore, can flow longer distances with lesser amount of water before this potential energy is dissipated. This becomes particularly significant if the specific gravities of different aggregates differ significantly. The waste foundry sands have low specific gravity, and therefore, can be expected to require more water for flow.

The amount of cement content used in generating the flow curves was around 60 to 40 kg/m$^3$. As explained in section 4.2.4, a certain amount of cement is initially added to the mix. But, in further steps, only fly ash and water are added. Therefore, the proportion of cement goes on decreasing in the mix. However, it was found, by adding different amounts of cement , that the amount of cement does not noticeably change the flow curve. Moreover, the range of cement content in flowable fill for the low strength applications is not very large. Therefore, the effect of cement content on flow is not separately considered. However, it is included in the calculation of the water-solid ratio.

Figures 4.10 and 4.11 show the flow curves for different sands with two fly ashes. Several observations may be drawn from these Figures. The mixes with river sand, R and virgin sand, V(N) require considerably less water compared to the mixes with WFSs N, A and G. The difference in specific gravity seems to be the main reason for this. The sands R and V(N) have higher specific gravity, and therefore the mixes containing these mixes possess higher potential energy due to their higher weight before the cylinder is lifted in the flow test, and therefore, cause higher flow. That is, these mixes are able to achieve the required flow with lesser amounts of water.

The gradation does not seem to influence the water demand significantly. The well graded sand, R required only slightly less water compared to the uniformly graded fine virgin sand, V(N).

In Figure 4.10 and 4.11, the flow curves for mixes with WFSs N and G start from zero fly ash content. That is, these sands can be made to flow without the help of fly ash. An

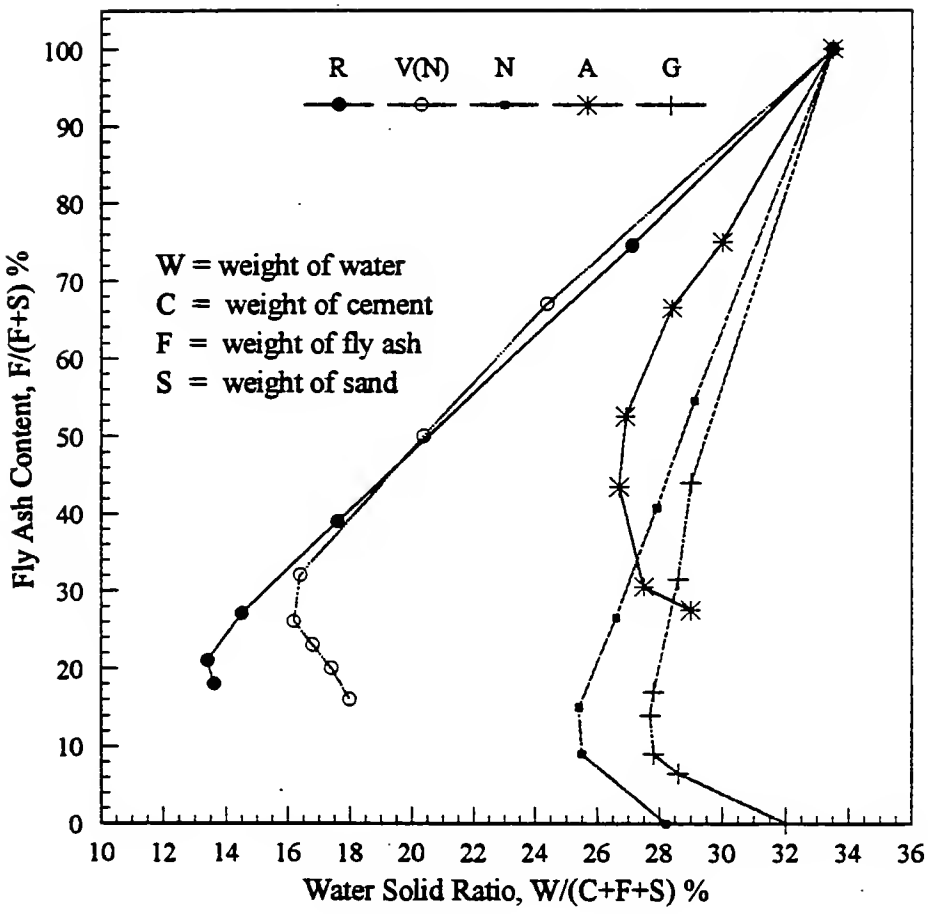


Figure 4.10 Flow Curves for Mixes with Fly Ash, GI, and Different Sands. Spread = 23cm (9 in.).

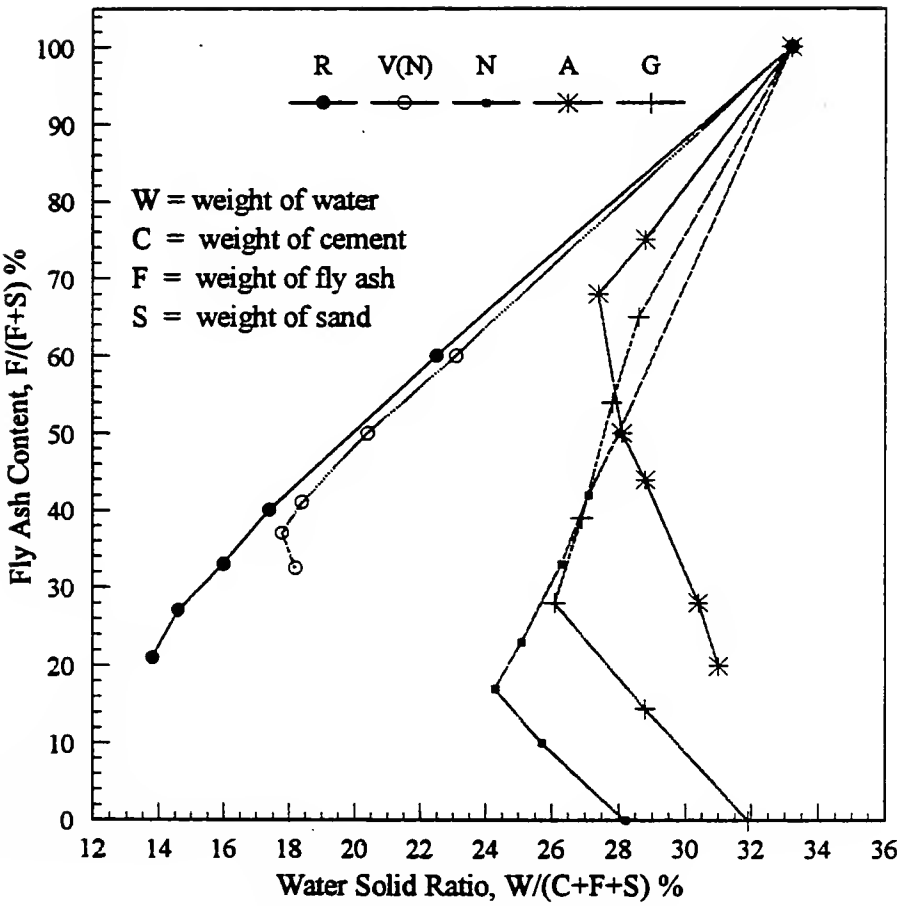


Figure 4.11 Flow Curves for Mixes with Fly Ash, SC, and Different Sands. Spread = 23cm (9 in.).

important and necessary condition for flow to take place is that the particle system in the mix should be able to hold the water within its body, without letting the water seep out in a short period of time. Presence of fly ash in flowable fill helps to retain the water between the solid particles during flow. The WFSs contain a small amount of clay. When water is added, the clay comes out as a suspension, and helps retain the water in the system. Thus, WFSs N and G are able to flow without any fly ash. However, WFS A could not flow without fly ash. It seems that the clay coating the sand particles in this sand does not readily come out after adding the water.

Comparision of Figures 4.10 and 4.11 indicate that the flow curves with the two fly ashes essentially have similar characteristics. The difference may be attributed to the differences in fineness and gradation of fly ashes.

### 4.3.4 Significance and Use of Flow Curves

In the last section, the mechanics of flow curves was discussed. The most significant feature of flow curves is the Point of Minimum Water Demand (PMWD), which gives the minimum amount of water that can produce the required flowability for a given combination of sand and fly ash. Every point on the flow curve represents the same flowability. However, the ideal point for choosing the proportion of sand and fly ash for design purposes is the PMWD for the following reasons.

It was earlier noted that the approach to the design of flowable fill should be to produce a dense, less porous material. The PMWD gives the minimum water-solid ratio, and therefore, should correspond to the minimum porosity. Minimum water in the mix also results in saving of cement which will be discussed in Chapter 6.

It is also important to consider, while designing a mix, the ease of handling the flowable fill, the homogeneity of the mix, and the possibility of segregation. At high fly ash contents (above PMWD), the mix becomes highly viscous and sticky, and it takes a longer time to thoroughly mix the ingredients. This might cause delays in the field, and also may necessitate special equipment in the field to handle high fly ash content mixes.

The PMWD gives two parameters: fly ash content ( F/(F+S) ), and water-solid ratio (W/(C+F+S)). These parameters will be used in designing the flowable fill mixes which will be explained in Chapter 6.

## 4.4 Summary

Flowability is the most important attribute of flowable fill. This property of flowable fill makes it possible to place the material without any compaction, and is the main reason for many innovative applications for this material. In this chapter, flow behavior of both dry material and flowable fill slurry were studied. The flow characteristics of dry material was studied using a Tobin's flow cone test. The flow behavior of flowable fill was studied using a 7.6cm × 15cm (3 in. × 6 in.) open ended cylinder. This is a very simple test, and has an advantage over any flow cone tests because the flow cone test results are influenced by the maximum particle size. But in case of the open ended cylinder test the diameter of the cylinder is very large compared to any partice size in flowable fill, therefore, the results are independent of particle size effects.

The flow of sand through the flow cone showed that the waste foundry sands were relatively more angular compared to the natural sands. This was judged by the low % solid volume of these sands in the flow test. The sand grains in WFSs are coated with clay particles. This might have induced the apparent angularity to the WFSs. The flow of dry sand-fly ash mixtures proved that the fly ash particles act as lubricants and improve the flow of dry sand. However, higher amount of fly ash obstructs the flow of sand.

The most important contribution of the chapter is the formulation of "***flow curves***" which not only help explain the mechanics of flow, but also help in designing the flowable fill mixes. Two different phenomena control the flow behavior at low fly ash content and at high fly ash content. At low fly ash content, the fly ash acts as a lubricant, and the spherical shape of the fly ash particles is advantageously used. At high fly ash content, viscous forces dominate the flow, and the fly ash particles tend to flocculate thus losing the advantage due to the spherical shape of the fly ash particles. There is a transition where the water demand

is minimum. This point on the flow curve is named "***Point of Minimum Water Demand* (PMWD)**". The WFSs needed more water to produce the required flowability. The difference in specific gravity of natural sand and WFSs seems to be the main reason for this. The flowable fill mixes containing sands with higher specific gravity require less water, because this mix will have higher potential energy in the open ended cylinder and therefore can flow better when the cylinder is lifted.

Flow curves can be used in designing dense, less porous and more economical mixes. The proportion of sand and fly ash corresponding to PMWD is ideal for mix design. The minimum water-solid ratio at this point ensures dense and a less porous final product.

# CHAPTER 5. HARDENING CHARACTERISTICS

## 5.1 Introduction

After the flowable fill is placed, it starts hardening, and attains most of its strength in about a month. However, the short term strength up to about a day or so is important, because it determines if the flowable fill can support foot traffic and allow further loading such as placing pavement courses. The hardening characteristics are evaluated in the laboratory by a mortar penetrometer. A portable version of this penetrometer is available and can conveniently be used in the field. There has been no useful criterion to evaluate the hardening behavior of flowable fill. Generally, the flowable fill is considered to have hardened if it can be walked upon. In this chapter, study to establish the penetration resistance necessary for walkability is reported. A soil pocket penetrometer is also used to estimate the unconfined compressive strength, and thereby the bearing capacity of flowable fill during the hardening stage. Finally, it is important to recognize the fact that the field conditions will be different from the laboratory, particularly in terms of drainage conditions. The effect of drainage condition on hardening behavior was also investigated.

## 5.2 Materials

Five sands, R, N, A, G and V(N), and two class F fly ashes, SC and GI, were used in this study. The sand, R is a well graded river sand. The sands, N, A, and G are waste foundry sands (WFSs). The sand, V(N) is a clean virgin sand which comes out as WFS, N after use in the metal casting process. The index properties of sands were given in Chapter 3.

Waste foundry sands and virgin foundry sand, V(N) were uniformly graded materials. The WFSs contain small amounts of clay and organic matter. The specific gravity of WFSs is lower compared to that of river sand, R, and virgin sand, V(N).

## 5.3 Experimental Program

### 5.3.1 Mixes

The proportions for the mixes chosen for the penetration resistance study are shown in Table 5.1. The points on the flow curves corresponding to the proportions of these mixes are also shown in Figures 5.1 and 5.2. The position of a particular mix on the flow curve immediately shows the proportion of fly ash and sand in the mix. Two fly ashes, GI and SC, and four sands (river sand, R, and waste foundry sands, N, A, and G) are contained in these mixes. The number of each mix represents the fly ash and sand used in the mix. For example, SC-R1 is a mix containing fly ash, SC and sand, R. There may be several mixes containing fly ash, SC and sand, R with different proportions of sand and fly ash, and also different cement contents, which would then be designated as SC-R1, SC-R2, SC-R3, etc. There are some mixes with fly ash and cement, but without sand. These mixes are designated after the fly ash. For example, SC2 is a mix containing fly ash SC, without any sand. Following the same convention, N3 is a mix containing WFS N, without any fly ash.

### 5.3.2 Penetration Resistance

The flowable fill hardens with time. The hardening characteristics were measured by the penetration resistance test (ASTM C 403). In this test, a cylindrical tip is pressed 2.54cm (1 in.) into the flowable fill, and the resistance offered by the flowable fill is measured in pounds. This value, divided by the cross sectional area of the tip, is taken as the penetration resistance. Tips of different diameters are available, and the choice depends on the strength of the material. The penetration resistance readings were taken with time up to 24 hours. The test setup for penetration resistance is shown in Figure 5.3. The metal mold used to

Table 5.1 Mix Proportions, 28-day Strength and Bleeding Data

| Mix Number | Cement kg/m$^3$ | Fly ash kg/m$^3$ | Sand kg/m$^3$ | Water kg/m$^3$ | 28-day strength kPa(psi) | Bleeding % |
|---|---|---|---|---|---|---|
| SC-R1 | 30 | 392 | 1474 | 262 | 738(107) | 2.1 |
| N3 | 50 | 0 | 1396 | 408 | 338(49) | 1.1 |
| SC-N2 | 50 | 254 | 1242 | 376 | 834 (121) | 1.2 |
| G3 | 50 | 0 | 1339 | 444 | 676 (98) | 3.6 |
| SC-G4 | 50 | 254 | 1157 | 409 | 655 (95) | 4.1 |
| SC-A3 | 50 | 258 | 1032 | 415 | 683 (99) | 1.3 |
| SC-2 | 50 | 1284 | 0 | 440 | 965 (140) | 1.3 |
| GI-R5 | 30 | 378 | 1512 | 257 | 621 (90) | 1.9 |
| GI-R1 | 56 | 374 | 1494 | 258 | 2096(304) | 1.8 |
| GI-R2 | 75 | 370 | 1480 | 258 | 3585(520) | 1.6 |
| GI-N5 | 50 | 161 | 1300 | 381 | 469 (68) | 3.0 |
| GI-G5 | 50 | 143 | 1284 | 408 | 717 (104) | 4.8 |
| GI-A4 | 50 | 361 | 976 | 402 | 545 (79) | 2.1 |
| GI-A2 | 70 | 356 | 963 | 403 | 1048(152) | 1.9 |
| GI-2 | 50 | 1295 | 0 | 449 | 0 | 1.7 |

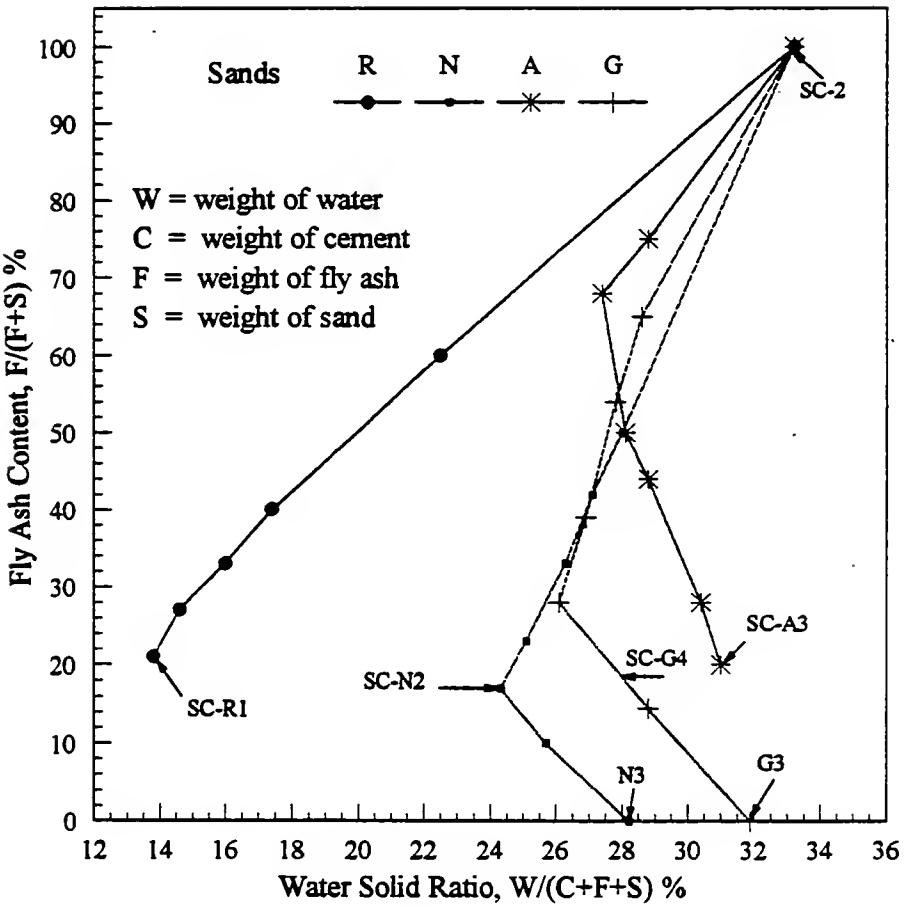


Figure 5.1 Flow Curves Showing Positions of Mixes with Fly Ash SC and Different Sands

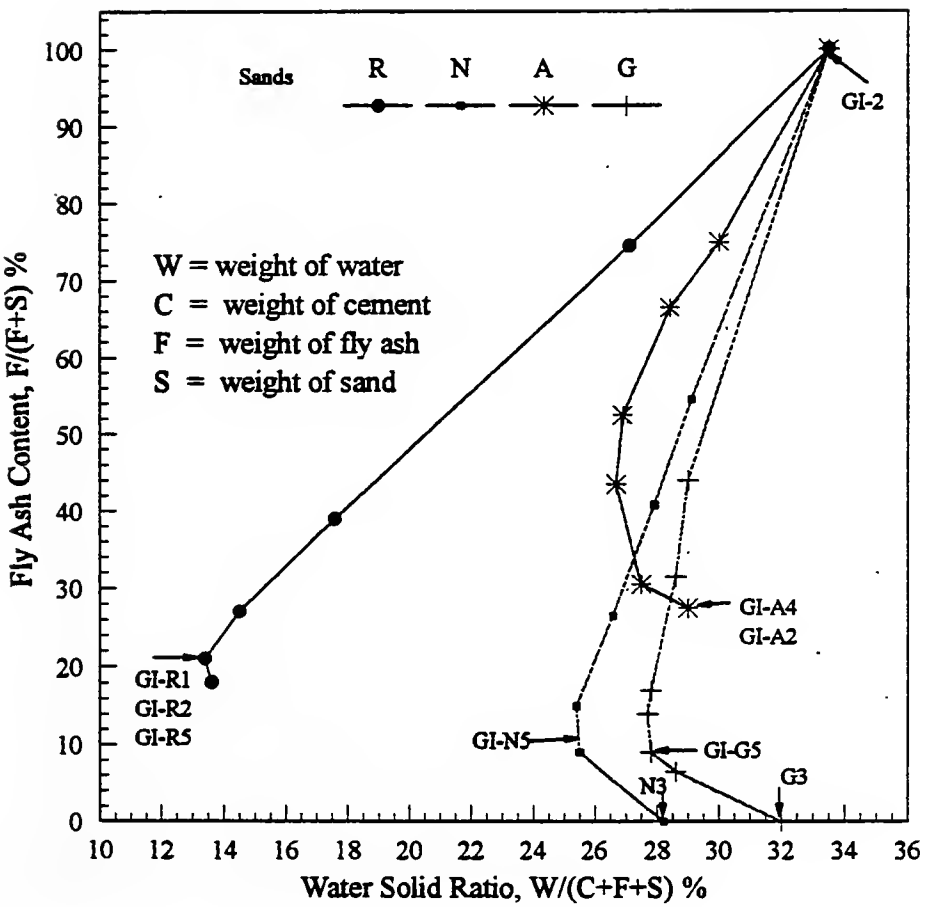


Figure 5.2 Flow Curves Showing Positions of Mixes with Fly Ash GI and Different Sands

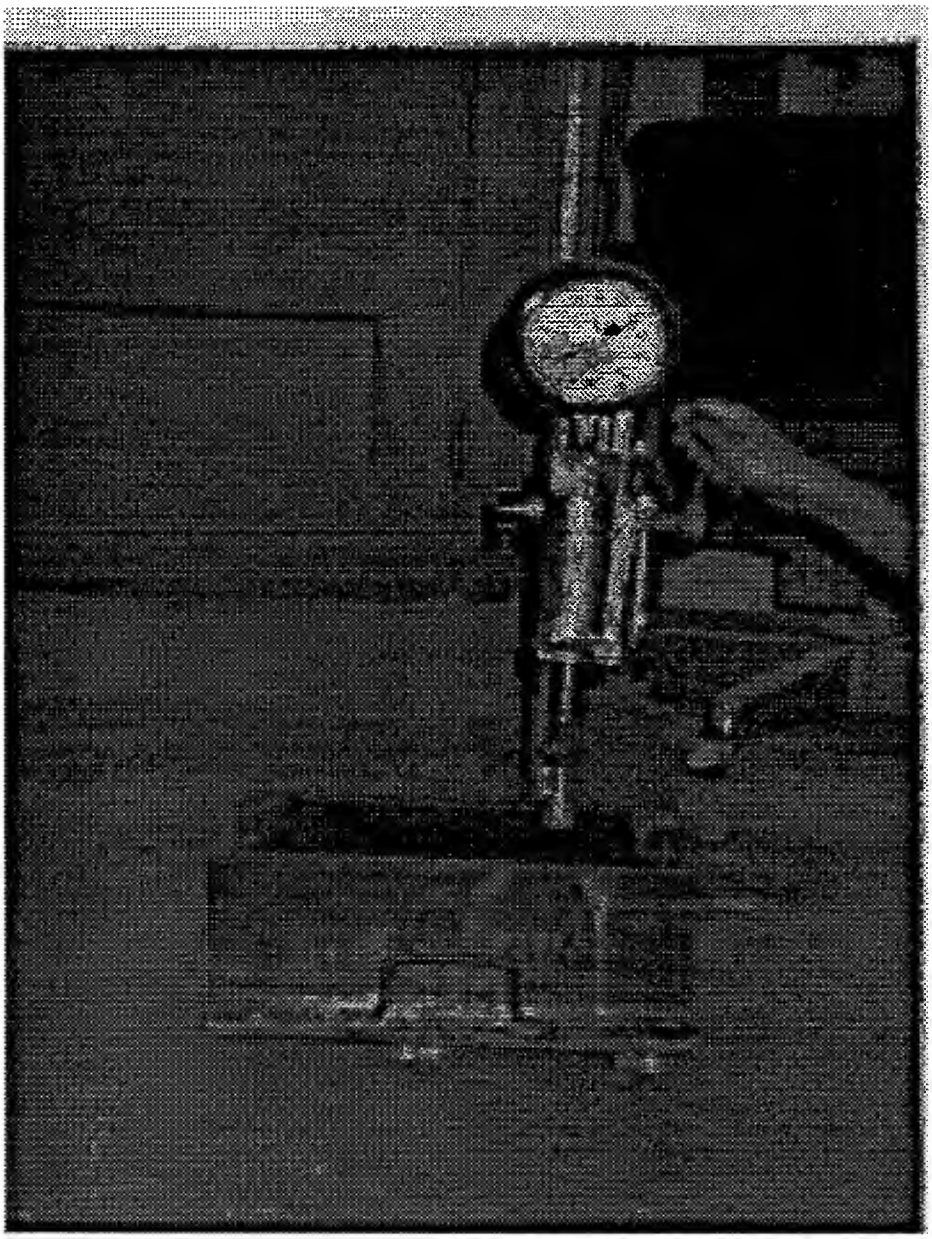

Figure 5.3 Penetration Resistance Test Setup

place flowable fill for this test measured 18cm wide, 30cm long, and 15cm deep. The mold was designed to be a three piece set, so that it can be easily dismantled and cleaned after the test. The joints in the mold were sealed with vacuum grease so that drainage is allowed only through the top surface of the material. Any free bleeding water was removed before each measurement of penetration resistance. A portable version of this penetrometer is shown in Figure 5.4.

### 5.3.3 Soil Pocket Penetrometer Test

The usefulness of the above penetration resistance test is limited because the penetration resistance is not correlated with any strength parameter of the material. To overcome this difficulty, a soil pocket penetrometer was used to estimate the unconfined compressive strength of the material (Figure 5.5). The penetration resistance test and pocket penetrometer were operated at the same time on the same flowable fill mix so that the penetration resistance could be correlated with the unconfined compressive strength of the material. The soil penetrometer has cylindrical tips of different diameters. The resistance of the material when the tip is pushed 1cm into the material is measured in kilograms. Based on Bucchi(1972), these data are used to calculate the unconfined compressive strength of the material.

### 5.3.4 Bleeding

The bleed water that comes to the surface in the penetration resistance test mold is measured with time until the bleeding stops. This test is done in conjunction with the penetration resistance test on the same sample. The bleed water that comes to the surface was removed by a syringe without disturbing the flowable fill in the mold.

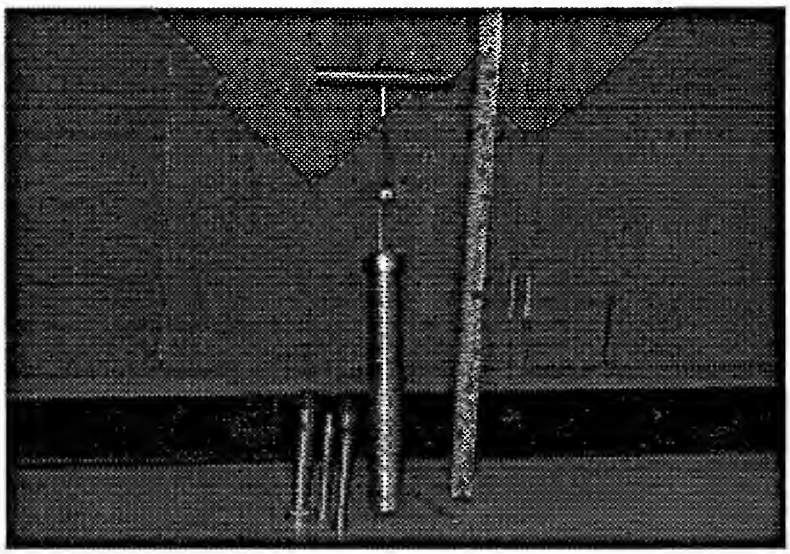

Figure 5.4 Portable Penetrometer

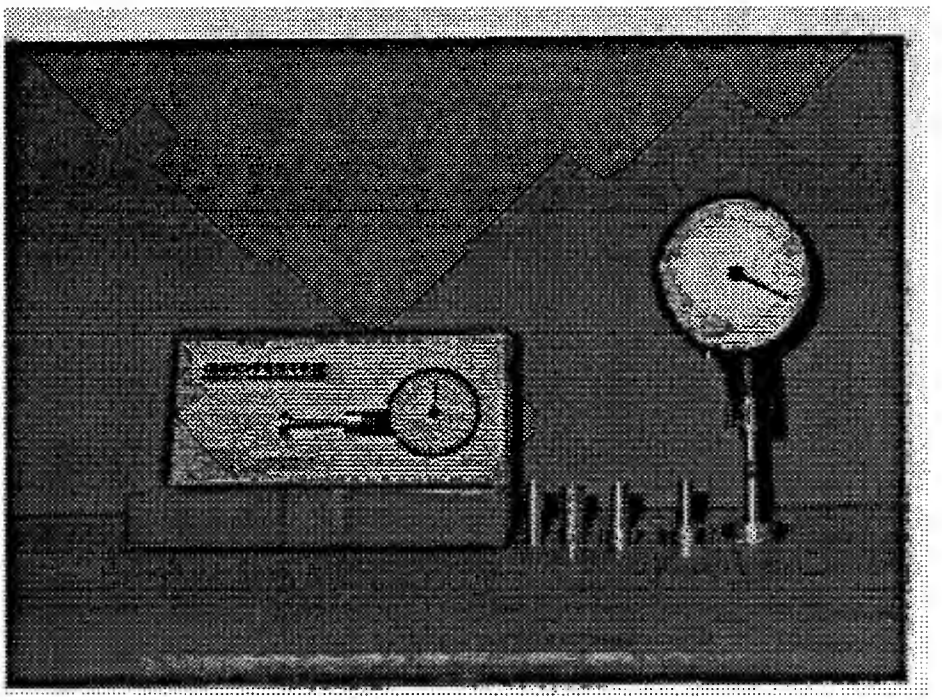

Figure 5.5 Soil Pocket Penetrometer

### 5.3.5 Geotextile Drainage Layer

To investigate the effect of drainage conditions on hardening characteristics of the flowable fill, geotextile drainage layers were introduced on all vertical sides and the bottom of the penetration resistance mold. That is, all the inside surface of the mold is completely covered with the drainage layer. The bottom layer extended beyond the walls of the mold to the outside so the water collected in the drainage layer could be easily released. The side walls of the mold were placed over this bottom layer, but were not fastened tightly so that the drainage layer right below the wall would work efficiently. With this arrangement, penetration resistance was measured in the usual manner.

### 5.3.6 Walkability Study

In order to find the penetration resistance corresponding to walkability, flowable fill was placed in several molds of the same size as the penetration resistance mold. A person wearing shoes was asked to stand on the material putting the whole body weight on one foot as the material hardened. When the material was able to sustain the load without making an indentation more than 2 to 3 mm, the penetration resistance was also measured. The average weight of a person used for this experiment was around 77 kg (170 lb), and the average contact area of shoe was approximately 161 $cm^2$ (25 $in.^2$). The experiment was repeated for all the mixes.

## 5.4 Results

### 5.4.1 Penetration resistance

Figures 5.6 through 5.8 show the penetration resistance test results for several mixes. The first point of observation on each curve is joined to the origin. This is an approximation because the fresh flowable fill will not have a measurable penetration resistance for some

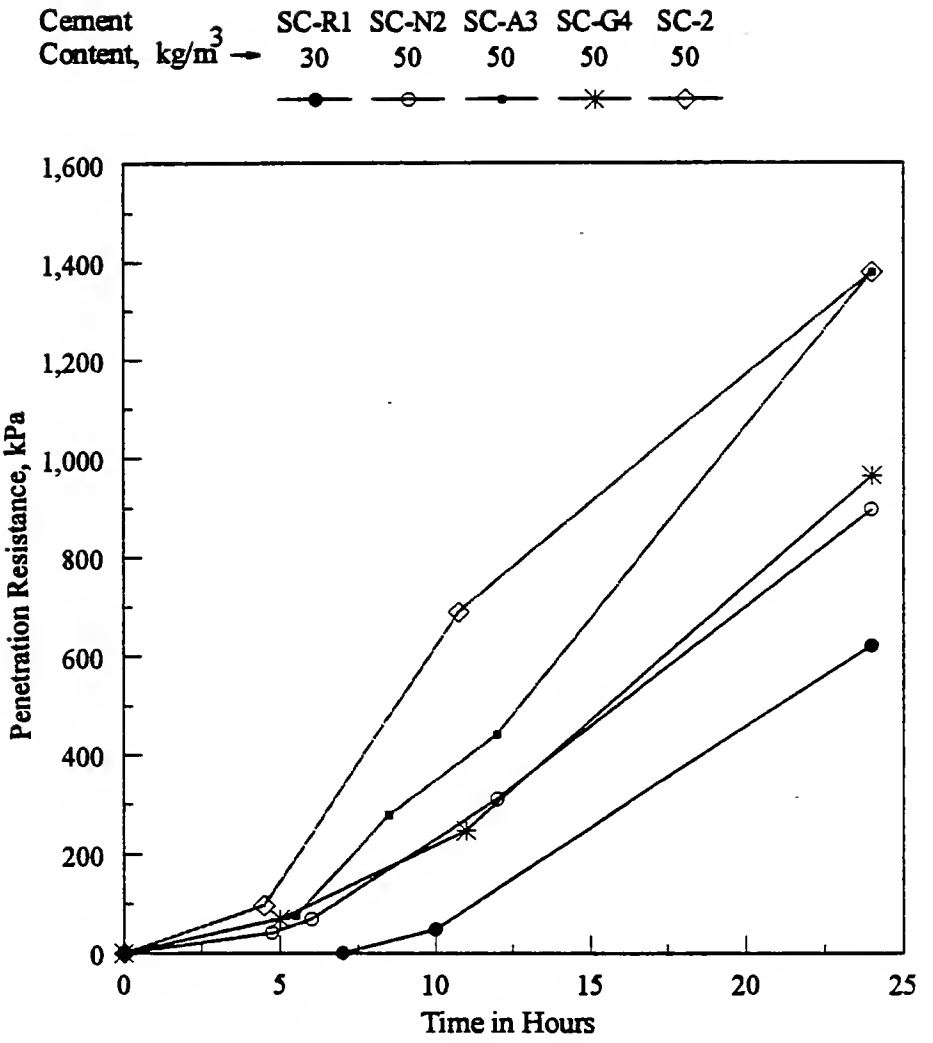


Figure 5.6 Penetration Resistance Test Results for Mixes Containing Fly Ash SC and Different Sands

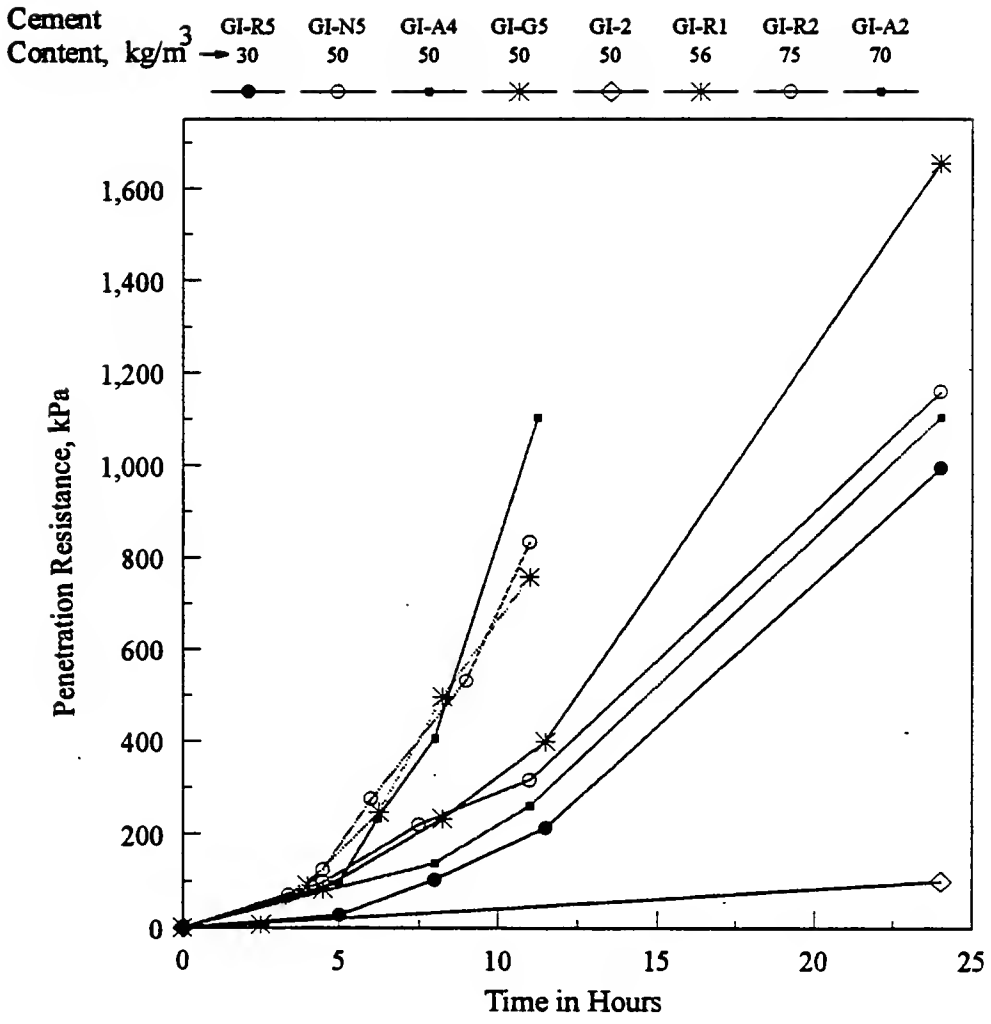


Figure 5.7 Penetration Resistance Test Results for Mixes Containing Fly Ash GI and Different Sands

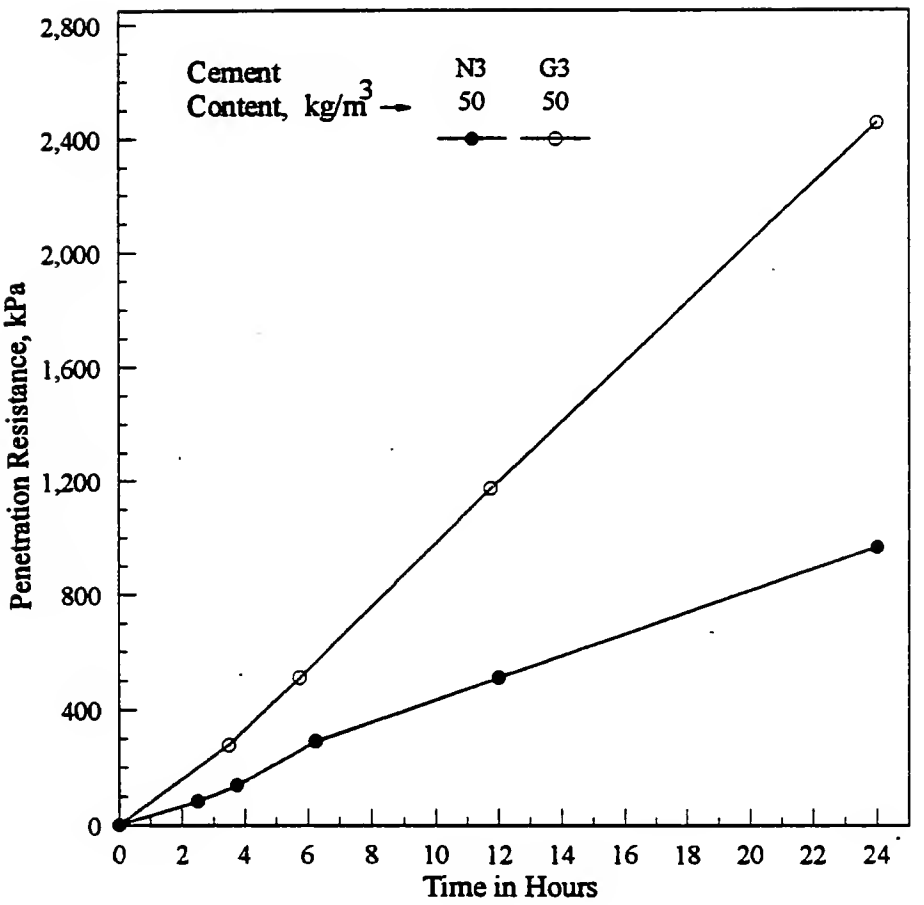


Figure 5.8 Penetration Resistance Test Results for the Mixes N3 and G3 Containing Only WFSs.

length of time, and therefore the curves should start not from the origin, but from a non-zero value on the time axis. Identifying such a point requires frequent readings to be taken. This was not possible because of the limited surface area of the mold. There is much scatter in the results from one mix to the other, and no generalization is possible.

The major factors affecting the early strength (penetration resistance) gain are the cement content in the mix, the environment conducive to cement hydration, the nature of fly ash, and the drainage condition around the flowable fill. The early penetration resistance does not correlate well with the ultimate strength of the mix. For example, the mix SC-R1 with a 28-day unconfined compressive strength of 738 kPa (Table 5.1) has a 24-hour penetration resistance of 210 kPa, whereas mix SC-G4 with a smaller 28-day strength of 655 kPa, has a higher 24-hour penetration resistance of 960 kPa.

In Figure 5.6, all mixes except SC-R1 have a cement content of 50 kg/m$^3$. However, there is considerable difference in hardening behavior between these mixes, containing different sands but the same fly ash and the same amount of cement. Some waste foundry sands seem to accelerate the cement hydration, thereby increasing the early strength.

Figure 5.8 shows penetration resistance test results for two mixes containing only WFS and no fly ash. Some WFSs could be made to flow without adding any fly ash because of presence of clay in them. The mixes N3 and G3 are shown in Figure 5.1. It can be seen from Figure 5.8 that the mix G3 containing WFS G hardens considerably faster than the mix N3 containing WFS N, though both the mixes had the same cement content of 50 kg/m$^3$.

The effect of increasing cement content on hardening behavior of mixes containing the same sand and fly ash can be seen from Figures 5.9 and 5.10. The higher amount of cement content causes the flowable fill to harden faster. However, increasing the cement content beyond a certain amount does not necessarily do so as can be seen for the mixes with cement contents of 56 kg/m$^3$ and 75 kg/m$^3$ in Figure 5.9.

To see the effect of the source of fly ash on hardening behavior, mixes with 100% fly ash were prepared (SC-2 in Figure 5.1 and GI-2 in Figure 5.2). Figure 5.11 shows the penetration resistance test results for these two mixes. The mix SC-2 developed a high penetration resistance. However, the mix GI-2 with the other fly ash, GI developed a very

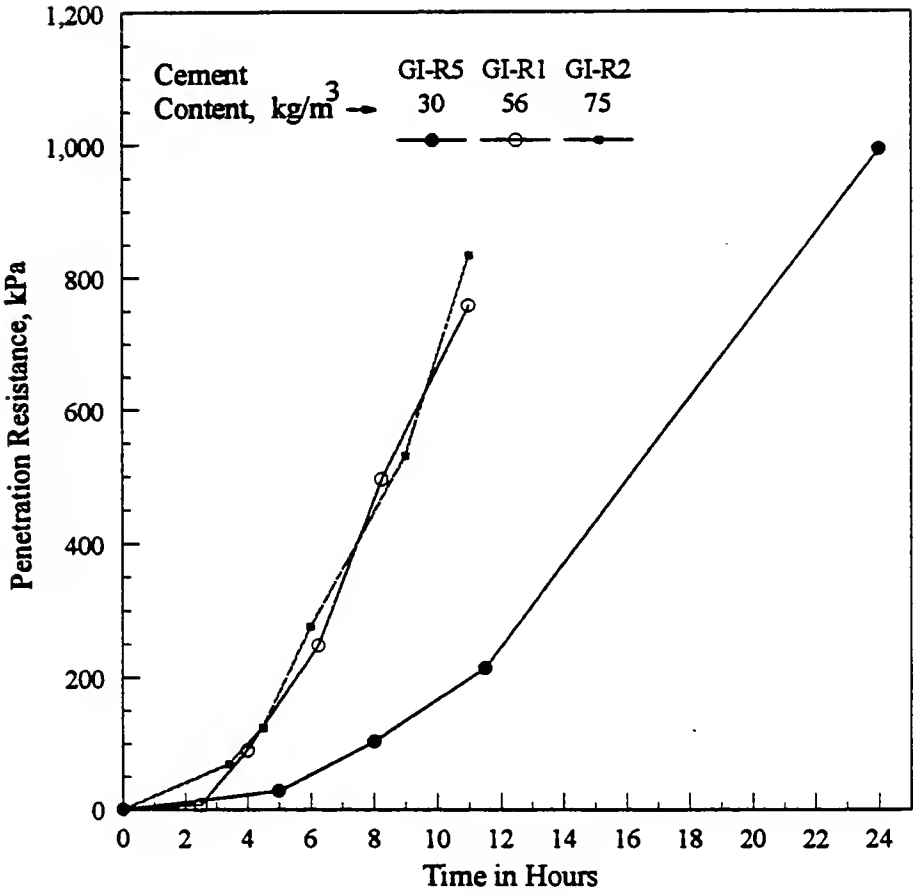


Figure 5.9 Effect of Cement Content on Penetration Resistance for Mixes Containing Fly Ash GI and Sand R

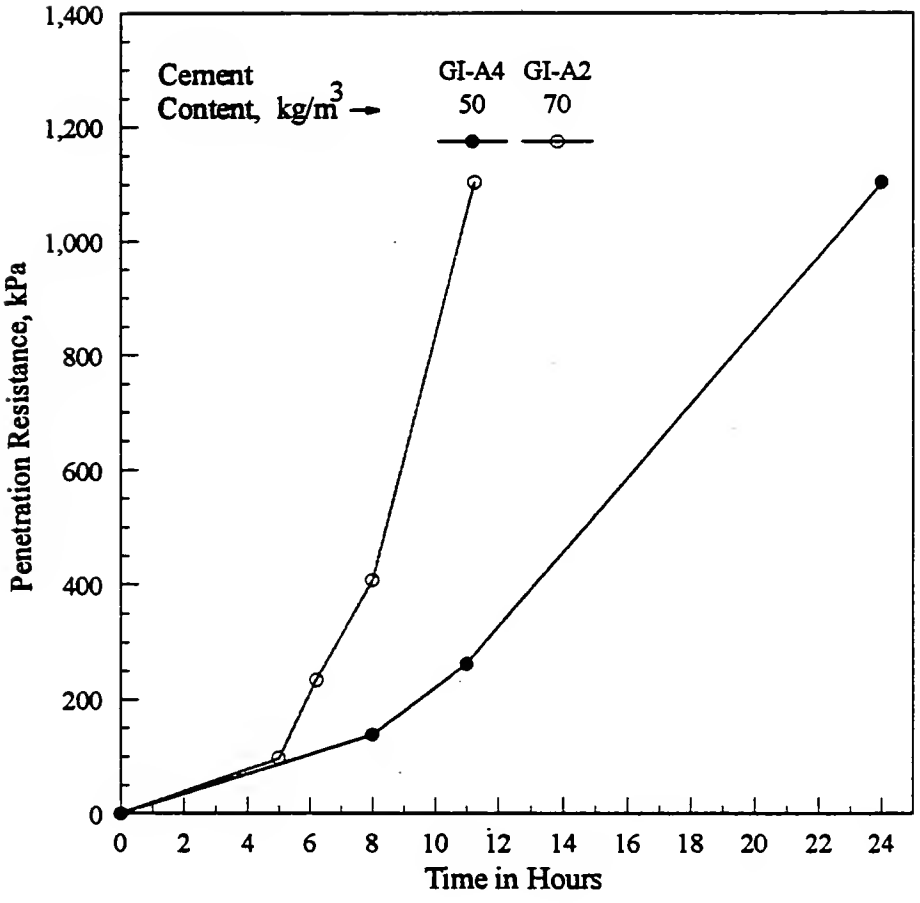


Figure 5.10 Effect of Cement Content on Penetration Resistance for Mixes Containing Fly Ash GI and WFS A

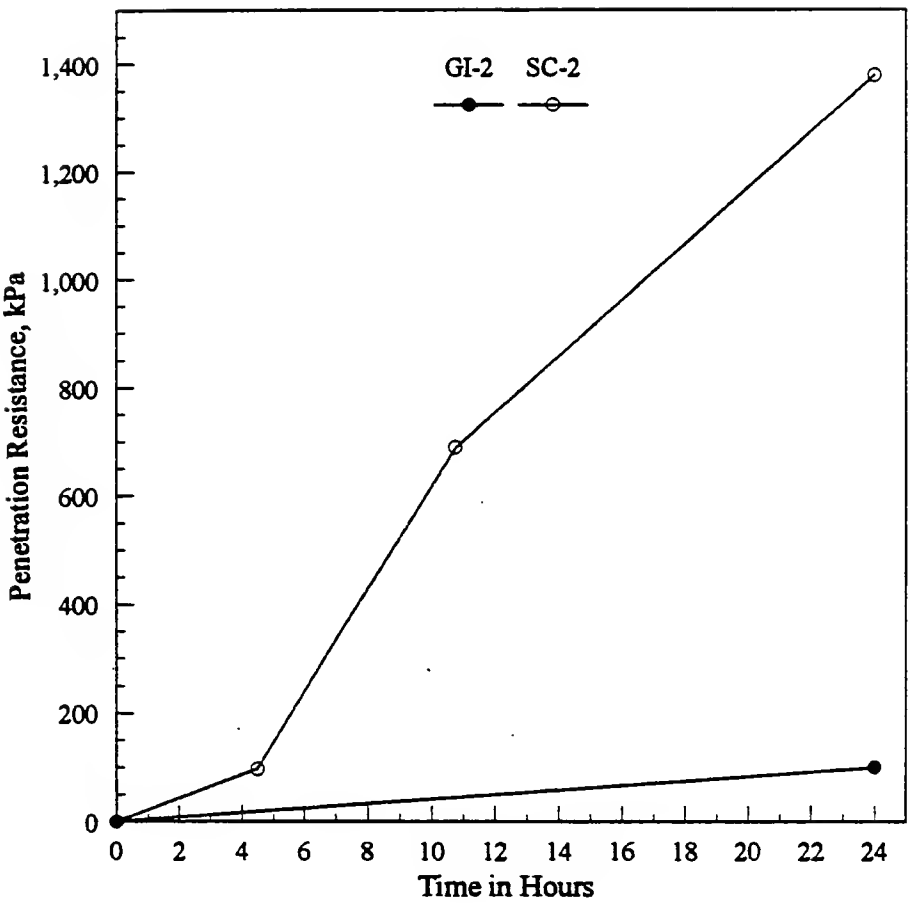


Figure 5.11 Penetration Resistance Test Results for Fly Ash Only Mixes with Fly Ashes SC and GI with a Cement Content of 50 kg/m$^3$

small penetration resistance. The mix also did not have a measurable 28-day compressive strength. It was observed that the mix exhibited considerable swelling in one to three days, and this must have resulted in the loss of both early and ultimate strength development. However, the mixes containing sand and smaller amount of this fly ash GI did not show any swelling potential. Therefore, the behavior of fly ash in a fly ash only mixes , i.e., without any sand, will be different from its behavior in mixes which contain both fly ash and sand.

### 5.4.2 Bleeding Considerations

Bleeding is another consideration in the design of flowable fill. The phenomenon of bleeding is common to all flowable fill mixes. The flowable fill when placed is in a condition where particles are almost in a floating state, and they do not have much particle-to-particle contact. Therefore, the shear strength of the material at this stage is zero. As the excess bleed water seeps out, particles tend to settle and establish some contacts with each other. This helps the material to gain some frictional strength. The bond strength due to cement hydration also starts developing simultaneously, this process being more active after the bleeding is over. It can be expected that higher amount of bleeding would result in more compact structure and less void ratio in the material, and thereby would give a higher frictional strength. However, excessive bleeding is not desirable because it is more often a sign of a bad mix, which might not give a good flow and also might result in segregation. It will also result in excessive initial subsidence of the surface after placement. Table 5.1 gives the percentage of total bleeding, and the time of bleeding defined as the time elapsed between mixing of flowable fill ingredients and bleeding measurements. The percentage of total bleeding is defined as the total cumulative volume of bleed water expressed as a percentage of total initial volume of flowable fill in the mold. The bleeding time varied from 1.5 hours to 5 hours. The shorter bleeding time results in higher early penetration resistance.

### 5.4.3 Effect of Drainage on Penetration Resitance

The effect of drainage on hardening behavior is shown in Figures 5.12 and 5.13. The introduction of a geotextile drainage layer resulted in shorter bleeding time, and early onset of strength gain as indicated by higher penetration resistance even before the mix without the geofabric drainage layer gained any strength. It was observed that bleeding was over in less than half hour for both the mixes SC-R1 and GI-N5 when drainage layer was provided, whereas it required 4 hours and 2.25 hours, respectively, for these mixes when the drainage layer was not present. The difference in penetration resistance kept increasing up to 24 hours. It is not very clear why the difference keeps increasing even after the bleeding is over in both cases (with and without drainage). It was also observed that the total amount of bleeding was higher for both the mixes when the drainage layer was present. This might have resulted in lower void ratio. The reduction in void ratio alone can contribute to the higher penetration resistance, assuming that there is no change in bond strength. The effect of small reduction in void ratio on bond strength if any is not known. It is also to be seen if the drainage condition has any effect on ultimate strength of the material.

It should be noted that the drainage condition in the field depends on the nature of the surrounding soil. Granular soils with higher permeability would speed up the process of bleeding in flowable fill, whereas clayey soil with lower permeability would prolong the time of bleeding.

### 5.4.4 Unconfined Compressive Strength Vs Penetration Resistance

The penetration resistance test, though very useful in comparing hardening characteristics of different mixes, is not helpful in evaluating a given mix in the laboratory, because there is no agreement as to what should be the penetration resistance of flowable fill mixes during the early period of hardening. The penetration resistance should be related to the bearing capacity of the material in order for it to be a useful parameter. The soil pocket penetrometer was used to estimate the unconfined compressive strength of the material during the hardening stage. The pocket penetrometer, whose design is based on the work of

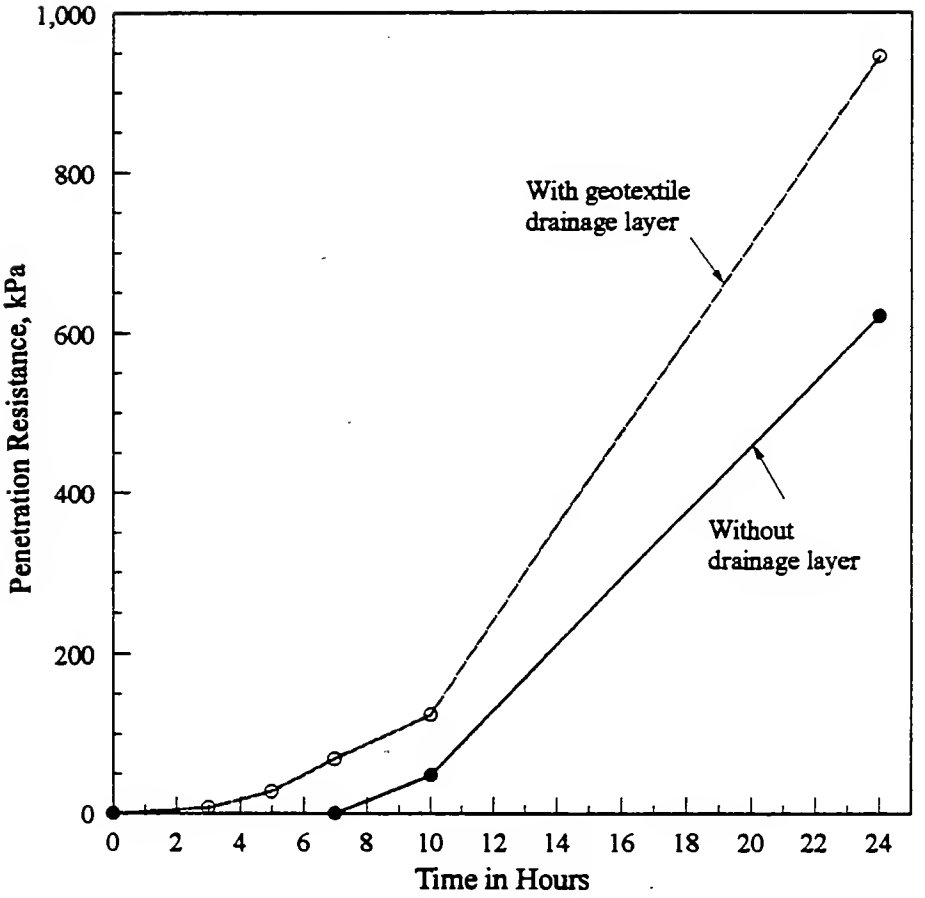


Figure 5.12 Effect of Drainage on Hardening Behavior of Mix SC-R1

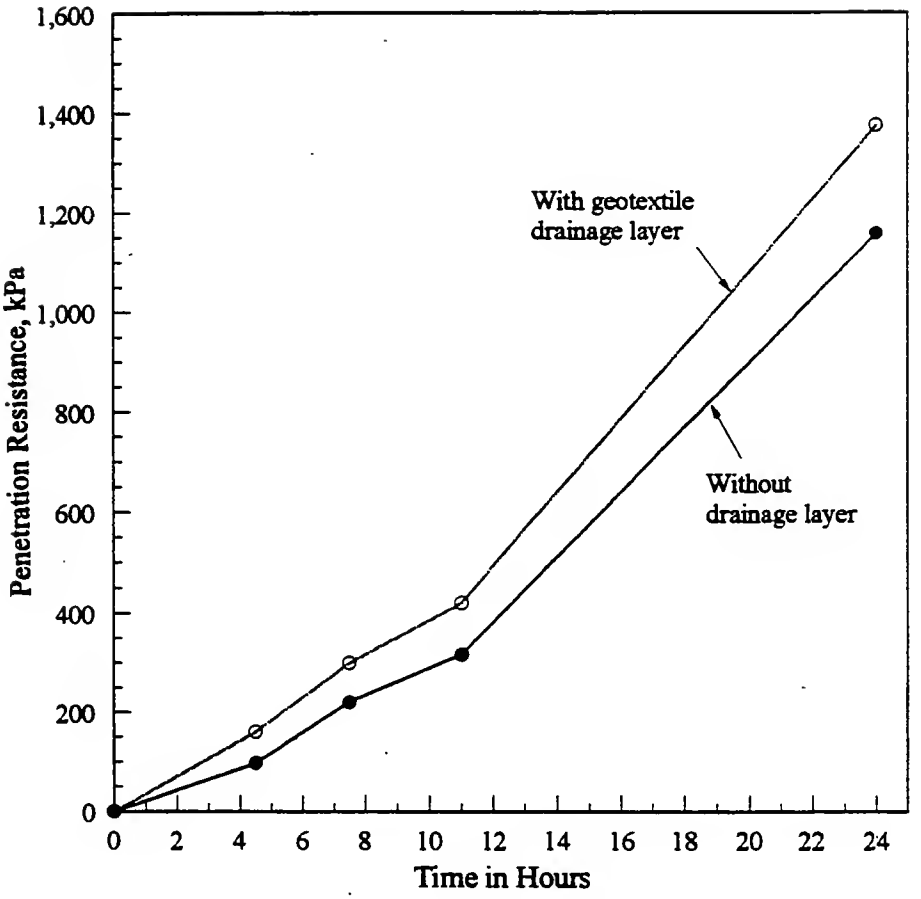


Figure 5.13 Effect of Drainage on Hardening Behavior of Mix GI-N5

Bucchi(1972), is meant to be used in soil to estimate the unconfined compressive strength, cohesion, c , and angle of internal friction, $\phi$. The strength of flowable fill during hardening can be thought of as having two components: frictional strength and the bond strength which is somewhat similar to cohesion, c in cohesive soils. Therefore, it is assumed that this instrument would give a reasonable estimate of unconfined compressive strength of flowable fill during the hardening stage.

Bucchi(1972) assumes that when the circular tip of the penetrometer is pushed into the soil to a quarter of an inch, the soil would undergo bearing capacity failure, and therefore that the Terzhaghi bearing capacity equations can be used. Thus, using Terzhaghi's equation for a circular footing,

$$q_f = 1.3 \times 5.7\, c_u = 7.41\, c_u = 3.71\, q_u \qquad (5.1)$$

where $q_f$= ultimate bearing capacity

$c_u$= undrained cohesion

$q_u$= unconfined compressive strength

$$q_f = \frac{Q}{\pi R^2}\ kg/cm^2 \qquad (5.2)$$

where Q = maximum load recorded by pocket penetrometer dial in kg during penetration test.

R = radius of the tip in cm

Equating Equations 1 and 2,

$$c_u = 0.043\ \frac{Q}{R^2}\ kg/cm^2 \qquad (5.3)$$

Therefore,

$$q_u = 2\, c_u = 0.086\ \frac{Q}{R^2}\ kg/cm^2 = 86\ \frac{Q}{R^2}\ kPa \qquad (5.4)$$

where $q_u$= unconfined compressive strength in kg/cm$^2$

Figure 5.14 shows the relation between penetration resistance and unconfined compressive strength determined from the soil pocket penetrometer. The unconfined compressive strength of flowable fill during the initial hardening period can be estimated for a given penetration resistance from Figure 5.14. Then the bearing capacity can be estimated from Equation 5.1.

The penetration resistance test is preferred to the use of the pocket penetrometer in the field because of its higher penetration of 2.54 cm (1 in.) against 0.6 cm (1/4 in.) penetration of the pocket penetrometer. The higher penetration helps to avoid any small surface drying effects.

### 5.4.5 Walkability

The walkability is a useful criterion to evaluate and compare hardening characteristics of different flowable fill mixes. Walkability here refers to that condition that allows person with shoes can walk on the flowable fill without causing settlements in excess of 2 mm. The time required for a particular mix to achieve this strength is defined here as "walkable time" for that mix. It was attempted to find the penetration resistance corresponding to walkability so that walkable time for any mix can be determined from penetration resistance curves such as in Figures 5.6 and 5.7. Based on the walkability tests on various mixes, it was found that the penetration resistance at that stage varied from 413 kPa to 448 kPa (60 to 65 psi) depending on the weight of a person. Based on these results, the walkable time is defined as time required to achieve a penetration resistance of 448 kPa (65psi). For example, for the mix SC-N2, the walkable time is around 14.4 hours (Figure 5.15). It should be remembered that in the field the walkable time may be shortened by as much as 50% depending on the drainage conditions in the surrounding soil.

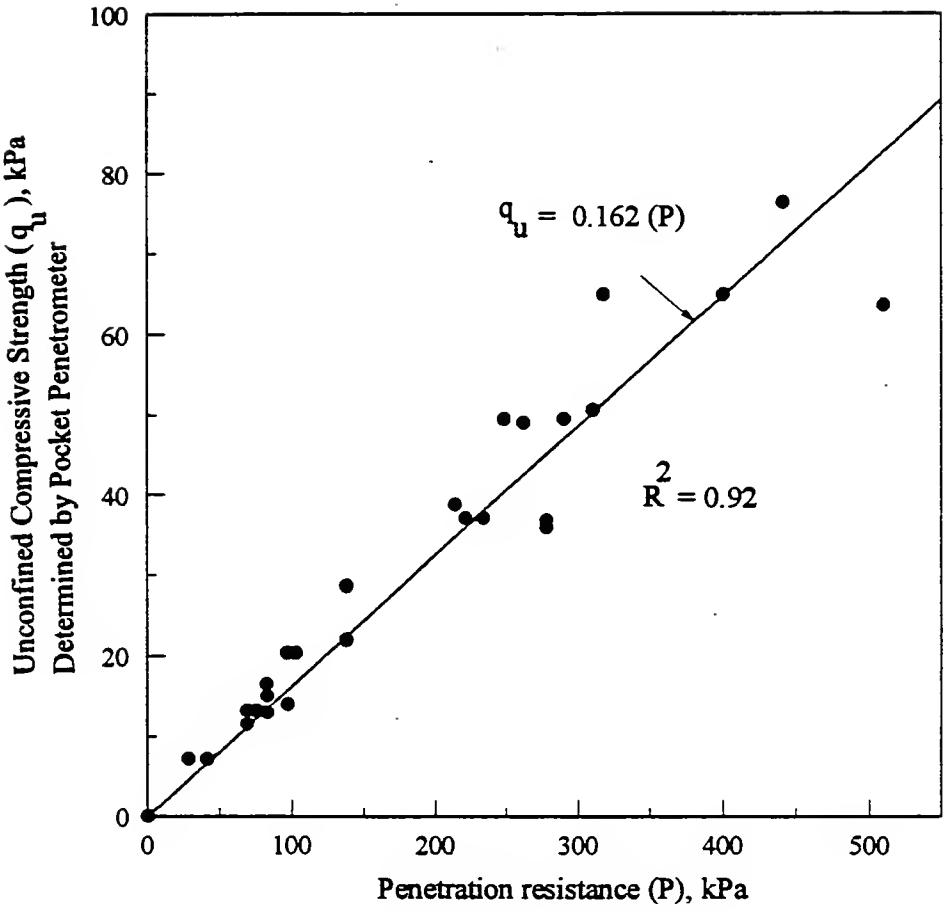


Figure 5.14 Penetration Resistance Vs Estimated Unconfined Compressive Strength

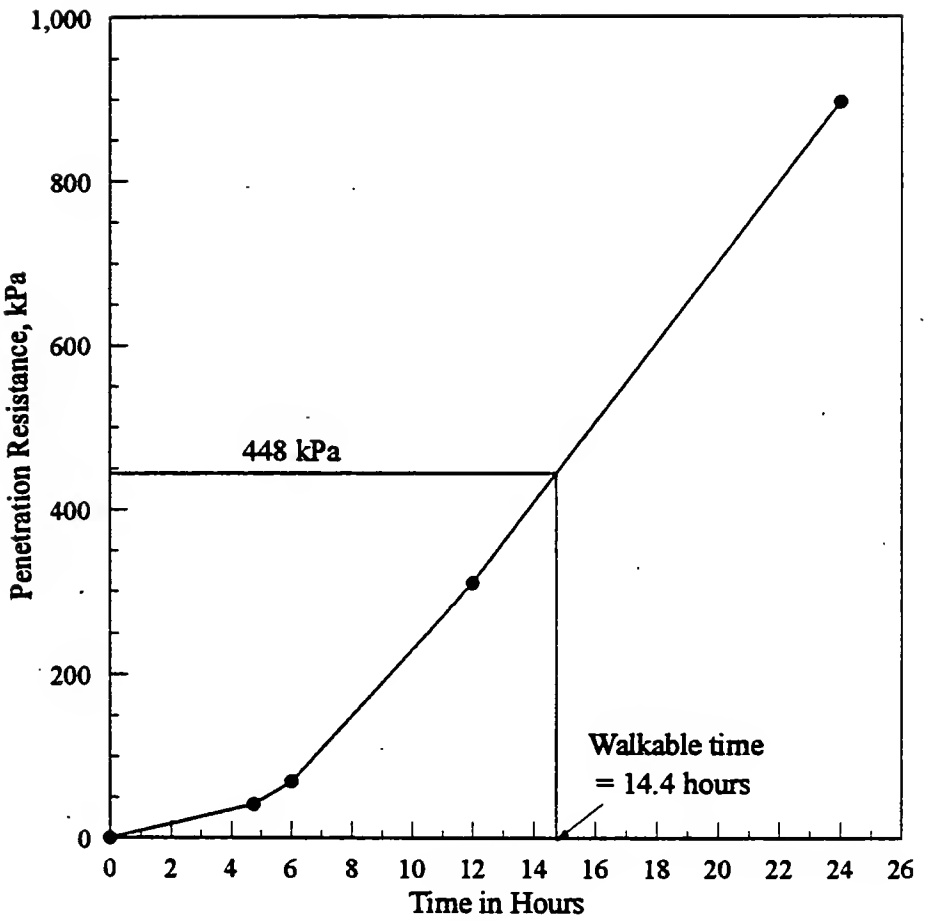


Figure 5.15 Example of Walkable Time Determination

## 5.5 Summary

The process of hardening of flowable fill involves two things. As the bleed water departs, the material develops some frictional strength, and also a bond strength which increases with the process of hydration of cement. The penetration resistance test helps compare the hardening behavior of different mixes. The major factors affecting penetration resistance are found to be the cement content, type of fly ash, drainage conditions, and the factors that may accelerate the hydration of cement. The introduction of a geotextile drainage layer increased the penetration resistance compared to the one without drainage layer. The increase seems to be due to an increase in frictional resistance of the material due to better drainage. The drainage condition in the field depends on the nature of the surrounding soil, which may control the early strength behavior.

The penetration resistance test is not a very useful test unless it is correlated with some strength parameter of flowable fill. The penetration resistance gave a good correlation with the unconfined compressive strength estimated by a soil pocket penetrometer. The unconfined compressive strength can also be used to calculate the bearing capacity of the hardening flowable fill. The flowable fill is considered to have hardened if it can support foot traffic. It was found that the penetration resistance necessary to ensure walkability on the material was around 448 kPa (65 psi). The time necessary to attain 448 kPa (65 psi) penetration resistance is defined as walkable time, which is a useful parameter in evaluating and comparing different mixes. The walkable time in the field may be reduced considerably depending on the drainage conditions in the surrounding soil.

# CHAPTER 6. STRENGTH AND MIX DESIGN METHODOLOGY

## 6.1 Introduction

The 28-day compressive strength for flowable fill or Controlled Low Strength Material (CLSM) is to be limited to, 1035 kPa (150 psi) to 8274 kPa(1200 psi) according to ACI Committee 229 (1995). This upper limit of 1200 psi is specified to include some high strength applications, and also to draw a distinction between this material and concrete. However, for most applications, an unconfined compressive strength of around 1035 kPa(150 psi) is recommended. This low strength allows possible future excavation. The low strength also ensures that flowable fill behaves more like a soil. Thus, higher strength is undesirable in flowable fill unlike in concrete. This is an important aspect to be considered in the design of flowable fill. It should be recognized that the 28-day compressive strength of 1035 kPa (150 psi) is specified on the presumption that most of its strength is attained in 28 days. However, the development of strength continues for a long time, and in some cases, the magnitude of increase in strength above that of 28-day strength may be quite large. There has been no standard mix design procedure for flowable fill. Generally, a standard mix is adopted. That is, the proportions of flowable fill ingredients are kept constant. This procedure does not necessarily produce a good material, because the properties of flowable fill ingredients might vary a great deal depending on the source of the material. This is particularly true in case of waste foundry sands and fly ashes. This study provides a general framework and step by step procedure for the mix design of flowable fill. The suggested procedure aims at producing a flowable fill which is dense and less porous, and uses as little cement as possible for a given combination of sand and fly ash.

## 6.2 Experimental Program

### 6.2.1 Unconfined Compressive Strength

The unconfined compressive strength was conducted on 7.6cm × 15.2cm (3 in. × 6 in.) samples at 28 days. Some mixes were also tested at 3 days, and some were tested at 90 days to study the long term strength development of flowable fill. A total of 29 mixes with different combinations and proportions of fly ashes and sands, and with different cement contents were studied. All the mixes were tested at 28 days. Seventeen of these mixes were tested at 90 days.

A computerized compressive testing machine with stress-control arrangement was used. A loading rate of 0.24 MPa/sec (35 psi/sec) was used. The samples were tested without capping. Three to four companion samples were tested each time and the average was taken as the compressive strength.

### 6.2.2 Mixes

The mix proportions for 29 mixes are shown in Table 6.1. The points on the flow curves corresponding to the proportions of these mixes are also shown in Figures 6.1 and 6.2. The position of a particular mix on the flow curve immediately indicates the proportion of fly ash and sand in the mix. Two fly ashes, GI and SC, and five sands R, N, A, G, and V(N) are covered in these mixes. The sand, R is a well graded river sand. N, A, and G are waste foundry sands (WFSs), and V(N) is a clean virgin sand which comes out as WFS, N. The number of each mix represents the fly ash and sand used in the mix. For example, SC-R1 is a mix containing fly ash SC and sand R with different proportions of sand and fly ash, and also different cement contents, which would then be designated as SC-R1, SC-R2, SC-R3, etc. Mixes SC2 and GI2 are the mixes containing fly ashes, SC and GI respectively, and

Table 6.1 Mix Proportions and Unconfined Compressive Strength

| Mix No. | Cement kg/m³ | Fly ash kg/m³ | Sand kg/m³ | Water kg/m³ | 3-day Strength kPa | 28-day Strength kPa(psi) | 90-day Strength kPa | W/C |
|---|---|---|---|---|---|---|---|---|
| SC-R1 | 30 | 392 | 1474 | 262 | 131 | 738(107) | 848 | 8.73 |
| SC-N1 | 35 | 257 | 1255 | 376 | 165 | 414(60) | 476 | 10.7 |
| SC-N2 | 50 | 254 | 1242 | 376 | 214 | 834 (121) | 1082 | 7.52 |
| SC-N8 | 30 | 257 | 1256 | 375 | 131 | 365(53) | - | 12.5 |
| SC-N4 | 50 | 122 | 1313 | 386 | 165 | 483(70) | - | 7.72 |
| SC-G1 | 35 | 409 | 1052 | 392 | - | 365(53) | 455 | 11.2 |
| SC-G2 | 50 | 405 | 1041 | 392 | - | 490(71) | 524 | 7.84 |
| SC-G4 | 50 | 254 | 1157 | 409 | 228 | 655 (95) | - | 8.18 |
| SC-A3 | 50 | 258 | 1032 | 415 | 207 | 683 (99) | - | 8.3 |
| SC-2 | 50 | 1284 | 0 | 440 | - | 965 (140) | - | 8.8 |
| GI-R1 | 56 | 374 | 1494 | 258 | - | 2096(304 | 2620 | 4.61 |
| GI-R2 | 75 | 370 | 1480 | 258 | - | 3585(520 | 4143 | 3.44 |
| GI-R5 | 30 | 378 | 1512 | 257 | 276 | 621 (90) | - | 8.57 |
| GI-R7 | 35 | 377 | 1508 | 257 | 303 | 827(120) | - | 7.34 |
| GI-R8 | 40 | 376 | 1505 | 257 | 386 | 1055(153 | | 6.43 |

Table 6.1 (continued)

| | | | | | | | | |
|---|---|---|---|---|---|---|---|---|
| GI-R9 | 45 | 375 | 1501 | 258 | 359 | 1138(165 | - | 5.73 |
| GI-V(N)1 | 56 | 443 | 1344 | 299 | - | 1317(191 | 1710 | 5.34 |
| GI-V(N)2 | 73 | 439 | 1318 | 296 | - | 1793(260 | 2296 | 4.05 |
| GI-N5 | 50 | 161 | 1300 | 381 | 221 | 469 (68) | - | 7.62 |
| GI-N7 | 60 | 160 | 1295 | 382 | 255 | 517(75) | - | 6.37 |
| GI-N4 | 50 | 86 | 1346 | 392 | - | 510(74) | - | 7.84 |
| GI-G5 | 50 | 143 | 1284 | 408 | 283 | 717 (104) | - | 8.2 |
| GI-G4 | 50 | 55 | 1322 | 428 | | 703(102) | - | 8.56 |
| GI-A4 | 50 | 361 | 976 | 402 | 303 | 545 (79) | - | 8.04 |
| GI-A6 | 60 | 358 | 969 | 402 | 352 | 910(132) | - | 6.7 |
| GI-A2 | 70 | 356 | 963 | 403 | - | 1048(152 | - | 5.76 |
| GI-2 | 50 | 1295 | 0 | 449 | - | 0 | - | 8.98 |
| N3 | 50 | 0 | 1396 | 408 | 138 | 338(49) | - | 8.2 |
| G3 | 50 | 0 | 1339 | 444 | - | 676 (98) | - | 8.9 |

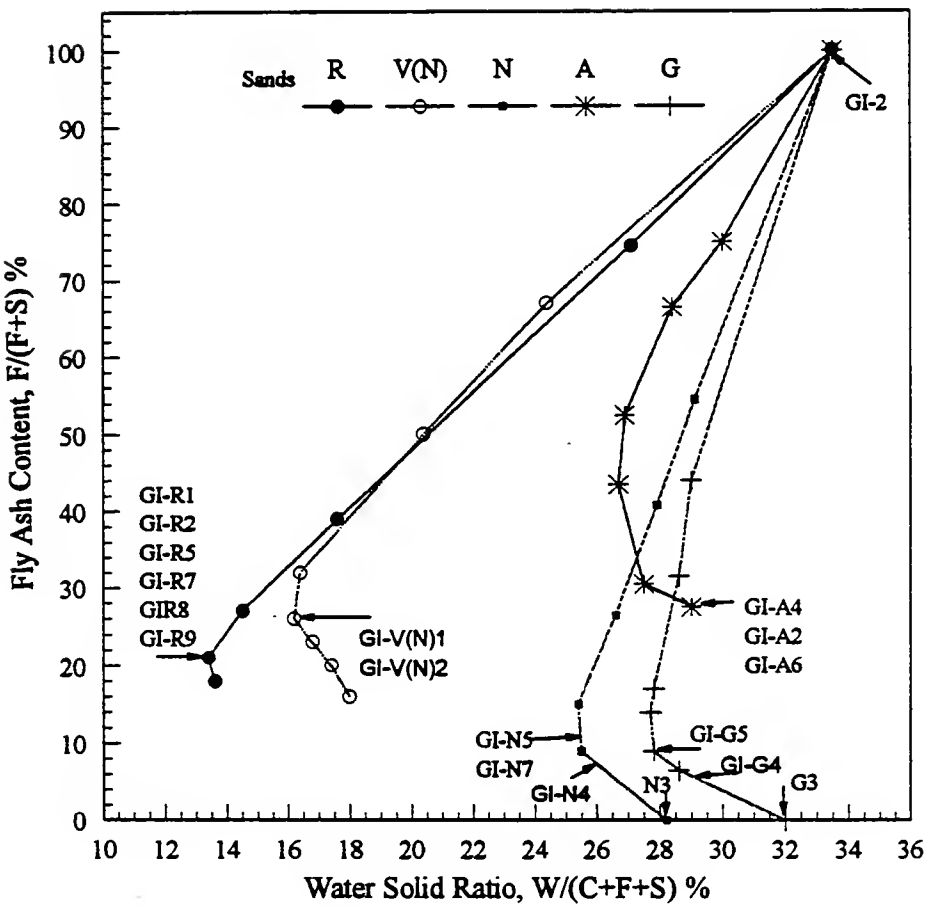


Figure 6.1 Flow Curves with Fly Ash GI and Different Sands Showing Positions of Different Mixes Used for Strength Testing

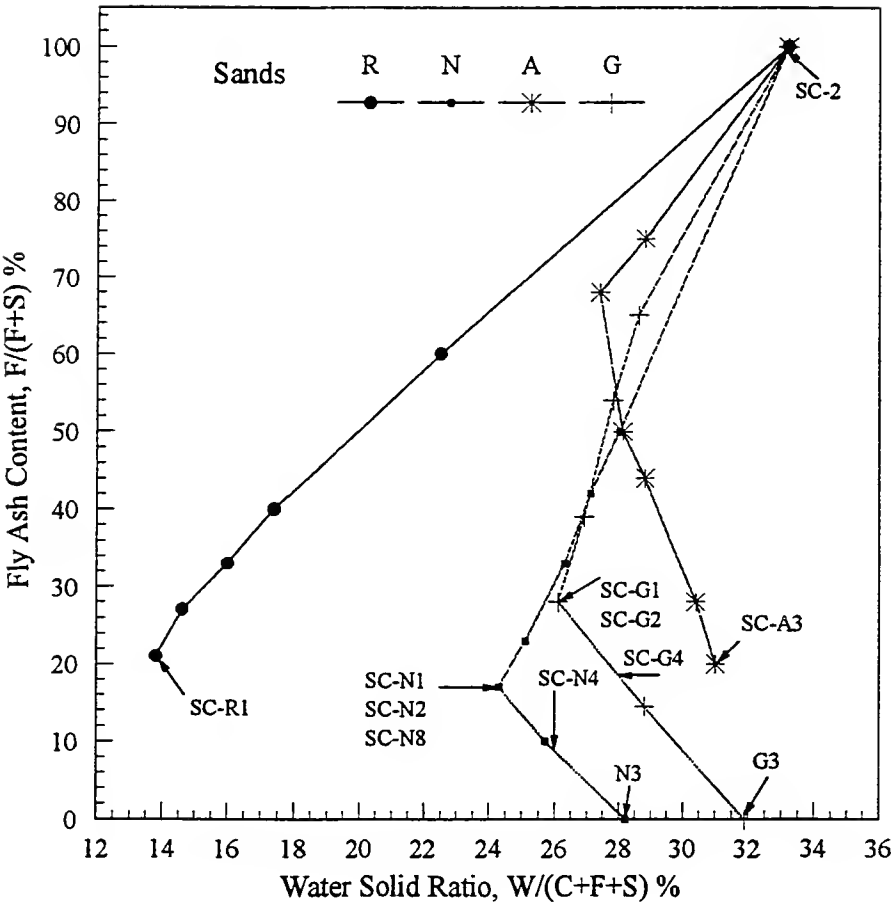


Figure 6.2 Flow Curves with Fly Ash SC and Different Sands Showing Positions of Different Mixes Used for Strength Testing

and contain no sands. The mixes N3 and G3 contain WFSs, N and G respectively, and contain no fly ash. All the mixes essentially contain some amount of portland cement.

### 6.2.3 Sample Preparation

Mixing was done either in a 5 cubic foot stow mortar and plaster mixer, or was hand mixed when the samples were to be tested only for 28-day strength. The fly ash, sand, and cement are first mixed thoroughly, and then the water is added and the mixing continued for about 5 minutes to get a homogeneous mix. The inside surface of the PVC mold is lightly coated with mineral oil before pouring the flowable fill in it, so the material would not stick to the mold. The mix is then poured into the 7.6cm × 15.2 cm cylindrical PVC molds with a spoon. The PVC mold was then lightly tapped with a metallic rod, and the surface was levelled by striking off the excess material by a straight edge. The molds were then transferred to the humidity chamber. The molds were removed from the humidity chamber after three days, and demolded. A small hole (2 to 3 mm dia) was drilled at the center of the bottom of the PVC mold before placing flowable fill in it. This enabled the use of air pressure to force the samples out of the mold. If the samples could not be removed easily with air pressure, the mold was submerged in warm water for a few minutes and the air pressure was applied again.

## 6.3 28-day Strength

The mix proportions of 29 mixes and their 28-day compressive strengths are shown in Table 6.1. Referring to Figure 6.1 and 6.2, most of the mixes correspond to the Point of Minimum Water Demand (PMWD). It was noted in Chapter 4, that the proportions corresponding to PMWD would give the ideal mix in terms of flow and homogeneity of the material. And, the mixes above PMWD on flow curves (i.e. mixes with high fly ash content) would increase the mixing time and would be sticky. The mixes below PMWD (i.e. smaller amount of fly ash) might result in heavy segregation. However, some mixes with low fly ash

content were also tested for strength. The mixes with WFS A does not give a very distinct point of Minimum Water Demand (PMWD), and PMWD is obtained at a very high fly ash content. Therefore, proportions corresponding to the lower end of the flow curve are chosen for the mixes.

The mixes with the river sand needed less cement to develop the same strength compared to the mixes with WFSs. For example, the mixes SC-R1, GI-R5, GI-R7 and GI-R8 with cement contents ranging from 30 to 40 kg/m$^3$ developed a 28-day strength of 621 kPa(90 psi) to 1055 kPa (153 psi). On the other hand, the mixes with WFSs needed more than 50 kg/m$^3$ of cement to develop comparable strength. It will be seen in section 6.3.3, that the smaller water demand in mixes containing clean river sand, R is mainly responsible for its higher strength. The strength of mixes containing WFSs depends also on the source of WFS.

### 6.3.1 Effect of Source of Fly Ash on Strength

The fly ash only mixes SC-2 and GI-2 (see Figures 6.1 and 6.2) were chosen only to see the influence of the source of fly ash on strength. Both the mixes had a cement content of 50 kg/m$^3$. The mix SC-2 developed a 28-day strength of 965 kPa(140 psi); on the contrary, the mix GI-2 failed to develop any strength. It was observed that the mix GI-2 exhibited considerable swelling in two to three days after mixing. This might have resulted in complete loss of strength. However, in the mixes containing sands, the fly ash GI did not show any swelling potential, and developed normal strength. Therefore, it can be concluded that the behavior of fly ash in a fly ash only mix would be totally different from its behavior in mixes containing sands.

### 6.3.2 Components of Strength

Flowable fill can be considered to have two components of strength: particulate and non-particulate. Non-particulate or cementation component of strength is due to the cementation bonds between particles created by the hydration products of cement. The

cementation component of strength certainly increases with the increase in cement content. It also depends on the particle matrix of flowable fill: a dense packing of sand and fly ash particles can be expected to enhance the effect of cementation, because a denser packing brings the sand as well as fly ash particles closer, and therefore, these particles can more effectively be bonded to each other with the same amount of hydration products as in a loose matrix of sand and fly ash particles.

Particulate component of strength is analogous to that of granular soil. This has again two components: pure friction and dilatancy. The pure friction depends on the nature of the materials, both sand and fly ash. Dilatancy mainly depends on the density of the material and the confining pressure. The dilatancy is the phenomenon of tendency to increase in volume under the application of shear stress. Higher the density, higher will be the dilatancy. An extra work has to be done by the external loads against these dilating particles, thus the dilatancy gives rise to additional strength. The aspect of dilatancy will further be addressed in Chapter 8. It is difficult to isolate frictonal and dilational components of strength. Hence, it is conventional to lump both these components together as frictional strength, which is in reality the apparent friction. Therefore, it can be stated that frictional strength increases with increasing density. It should be noted that during unconfined compressive strength testing, there will be both normal and shear stresses on different inclined planes in the sample. This will contribute to the frictional strength of the material.

### 6.3.3 W/C Ratio Vs Unconfined Compressive Strength

There are several factors which affect the strength: cement content, the nature of sand and fly ash, amount of fly ash in the mix, the porosity or void ratio, the frictional characteristics of the materials, etc. However, it is important for engineers to identify the most influencing parameters so that the prediction would be possible with as few parameters as possible. It was found that water-cement ratio alone is the single most important parameter that affects the strength of flowable fill. The relation between W/C ratio and 28-day compressive strength is shown in Figure 6.3. The relation could be approximated by a

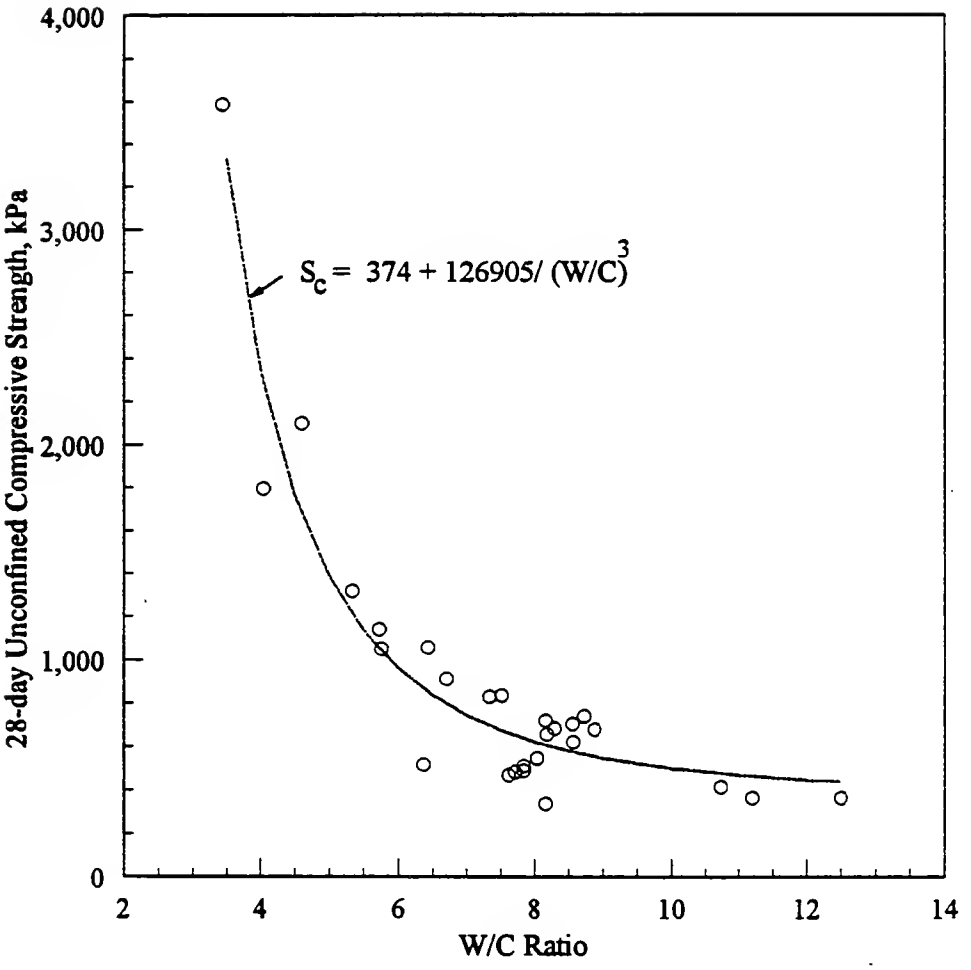


Figure 6.3 W/C Ratio Vs Unconfined Compressive Strength

cubic equation:

$$S_c = 374 + \frac{126905}{(W/C)^3} \qquad (6.1)$$

where $S_c$ = unconfined compressive strength at 28 days in kPa

W/C = water-cement ratio

Considering the variation in the properties of sands and fly ashes used in this study, the correlation can be considered to be good ($R^2 = 0.92$). The amount of water added to the mix directly influences the void ratio of the material. Higher the water content, higher will be the void ratio, and consequently lower will be the frictional component of strength (pure friction plus dilatancy), and vice versa. Also, higher void ratio reduces the effectiveness of the cementation bonds as noted in section 6.3.2. Strength can also be expected to be directly proportional to the cement content. Thus, W/C ratio is an appropriate and logical parameter to predict strength.

Examination of the curve in Figure 6.3 reveals a very interesting fact. At very high W/C ratio, the curve almost becomes asymtotic to the x-axis. At this W/C ratio, the cementation perhaps is ineffective, and all the strength can be attributed to the frictional component of strength. At low W/C ratio, the curve becomes increasingly steeper. This means that small changes in W/C ratio cause large changes in strength. This implies that the material is tending to behave more like a concrete. In the intermediate W/C ratio, both frictional and cementation components of strength control behavior of flowable fill.

It is clear from the foregoing discussion that the W/C ratio concept in flowable fill should not be confused with that of concrete. In flowable fill, the water content and cement content independently affect the strength as explained earlier, and therefore the W/C ratio works well in predicting strength. Thus W/C ratio, though conceptually different in concrete and flowable fill, are operationally equivalent.

## 6.4 90-day Strength

The 90-day compressive strength testing results are shown in Table 6.1 and Figure 6.4. The factors affecting long term strength are not exactly known. The hydration of cement might continue for a long time beyond 28 days. A part of the fly ash might be participating in the pozzolanic reaction depending on the nature of the fly ash, and availability of calcium hydroxide. The 90-day strength was in some cases as high as 30% more than the 28-day strength. On an average, 15-25% increase in 90-day strength with respect to 28-day strength may be expected.

## 6.5 Mix Design Methodology

In designing flowable fill, the target 28-day compressive strength can be 550 kPa (80 psi) to 1035 kPa (150 psi). According to Equation 6.1, the W/C ratio corresponding to these strengths are 8.9 and 5.7 respectively. Therefore, an upper bound and lower bound of 9.0 and 5.5 for W/C ratio will be chosen here. The equations necessary for mix design will be presented now.

From Figure 6.5,

$$k_1 = \frac{F}{(F + S)} \tag{6.2}$$

$$k_2 = \frac{W}{(C + F + S)} \tag{6.3}$$

Let W/C ratio be denoted by $k_3$.

$$k_3 = \frac{W}{C} \tag{6.4}$$

where F = fly ash content in $kg/m^3$

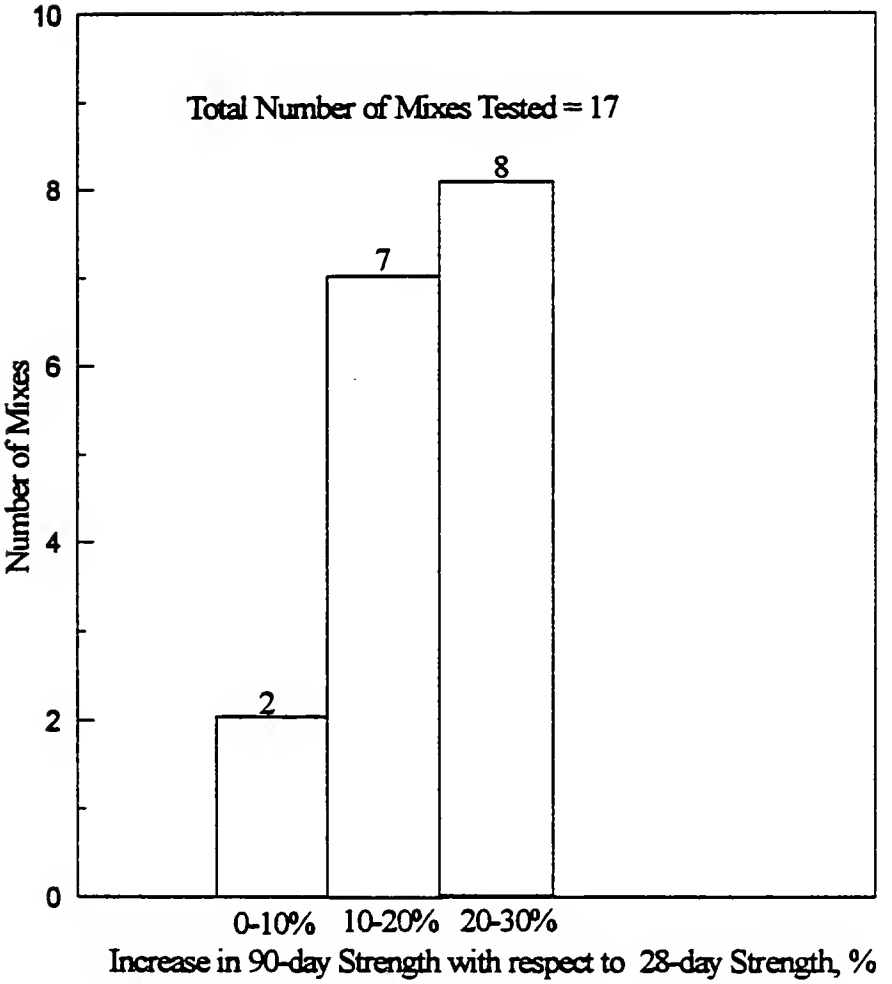


Figure 6.4 Results of Unconfined Compressive Strength Tests at 90 days

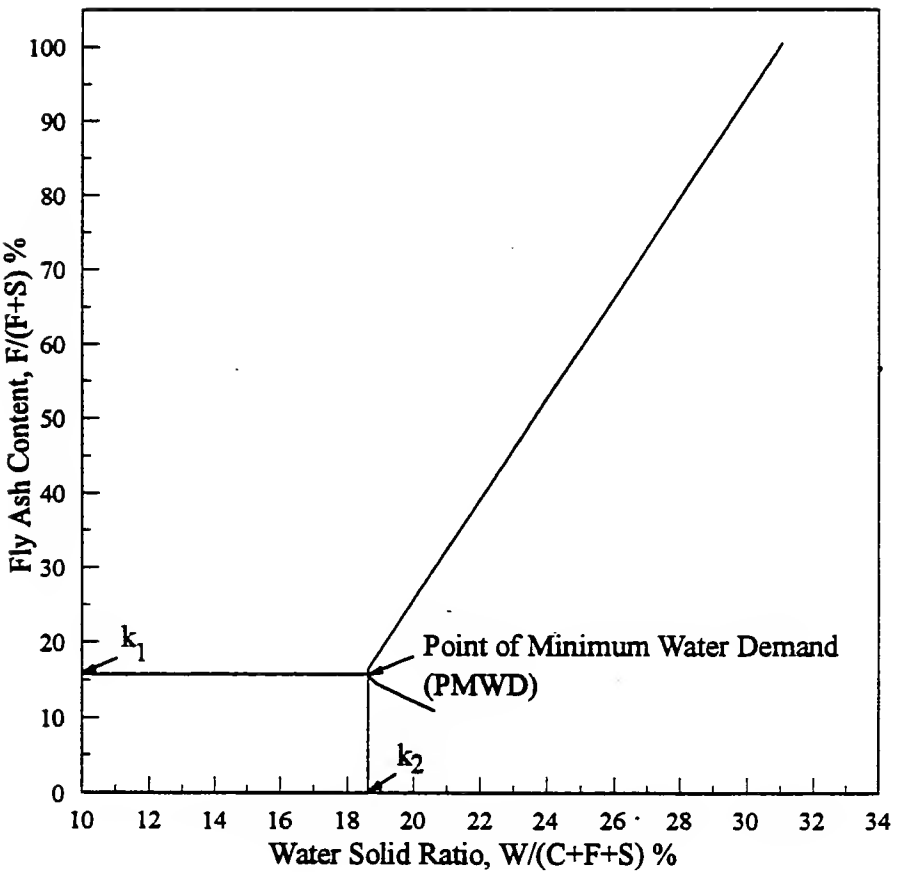


Figure 6.5 Mix Design Parameters $k_1$ and $k_2$ from Flow Curve

S = sand content in kg/m$^3$

W = water content in kg/m$^3$

C = cement content in kg/m$^3$

Assuming that the air content in the flowable fill is negligibly small, the volume of all the ingredients together should give unit volume (1 m$^3$ in this case). There will be small amount of air entrapped in the flowable fill system. However, since there is ample water, enough to fully saturate the system, this assumption seems to be reasonable. Therefore,

$$\frac{W}{1000\times G_w} + \frac{F}{1000\times G_F} + \frac{S}{1000\times G_s} + \frac{C}{1000\times G_c} = 1 \qquad (6.5)$$

where $G_w$ = specific gravity of water (=1)

$G_F$ = specific gravity of fly ash

$G_s$ = bulk specific gravity of sand

$G_c$ = specific gravity of cement

Equation 6.2 can be rewritten as

$$S = \frac{F\,(1-k_1)}{k_1} \qquad (6.6)$$

Using Equations 6.2 through 6.4,

$$W = \frac{F}{\left(\frac{k_1}{k_2} - \frac{k_1}{k_3}\right)} \qquad (6.7)$$

Equation 6.5 can be expressed to relate F and C as

$$F\left(\frac{k_2}{k_1} + \frac{1}{G_F} + \frac{(1-k_1)}{k_1\,G_s}\right) = 1000 - k_2\,C - \frac{C}{G_c} \qquad (6.8)$$

Equation 6.5 can be rearranged using Equations 6.4, 6.6, and 6.7 to get an expression for F in terms of design parameters $k_1$, $k_2$, $k_3$ and specific gravities of the ingredients as

$$F\left\{\frac{k_2\,(k_3\,G_c+1)}{k_1\,G_c\,(k_3-k_2)}+\frac{1}{G_F}+\frac{(1-k_1)}{k_1}\times\frac{1}{G_s}\right\}=1000 \qquad (6.9)$$

Specific gravity for cement ($G_c$) may be assumed to be 3.17.

The following steps may be adopted in designing the mix.

1. Generate the flow curve for a given combination of sand and fly ash as explained in Chapter 4, and determine the parameters $k_1$ and $k_2$ from the flow curve. Normally, $k_1$ and $k_2$ corresponding to Point of Minimum Water Demand (PMWD) may be chosen. Some waste foundry sands with very low specific gravity (e.g. WFS A) may attain PMWD at a very high fly ash content. In such cases, $k_1$ and $k_2$ corresponding to the lower end of the flow curve may be chosen ( for example, for WFS A and fly ash SC, $k_1 = 0.2$ and $k_2 = 0.31$ may be selected from Figure 6.2). As a rule of thumb, if PMWD is attained at $k_1$ greater than 0.25, mix proportions corresponding to $k_1$ from 0.2 to 0.25 may be chosen.

2. Determine the weights of fly ash (F), sand (S), water (W), and cement (C) using the Equations 6.9, 6.6, 6.7 and 6.4 in order, for two W/C ratio ($k_3$) values of 5.5 and 9. These mixes are expected to give a 28-day compressive strength of 1035 kPa (150 psi) and 550 kPa (80 psi) respectively, based on Equation 6.1.

   (Note: If there is no stringent limit on the 28-day strength, mix proportions for a W/C ratio of 7.4, can be calculated. This mix may be adopted and no further steps are necessary. The expected 28-day compressive strength of this mix is 690 kPa(100 psi) based on Equation 6.1.)

3. Make these two mixes, prepare samples, and test them for compressive strength at 28 days. The accelerated strength test (Chapter 9) may be adopted if the 28-day strength is to be quickly estimated.

4. The two values of 28-day strength obtained in step 3 correspond to two cement contents corresponding to W/C ratios of 5.5 and 9.0. Based on these strengths, the cement content necessary for an expected 28-day strength of 670 kPa (100 psi) may be calculated by interpolation between the two cement contents obtained above, assuming that the strength would vary linearly with cement content between these two cement contents. The proportions of other ingredients can be calculated in either of the two ways ( a or b) explained below.

   a) From the cement content (C), obtained above, fly ash content(F) can be calculated from Equation 6.8. Sand and water content may be obtained by Equations 6.6 and 6.3 respectively. This is the final mix to be adopted.

   b) Alternatively, from the new cement content (C), calculate the new W/C ratio. The water content (W) is same as calculated in step 2. Now, the fly ash content (F) and sand content (S) can be calulated in the same way as in step 2. Note that the water content(W) remains the same for all the mixes for a given value of $k_1$ and $k_2$. The mix proportions obtained in this step are the final proportions to be adopted.

Example:

For WFS A and fly ash SC, choose $k_1 = 0.2$, $k_2 = 0.31$ from Figure 6.2. Since PMWD is at a very high fly ash content for this combination of sand and fly ash, the $k_1$ and $k_2$ are chosen from the lower portion of the flow curve as explained in Step 1 of mix design procedure. Let us now calculate the mix proportions for two W/C ratios 5.5 and 9.0, using Equations 6.9, 6.6, 6.7 and 6.4.

$G_s = 2.25$, $G_F = 2.36$, $G_c = 3.17$

For $k_3 = 5.5$ (Expected 28-day compressive strength = 1035 kPa (150 psi)

$F = 254$ kg/m$^3$

$S = 1016$ kg/m$^3$

$W = 417$ kg/m$^3$

C = 76 kg/m$^3$

For $k_3$ = 9 (Expected 28-day compressive strength = 550 kPa (80 psi)

F = 259 kg/m$^3$

S = 1036 kg/m$^3$

W = 416 kg/m$^3$

C = 46 kg/m$^3$

Let us assume that the 28-day strengths for these mixes were estimated (either by testing at 28 days in the normal method or by accelerated strength testing at 3 days suggested in Chapter 9) to be 1100 kPa (160 psi) and 482 kPa (70 psi). By intrapolation, the cement content necessary for a target strength of 690 kPa (100 psi) can be calculated as follows:

$$C = 46 + \frac{(76 - 46)}{(150 - 80)} \times (100 - 80) \qquad (6.10)$$

$$= 55 \text{ kg/m}^3$$

Calulate the weights of fly ash, sand and water from the Equations 6.8, 6.6 and 6.3 respectively. Alternatively, a new W/C ratio may now be calulated as, 416/55 = 7.6. The water content in all the mixes remains approximately constant (In the above two mixes water content was 416 and 417 kg/m$^3$). From the new value of $k_3$ = 7.6, the proportions of fly ash and sand may be calculated from Equations 6.9 and 6.6. Thus, the final proportions of the mix are

C = 55 kg/m$^3$

W = 416 kg/m$^3$

F = 257 kg/m$^3$

S = 1028 kg/m$^3$

Note that the weight of the sand is SSD weight. The dry weight of the sand to be taken for the mix will be 1028/1.055 = 974 kg/m$^3$ ( the absorption was 5.5 % for this sand), and the total water to be added to the mix will be, 416 + (1028-974) = 470 kg/m$^3$.

## 6.6 Summary

The strength of flowable fill is one of the important parameters in the design. The strength should be limited to certain values to allow possible future excavation. Based on this criterion, an upper limit for 28-day unconfined compressive strength equal to 1035 kPa (150 psi) is generally recommended. In this study, based on the strengths of large number of mixes, a relation between W/C ratio and 28-day unconfined compressive strength was suggested. There are several factors affecting the strength of flowable fill: cement content, water content, properties of sand, source of fly ash, proportion of sand and fly ash in the mix, etc. However, the success of engineering lies in identifying the most important parameters, in order to be able to make predictions using minimum number of parameters.

The two important parameters affecting the strength were identified to be the water content and cement content in the mix. The water content here refers to the initial mixing water. The amount of water in the mix influences the void ratio of the material, and affects the frictional component of the strength. The void ratio also affects the effectiveness of cementation bonds. Lower void ratio means a denser packing of sand and fly ash particles; therefore, these closely spaced particles can more effectively bonded with the same amount of hydrated cement paste than with a loosely packed fly ash and sand matrix. Thus, the strength is inversely related to water content. The strength increases with an increase in cement content. Combining these two parameters, W/C ratio is a logical and appropriate parameter to predict the strength. Distinction should be made between concrete and flowable fill. In concrete, the cementation is predominantly responsible for strength, where as in flowable fill, both frictional and cementation components contribute to strength.

There has been no methodical procedure for designing flowable fill mixes. The mix design procedure suggested here takes into account flowability requirement and 28-day unconfined compressive strength. However, hardening characteristics are not taken into account. The parameters needed for the design of flowable fill are $k_1$, $k_2$, $k_3$ and specific gravities of sand and fly ash. The parameters $k_1$ and $k_2$ are obtained from the flow curves. The W/C ratio($k_3$) is assumed based on the relation established between 28-day compressive strength and W/C ratio.

The ultimate strength will be different from the 28-day strength. The hydration of cement might continue for a long time beyond 28 days, and some fly ash may participate in pozzolanic reaction beyond 28 days depending on the availability of calcium hydroxide. The strength test results at 90 days on seventeen different mixes indicated that the 90 day strength could be as much as 30 % higher than the 28-day strength. On an average, a 20 to 25% increase in ultimate strength above that of 28-day strength may be expected.

# CHAPTER 7. PORE STRUCTURE, PERMEABILITY AND ENVIRONMENTAL ASPECTS

## 7.1 Introduction

Void ratio is a fundamental description for soils. However, this is not adequate to define the pore structure of the material. On the other hand, the distribution of pore sizes within the soil mass gives more information about the pore structure, micro structure, and fabric of the material; thus knowledge about pore size distribution should lead to a more fundamental understanding of the soil behavior.

The pore structure of flowable fill has never been investigated in the past. The development and application of this material is based on its unique property, namely, flow. One would expect that such an uncompacted fill would result in a highly porous and loose structure. However, experience shows that this is not true. It is always desirable to have a compact, dense, and less porous material. The multiphase nature of flowable fill containing sand, fly ash, and hydrated cement makes the microstructure of this material more complex. In this study, the mercury intrusion porosimetry technique was used to study the pore structure of flowable fill.

Permeability of flowable fill is another important parameter. Flowable fill contains waste materials- fly ash and waste foundry sand in this case. It is undesirable to release any toxic material into the environment from within the flowable fill. Low permeability of a material reduces the chance of any such toxic component being leached out. Permeability was determined using constant head permeability test.

The nature of the pore solution in terms of pH and toxicity was studied. The pore solution was squeezed/expressed out of the flowable fill samples using a high pressure pore solution device. One of the concerns about flowable fill is whether it is corrosive. This is

important where flowable fill is placed around metallic pipes or parts. The pH of its pore solution indicates the potential corrosivity of flowable fill. The toxicity test done on the expressed pore solution was a bacterial bio assay test, Microtox™ , by the environmental research group at Purdue University (Bastion and Allman, *Unpublished data*). The test was particularly developed to screen out potentially hazardous waste foundry sands.

## 7.2 Experimental Program

### 7.2.1 Mixes

Eleven mixes covering two fly ashes, a natural river sand, and three waste foundry sands were chosen for this study: five mixes contained fly ash, SC, and five mixes contained fly ash, GI; one mix contained only WFS without any fly ash. The mix proportions for these mixes are given in Table 7.1. Other properties for these mixes have been dealt with in the previous chapters.

The SC-R1 is a mix containing fly ash, SC, and natural river sand, R. The SC-N2, SC-G4, SC-A3 are the mixes with fly ash, SC, and WFS, N, G, and A respectively. SC-2 is a mix containing fly ash, SC, and has no sand in it. Similarly, GI-R5, GI-N5, GI-G5, and GI-A4 contain fly ash, GI, and sands, R, N, G, and A, respectively. The GI-2 is a mix containing fly ash, GI and contains no sand. The mix, G3 contains WFS, G, and contains no fly ash. All the mixes containing fly ash and sand were so proportioned as to have a minimum water requirement to get the required flowability, based on the flow curves explained in Chapter 4. The samples were cured in humidity chamber for 28 days.

Table 7.1 Mix Proportions

| Mix Number | Cement $kg/m^3$ | Fly ash $kg/m^3$ | Sand $kg/m^3$ | Water $kg/m^3$ |
|---|---|---|---|---|
| SC-R1 | 30 | 392 | 1474 | 262 |
| SC-N2 | 50 | 254 | 1242 | 376 |
| G3 | 50 | 0 | 1339 | 444 |
| SC-G4 | 50 | 254 | 1157 | 409 |
| SC-A3 | 50 | 258 | 1032 | 415 |
| SC-2 | 50 | 1284 | 0 | 440 |
| GI-R5 | 30 | 378 | 1512 | 257 |
| GI-N5 | 50 | 161 | 1300 | 381 |
| GI-G5 | 50 | 143 | 1284 | 408 |
| GI-A4 | 50 | 361 | 976 | 402 |
| GI-2 | 50 | 1295 | 0 | 449 |

## 7.2.2 Mercury Intrusion Porosimetry (MIP)

### 7.2.2.1 Background and Experimental Technique

Mercury Intrusion Porosimetry is a widely used technique to define the pore space. Washburn (1921) was the first to suggest a theoretical basis for MIP. The use of this technique remained limited because of the difficulty in generating high pressures. In the 1960's when hydraulically pressured commercial instruments became available, the use of MIP became wide spread. Diamond (1970, 1971) and Sridharan et al.(1971) were the first to apply this technique to determine the pore structure of compacted clays. The technique is found to be a useful tool in the study of microstructure and fabric of soils. The technique is routinely used in cement and concrete related research, and other building materials. One of the advantages of MIP over other techniques is that pore sizes spanning over a wide range can be measured. The MIP is based on the capillary law governing the penetration of liquid into small pores as in the following equation.

$$p = \frac{-4\ \gamma\ \cos\theta}{d} \qquad (7.1)$$

where p: pressure required to cause the intrusion

d: diameter of the pore being intruded

$\gamma$: surface tension of mercury

$\theta$: contact angle between the mercury and the pore wall

There are several factors which may affect the reliability of the pore size results from MIP.

i) Equation 7.1 gives an equivalent pore diameter of the intruded cross section of the pore. However, pores in most materials are rarely cylindrical.

ii) The real pore structure is very complicated. Entrance to a void may lead to an area which is larger than the entrance equivalent diameter. This effect is known as *bottle neck* or *ink bottle* effect. This might lead to an overestimation of smaller pore volume and underestimation of larger pore

volume. Therefore the diameter obtained in the Equation 7.1 is a limiting pore diameter.

iii) Contact angle ($\theta$) between mercury and the material is a function of the solid composition of the material, and determination of exact $\theta$ is very difficult. Fortunately, the results are not very sensitive to small changes in $\theta$.

iv) Intruded pore diameters are limited by the minimum and the maximum pressure that can be used in a certain porosimeter.

v) The small sample (about 1cc) may not be representative of the real material.

Inspite of these limitations, MIP is found to be a reliable technique, and gives a good reproducible results. The significance of errors and limitations in MIP has been discussed by Ritter and Drake (1945) and Brakel et. al. (1981).

Most of the recent porosimeters (example: AutoPore, and Quantachrome) are fully automated and are operated by a computer. Sample size is limited by the volume of the penetrometer which can be used with a particular equipment. Typically, penetrometer volume ranges between 3 to 15 cc with a mercury intrusion capacity (which depends on the capacity of the stem of the penetrometer) of about 0.38 to 4 cc. The volume of mercury forced into the pores of the samples causes a decrease in the level of mercury within the stem of the penetrometer. This change in volume is measured by the change in capacitance of the cylindrical co-axial capacitor formed by an outer metallic shield around the penetrometer stem and the inner column of mercury. Capacitance changes are converted to volume changes using a calibration factor (Micromeritics, 1987).

Before applying the pressure, the penetrometer containing the dry sample is evacuated. Under the applied vacuum, the penetrometer is flooded with mercury at a low pressure. After the mercury filling, the mercury supply is detached and the pressure is increased by pneumatic means in the low pressure chamber. After 25 psi pressure, the penetrometer containing the sample and mercury is transferred to the high pressure chamber where the pressure is increased by hydraulic means up to the maximum capacity of the equipment.

7.2.2.2 Drawbacks

The pores ranging from several hundred microns down to several tens of microns are intruded from 0 to 25 psi pressure. There are specific problems associated with low pressure and high pressure regions (Winslow, 1984) which are explained below.

Low pressure region

a) Reluctance of mercury to enter pores overcoming the local irregularities at low pressures (below 1/5 atmosphere), might overestimate the smaller pores.

b) Actual pressure acting at the entrance of different pores is different due to the head of mercury filling the penetrometer. The effect may be significant at low pressure regions.

c) Insufficient evacuation of the penetrometer and sample before applying low pressure can cause significant error due to the compression of the entrapped air.

High pressure region

a) Generation of high pressure causes the temperature of the system to rise significantly.

b) High pressure compresses the sample, the mercury, and the penetrometer causing apparent intrusion or extrusion depending on the compressibility of the different components.

Details about different corrections due to temperature, compressibility of mercury, penetrometer, and sample are discussed by Winslow (1984). The features of the porosimeter used for the present study are given in Table 7.2.

The flowable fill samples after 28 days were removed from the humidity chamber, oven dried, and pieces of around 1 cc were taken. The oven drying method of drying was used because oven drying did not result in either damage or shrinkage of the samples. This was because of the presence of cementation.

Table 7.2 Mercury Intrusion Porosimeter Details

| | |
|---|---|
| Equipment | Autopore II 9220 |
| Operating Software | Autopore, version 1.07 |
| Pressure | |
| Range | 0.8 to 60,000 psi |
| Low Pressure Range | 0.8 to 25 psi |
| High Pressure Range | 25 to 60,000 psi |
| Increment | Step Increment, uniform logarithmic interval of about 0.25 |
| Pore Diameter Range | 360 to 0.001 microns |
| Sample Size | Around 1 cc |
| Drying Method | Oven Drying |
| Sample Evacuation Presssure | 15 to 20 micrometer of Hg |
| Penetrometer size | |
| Bulb | 6 cc |
| Stem | 0.392 cc |
| Contact Angle | 123 degrees |
| Surface Tension | 480 dyne/cm |

### 7.2.3 Constant Head Permeability Test

Permeability tests were carried out in accordance with ASTM D5084 on 7.62cm x 15 cm cylindrical samples after the age of 28 days. A back pressure of around 550 kPa (80 psi) was applied and maintained until a B value of 0.97 or higher was obtained. Then, a constant head permeability test was carried out with a hydraulic gradient of around 10.

### 7.2.4 pH and Bio Assay Test (Toxicity Test)

The pH and bio assay tests were carried out on the expressed pore solution from flowable fill samples after 28 days. A high pressure pore solution device (Dolch and Diamond, 1995), which can apply a force up to 25000 pounds on samples confined by a rigid die body, was used to express the pore solution from the flowable fill samples. The details of this device are shown in Figure 7.1. This device was specially built to use in concrete research at Purdue University. The pH of the pore solution was determined using a pH meter (CORNING 340 pH meter).

The bio assay test, Microtox™ was developed by the environmental group at the Purdue University (Bastion and Allman, *personal communication*) to screen out potentially hazardous waste foundry sands. This is an indirect way of estimating the toxicity of the leachate or the solution to be tested. The test involves measuring the toxic effect of the solution on the bacteria "photobacterium phosphorium". The bacteria glow; and this light output can be measured. When these bacteria are exposed to a toxic leachate environment, the light output decreases, and this decrease in light output with respect to the control condition is an indirect measure of the environmental quality of the leachate. A percentage difference of above 30 would be considered toxic. A negative value would indicate that the condition in the test sample is more favorable to the bacteria compared to the condition in the control sample.

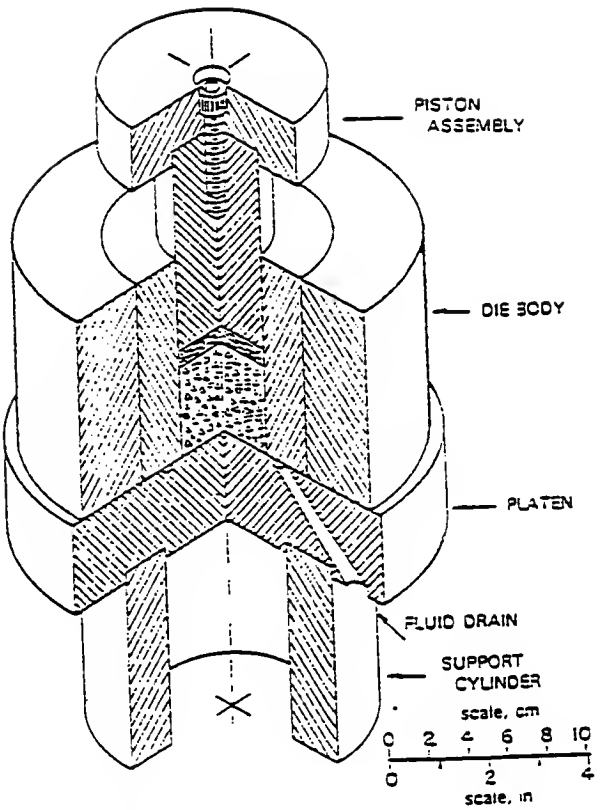


Figure 7.1 High pressure pore solution device in use at Purdue University. Specimen is confined by a rigid die body. Up to 250,000 pounds of force is applied to the piston, resulting in stresses sufficient to remold the concrete and expel the pore solution (Dolch and Diamond, 1995).

## 7.3 Results

### 7.3.1 Pore Structure

Figures 7.2 through 7.12 show the pore size distribution (PSD) curves for all the samples. The dashed line is the average of the two tests (solid lines) for each sample. Note that the average line was the weighted average (i.e. proper weightage assigned depending on the weight of the two specimens taken from each sample), and therefore does not fall exactly at the center of the two solid curves.

Figure 7.13 shows the PSD curves for all the samples. The curves mainly form three bands in terms of total intruded pore volume. The fly ash only mixes have highest total intruded pore volume (the top most two curves). The mixes containing river sand, R give least total intruded pore volume (the bottom most two curves). The mixes with WFS have an intermediate total intruded pore volume.

The conventional way of plotting intruded volume in cc/gm as ordinate is misleading for a material like flowable fill containing components having different specific gravities in different proportions: One gram dry weight of two mixes, for example, could have markedly different solid volume depending on the proportions of sand, fly ash, and cement, because each of these components have different specific gravities; therefore, comparing intruded volumes of different mixes in cc/gm is not appropriate. In Figure 7.14 is shown the PSD curves taking intruded volume in cc/cc of solid volume. By knowing the solid density in gm/cc (which is an average solid density) from the MIP result, the cumulative intruded volume in cc/gm at each stage can be easily converted to cc/cc of solid volume. The total intruded volume on this plot, incidentally, gives the void ratio of the sample.

The dry densities of the samples obtained by MIP are shown in Table 7.3. The mixes with river sand, produced highest density of 1800 to 2000 kg/m$^3$. Fly ash alone mixes gave lowest density of 1250 to 1300 kg/m$^3$. The density of the WFS mixes depends on the specific gravity of WFS used, and these densities were much lower compared to the mixes with river sand.

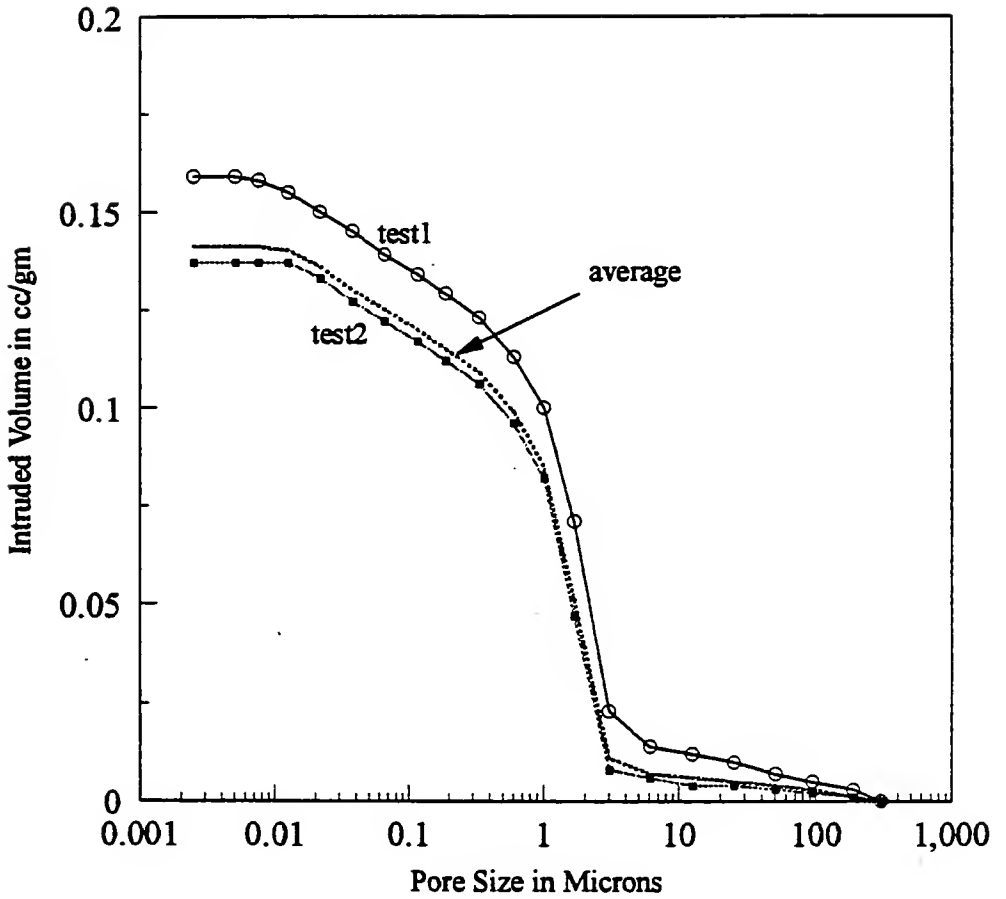


Figure 7.2 Pore Size Distribution for SC-R1

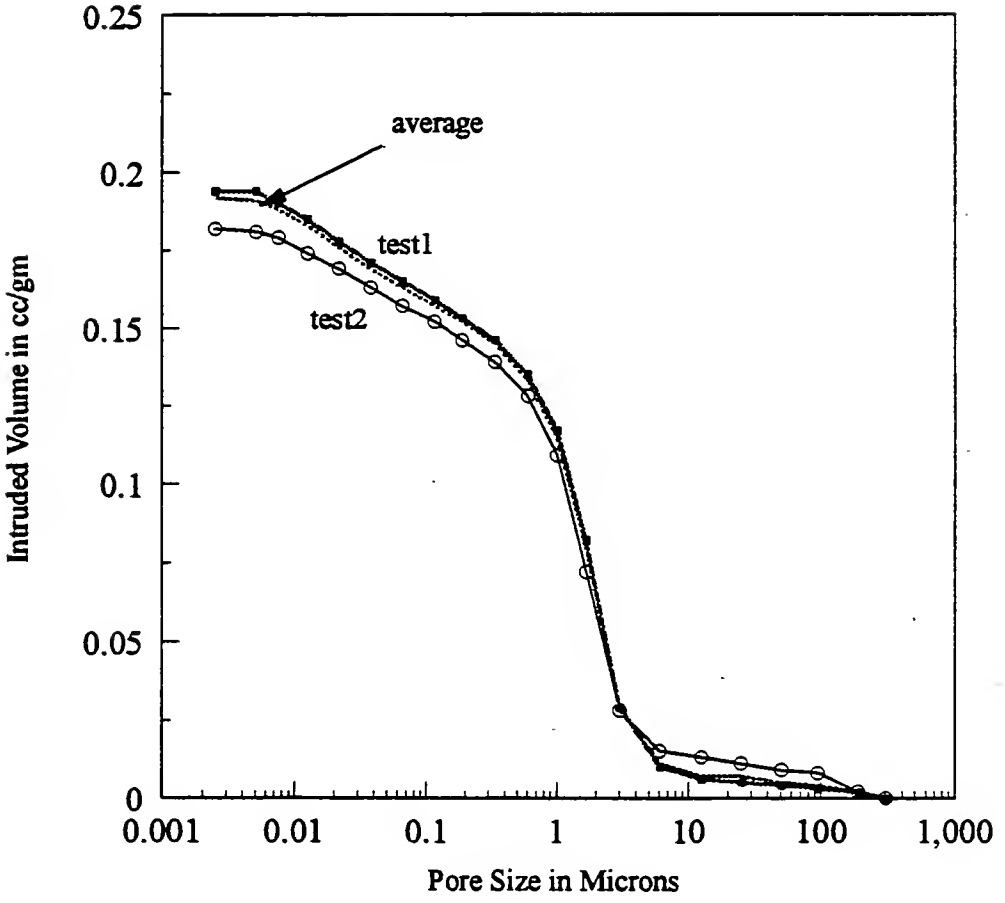


Figure 7.3 Pore Size Distribution for SC-N2

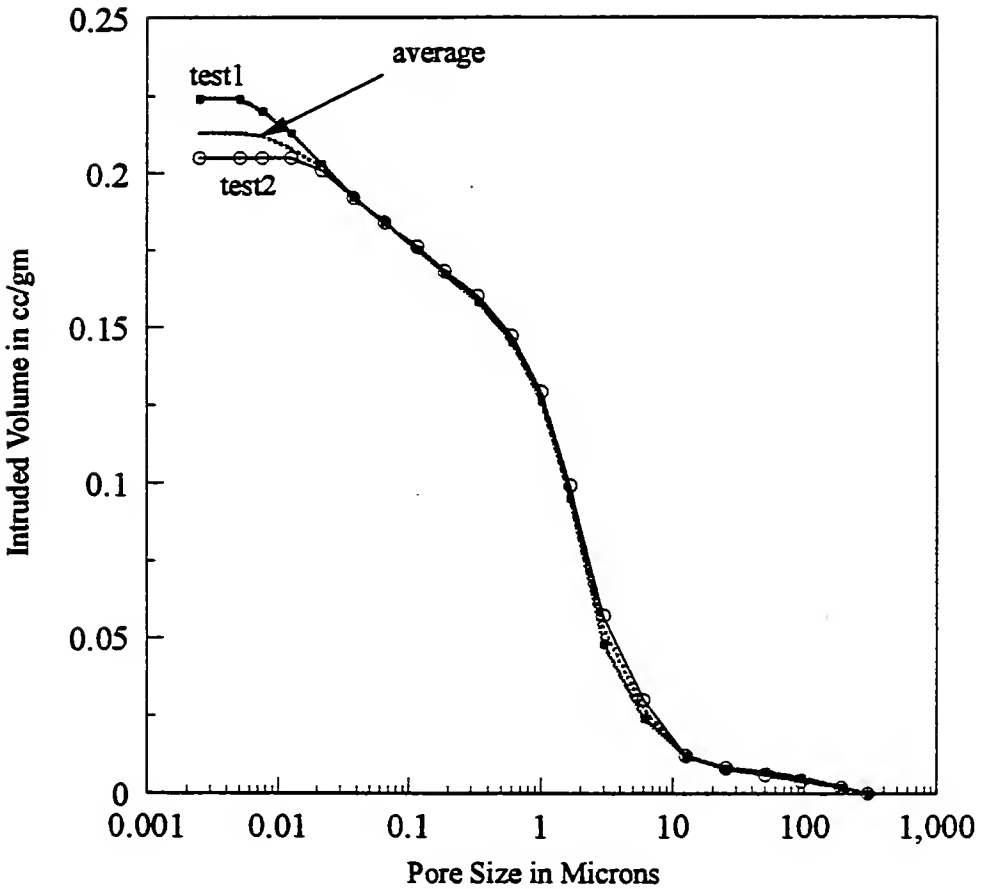


Figure 7.4 Pore Size Distribution for G3

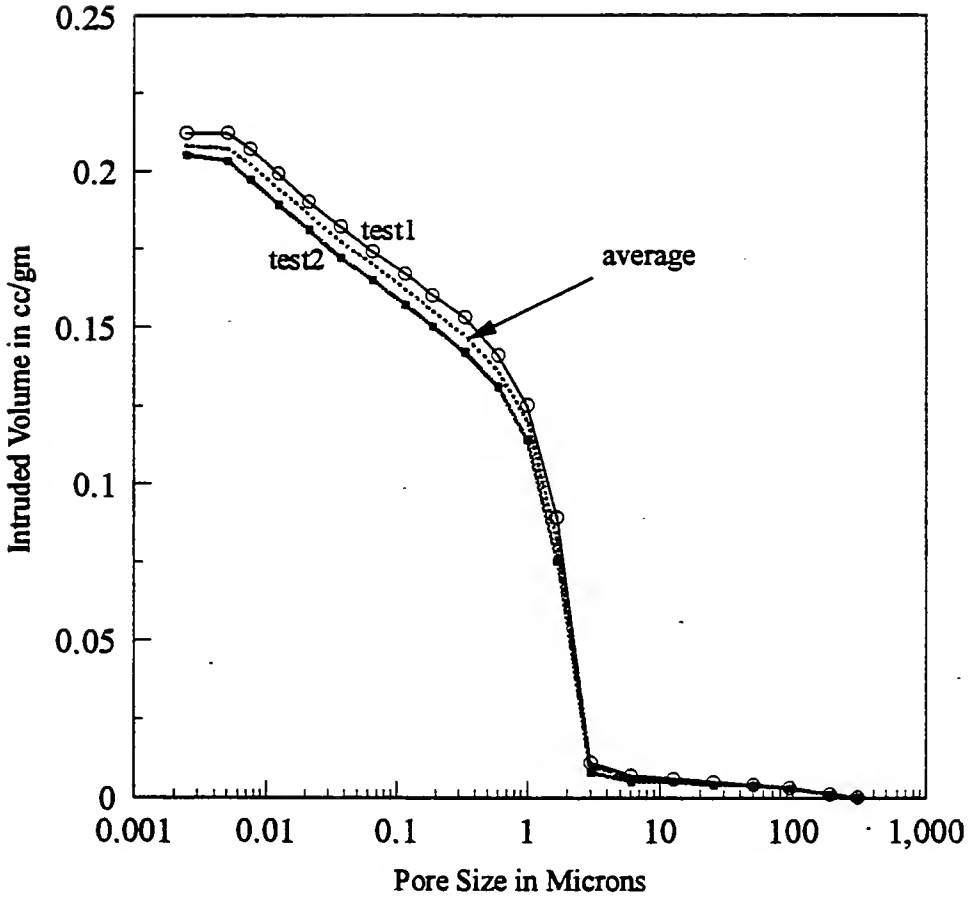


Figure 7.5 Pore Size Distribution for SC-G4

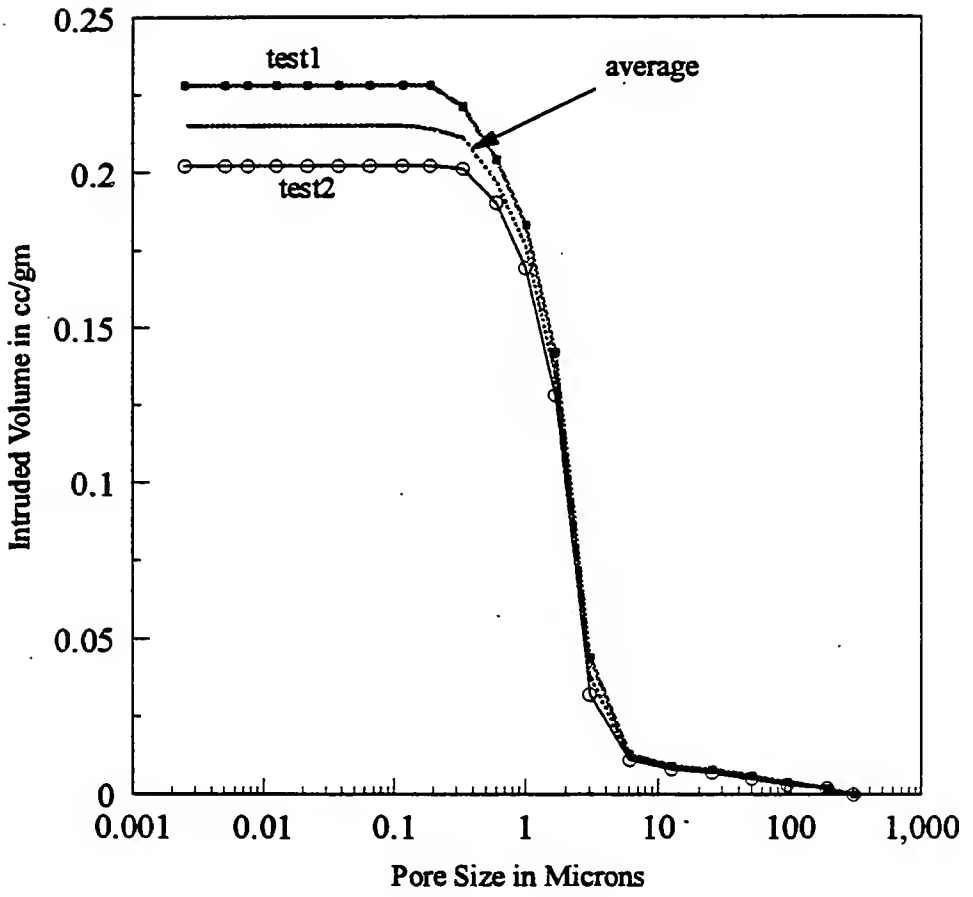


Figure 7.6 Pore Size Distribution for SC-A3

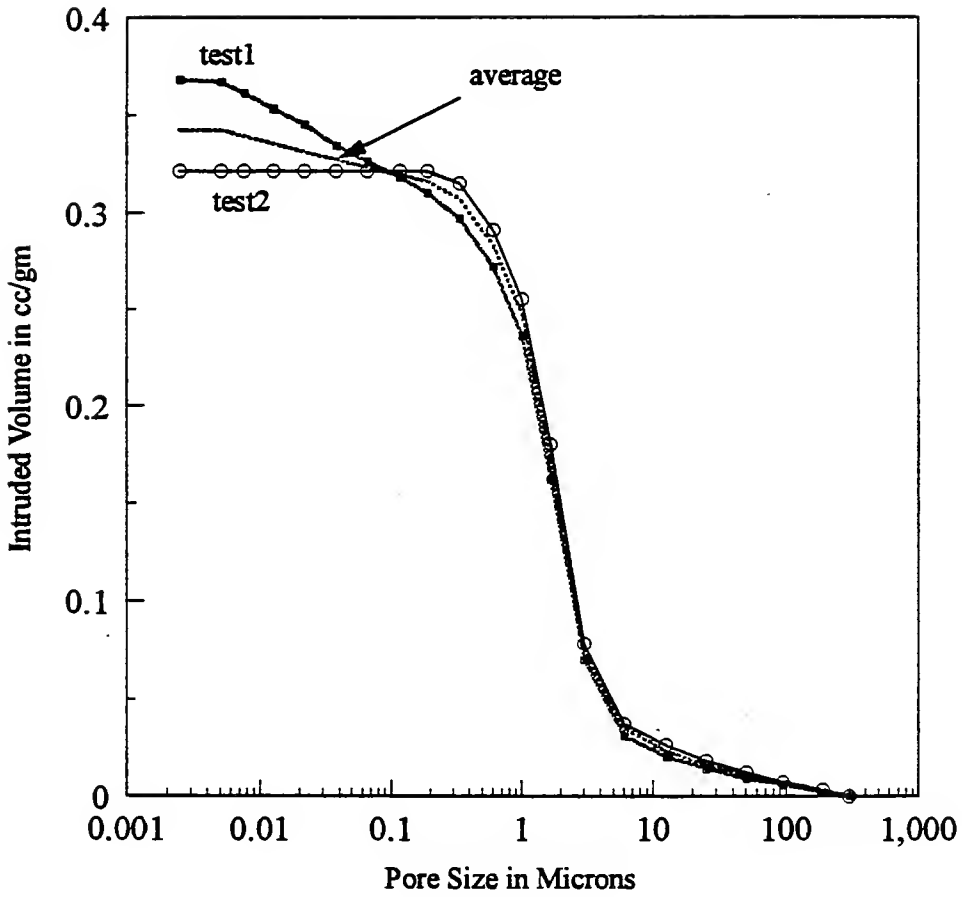


Figure 7.7 Pore Size Distribution for SC-2

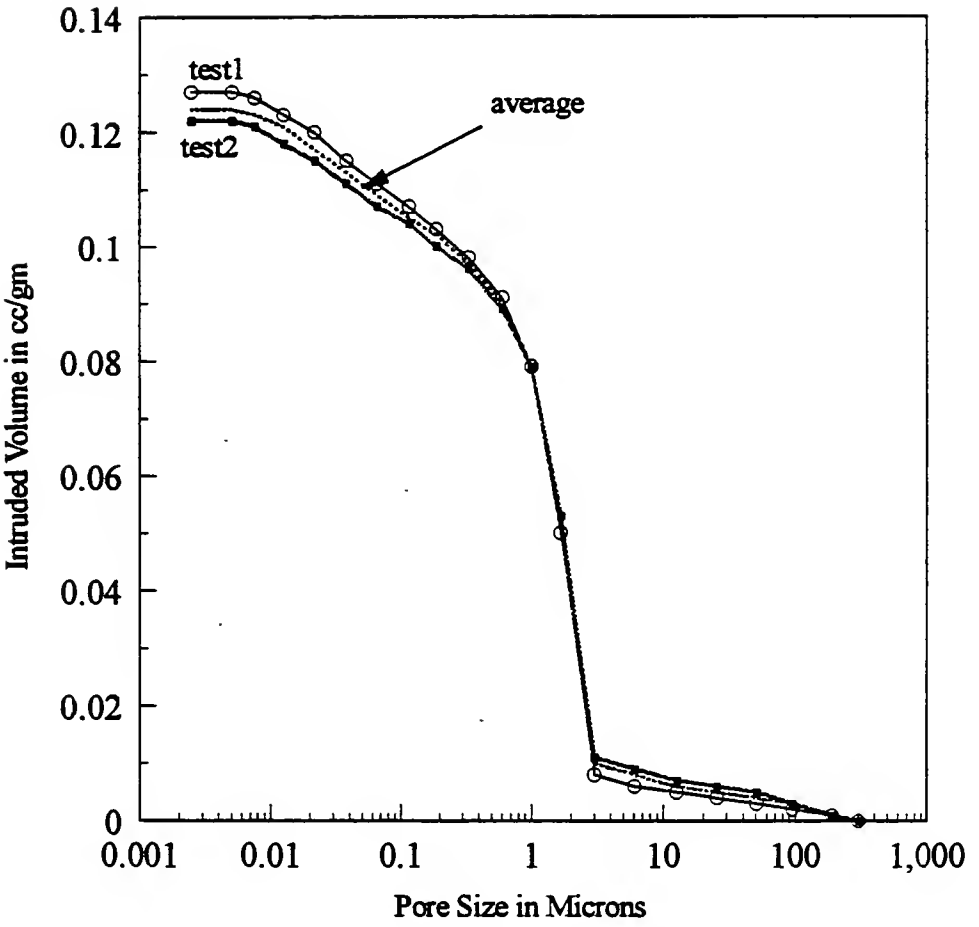


Figure 7.8 Pore Size Distribution for GI-R5

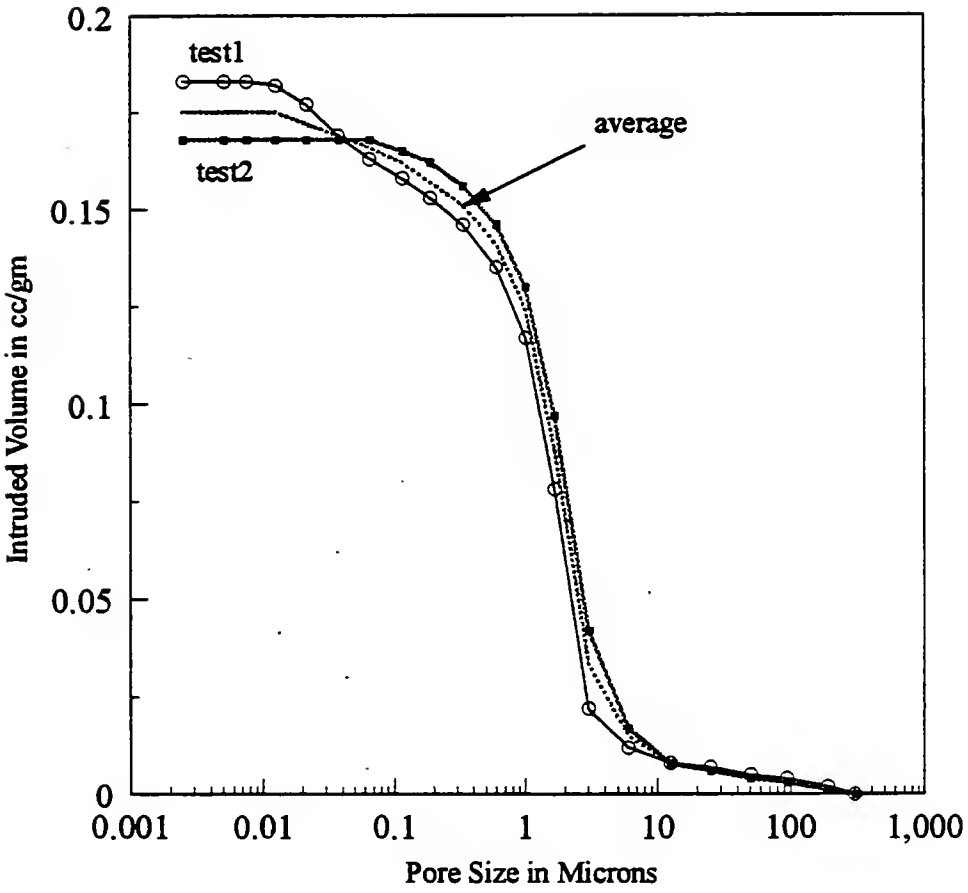


Figure 7.9 Pore Size Distribution for GI-N5

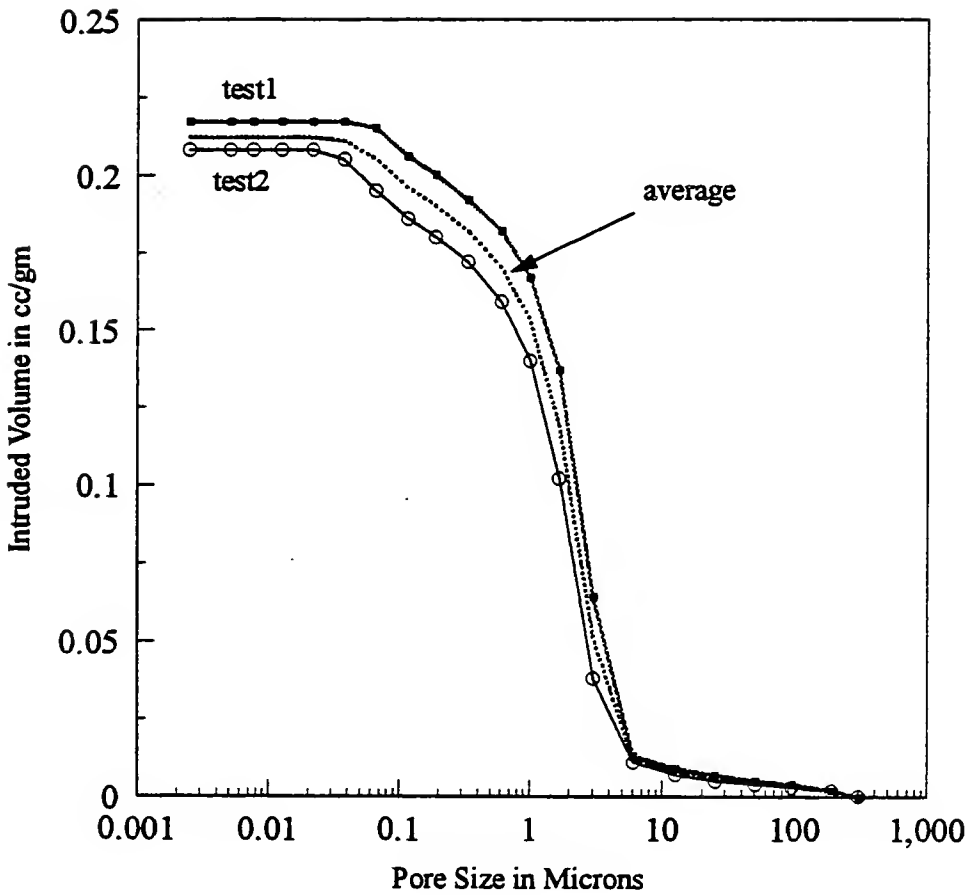


Figure 7.10 Pore Size Distribution for GI-G5

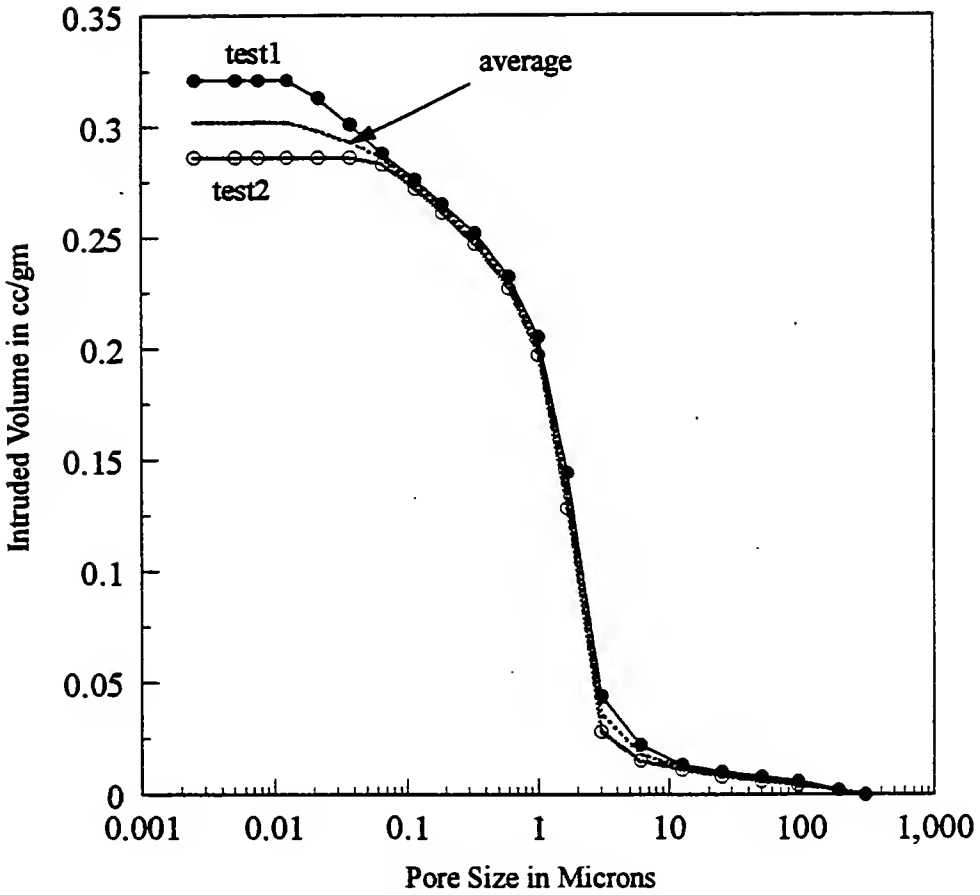


Figure 7.11 Pore Size Distribution for GI-A4

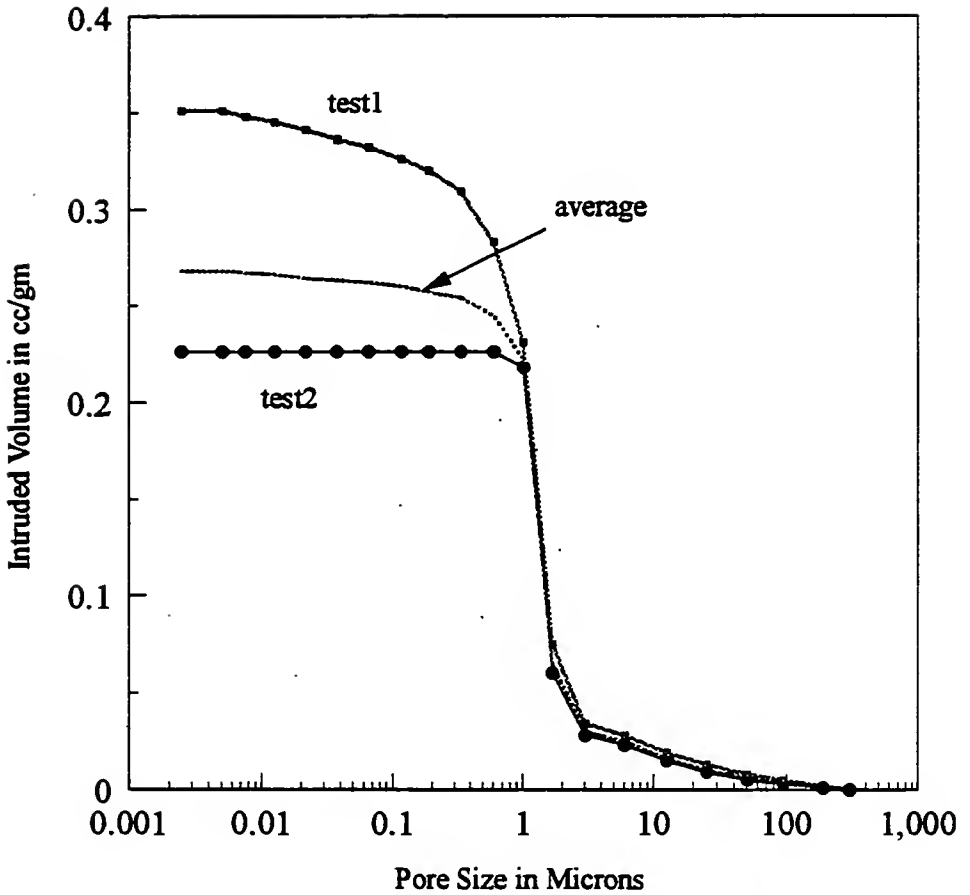


Figure 7.12 Pore Size Distribution for GI-2

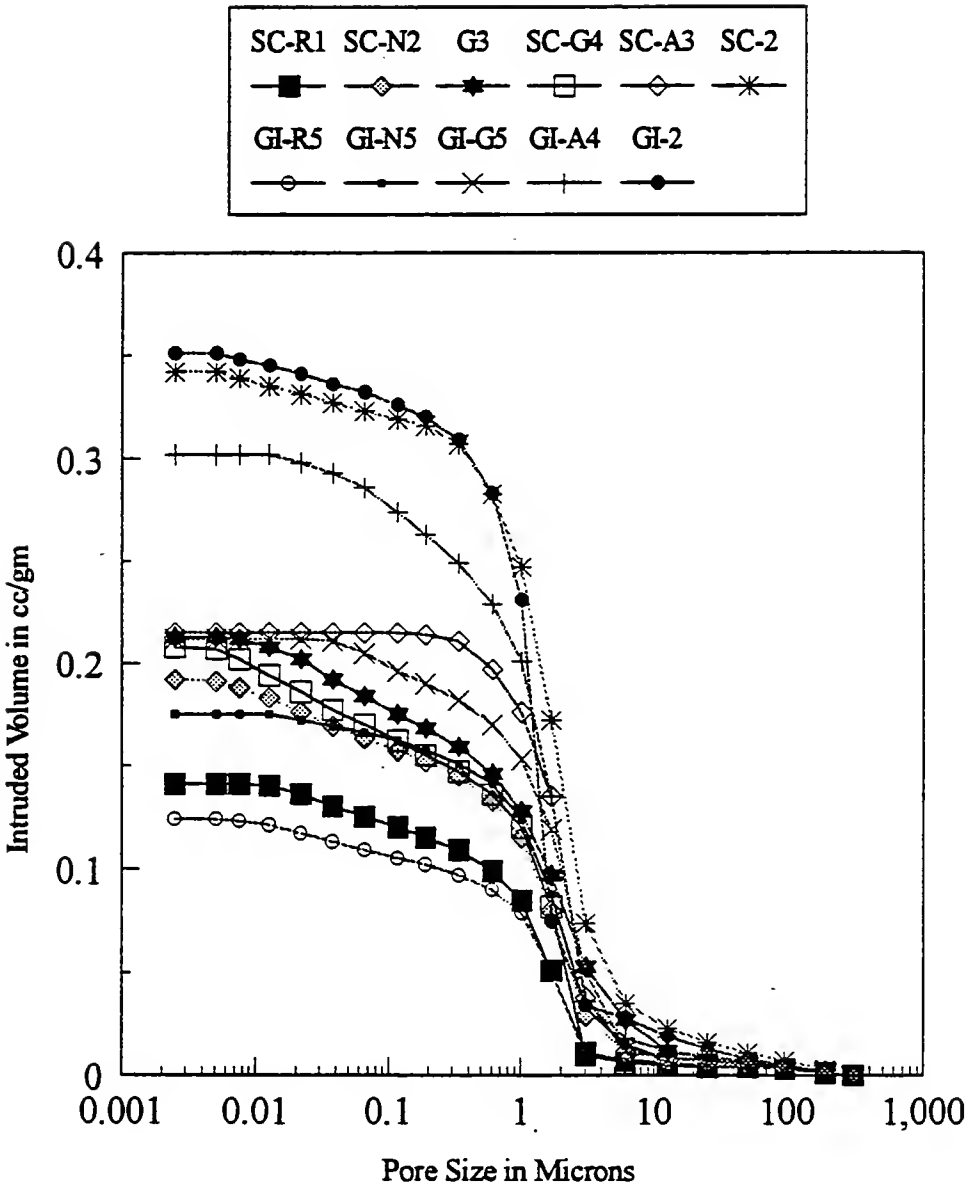


Figure 7.13 Pore Size Distribution for All the Samples

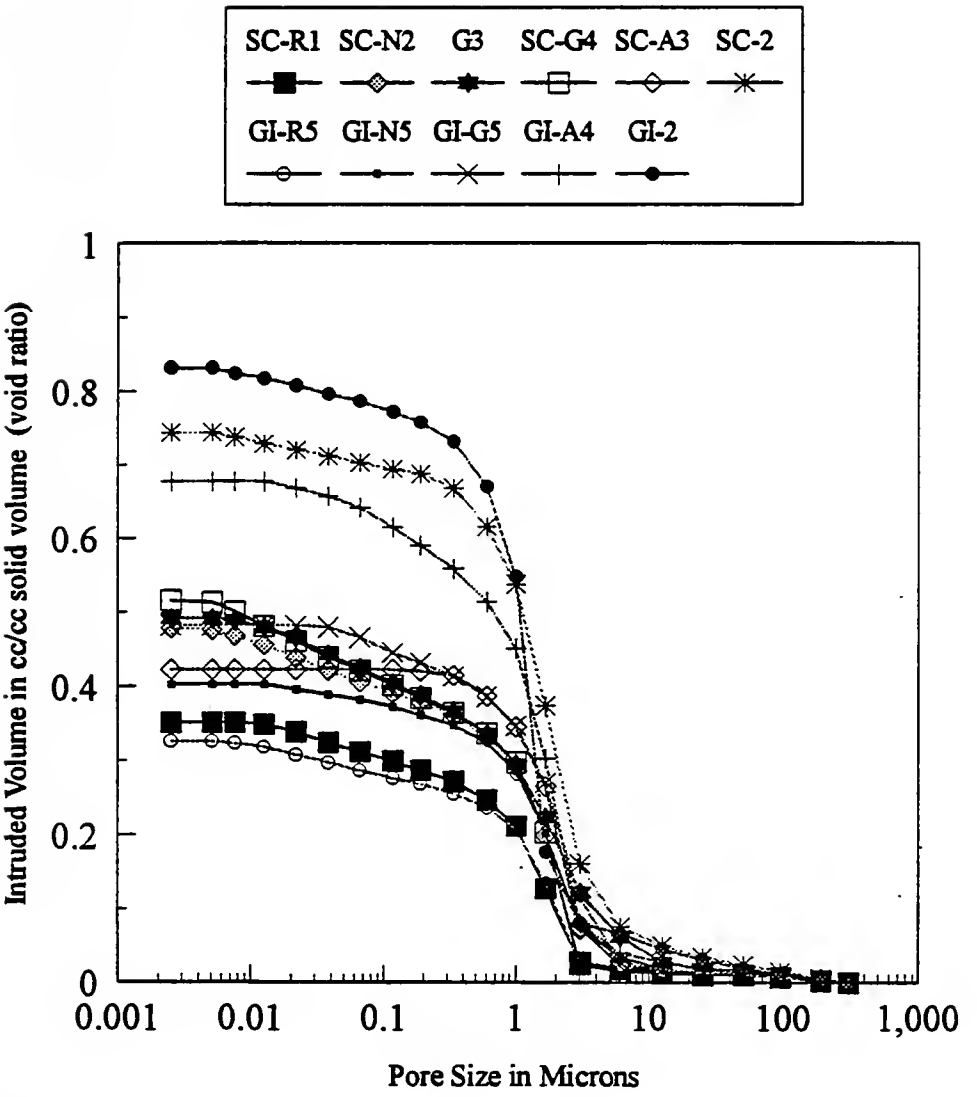


Figure 7.14 Modified Pore Size Distribution
(Void Ratio Distribution)

Table 7.3 Densities, Threshold Diameter and Void Ratio by MIP

| Mix Number | Bulk Density or Dry Density, gm/cc | Solid Density gm/cc | Threshold Diameter, microns | Void Ratio |
|---|---|---|---|---|
| SC-R1 | 1.8458 | 2.4922 | 3 | 0.351 |
| SC-N2 | 1.6863 | 2.3904 | 4 | 0.478 |
| G3 | 1.5442 | 2.3054 | 9 | 0.491 |
| SC-G4 | 1.6349 | 2.4781 | 3 | 0.515 |
| SC-A3 | 1.3812 | 1.9637 | 5 | 0.422 |
| SC-2 | 1.2443 | 2.1758 | 6 | 0.744 |
| GI-R5 | 1.9814 | 2.6293 | 3 | 0.326 |
| GI-N5 | 1.6385 | 2.2998 | 4 | 0.402 |
| GI-G5 | 1.5324 | 2.2708 | 6 | 0.481 |
| GI-A4 | 1.3348 | 2.243 | 3.5 | 0.677 |
| GI-2 | 1.2924 | 2.3676 | 3 | 0.635 |

The total intruded volume (cc/cc of solid volume) depends on many factors: the amount of mixing water, amount of cement, gradation of sand and fly ash etc.). However, the amount of water seems to have the major effect (Figure 7.15).

The diameter of pores at which the PSD curve becomes steep is known as the threshold diameter. The threshold diameters are shown in Table 7.3. The threshold diameter varied from 3 microns to 6 microns except for the mix G3 (WFS only mix) which had a threshold diameter of 9 microns. It is worth noting that a cement paste typically will have a threshold diameter around 0.1 micron. From Figure 7.15, it can be seen that the major percentage of pore volume for flowable fill lies between 3 microns and 0.4 microns. The intruded volume below 0.1 micron was very small. This portion of pores is perhaps due only to the hydrated cement paste. The main pore size distribution in flowable fill is due to the matrix of sand and fly ash particles.

### 7.3.2 Permeability

The results of permeability tests are shown in Table 7.4. The permeability did not seem to vary a great deal for different mixes. It ranged from $1.2 \times 10^{-5}$ cm/sec to $2.6 \times 10^{-6}$ cm/sec. The fly ash only mixes SC-2 and GI-2 have a slightly higher permeability values compared to other mixes. Increasing the fly ash content, therefore, does not necessarily help decrease the permeability. The advantage due to the fine particle size of fly ash is perhaps outweighed by the uniform spherical shape of these particles, resulting in more porous structure. It was seen in the last section that the fly ash only mixes had highest intruded pore volume. Both the total porosity and the size of the largest pores might control the permeability. The samples with river sand, R had smallest threshold diameter and least total intruded pore volume, and gave low permeability values.

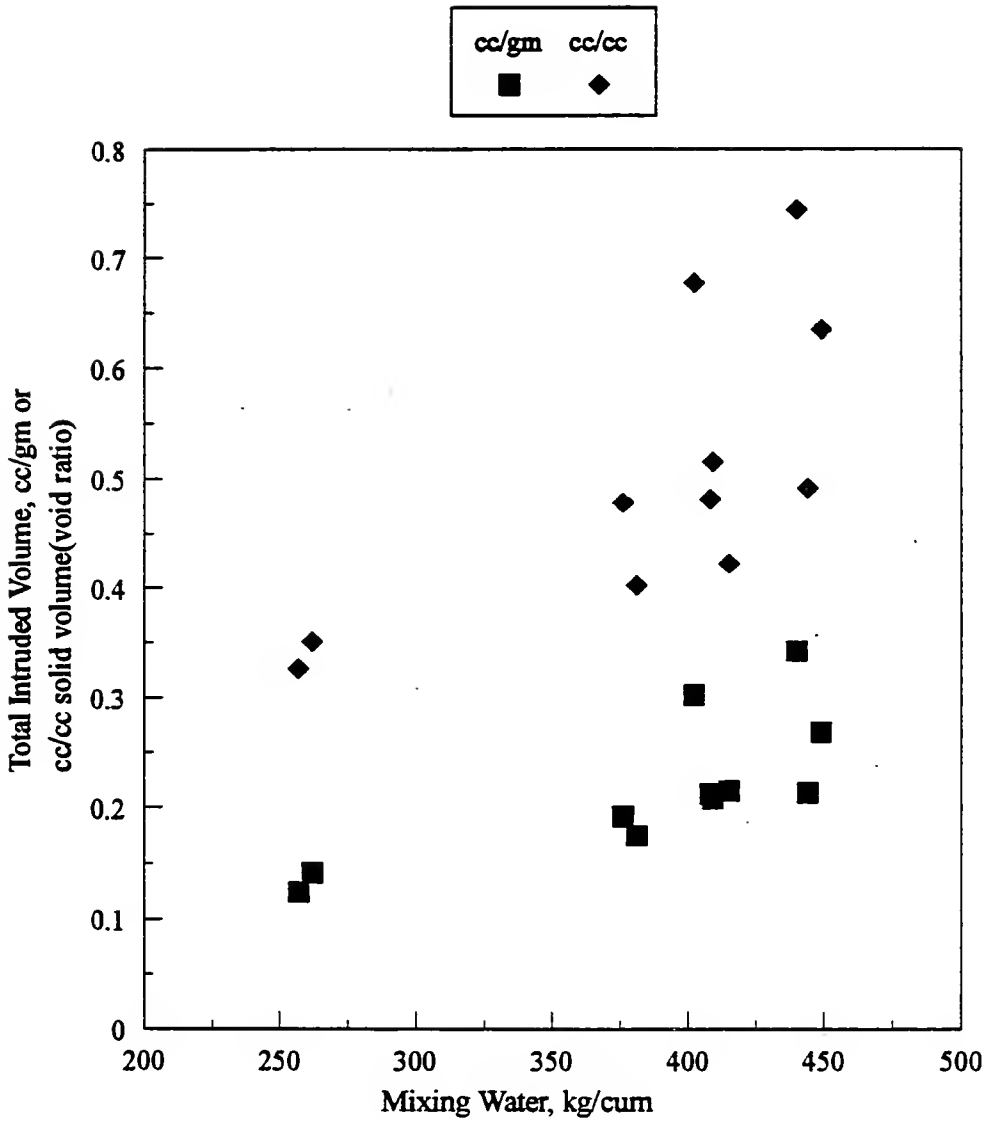


Figure 7.15 Influence of Mixing Water on Total Voids

Table 7.4 Permeability, pH, and Toxicity Test Results

| Mix Number | Sand Source | pH of bleed water | pH of pore solution | Toxicity, % difference from control value | | Permeability cm/sec |
|---|---|---|---|---|---|---|
| | | | | sand alone | pore solution | |
| SC-R1 | River sand | 11.5 | 11.3 | 34.9 | 30.2 | $8.8 \times 10^{-6}$ |
| SC-N2 | WFS, N | 11.5 | 12.0 | 33.3 | 83.2 | $4 \times 10^{-6}$ |
| G3 | WFS, G | 11.4 | 11.4 | -5.1 | - | - |
| SC-G4 | WFS, G | 11.5 | 11.6 | -5.1 | 6.4 | $1.9 \times 10^{-5}$ |
| SC-A3 | WFS, A | 11.5 | 11.9 | -4.6 | 0.5 | $1.2 \times 10^{-5}$ |
| SC-2 | No sand | 10.0 | 11.8 | - | -14.7 | $2.9 \times 10^{-5}$ |
| GI-R5 | River sand | 10.1 | 11.06 | 34.9 | - | $2.6 \times 10^{-6}$ |
| GI-N5 | WFS, N | 11.6 | 12.3 | 33.3 | 43.2 | $3.8 \times 10^{-6}$ |
| GI-G5 | WFS, G | 11.5 | 11.7 | -5.1 | 2.1 | $1.1 \times 10^{-5}$ |
| GI-A4 | WFS, A | 11.4 | 11.8 | -4.6 | 5.6 | $6.7 \times 10^{-6}$ |
| GI-2 | No sand | 10.0 | - | - | - | $1.7 \times 10^{-5}$ |
| N3 | WFS, N | 11.7 | 12.3 | 33.3 | 84.9 | - |
| G3 | WFS, N | 11.1 | - | -5.1 | | $1.4 \times 10^{-5}$ |

Note: Toxicity test "Bio assay" was done by Bastion(Purdue Univ.).

### 7.3.3 pH of Pore Solution

The pH for bleed water from fresh flowable fill, and for the pore solution expressed from the samples after 28 days are shown in Table 7.4. The pH of bleed water and pore solution were almost same. An average value of pH for pore solution was around 11, which shows the basic nature of the pore solution. The eleven mixes included different combinations: fly ash only mixes, WFS only mix, fly ash plus WFS mixes, fly ash plus natural river sand mixes. These combinations helped to determine what was the source of high pH. All the mixes contained portland cement. It can be easily seen that the high pH is mainly due to the presence of cement. Due to this high pH, all flowable fill mixes (including WFS) can be considered to be noncorrosive, if the waste foundry sands do not contain chlorides. From Table 3.3, it can be seen that WFSs had traces of chlorides, but this amount is very small to cause any concern about corrosivity.

### 7.3.4 Environmental Test Results

It was seen that the permeability of flowable fill is sufficiently low to prevent any free drainage of pore solution into the environmental. The bio assay tests were carried out to screen out potentially hazardous waste foundry sands. The bio assay test was done both on expressed pore solution, and the sand alone (Table 7.4). The results show that the mixes containing WFS, N is toxic with a high toxicity value more than 80. The mixes containing other WFSs had sufficiently low toxicity values to be considered as completely non-toxic. What is not very clear is the toxicity exhibited by the river sand as indicated by the toxicity value of around 34.9. The pore solution expressed from flowable fill sample, in some cases, showed higher toxicity compared to the WFS that was present in that sample. It is not very clear whether this higher toxicity of pore solution came from the fly ash that was present in the flowable fill sample. Further study needs to be done on bio assay testing before this method can be used effectively in evaluating the environmental quality of foundry sands.

## 7.4 Summary

The pore structure of eleven mixes of flowable fill was studied using Mercury Intrusion Porosimetry (MIP) technique. The MIP technique gives pore size distribution, the solid density, and also the bulk density (dry density). The conventional way of representing cumulative intruded volume in cc/gm is not appropriate for flowable fill since it contains different phases having different specific gravities. Therefore, a unit weight of different material would contain different amount of solid volume in them. A new unit, cc/cc of solid volume was chosen for cumulative intruded volume. This unit is equivalent to the void ratio. The fly ash only mixes had highest intruded volume or void ratio (around 0.8), the mixes containing river sand had smallest void ratio (around 0.3), and those with WFSs had intermediate void ratios (0.4 to 0.5). The threshold diameter ranged from 3 to 6 microns. The major portion of pore volume was in the diameter range of 3 to 0.4 micron. The pore volume due to pores less than 0.1 micron size was small, which is mainly due to the hydrated cement phase. The mixing of sand and fly ash in proper proportions reduces the porosity. Increasing the fly ash content does not necessarily reduce the porosity.

The permeability varied from $1.2 \times 10^{-5}$ cm/sec to $2.6 \times 10^{-6}$ cm/sec. Both the total porosity and the threshold diameter of pores seem to affect permeability. The mixes with river sand had smaller threshold diameter and smaller total intruded volume, and gave lower permeability value. The mixes with WFSs had comparable permeability values. The pH of both bleed water from fresh flowable fill, and expressed pore solution from flowable fill samples after 28 days of age showed that highly alkaline environment remains within the flowable fill. This was mainly due to the presence of cement. All flowable fill mixes including those containing WFSs can be considered to be non-corrosive.

The bio assay tests on expressed pore solution from flowable fill showed that some WFSs are totally non-toxic, and pose no danger to the environment. One WFS was found to be very toxic. The toxicity values of pore solution from flowable fill samples were sometimes higher than that of leachates from WFSs alone. The reason for this is not very clear.

# CHAPTER 8. STRESS-STRAIN-STRENGTH BEHAVIOR

## 8.1 Introduction

Flowable fill is meant to be used in place of soil; hence, an important question that an engineer needs to know is- does this material behave the way the soil does?. The answer to the question is neither obvious nor simple. Out of the many aspects of soil behavior when it is used as a construction material, of particular interest, is the response of soil to an externally applied load. The study of stress-strain-strength behavior addresses this aspect. Therefore, the objective of this chapter is to study the stress-strain-strength behavior of flowable fill.

In the normal backfill applications, for example, utility trenches, it is not very much essential to know the stress-strain behavior of flowable fill. However, the author foresees tremendous potential for this material to be used in other applications where more knowledge and understanding about its engineering behavior would be warranted. Example of such applications, to list a few, are: structural fill, backfill in reinforced earth structures, replacement for hydraulic fill, seepage cut-off applications in earth dams, impoundment liners, landfill liners, etc.

It can be stated hypothetically that flowable fill is a multiphase particulate material held together by cementation bonds; upon application of a load, there are two things that come into action- firstly the cementation bonds; secondly the interaction between different components of flowable fill, namely, fly ash-fly ash, fly ash-sand, and sand-sand interactions, which are loosely defined here as frictional characteristics. The stress-strain-strength behavior of flowable fill under different confining pressures is investigated in this Chapter. The effect of cement content and amount of fly ash is addressed. The behavior is discussed in the context of geotechnical engineering concepts.

## 8.2 Experimental Program

### 8.2.1 Samples

The samples of flowable fill were 7cm dia x 15cm length (2.8 in. x 6 in.), and tested after 28 days of curing. The fresh flowable fill mixes were poured into 7 cm x 15 cm PVC molds without any compaction, and kept in the humidity chamber (100% humidity); the samples were demolded after three days, and placed back into the humidity chamber until the day of testing.

Four mixes were chosen for this study: GI-R5, GI-R7, GI-R6 and GI-N7. The mixes GI-R5, GI-R7 and GI-R6 contained fly ash, GI and river sand, R. The mix GI-N7 contains fly ash, GI and waste foundry sand (WFS), N. The mixes GI-R5 and GI-R7 have a cement content of 30 kg/m$^3$ and 35 kg/m$^3$ respectively, other components being nearly the same. The mix GI-R6 is a high fly ash content mix, and was chosen to see the effect of amount of fly ash on the stress-strain behavior of flowable fill. The mix GI-N7 is chosen to see the effect of WFS in flowable fill. The mix proportions for the above mixes are as follows:

GI-R5: cement= 30 kg/m$^3$, fly ash= 378 kg/m$^3$, sand= 1512 kg/m$^3$, water= 257 kg/m$^3$

GI-R7: cement= 35 kg/m$^3$, fly ash= 377 kg/m$^3$, sand= 1508 kg/m$^3$, water= 257 kg/m$^3$

GI-R6: cement= 30 kg/m$^3$, fly ash= 686 kg/m$^3$, sand= 1029 kg/m$^3$, water= 314 kg/m$^3$

GI-N7: cement= 60 kg/m$^3$, fly ash= 160 kg/m$^3$, sand= 1295 kg/m$^3$, water= 382 kg/m$^3$

### 8.2.2 Triaxial Testing

Triaxial tests were performed using the MTS Soil Test System, with an IBM PC to control the test and do data acquisition. Consolidated drained triaxial (CD) tests were performed on all the mixes at four confining pressures ( 50 kPa, 100 kPa, 200 kPa, and 400 kPa). The samples were backsaturated with a back pressure ranging from 300 to 500 kPa.

When a B parameter of 0.98 or higher was obtained, the samples were consolidated to the desired pressure, and were then sheared. The axial strain rate adopted during shearing was around 4% per hour. Consolidated undrained triaxial (CU) tests were performed on samples GI-R5 and GI-R7 at three confining pressures (100 kPa, 200 kPa, 400 kPa). These samples were backsaturated in the same way as in drained tests. The axial strain rate during shearing was around 20% per hour. The dry density of the samples was obtained by oven drying the samples.

### 8.2.3 Unconfined Compressive Strength and Brazilian Tensile Strength Tests

Unconfined compressive strength was obtained in the MTS machine. Four samples of each mix were tested and the average was taken as the unconfined compressive strength. The Brazilian Tensile Strength test is an indirect tensile strength test. In this test, the cylindrical specimen is placed horizontally and loaded along the diameter as shown in Figure 8.1. The load is increased to cause diametric failure in tension. The tensile strength, $\sigma_{tf}$ is calculated as

$$\sigma_{tf} = \frac{2\,Q_f}{\pi DL} \tag{8.1}$$

where $Q_f$ is the failure load, D is the diameter of the specimen, and L is the length of the specimen. Average failure load of three to four samples for each mix was reported.

## 8.3 Test Results

### 8.3.1 Dry Density and Void Ratio

The dry density and void ratio for different samples are shown in Table 8.1. The dry density mainly depends upon the specific gravity and amount of sand in the mix, and the

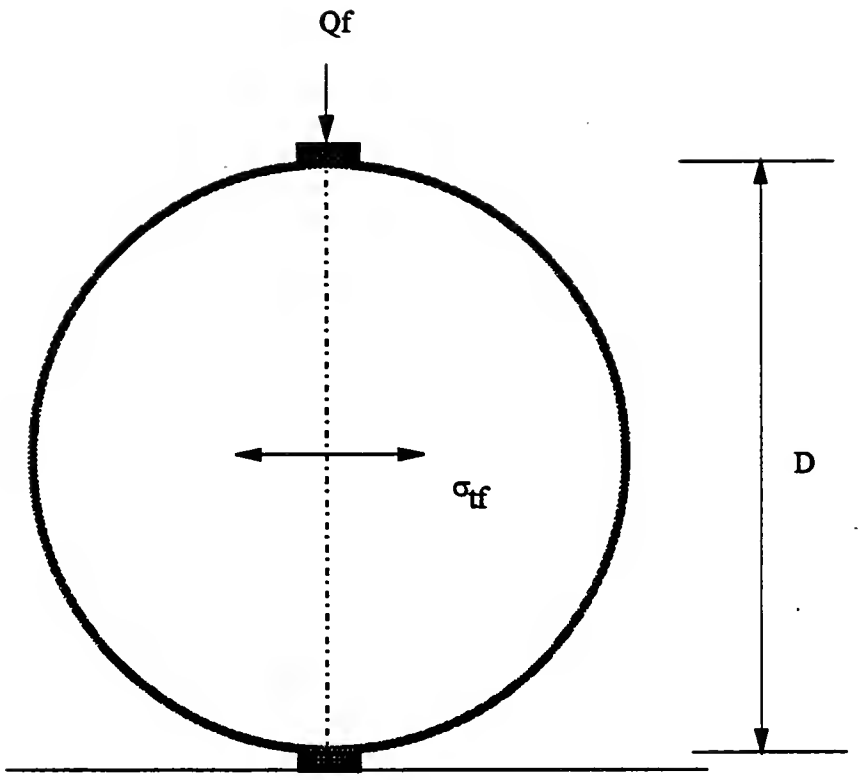


Figure 8.1 Brazilian Tensile Strength Test

Table 8.1 Properties of Flowable Fill Samples Chosen for Triaxial Testing

| Sample No. | Dry Density $kg/m^3$ | void ratio e | Unconfined Compressive Strength, kPa | Tensile Strength kPa | Specific Gravity of Sand | $e_{max}$ for sand | $e_{min}$ for sand |
|---|---|---|---|---|---|---|---|
| GI-R5 | 2000 | 0.32 | 700 | 155 | 2.69 | 0.69 | 0.45 |
| GI-R7 | 2020 | 0.30 | 1085 | 245 | 2.69 | 0.69 | 0.45 |
| GI-R6 | 1790 | 0.43 | 145 | 27 | 2.69 | 0.69 | 0.45 |
| GI-N7 | 1610 | 0.56 | 700 | 170 | 2.53 | 0.91 | 0.73 |

amount of water that needs to be added to get the required flowability. The dry density of mix GI-R6 is lower compared to the mixes GI-R5 and GI-R7, because the amount of sand is low, and the amount of fly ash is more in GI-R6. The specific gravity of fly ash is only 2.42 against 2.69 of river sand, R. The lower specific gravity of waste foundry sand, N results in a further lower value of dry density of mix GI-N7.

The void ratio is a fundamental parameter in soils, and can be estimated very easily. However, in flowable fill, the presence of three solid phases (sand, fly ash and cement) with different specific gravities makes the computation of void ratio difficult. Besides, the hydrated cement will have a different volume and specific gravity compared to its original values. The fly ash also would react to some extent. In this study, the fly ash used was class F, which does not react by itself. In the presence of cement, fly ash would undergo pozzolanic reaction. However, in flowable fill, the amount of cement is small, and therefore, a small amount of class F fly ash would react, leaving the rest of it inert. The cement after hydration contains non-evaporable water equal to around 23% of its original weight, and the hydrated cement paste will have around 54 % increase in the solid volume (Mindess and Young, 1981). It is assumed here that the weight of hydrated cement paste is 23 % higher than the original weight. The specific gravity of cement paste would then change from 3.17 to (3.17 x 1.23/1.54 ) 2.53. The equivalent specific gravity, $G_{eq}$ of the three phases is here defined as total weight of the three phases divided by the weight of water whose volume is equal to the volume of the three phases together. For example, the $G_{eq}$ and void ratio, e can be computed for mix GI-R5 as follows:

$$G_{eq} = \frac{1488+378+30\times1.23}{\frac{1488}{2.69}+\frac{378}{2.42}+\frac{30\times1.23}{2.53}} = 2.63 \qquad (8.2)$$

Note that the weight of sand specified in the mix (1512 kg/m$^3$) is the surface saturated dry weight. Dividing this weight by the absorption (1.6 % for this sand) would give an equivalent

$$e = \frac{G}{\gamma_d} - 1 = \frac{2.63}{2} - 1 = 0.32 \tag{8.3}$$

dry weight of 1488 kg/m$^3$ which is used in the calculation of $G_{eq}$. It is interesting to note that the void ratio computed from Mercury Intrusion Porosimetry was also 0.32.

### 8.3.2 Stress-Strain Response

Figures 8.2 through 8.17 show the results of consolidated drained triaxial (CD) tests on the four mixes GI-R5, GI-R7, GI-R6 and GI-N7 at different confining pressures. Figures 8.18 through 8.23 show the results of consolidated undrained triaxial (CU) tests on two mixes GI-R5 and GI-R7.

General shape of the stress-strain curves can be explained by referring to Figure 8.24. For example, the stress-strain curve at 400 kPa confining pressure for this sample starts off with a linear portion up to an axial strain of around 0.8%, and the sample tends to decrease in volume. The curve then becomes non-linear during which time the sample tends to further decrease in volume until a zero rate of volume change is reached, and the dilation follows. The deviator stress continues to increase and reaches a peak value. The deviator stress gradually decreases and tends to reach a residual value.

The peak strength does not necessarily coincide with the point of maximum rate of dilation (the point where the slope of volumetric strain vs axial strain curve is maximum), unlike in sands. The reason for this is that the strength of flowable fill samples has three components due to: cementation, friction, and dilation. The peak strength is obtained when sum of these components is maximum.

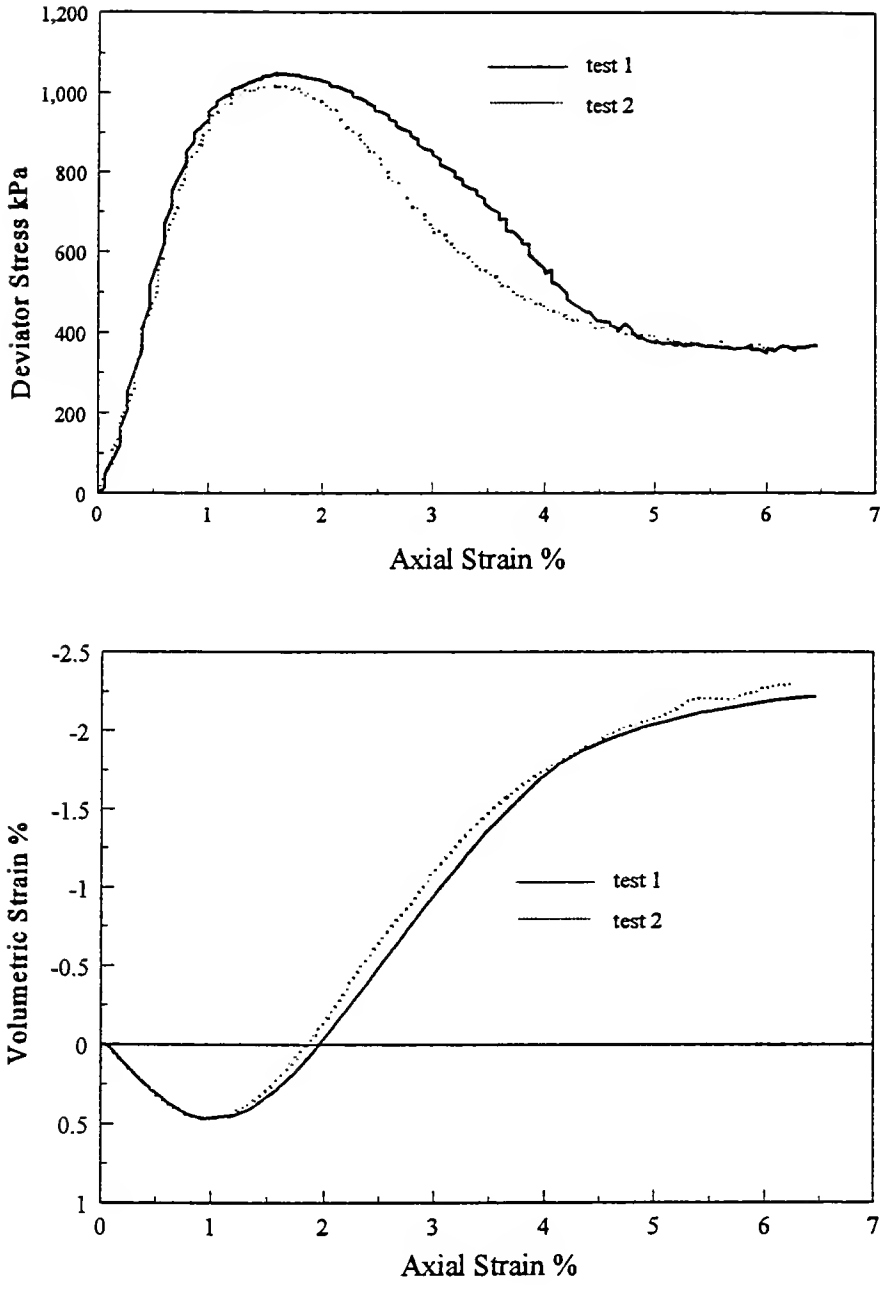


Figure 8.2 CD Triaxial Test on GI-R5 at $\sigma_3 = 50$ kPa

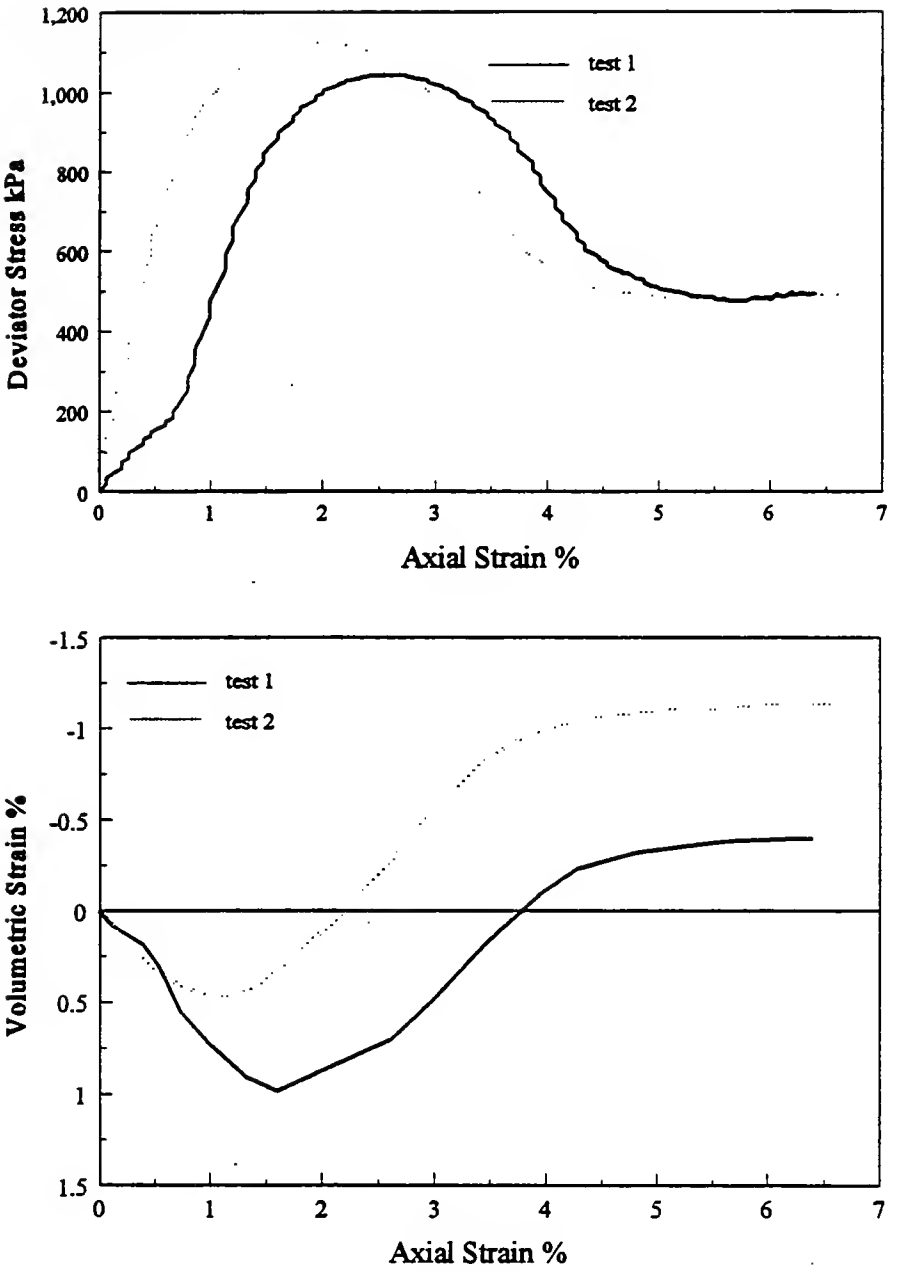


Figure 8.3 CD Triaxial Test on GI-R5 at $\sigma_3$ = 100 kPa

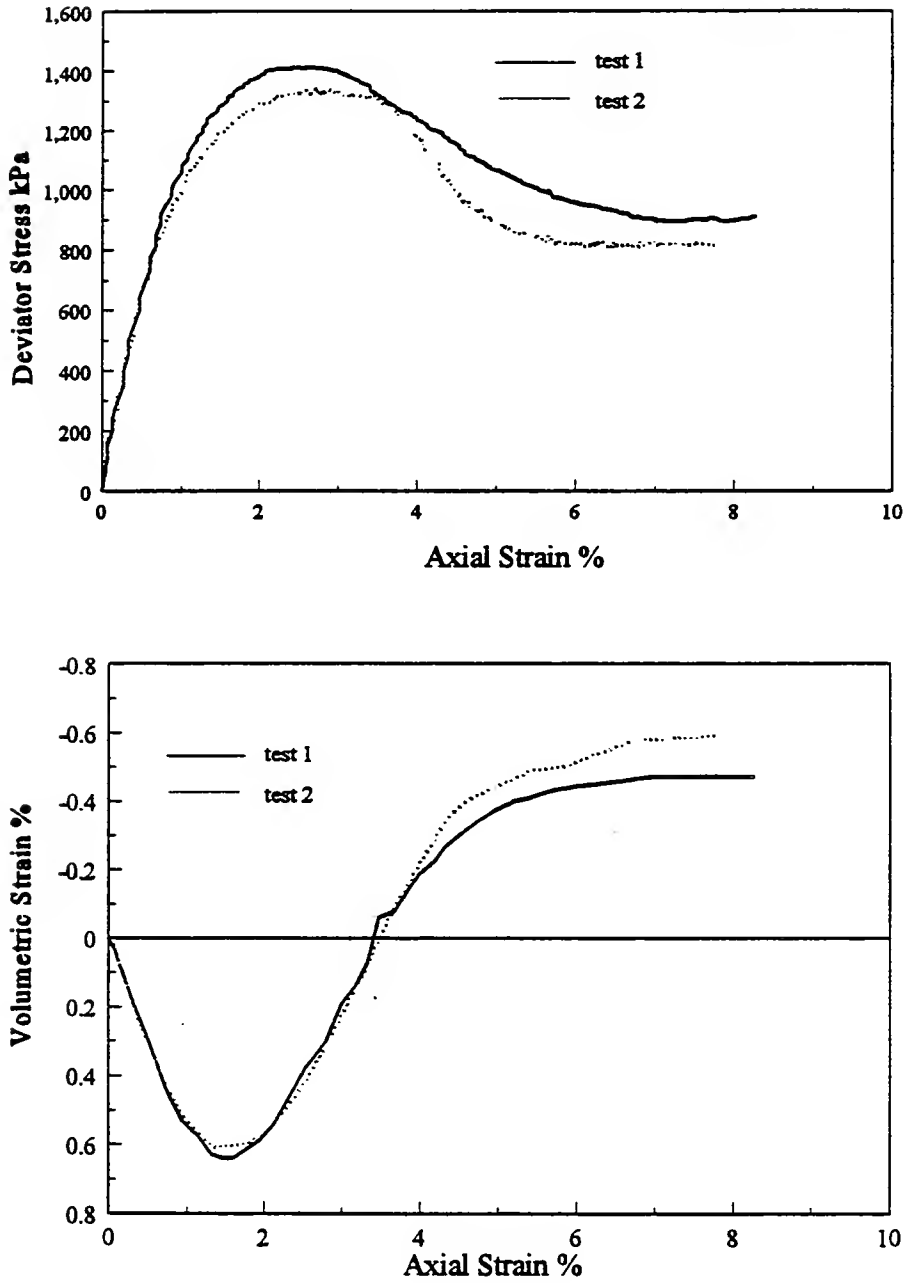


Figure 8.4 CD Triaxial Test on GI-R5 at $\sigma_3 = 200$ kPa

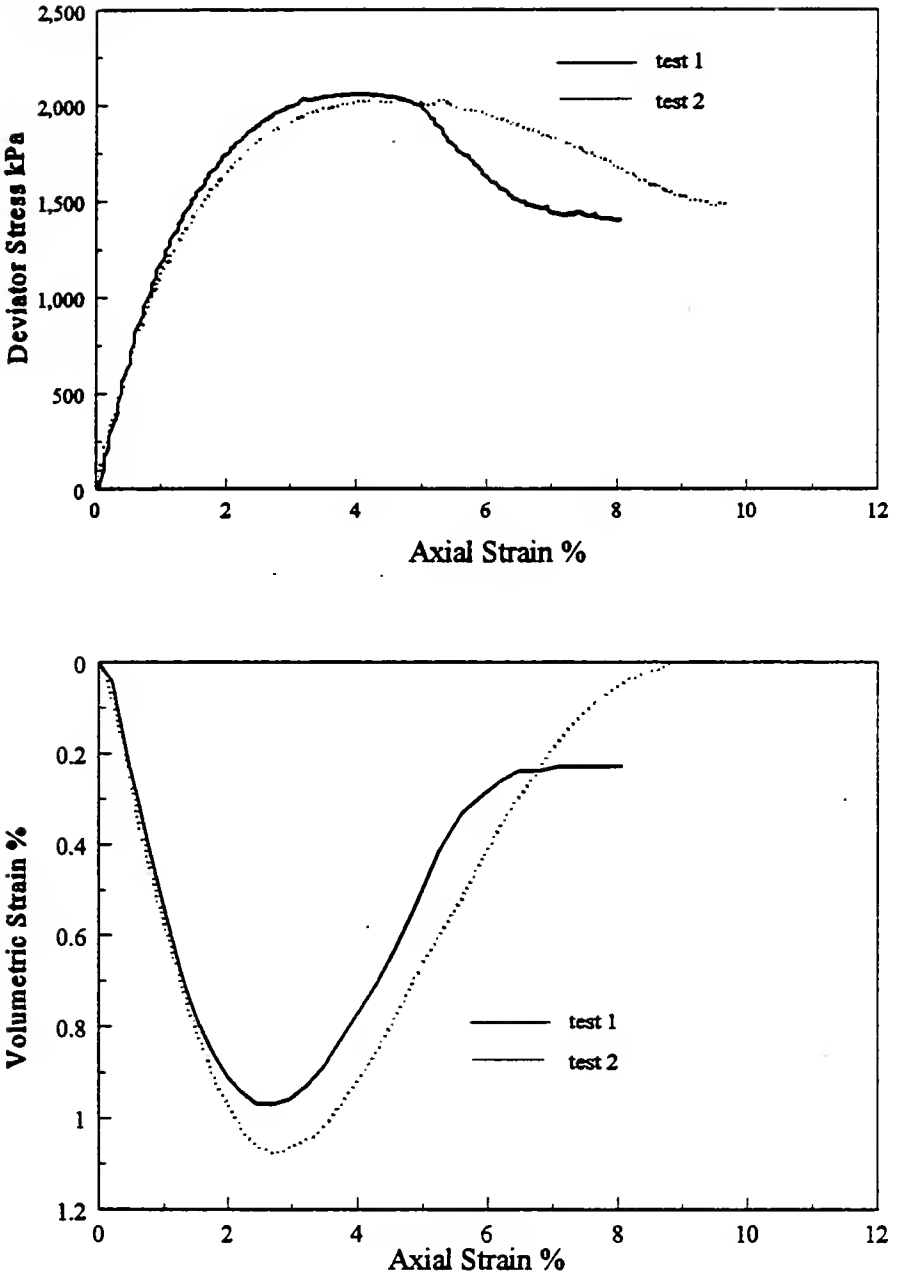


Figure 8.5 CD Triaxial Test on GI-R5 at $\sigma_3$ = 400 kPa

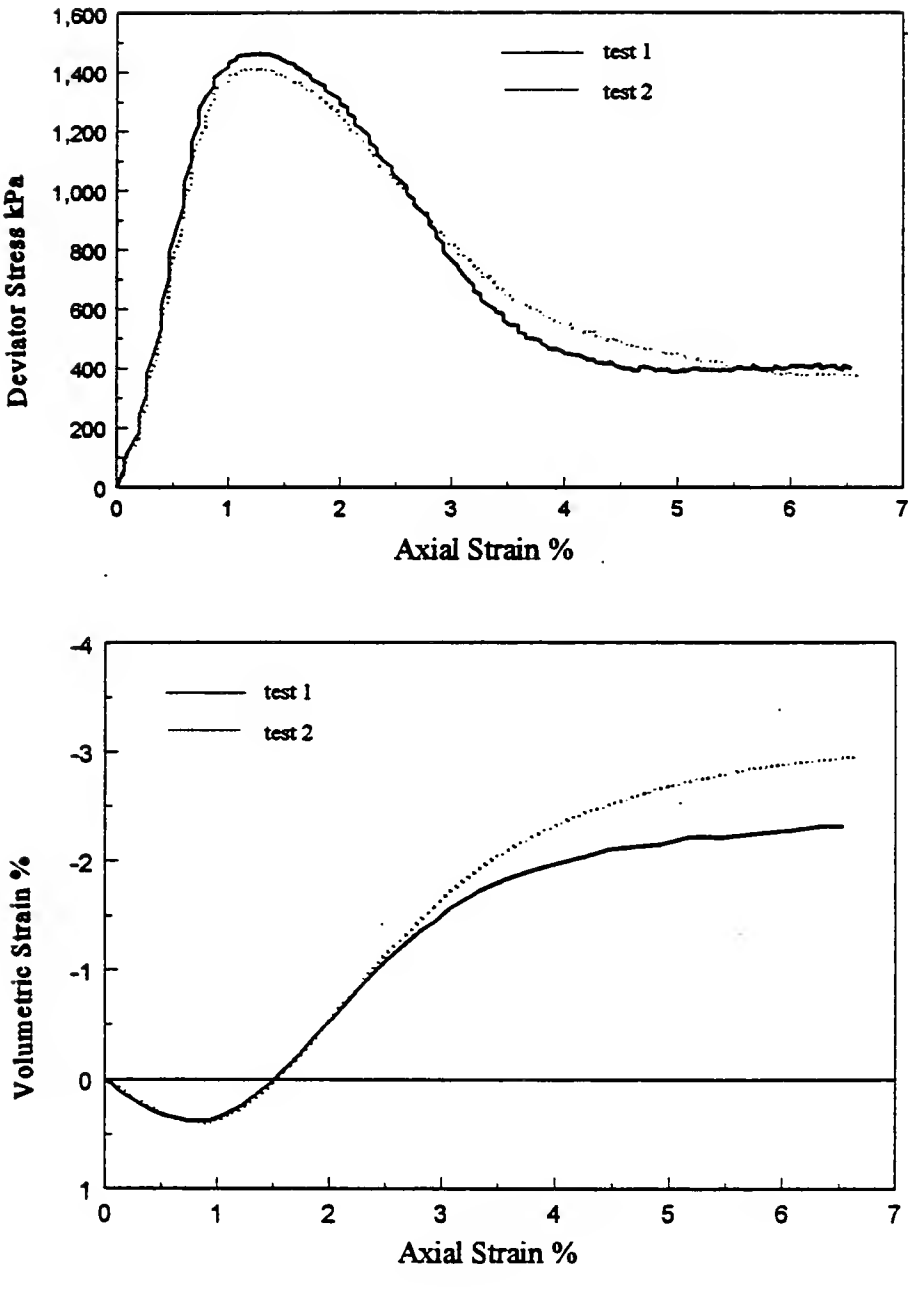


Figure 8.6 CD Triaxial Test on GI-R7 at $\sigma_3 = 50$ kPa

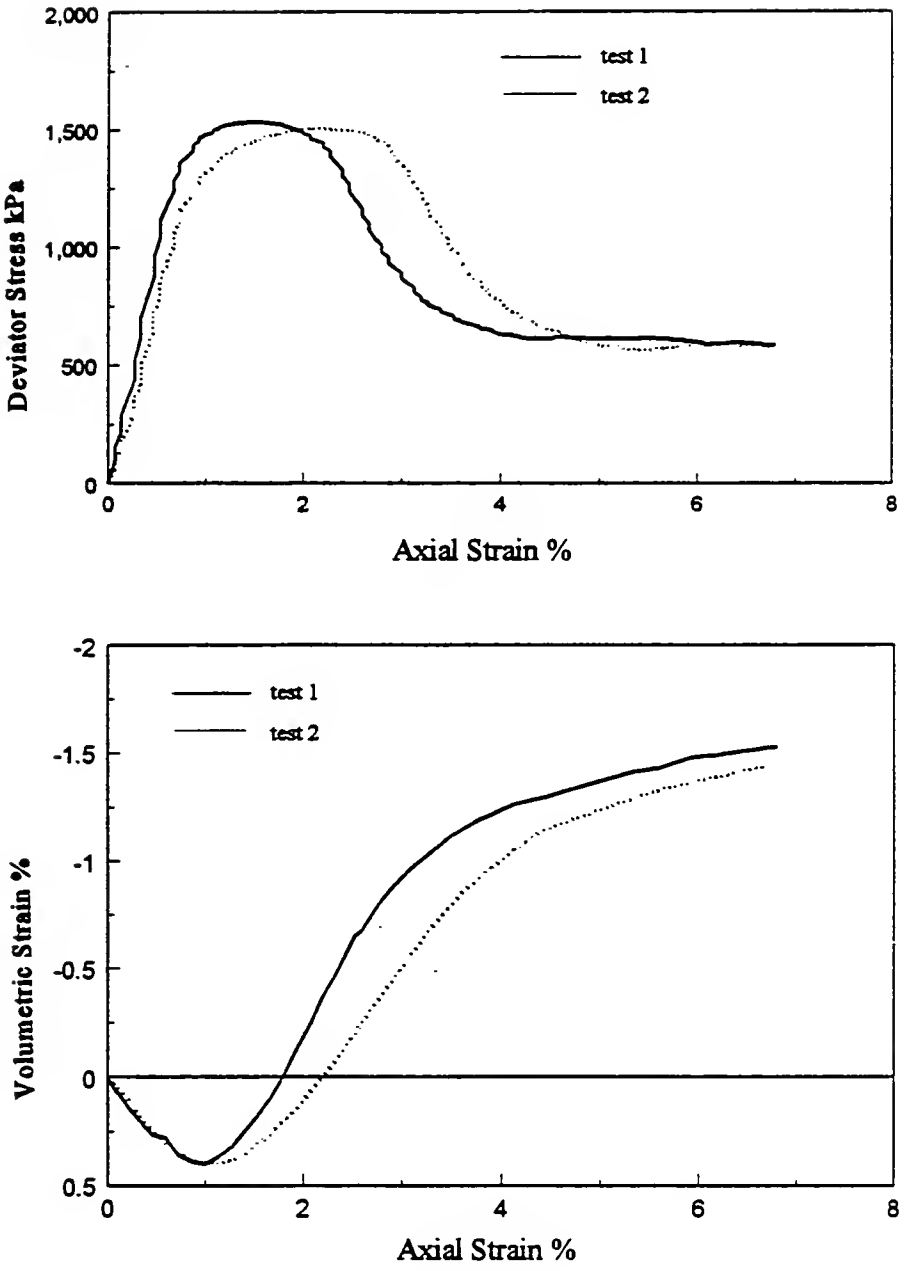


Figure 8.7 CD Triaxial Test on GI-R7 at $\sigma_3$ = 100 kPa

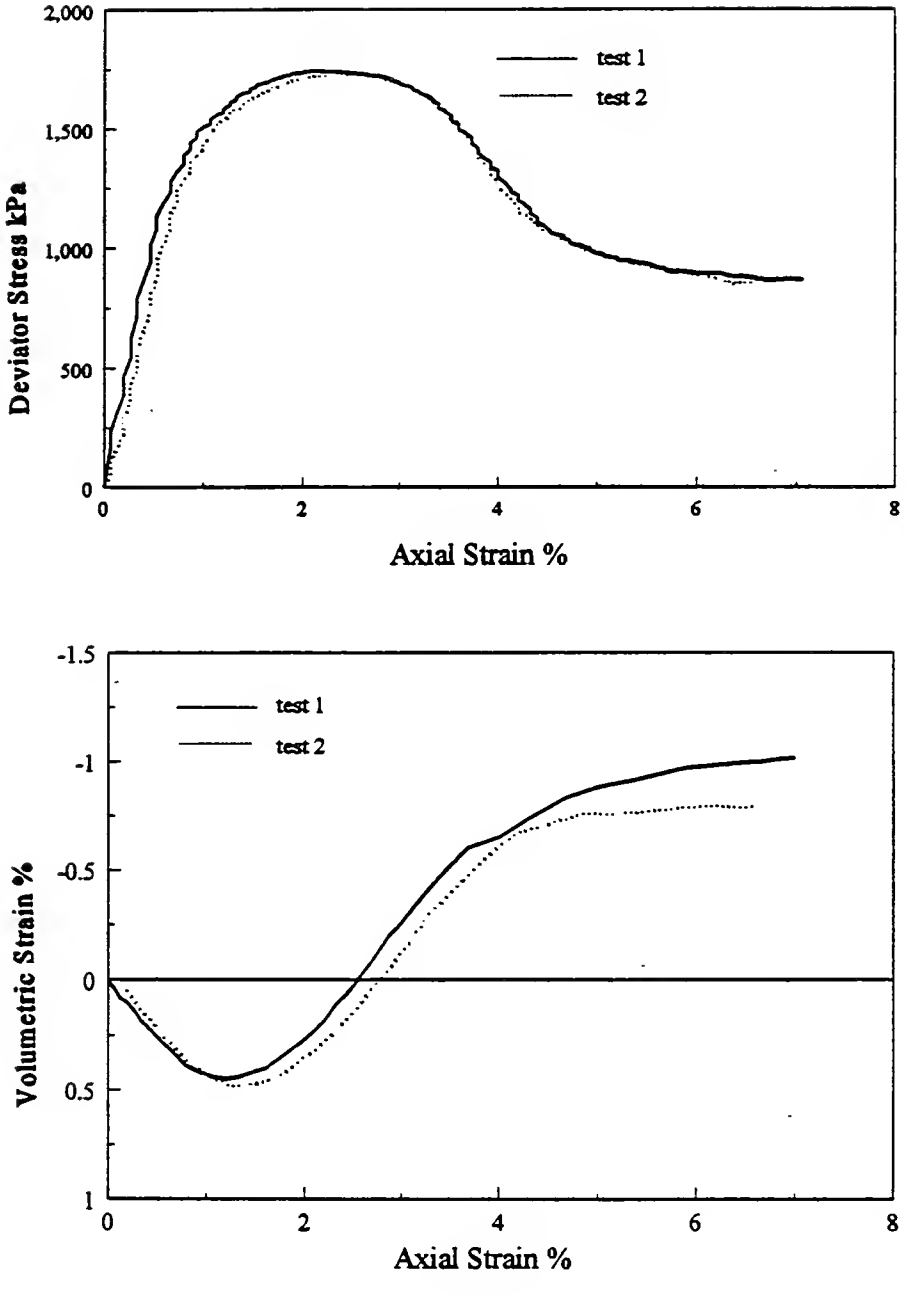


Figure 8.8 CD Triaxial Test on GI-R7 at $\sigma_3$ = 200 kPa

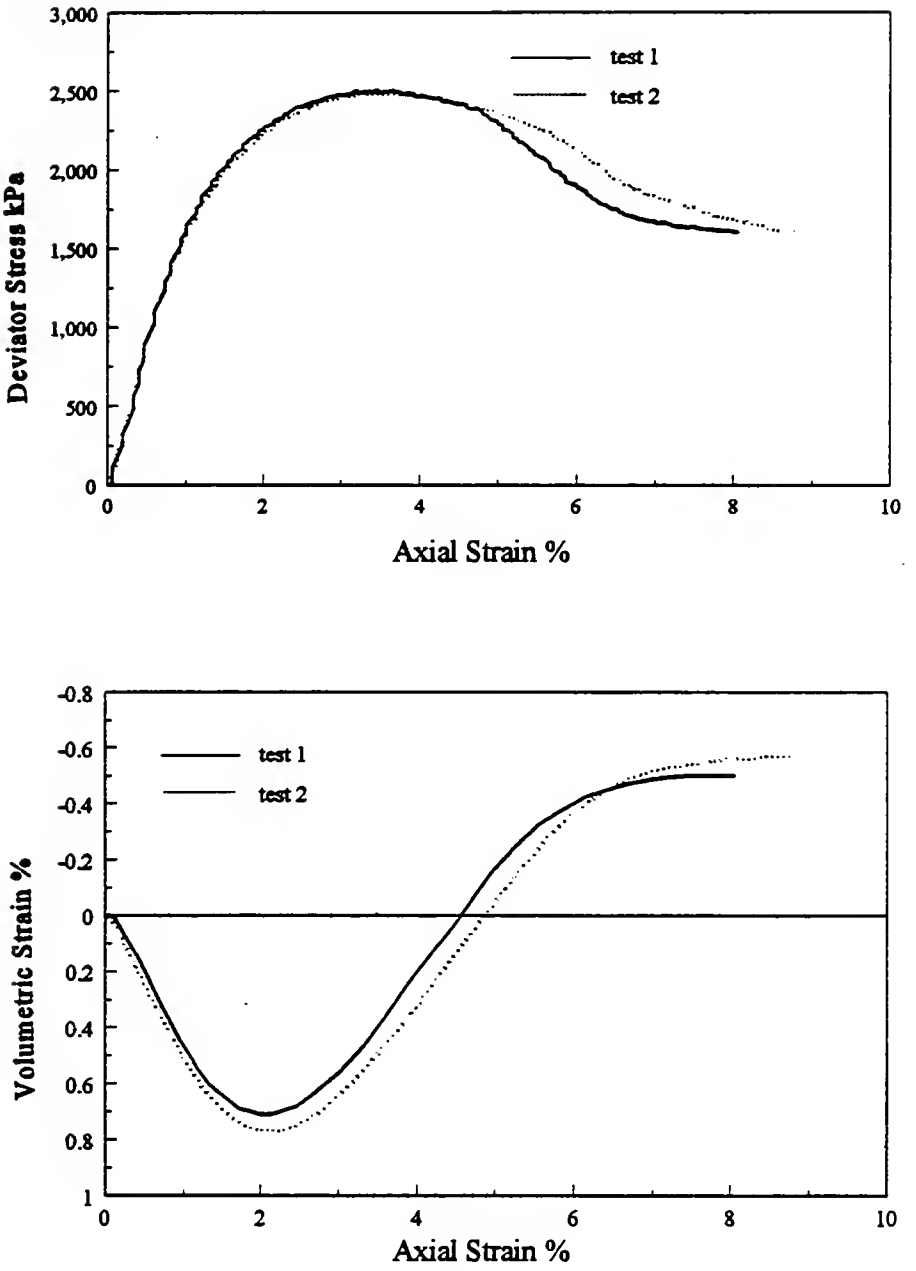


Figure 8.9 CD Triaxial Test on GI-R7 at $\sigma_3$ = 400 kPa

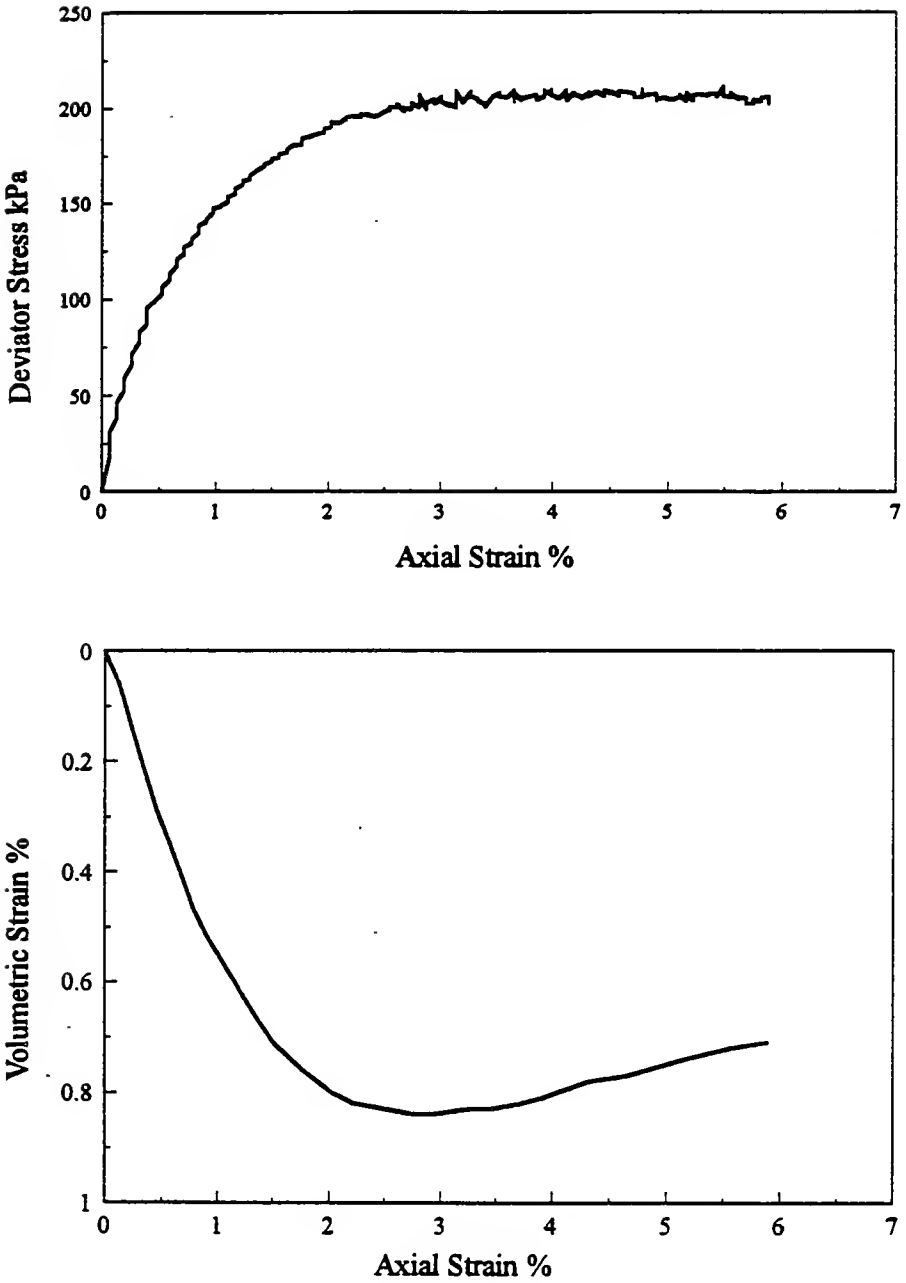


Figure 8.10 CD Triaxial Test on GI-R6 at $\sigma_3$ = 50 kPa

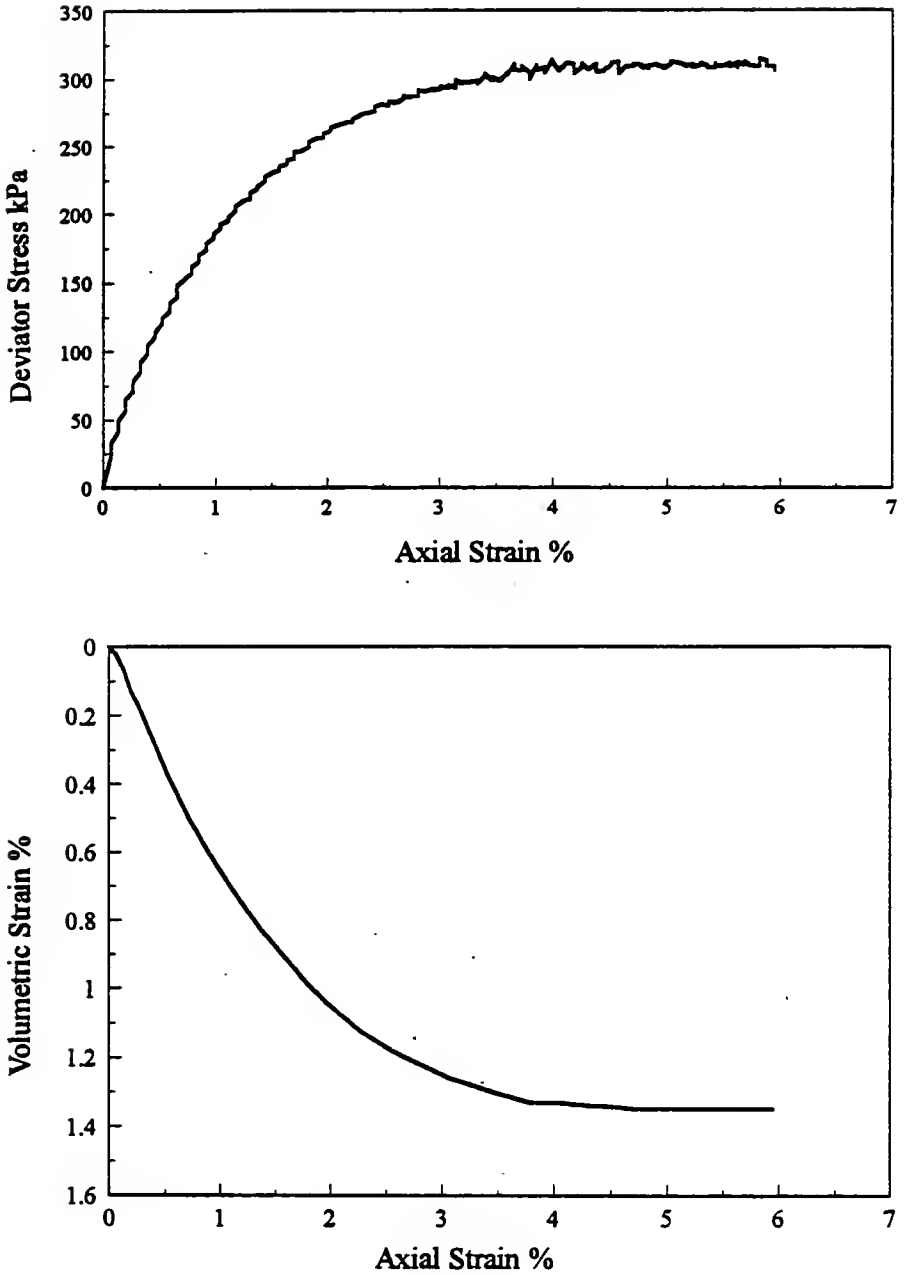


Figure 8.11 CD Triaxial Test on GI-R6 at $\sigma_3$ = 100 kPa

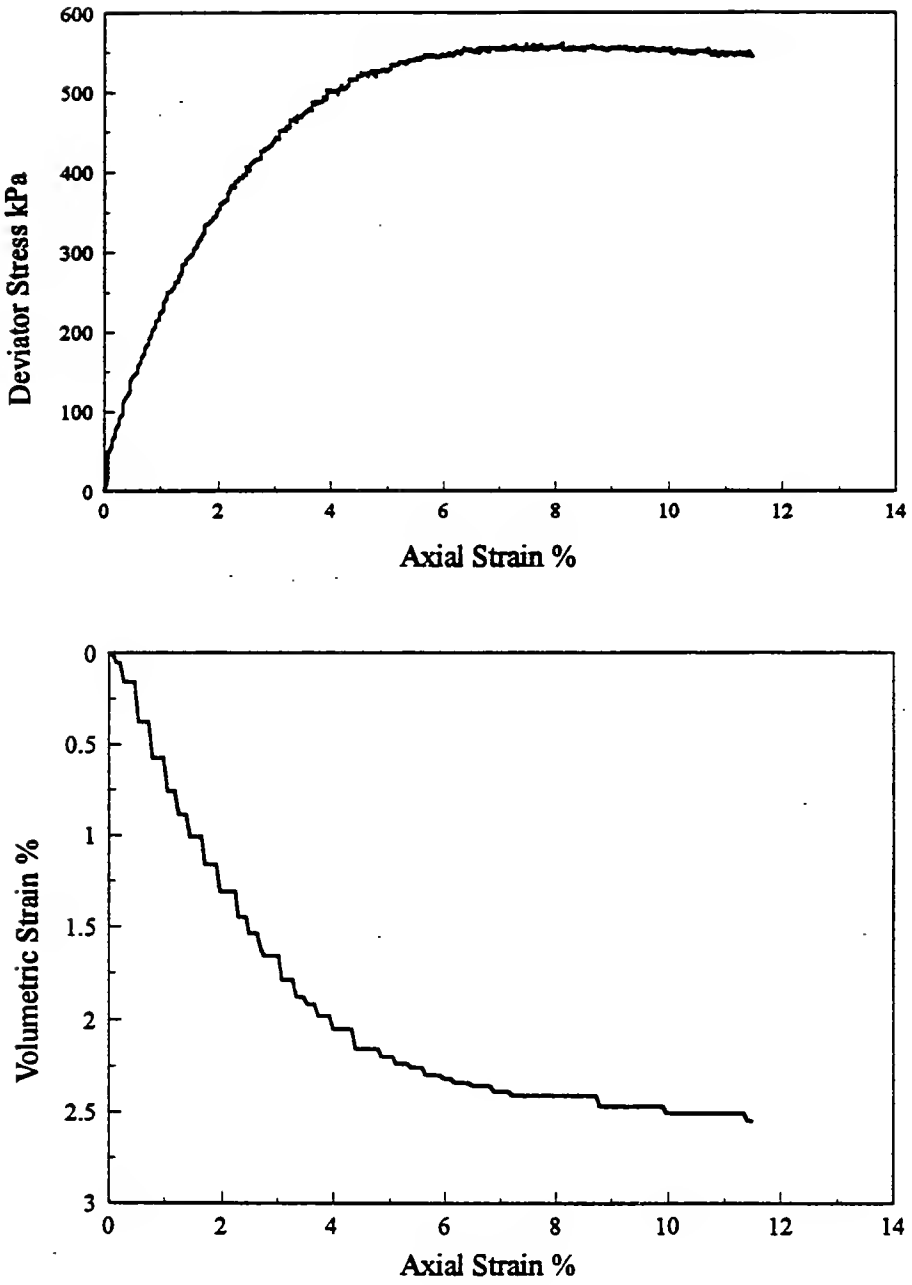


Figure 8.12 CD Triaxial Test on GI-R6 at $\sigma_3$ = 200 kPa

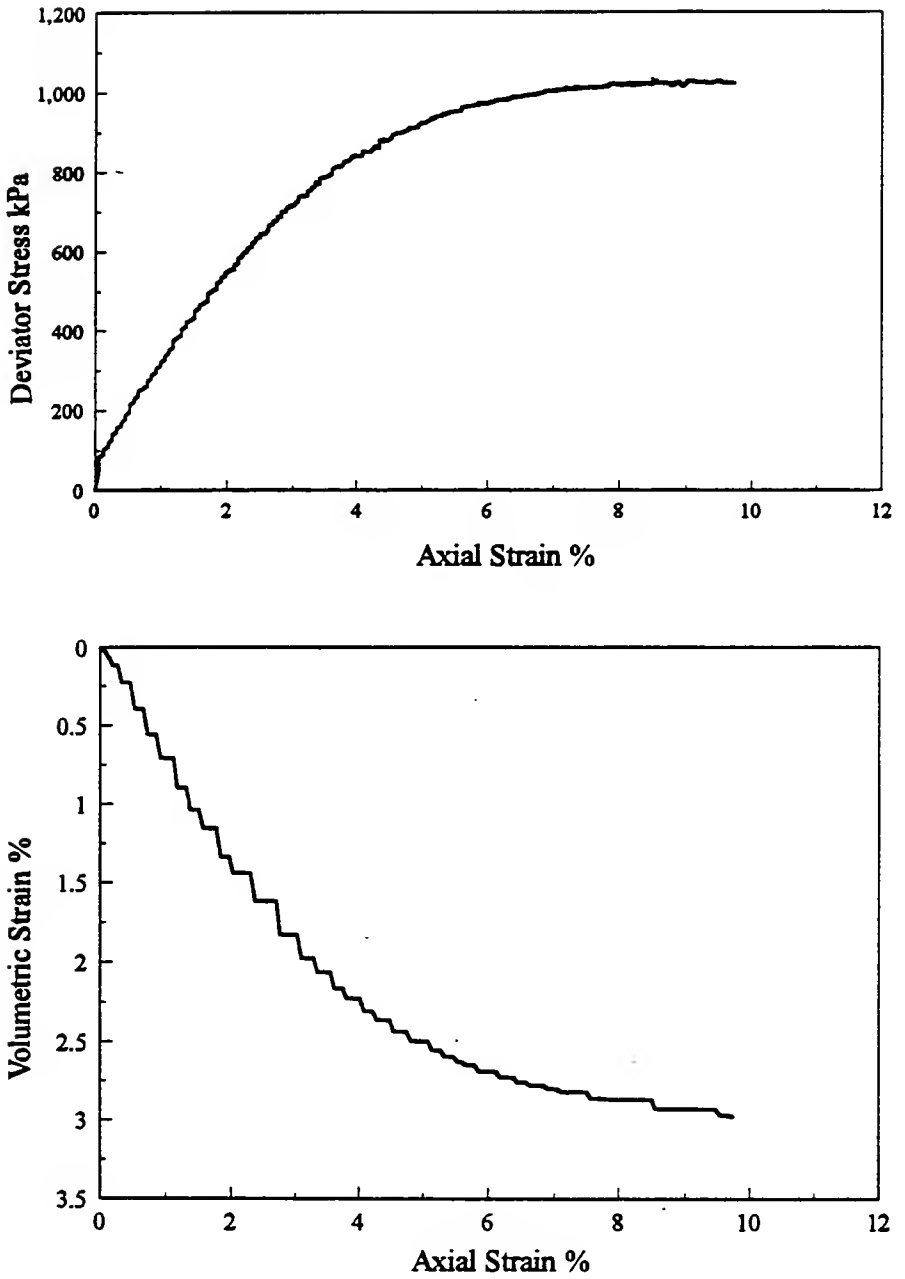


Figure 8.13 CD Triaxial Test on GI-R6 at $\sigma_3$ = 400 kPa

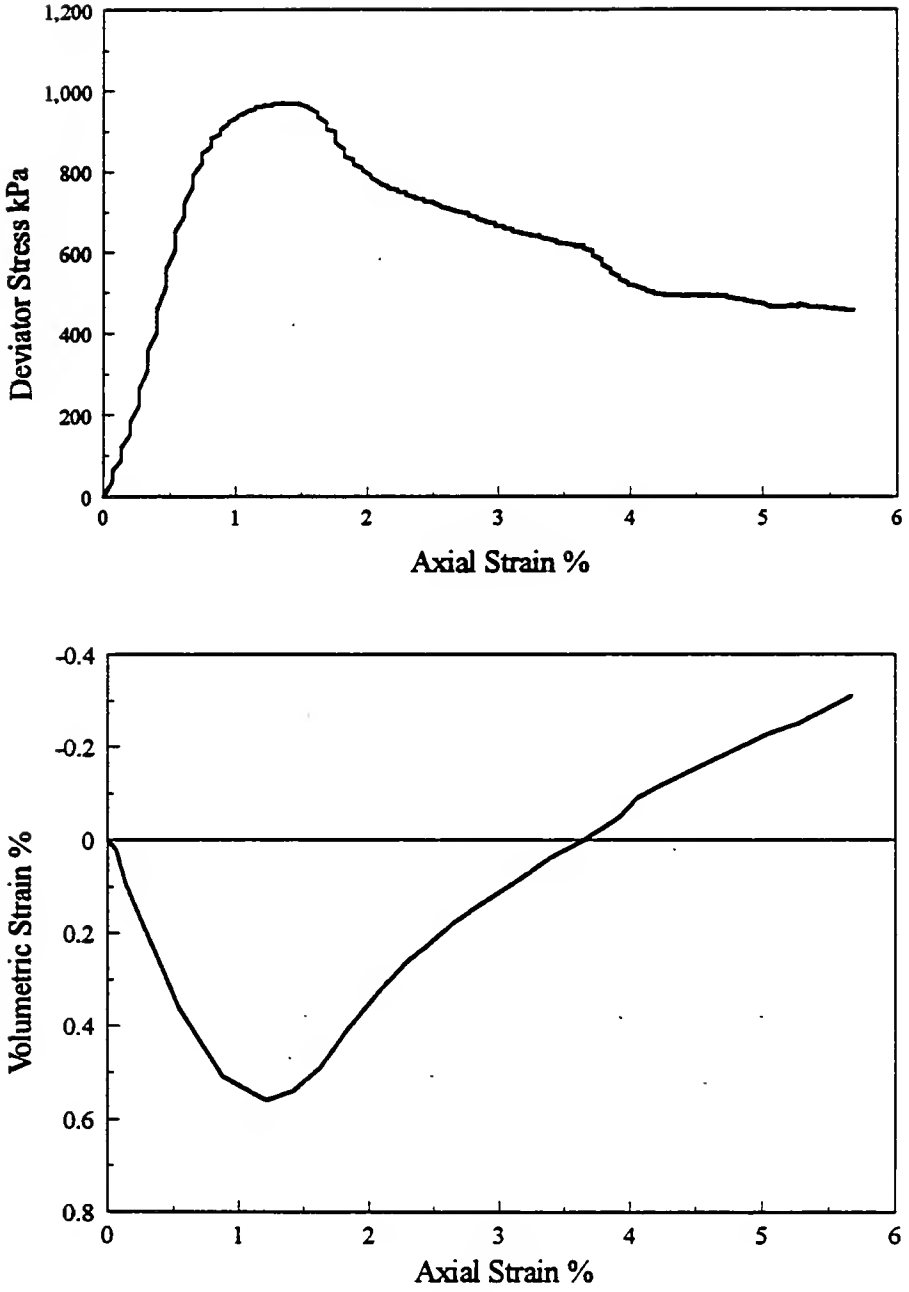


Figure 8.14 CD Triaxial Test on GI-N7 at $\sigma_3$ = 50 kPa

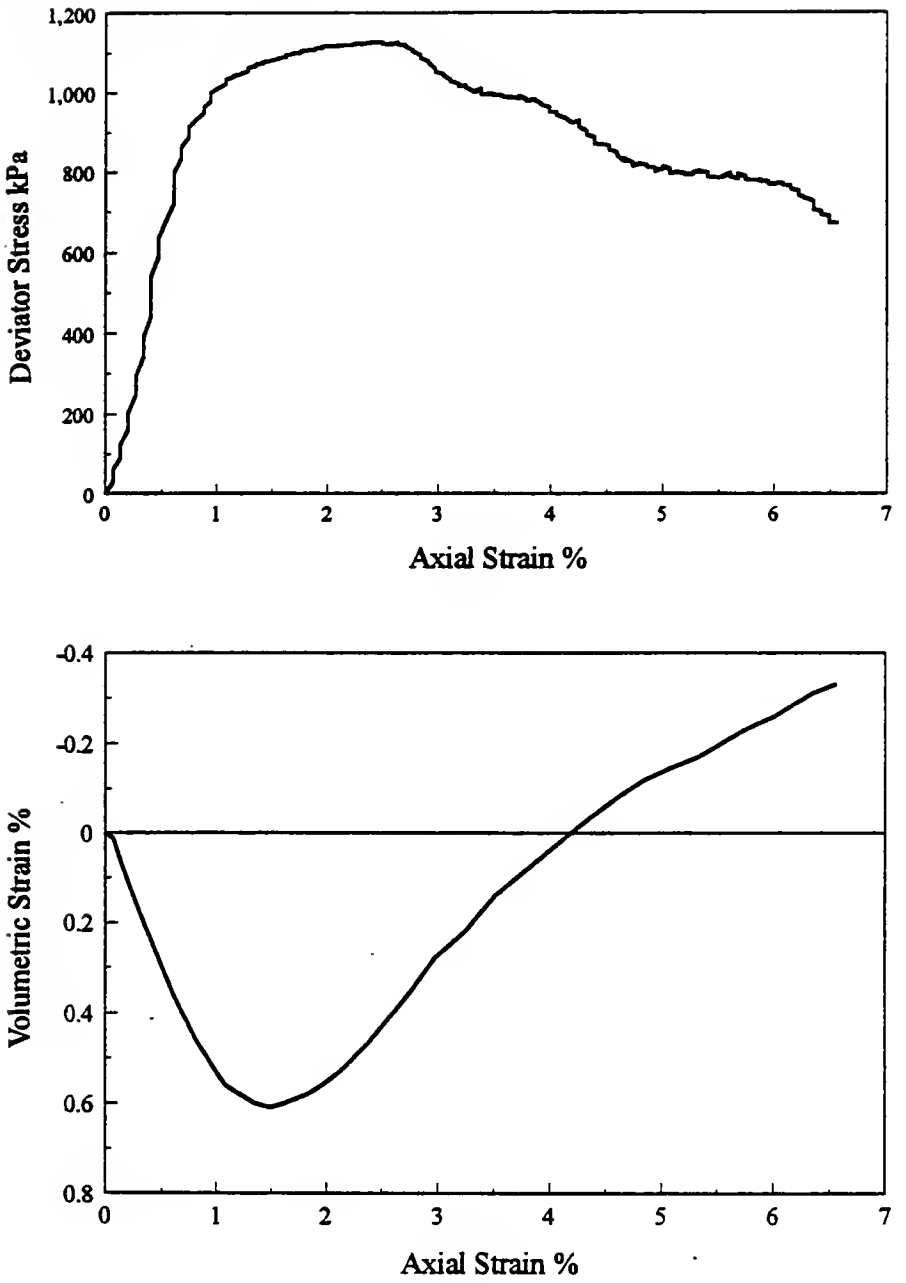


Figure 8.15 CD Triaxial Test on GI-N7 at $\sigma_3$ = 100 kPa

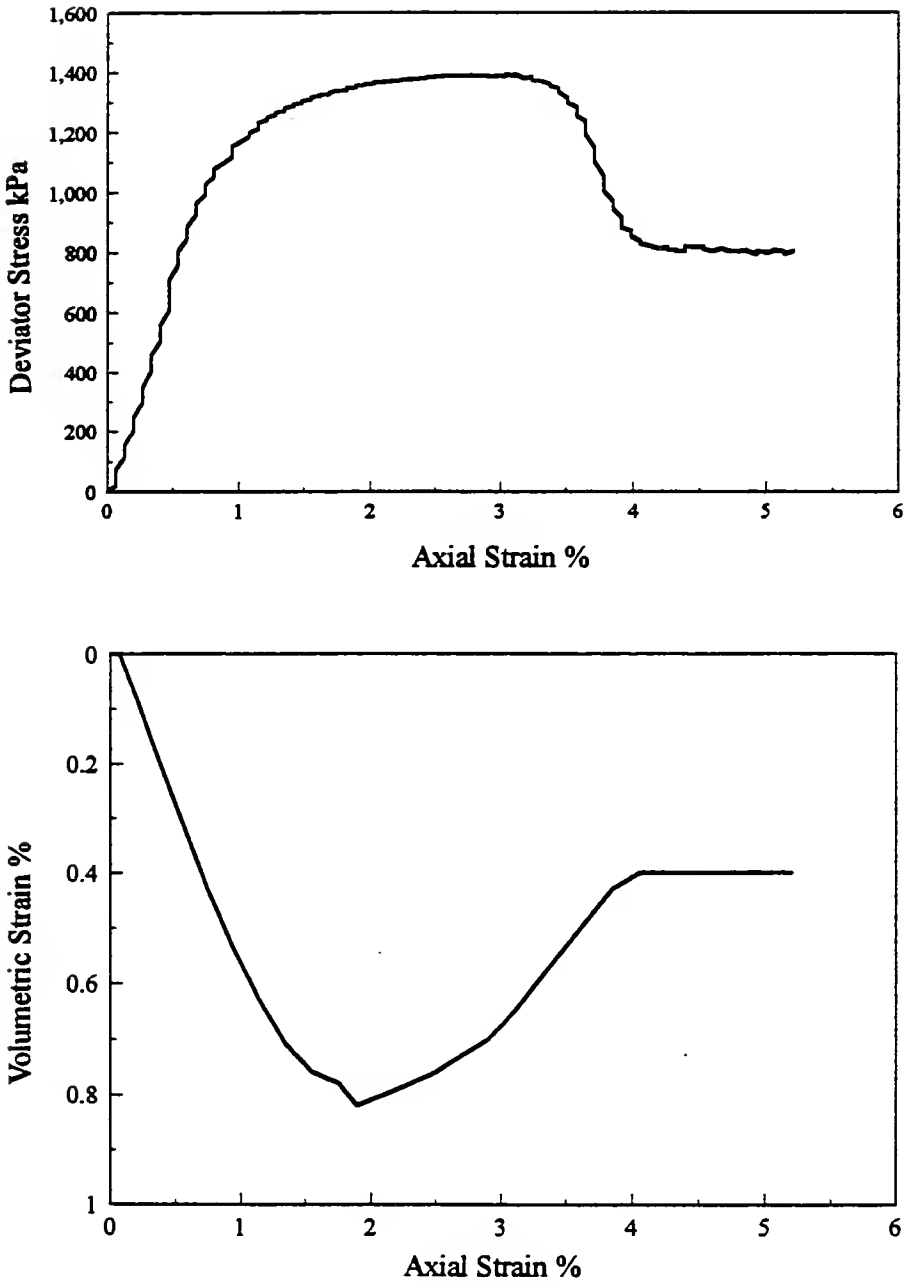


Figure 8.16 CD Triaxial Test on GI-N7 at $\sigma_3$ = 200 kPa

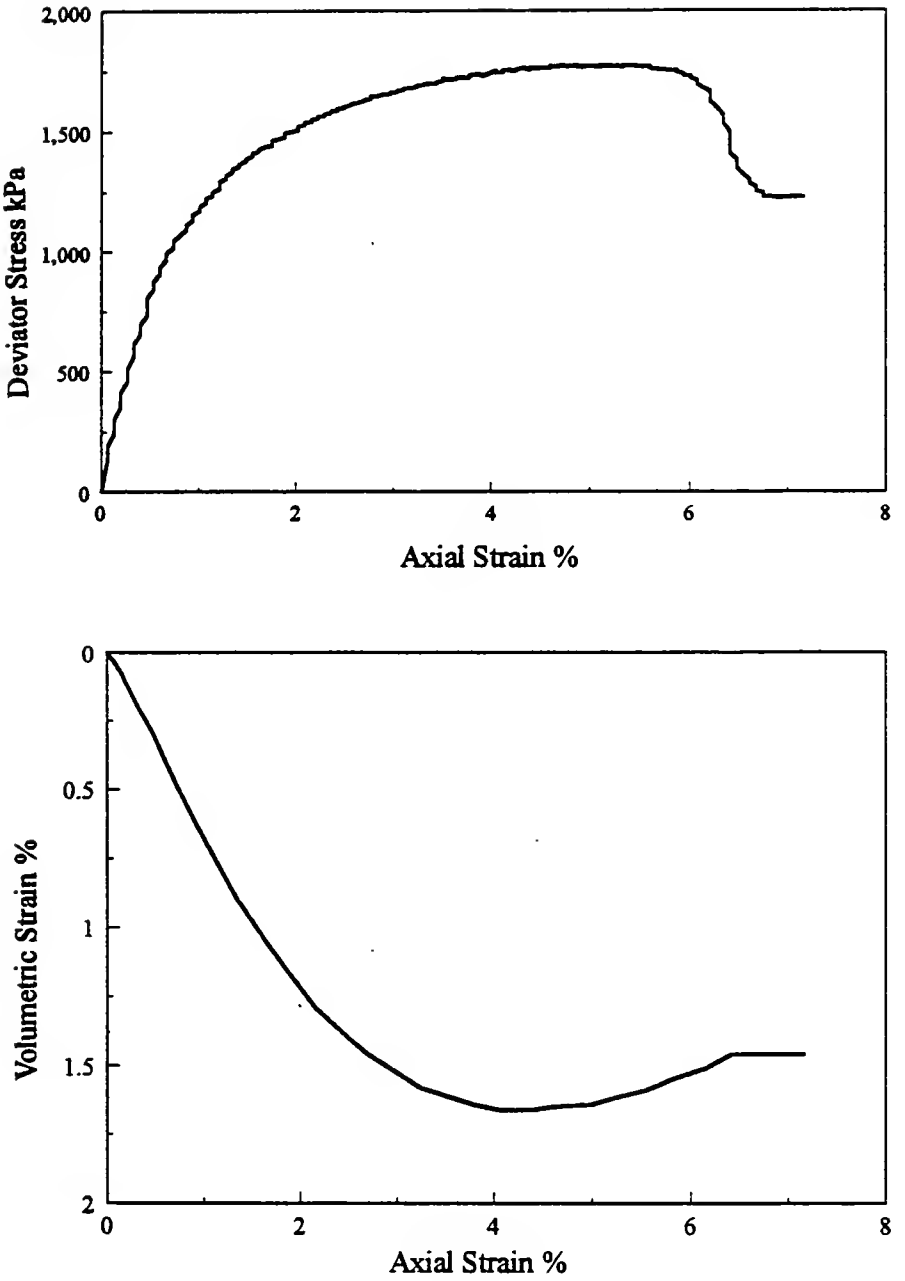


Figure 8.17 CD Triaxial Test on GI-N7 at $\sigma_3$ = 400 kPa

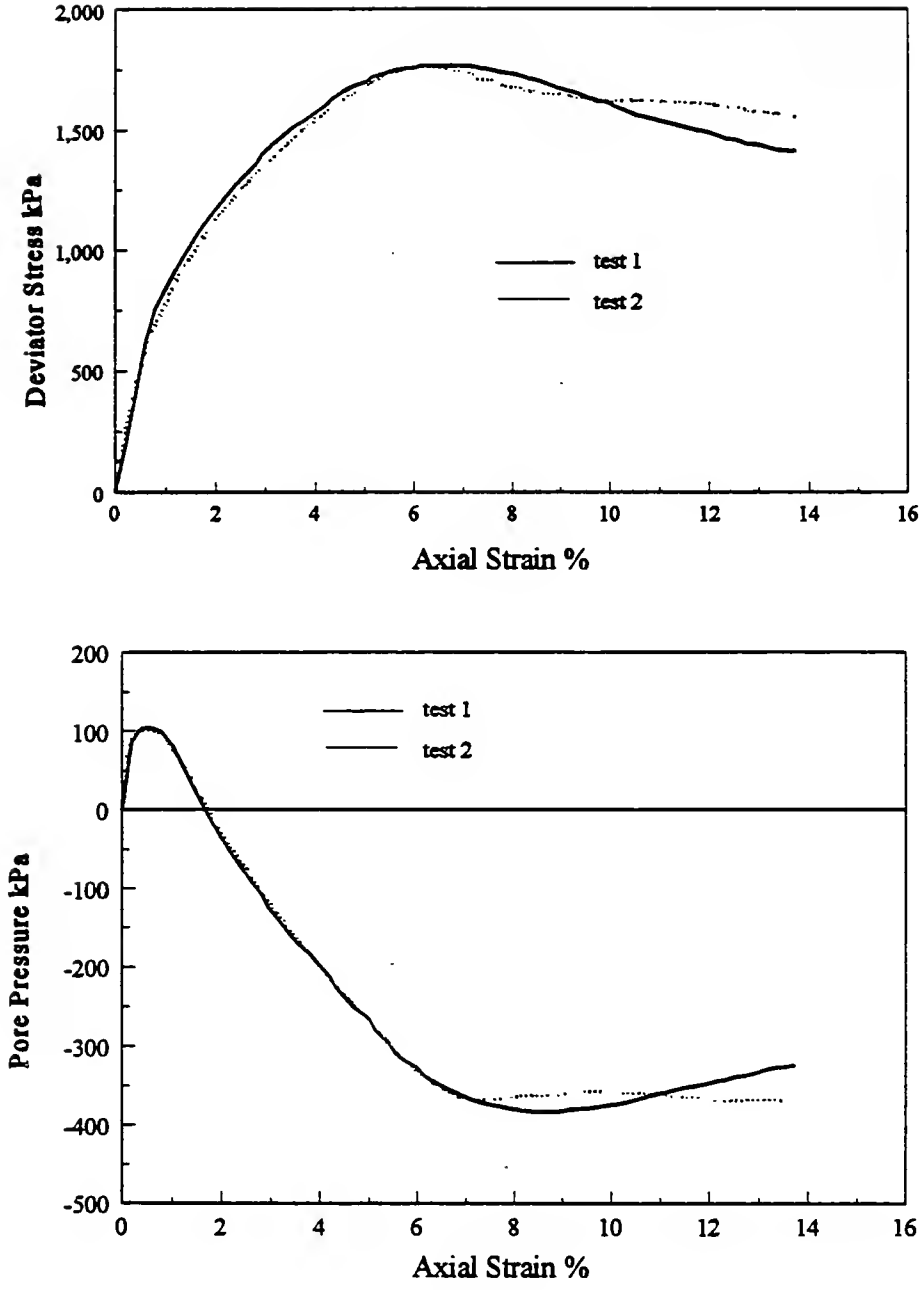


Figure 8.18 CU Triaxial Test on GI-R5 at $\sigma_3$ = 100 kPa

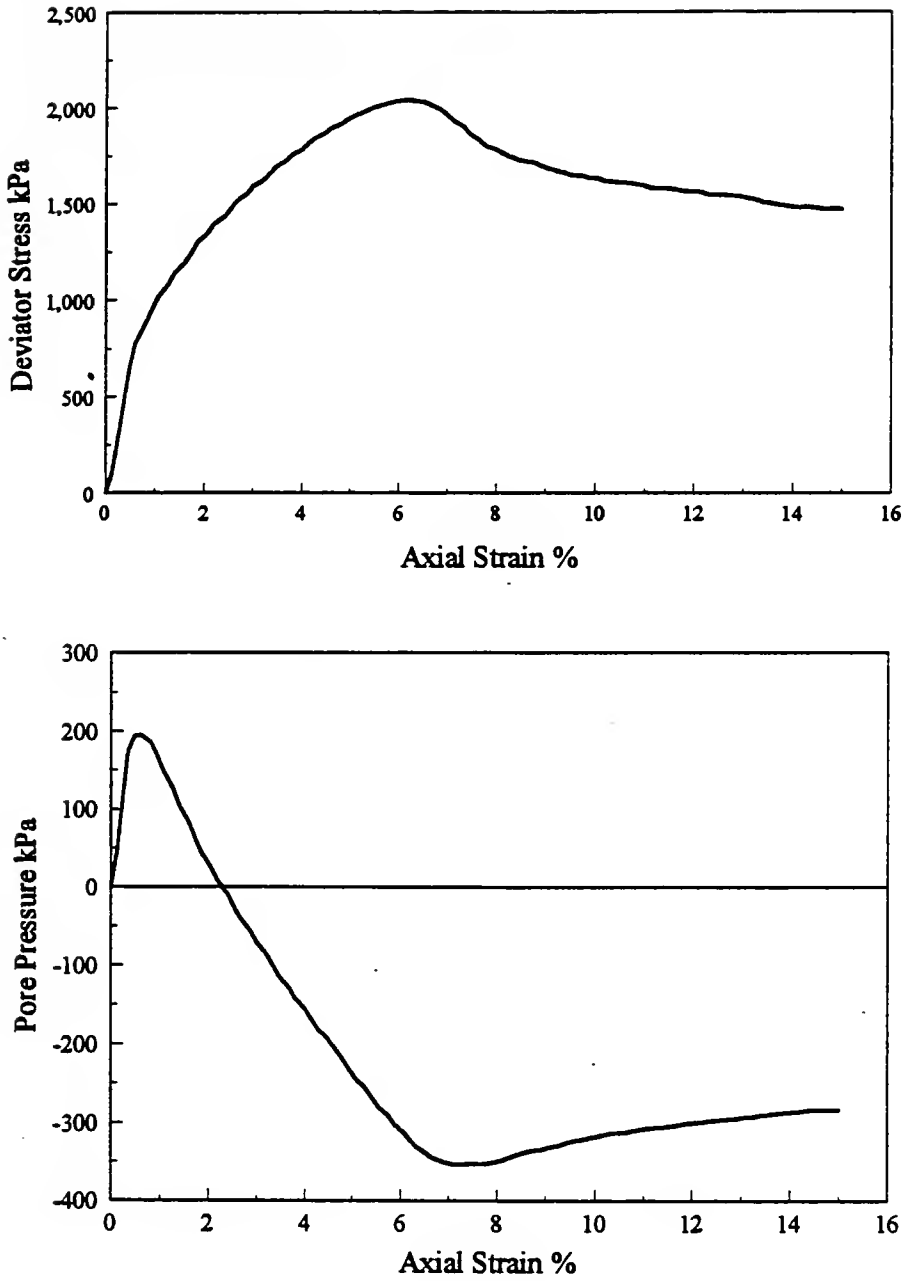


Figure 8.19 CU Triaxial Test on GI-R5 at $\sigma_3$ = 200 kPa

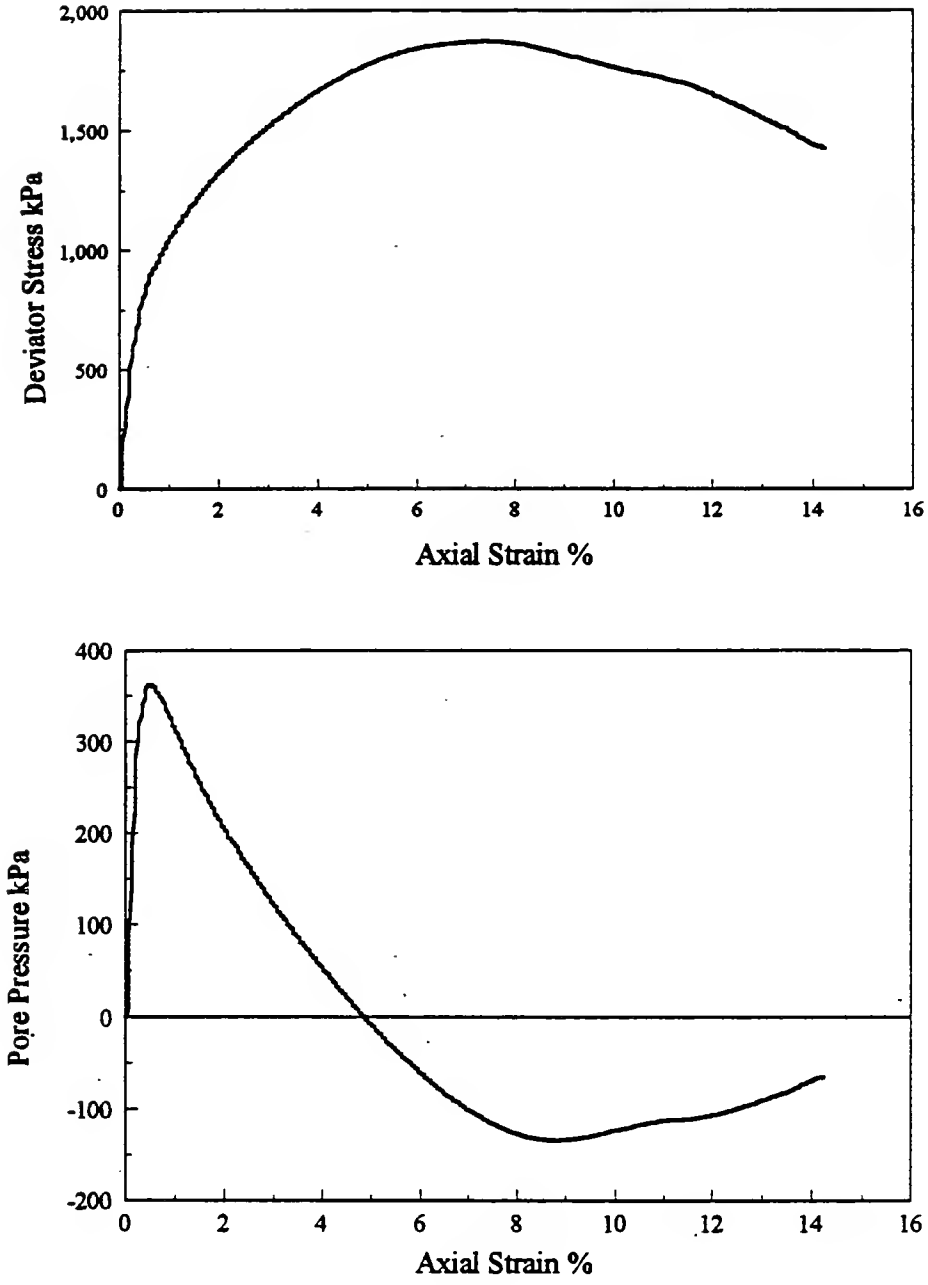


Figure 8.20 CU Triaxial Test on GI-R5 at $\sigma_3$ = 400 kPa

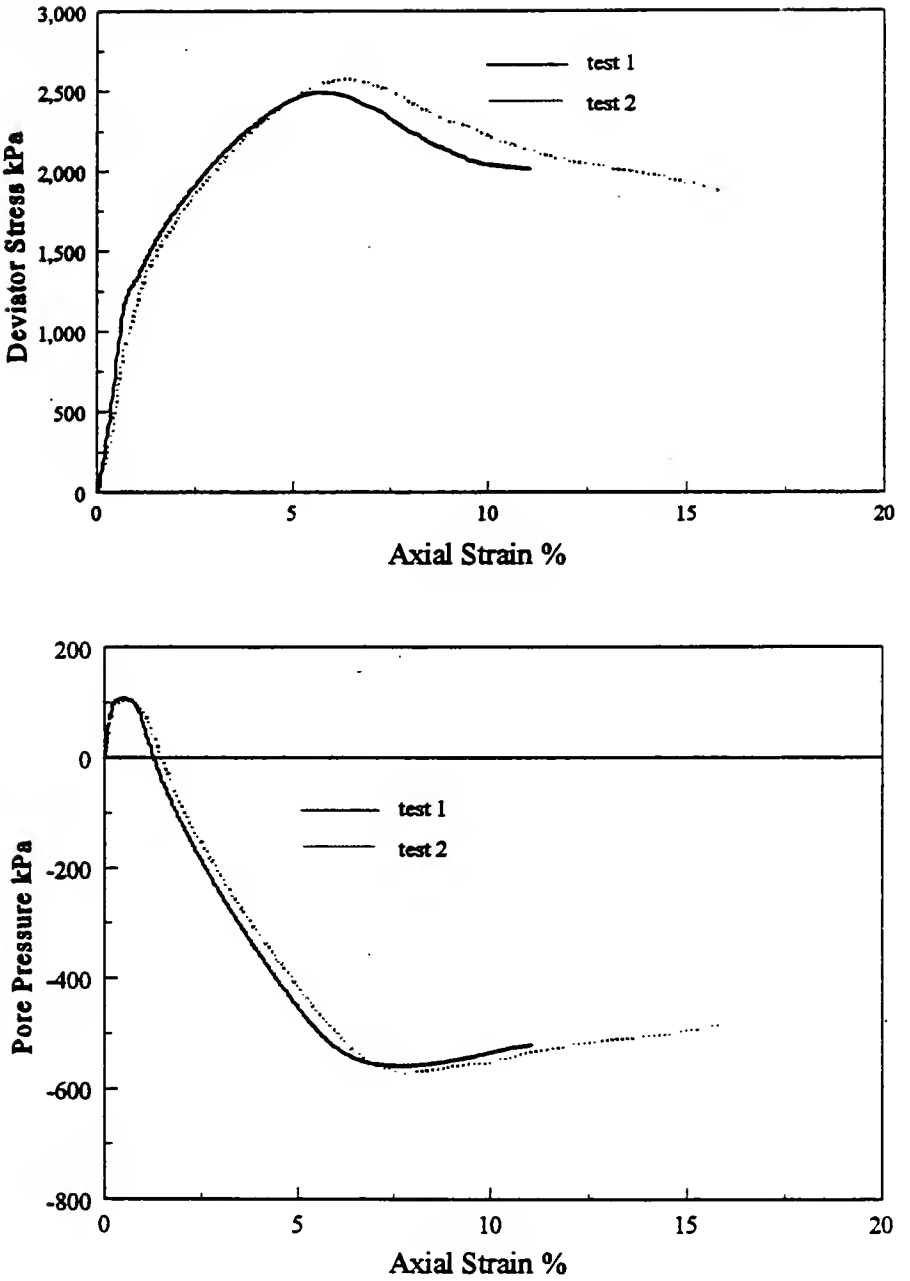


Figure 8.21 CU Triaxial Test on GI-R7 at $\sigma_3$ = 100 kPa

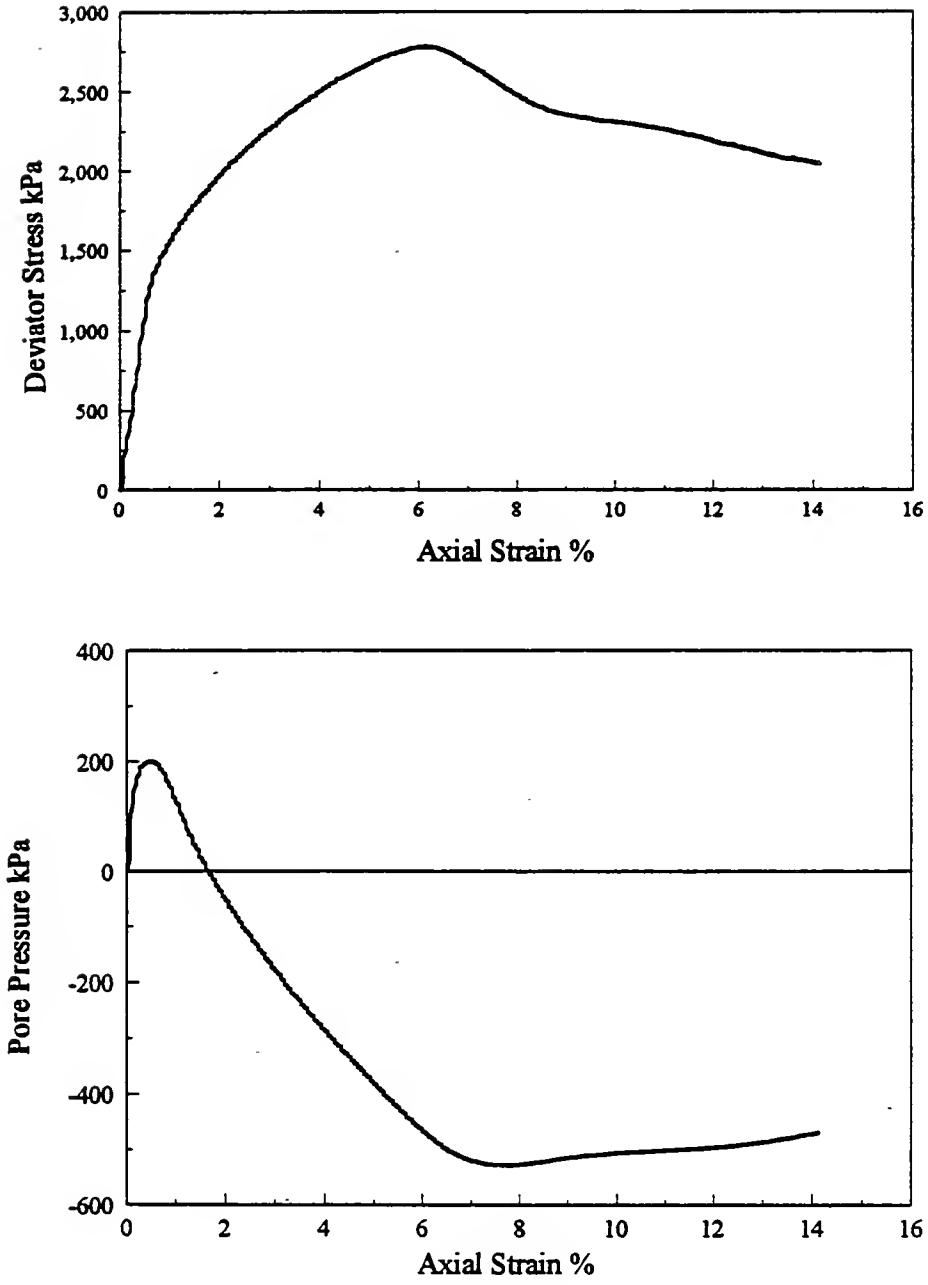


Figure 8.22 CU Triaxial Test on GI-R7 at $\sigma_3$ = 200 kPa

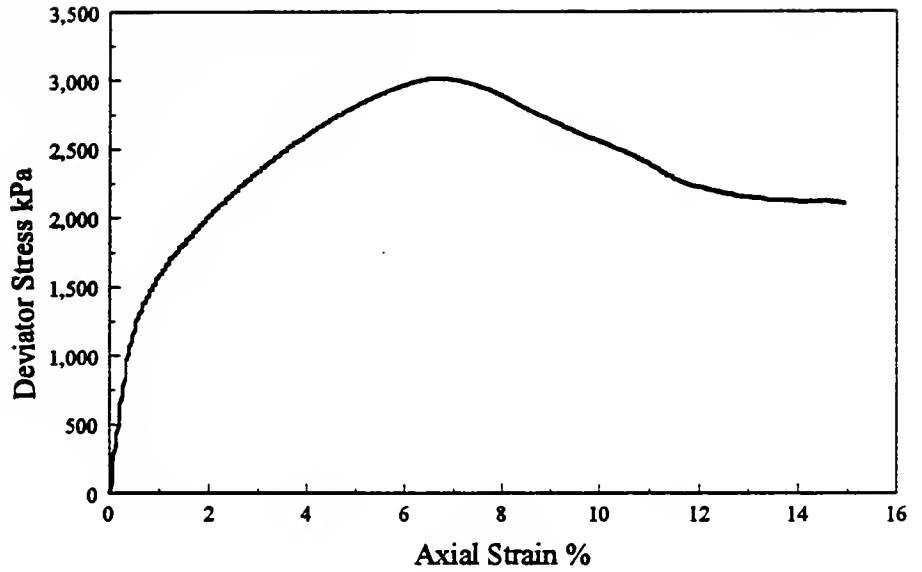


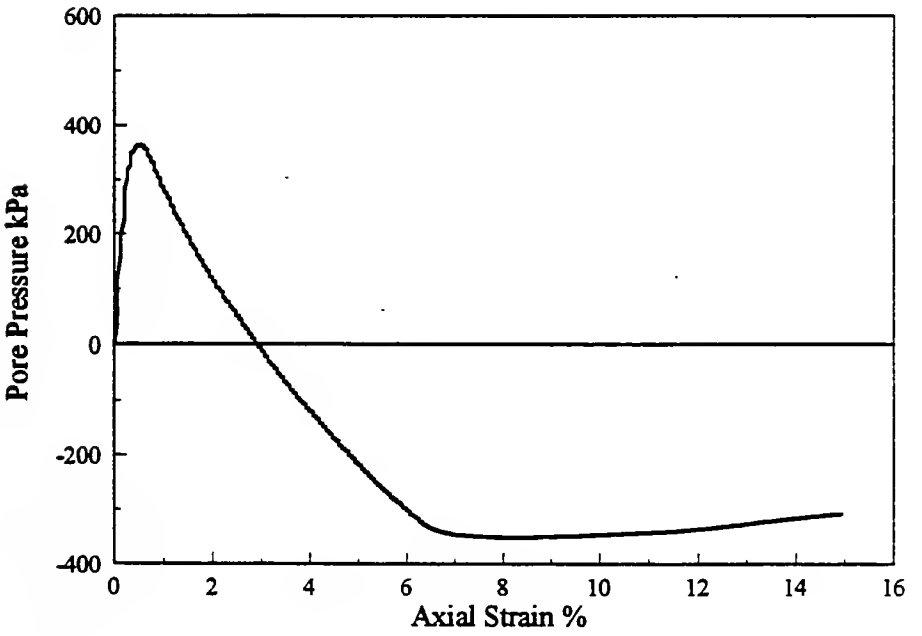


Figure 8.23 CU Triaxial Test on GI-R7 at $\sigma_3$ = 400 kPa

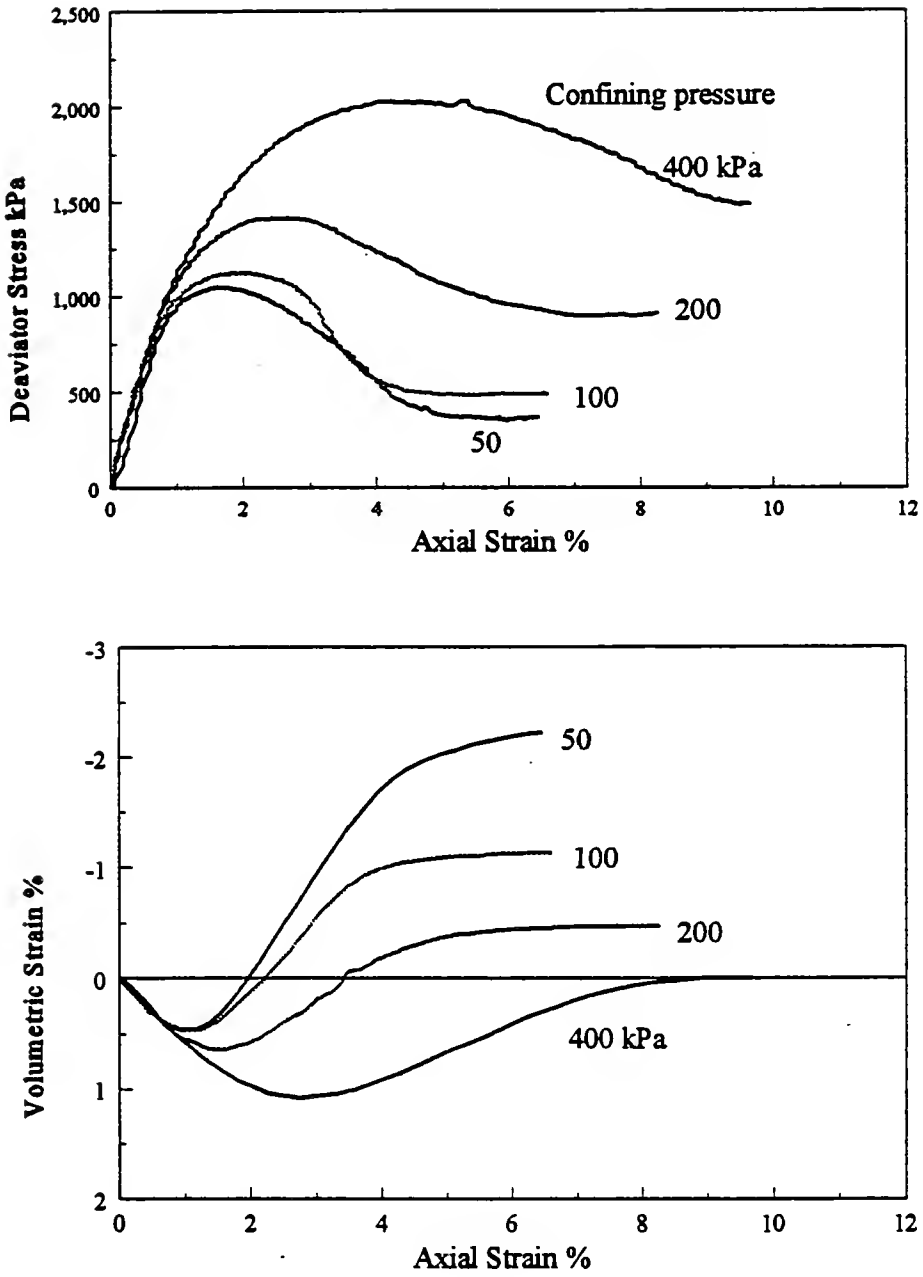


Figure 8.24 CD Triaxial Tests on GI-R5 at Different Confining Pressures

One would speculate that the stress-strain curve eventually reaches a residual or constant volume state or critical state when all the cementation bonds are destroyed during the process of shearing. However, there arises a practical difficulty of making measurements at large strains, to validate this hypothesis: The samples being highly dilatant develop a single distinct shear plane. The post peak shearing is essentially restricted to this narrow band of the sample. However, the measurements made will be interpreted on the assumption that the same phenomenon occurs throughout the sample. Therefore, at large strains, the measurements are not accurate.

For a cemented material, one would expect that the breaking of cementation bonds would result in a sharp peak in the stress-strain curve, and a dramatic post peak behavior with a sudden dip in the stress-strain curve. However, this sample, on the contrary, gives a broad peak, and a gradual decrease in post peak deviator stress.

It can be seen from Figure 8.24 that the increase in confining pressure results in an increase in strength, increases the strain at which peak occurs, and broadens the peak. The increase in confining pressure also decreases the tendency for dilation, decreases the maximum rate of dilation, decreases the amount of final dilation, and increases the strain at which dilation begins.

The mix GI-R7 (35 kg/m$^3$ cement content) is similar to mix GI-R5 (30 kg/m$^3$ cement content) except that it has a slightly higher cement content. The unconfined compressive strength of GI-R5 and GI-R7 were 700 kPa and 1085 kPa respectively (Table 8.1). The samples GI-R7 show stress-strain response similar to samples GI-R5 (Figure 8.25). The effect of increased cementation will be addressed in section 8.3.5.

The mix GI-R6 was designed to study the effect of high fly ash content. The amount of fly ash was 67 % by weight of sand against the value of 25% in the previous mixes GI-R5 and GI-R7. This gave a lower unconfined compressive strength of 145 kPa (Table 8.1). The stress-strain response (Figure 8.26) for these samples was devoid of strain softening which was present in GI-R5 and GI-R7 (Figure 8.24 and 8.25). The failure of the samples during testing was like a non-dilatant soil giving the shape of a barrel to the specimen at the end of the test. The cementation was weaker in these samples indicated by the unconfined

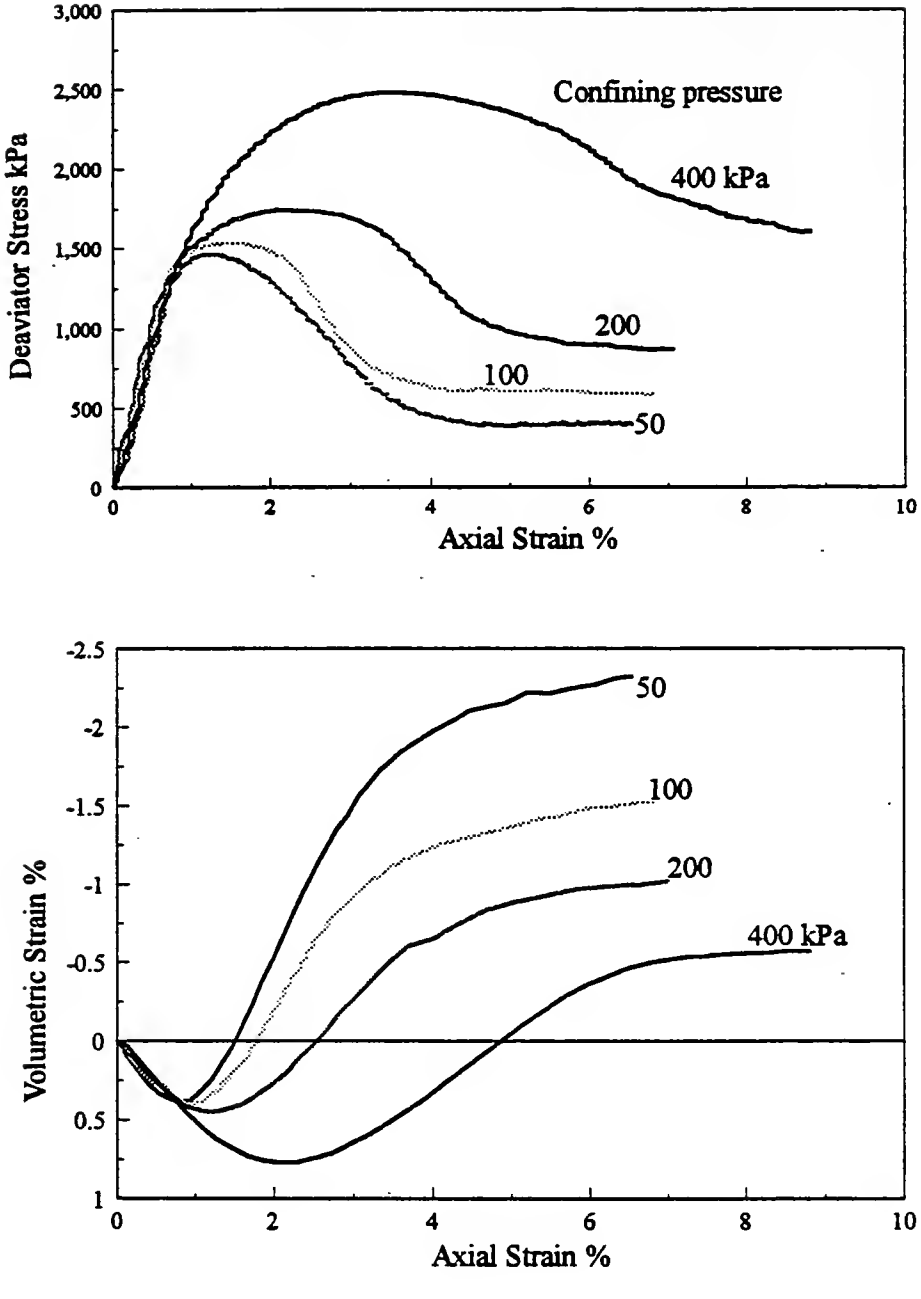


Figure 8.25 CD Triaxial Tests on GI-R7 at Different Confining Pressures

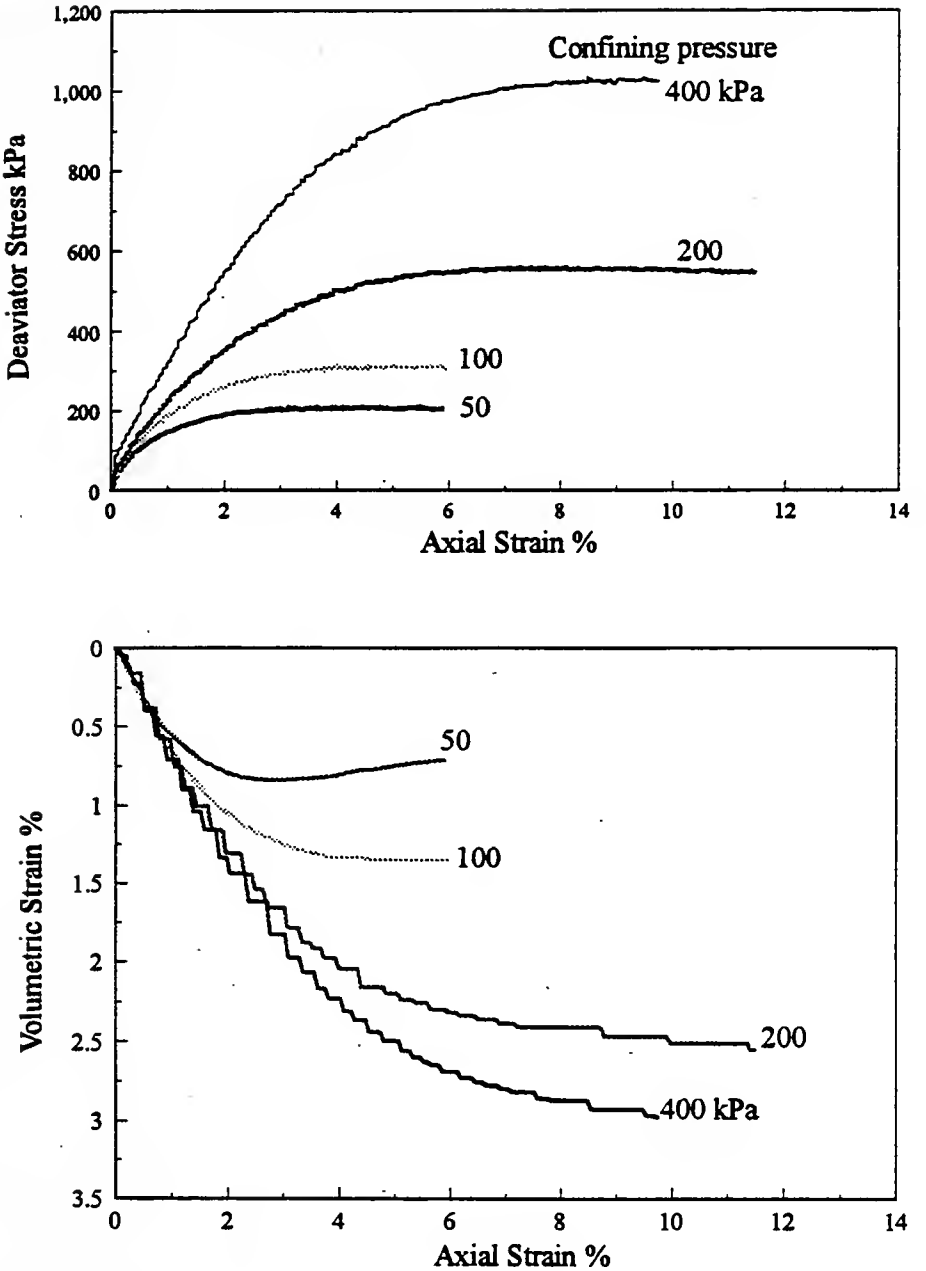


Figure 8.26 CD Triaxial Tests on GI-R6 at
Different Confining Pressures

compressive strength of only 145 kPa. The cementation bonds are perhaps completely broken somewhere before the peak is reached; consequently the peak strength does not contain any cementation component of strength. There was no tendency for dilation except at 50 kPa confining pressure. Volumetric strains were contractive at all other confining pressures, and an increase in confining pressure increases the volumetric strain. The behavior is comparable to that of loose sand. It should be noted that the void ratio for this sample was 0.43 (Table 8.1), and the void ratios for GI-R5 and GI-R7 were 0.32 and 0.3 respectively. The main reason for the higher value of void ratio in GI-R6 is the higher amount of water that needs to be added to get the required flowability. It should be recalled from Chapter 4 that increasing the fly ash content above a certain value would not benefit the flow of the material; on the contrary, it results in an increase of water demand to produce the same flow. The higher contraction in sample GI-R6 could be due to higher void ratio. Also, a higher amount of fly ash might have played an important role too. The fly ash seems to be more compressible than the sand. The fly ash particles are spherical in shape, thus less angular compared to sand; consequently, these samples with higher fly ash content could be expected to show less tendency towards dilation compared to the samples GI-R5 and GI-R7 with higher amount of sand.

The mix GI-N7 contains WFS, N (Figure 8.27). The stress-strain behavior is similar to that of samples GI-R5 and GI-R7 which contains river sand, R (Figure 8.24 and 8.25). The samples exhibit post peak strain softening, and were dilatant as can be seen from the volume change curves in Figure 8.27. However, the maximum rate of dilation and total dilation at each confining pressure were lower compared to GI-R5 and GI-R7. The waste foundry sand, N contained small amount of clay which must have caused the lower tendency for dilation. The behavior with respect to increasing confining stress was slightly different for these samples. An increase in confining stress would normally produce a relatively flatter post peak stress-strain curve like in Figures 8.24 and 8.25. However, from Figure 8.27, it can be seen that at confining pressures of 200 kPa and 400 kPa, there is a dramatic decrease in deviator stress after the peak , suggesting a sort of collapse in the structure. The reason for this phenomenon is not yet known.

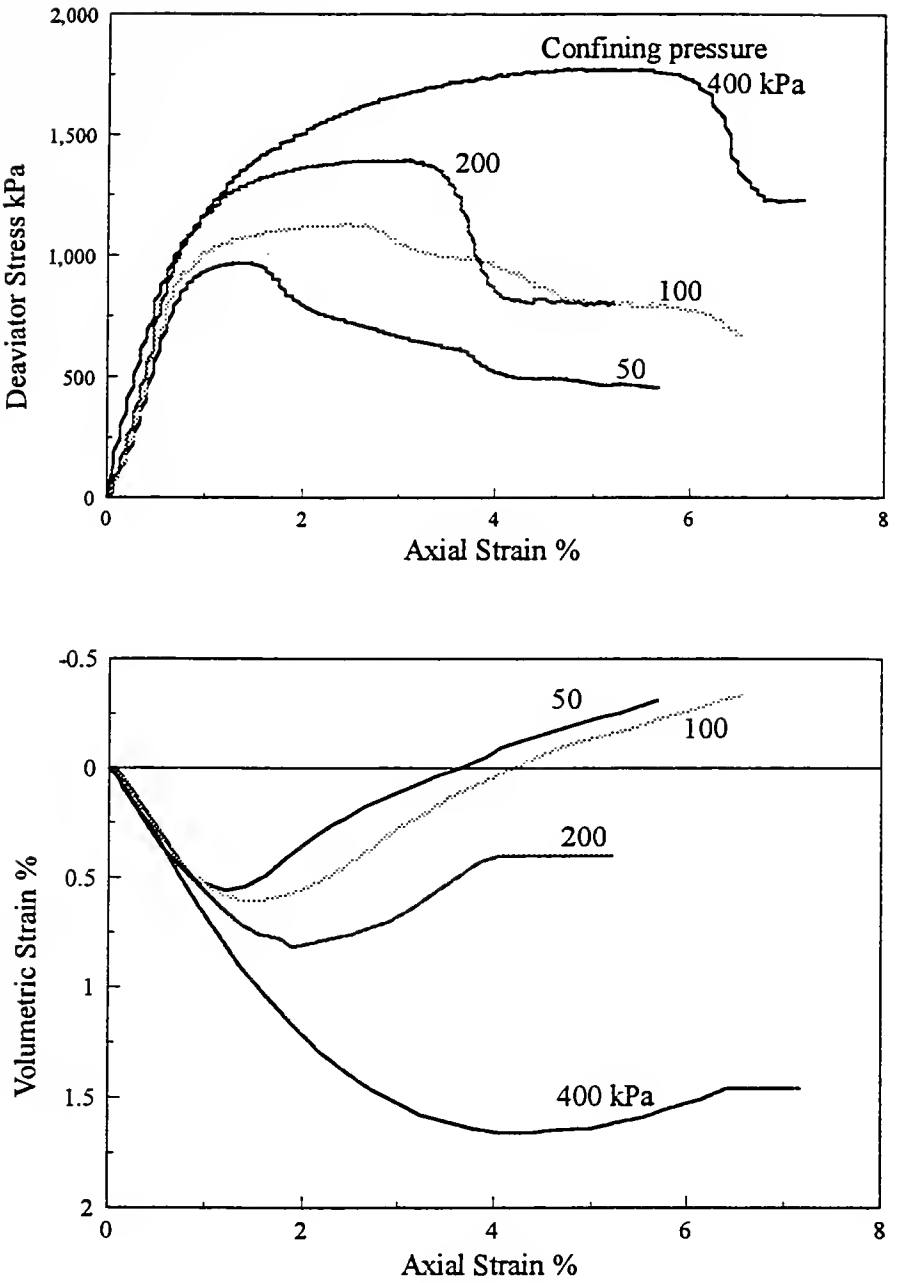


Figure 8.27 CD Triaxial Tests on GI-N7 at
Different Confining Pressures

Consolidated undrained triaxial test results for mixes GI-R5 and GI-R7 are shown in Figures 8.28 and 8.29 respectively. The initial portion of the stress strain curves is linear, followed by a non-linear response up to peak, and then strain softening. Shearing causes development of strong negative pore pressures. Increasing the confining pressure reduces the tendency for negative pore pressure development. From the knowledge of sand behavior, it is known that a dilation or volume expansion during drained shearing on a sample would translate into the development of negative pore pressure during undrained shearing of similar samples. This is found to be true for this material, too. Extending the same logic, the higher the tendency for dilation, the more negative should the pore pressure be. Interestingly, this is the case here. It was seen in Figures 8.24 and 8.25 that GI-R7 with a higher cement content showed higher dilation compared to GI-R5 with a lower cement content. Therefore, during undrained shearing samples GI-R7 developed more negative pore pressures compared to samples GI-R5 (Figures 8.28 and 8.29). In Figure 8.28, the peak deviator stress at 200 kPa is found to be higher than at 400 kPa which can not be explained.

### 8.3.3 Initial Tangent Modulus

The slope of the initial portion of the stress-strain curve is known as the initial tangent modulus. This is a useful parameter which gives the initial stiffness of the material and generally used in modeling the soil behavior. Figure 8.30 shows the variation of tangent modulus with confining pressure for different mixes on a log-log plot, normalized with respect to atmospheric pressure. The samples GI-R5, GI-R7 and GI-N7 with higher unconfined compressive strengths of 700, 1085 and 700 kPa respectively were much stiffer compared to the mix GI-R6 with a lower unconfined compressive strength of 145 kPa. The samples GI-R7 with a higher cement content were stiffer than sample GI-R5 with a lower cement content. However, the curves become flat at confining pressures above 100 kPa, implying the independence of stiffness on confining pressure. This means that the frictional component in the initial portion of the stress-strain curve is very small, and that the cementation is mainly responsible for resisting the load. Cementation bond strength can be considered to be

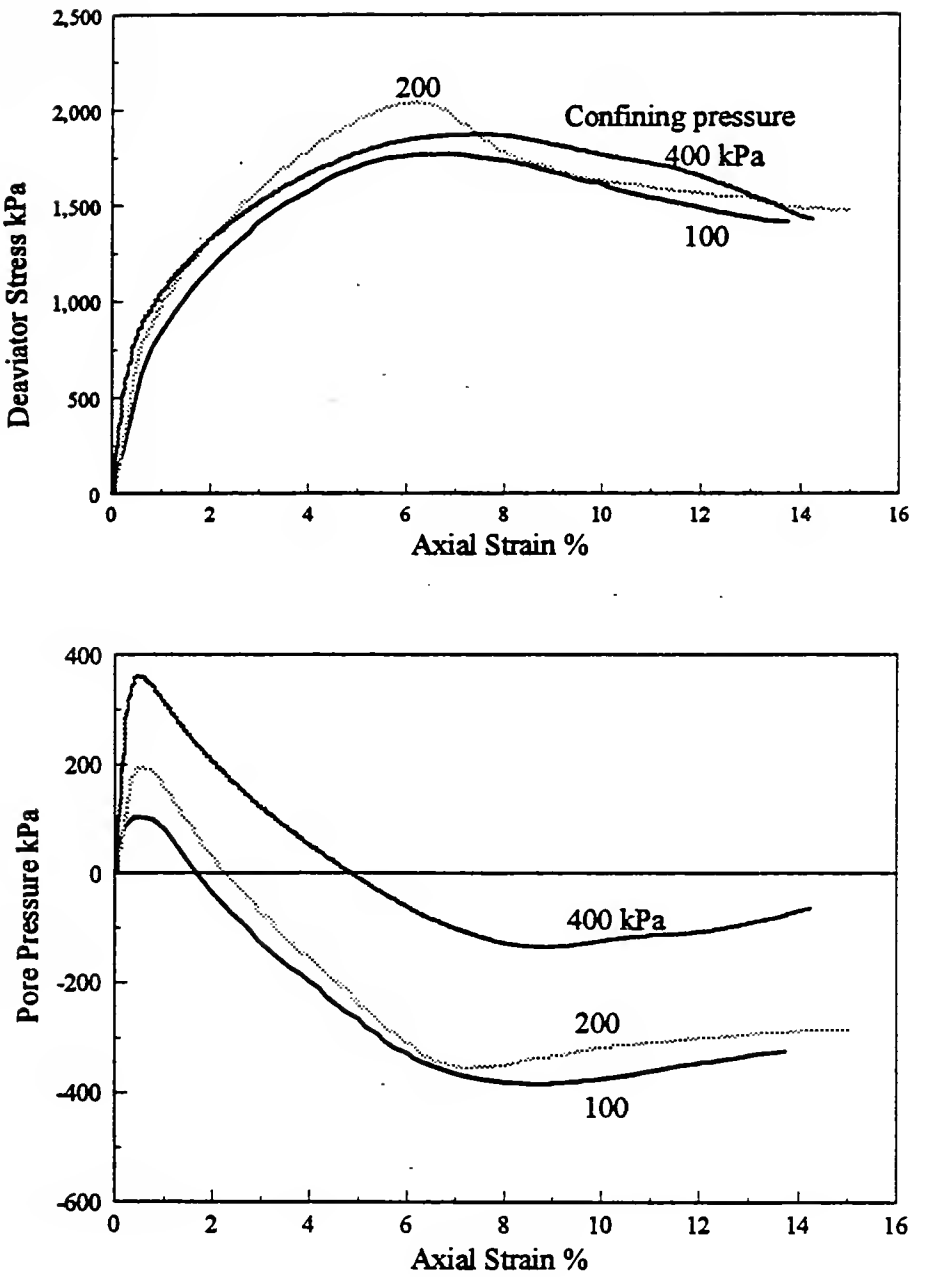


Figure 8.28 CU Triaxial Tests on GI-R5 at Different Confining Pressures

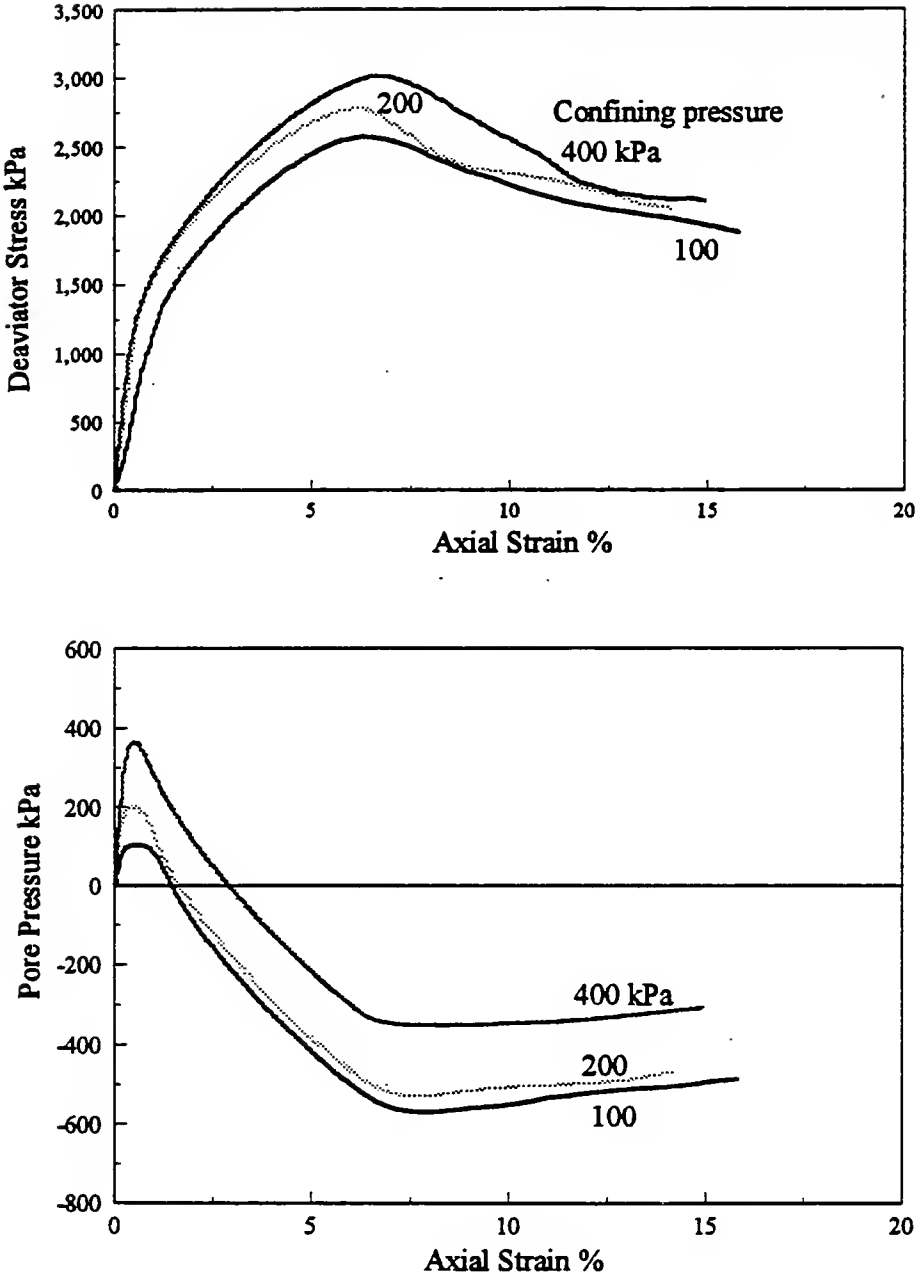


Figure 8.29 CU Triaxial Tests on GI-R7 at Different Confining Pressures

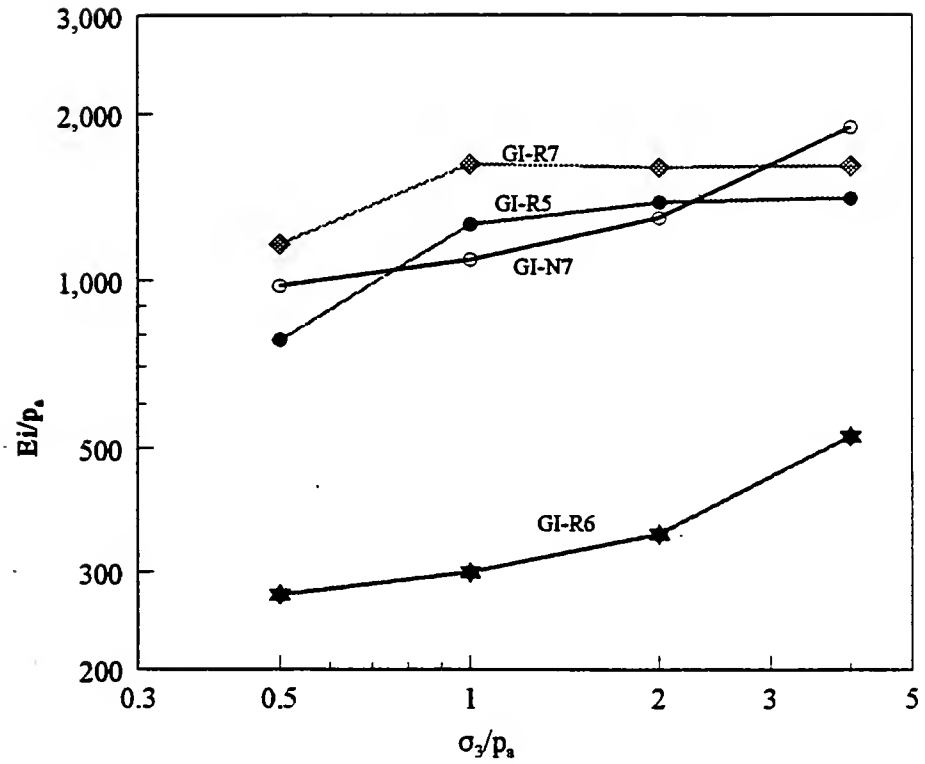


Figure 8.30 Variation of Initial Tangent Modulus with Confining Pressure

independent of confining pressures. In the non-linear portion of the stress-strain curve where cementation bonds start breaking up, frictional strength begins to get mobilized simultaneously. For samples GI-N7 containing WFS, N, the confining pressure had continued effect on the magnitude of the initial tangent modulus (i.e. it increased with increasing confining pressure). The presence of clay in WFS might have caused this difference in behavior. The samples GI-R6 had weak cementation bonds; as a result, frictional strength, and therefore, the confining pressure plays an important role in deciding the magnitude of the initial stiffness. This causes an increase in the initial tangent modulus with an increase in the confining pressure for samples GI-R6. A factor which is not considered here, is the stiffness of the triaxial apparatus, which may be important when small changes in stiffness should be measured.

### 8.3.4 Strength Characterictics

Having seen the stress-strain behavior of flowable fill at different confining pressure, the strength characteristics can be studied by drawing Mohr failure envelopes. A convenient way of drawing failure envelopes, without having to draw Mohr circles is to choose mean stress, $(\sigma'_1 + \sigma'_3)/2$ as abscissa, and shear stress, $(\sigma'_1 - \sigma'_3)/2$ as ordinate. The slope of the this strength line, $\psi$, and intercept, d, in this space can be related to strength parameters, $c_{ap}'$ and $\phi'$ by the following equations,

$$\sin\phi' = \tan\psi \tag{8.4}$$

$$c'_{ap} = \frac{d}{\cos\phi'} \tag{8.5}$$

Instead of conventional notation, c′ for cohesion, apparent cohesion, $c'_{ap}$ is used to indicate that this parameter includes cementation effects too. The strength lines for all the mixes are shown in Figures 8.31 through 8.34.

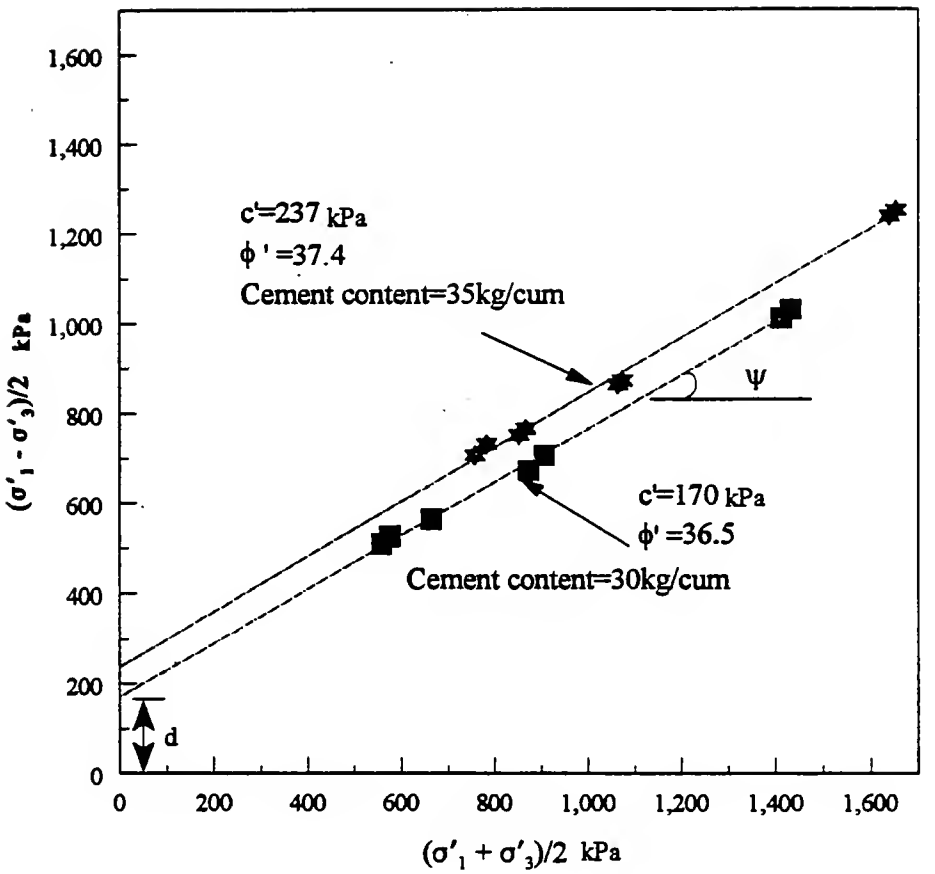


Figure 8.31 Peak Strength Lines for GI-R5 and GI-R7

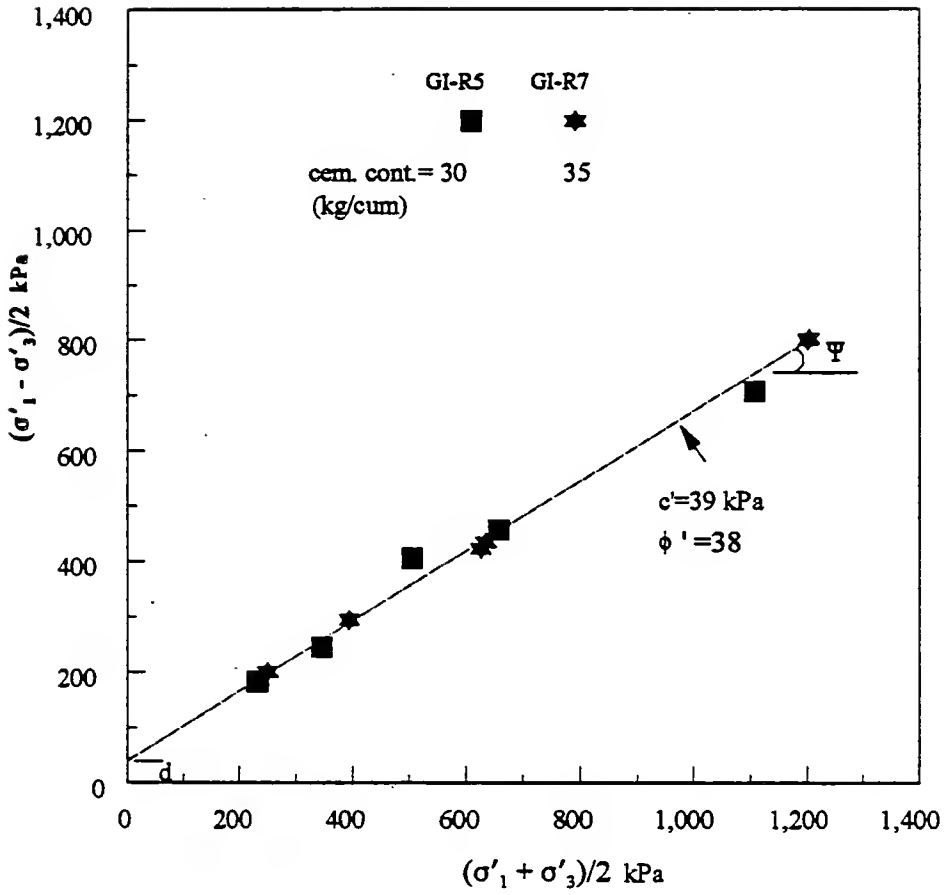


Figure 8.32 Residual Strength Lines for GI-R5 and GI-R7

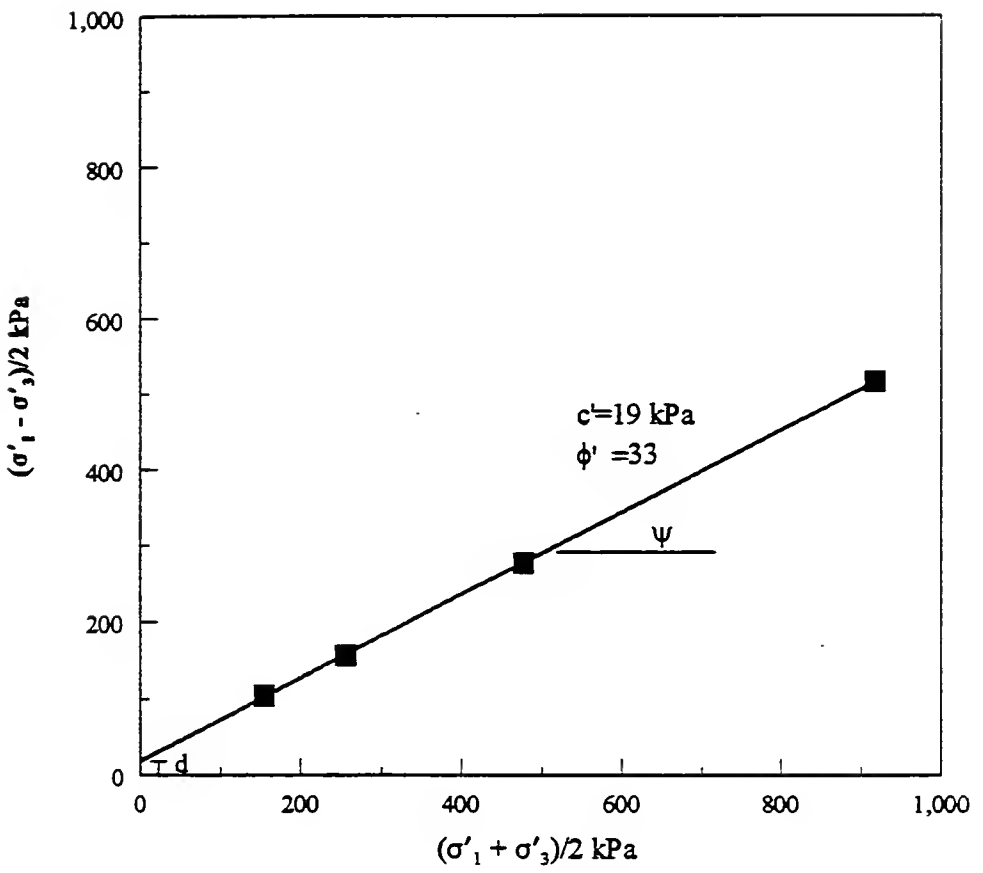


Figure 8.33 Peak and Residual Strength Lines for GI-R6
( High Fly Ash Content Mix)

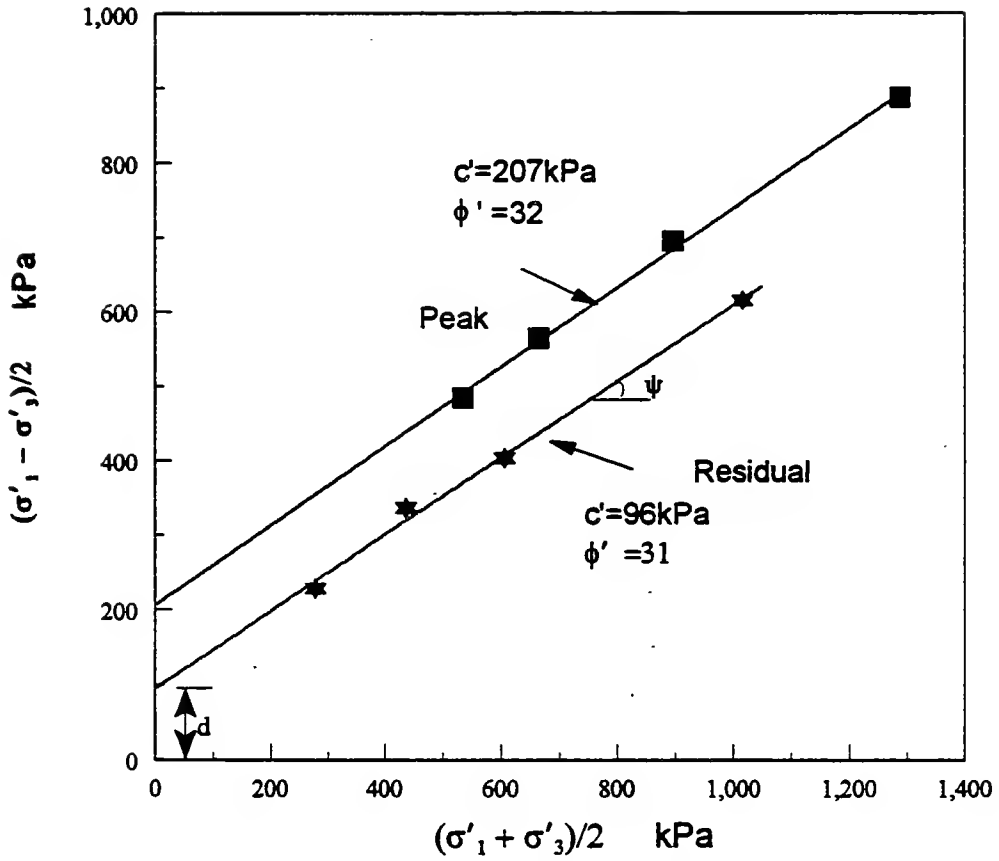


Figure 8.34 Strength Lines for GI-N7

The Figure 8.31 shows peak strength lines for samples GI-R5 (30 kg/m$^3$ cement content) and GI-R7 (35 kg/m$^3$ cement content). The strength lines are almost parallel giving $\phi'$ of 36.5° and 37.4° respectively. The apparent cohesion, $c'_{ap}$ was 170 kPa and 237 kPa respectively. The effect of higher cementation was to increase the $c'_{ap}$. It can be noted that the major component of strength at peak is due to friction.

The Figure 8.32 shows the residual strength lines for the above samples, GI-R5 and GI-R7. The failure points could be approximated by a common strength line. This is understandable because after the cementation bonds are broken completely, both the samples having the same proportion of sand and fly ash would be expected to reach the same ultimate strength. However, existence of a relatively small value of cohesion intercept, $c'_{ap}$ implies that there is something else present apart from pure friction. This is believed to be due to dilatancy component of strength. It can be seen from the volume change response (Figures 8.24 and 8.25) that at the end of the tests, the material is still dilating, and that the constant volume condition is not yet reached at this strain. The difficulty in carrying out shearing up to large strains to reach constant volume condition was noted in section 8.3.2.

The Figure 8.34 shows peak and residual strength lines for the mix GI-N7 containing WFS, N. The peak and residual failure friction angles were 32° and 31°, respectively. This is a reasonably good value though it is slightly reduced perhaps due to the presence of clay in WFS, compared to the values of friction angles for GI-R5 and GI-R7 (Figures 8.31 and 8.32).

The Figure 8.33 shows the strength line for the mix GI-R6 with high fly ash content. A friction angle of 33° and a small apparent cohesion, $c'_{ap}$ of 19 kPa are obtained. Since this sample did not show any post peak strain-softening behavior, only one strength line could be obtained.

It is important to recognize the fact that the method of drawing Mohr failure envelopes or strength lines does not necessarily separate the friction and cohesive component of strength completely, but is a convenient method of arriving at design parameters, $c'$ and $\phi'$. In pure sands, it is known that the friction angle varies with the level of confining pressure, and that the failure envelope becomes curved (concave downwards) as confining

pressure is increased. Therefore, the method of drawing a common envelope through these failure points yields a cohesion intercept, where as, in reality there is no such thing as cohesion in pure sands. This phenomena is partly due to the "dilatancy" of sand. The dilatancy or the tendency to increase in volume during shearing requires that an extra amount of work be done against this force, giving an additional strength to the sand. The dilatancy decreases with increasing confining pressure. In cemented materials like flowable fill, there is still another component of strength due to cementation, which makes its analysis much more complex.

### 8.3.5 Effect of Higher Cementation on Stress-Strain Behavior

The mixes GI-R5 and GI-R7 are so chosen as to have different amounts of cement (30 kg/m$^3$ and 35 kg/m$^3$ respectively), everything else remaining the same. It was seen in Section 8.3.4 that the effect of increased cementation was to increase apparent cohesion intercept, $c'_{ap}$. The stress-strain curves for these samples were shown in Figures 8.24 and 8.25. In Figure 8.35 through 8.38 are shown the stress-strain curves for both the samples together at each confining pressure. The samples GI-R7 with a higher cement content start off with slightly higher stiffness at all confining pressures, attain higher peak, and reaches approximately the same residual strength as that of samples GI-R5 with lower cement content. The important difference was observed in volume change behavior. The maximum rate of dilation and total amount of dilation were higher for GI-R7. It is not very clear why higher cementation causes higher dilation. The void ratio in GI-R7 was slightly lower because of higher cement content. This might have partly contributed to the higher dilation. The higher cementation also could have increased the roughness and angularity of the sand and fly ash particles resulting in higher dilation.

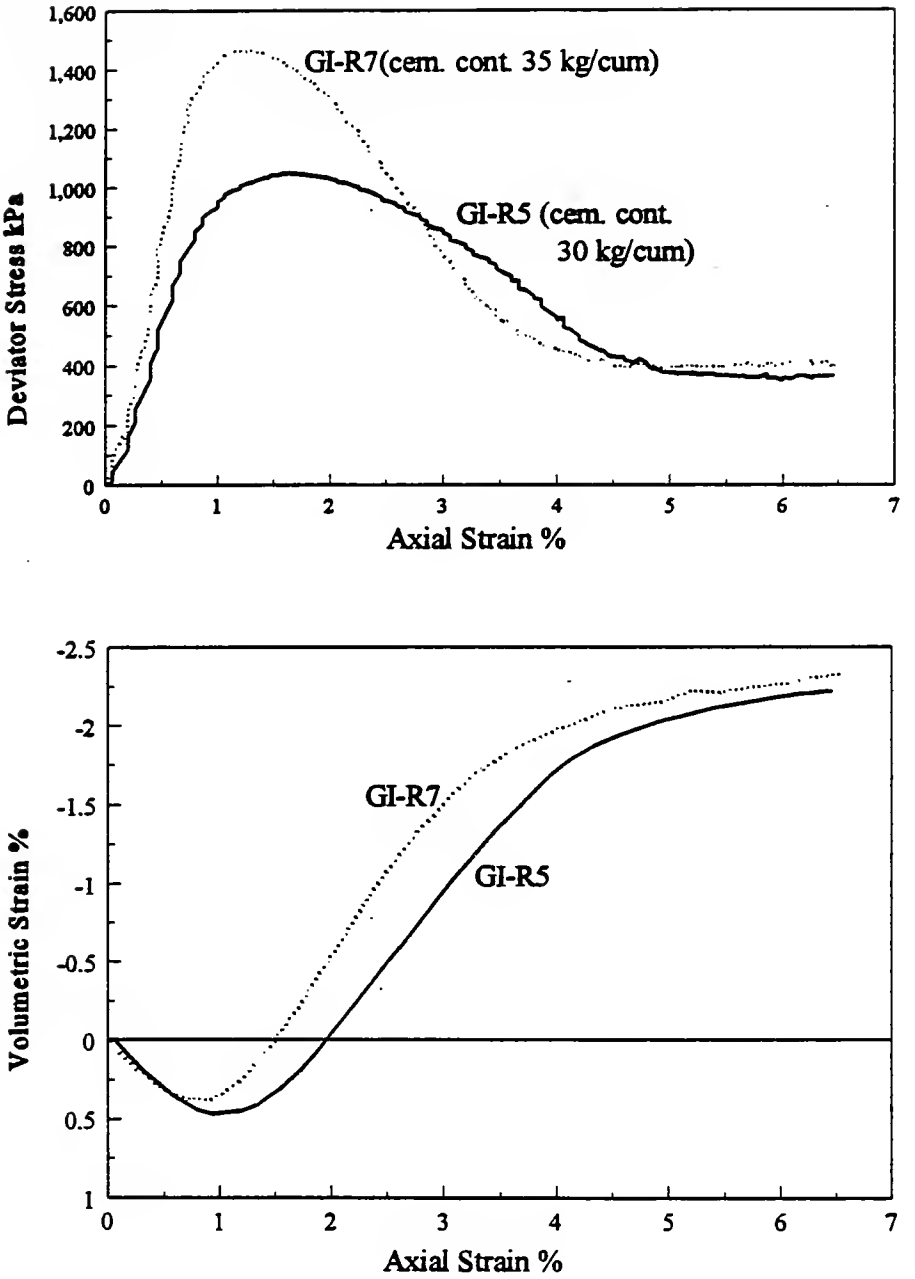


Figure 8.35 CD Triaxial Tests on GI-R5 and GI-R7 at $\sigma_3$ = 50 kPa (Effect of Cement Content)

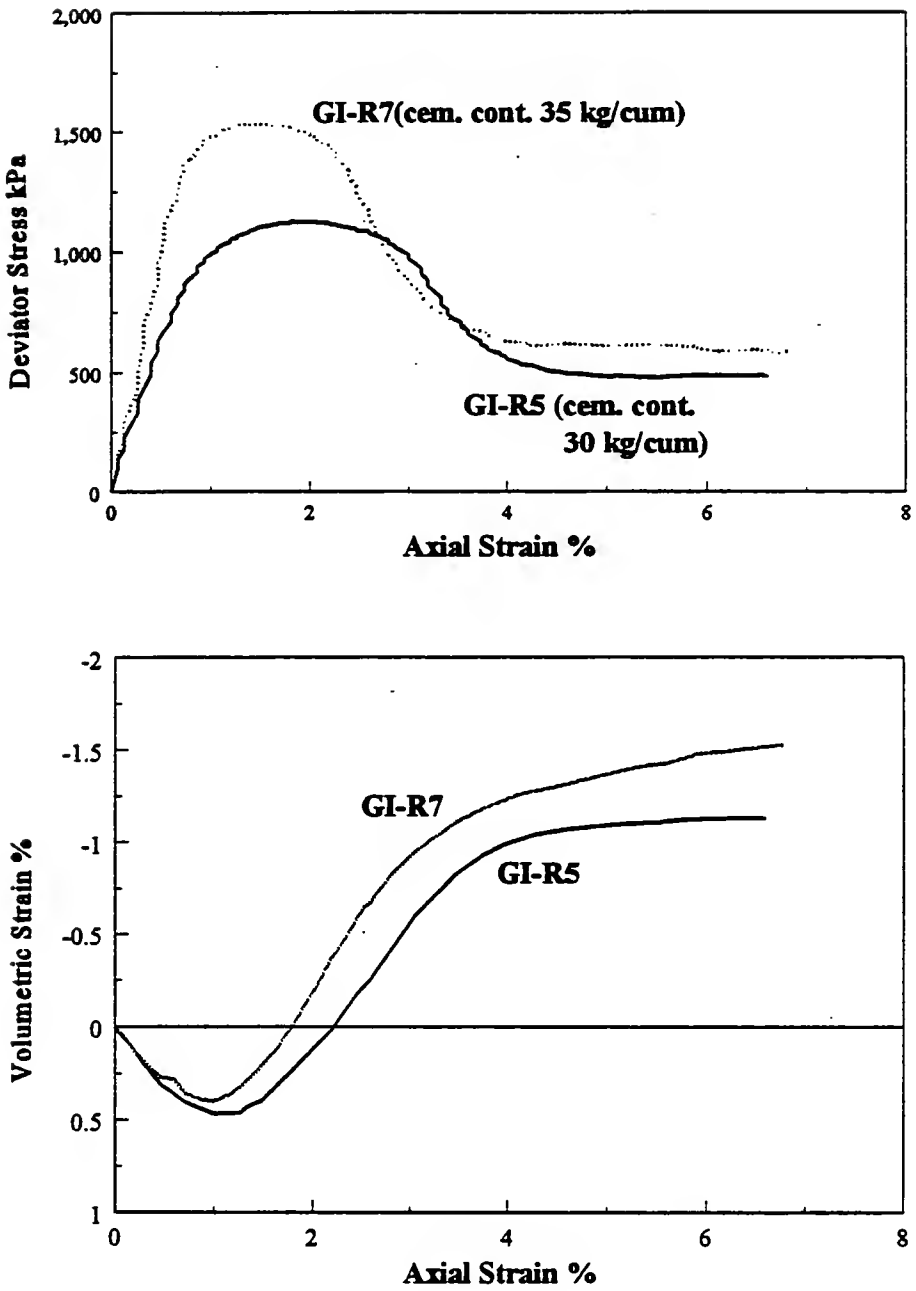


Figure 8.36 CD Triaxial Tests on GI-R5 and GI-R7 at $\sigma_3$ = 100 kPa
(Effect of Cement Content)

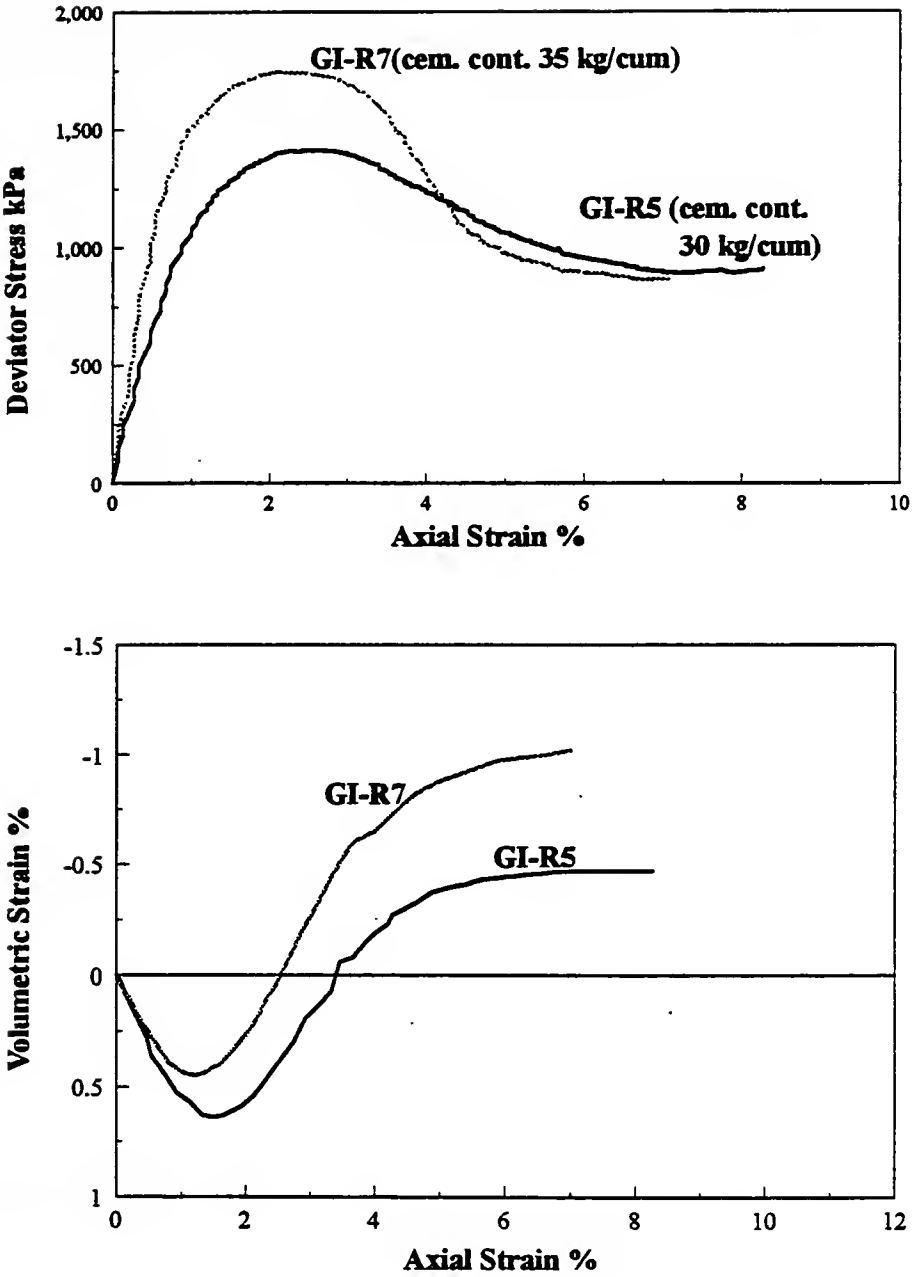


Figure 8.37 CD Triaxial Tests on GI-R5 and GI-R7 at $\sigma_3$ = 200 kPa
(Effect of Cement Content)

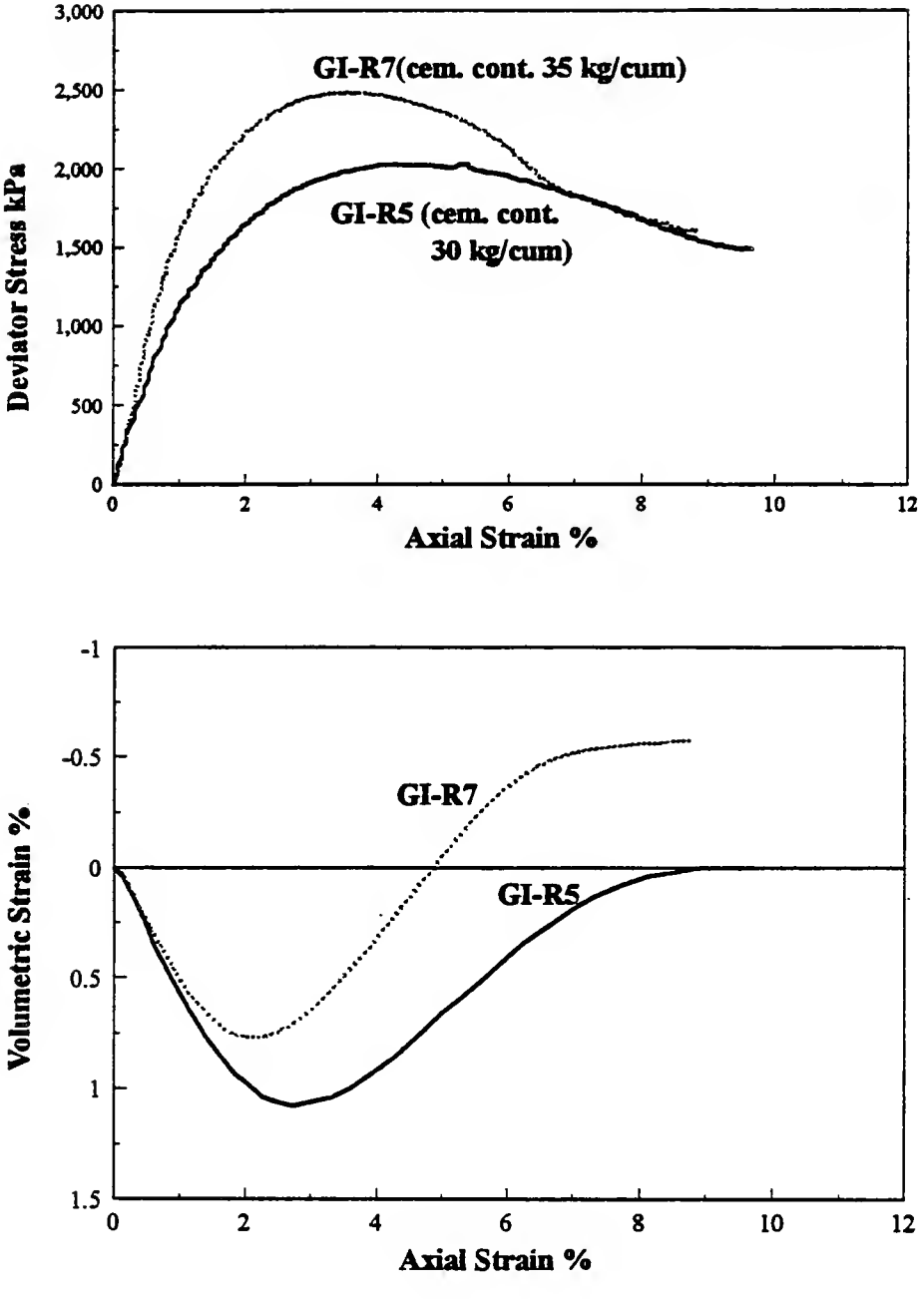


Figure 8.38 CD Triaxial Tests on GI-R5 and GI-R7 at $\sigma_3 = 400$ kPa (Effect of Cement Content)

### 8.3.6 Tensile Strength

In certain applications where tensile cracks are likely to develop, tensile strength is an important parameter. The relation between Brazilian tensile strength and unconfined compressive strength is shown in Figure 8.39. There seems to be a good correlation between the two parameters. The unconfined compressive strength is found to be approximately 4.3 times the tensile strength. It is reported that, in cemented sands, tensile strength may be 1/8 to 1/15 of compressive strength (Das et al. 1993, Sitar, 1979 ). Therefore, flowable fill seems to be stronger in tension compared to cemented sands.

### 8.3.7 Matrix of Sand and Fly Ash

The void ratios of flowable fill samples were much lower than the minimum void ratio, $e_{min}$ that can be achieved by the sand alone (Table 8.1). For example, void ratio for samples GI-R5 was 0.32, where as $e_{min}$ for the river sand, R was 0.45 (Table 8.1). That is, the presence of fly ash (and also cement to some extent) helps reduce the void ratio in flowable fill. However, if the sand skeleton alone within the flowable fill is considered, imagining that there are no other phases present, the sand is in a very loose state; in fact looser than the loosest possible state for this sand. For example, for the above mix, the void ratio of the sand skeleton within the flowable fill sample can be calculated knowing the amount of sand in a unit volume of flowable fill, and this void ratio for sample GI-R5 was 0.8. The maximum void ratio, $e_{max}$ for this sand was 0.69 (Table 8.1). This suggests that the sand grains are supported by fly ash particles, or the sand particles are embedded within the fly ash matrix. It is possible that sand grains do not really touch each other, they being seperated by the fly ash particles. During shearing, major interaction could be between fly ash-fly ash particles, particularly in high fly ash content mixes. A good friction angle in all the cases therefore implies that fly ash is not an inferior material in terms of frictional characteristics.

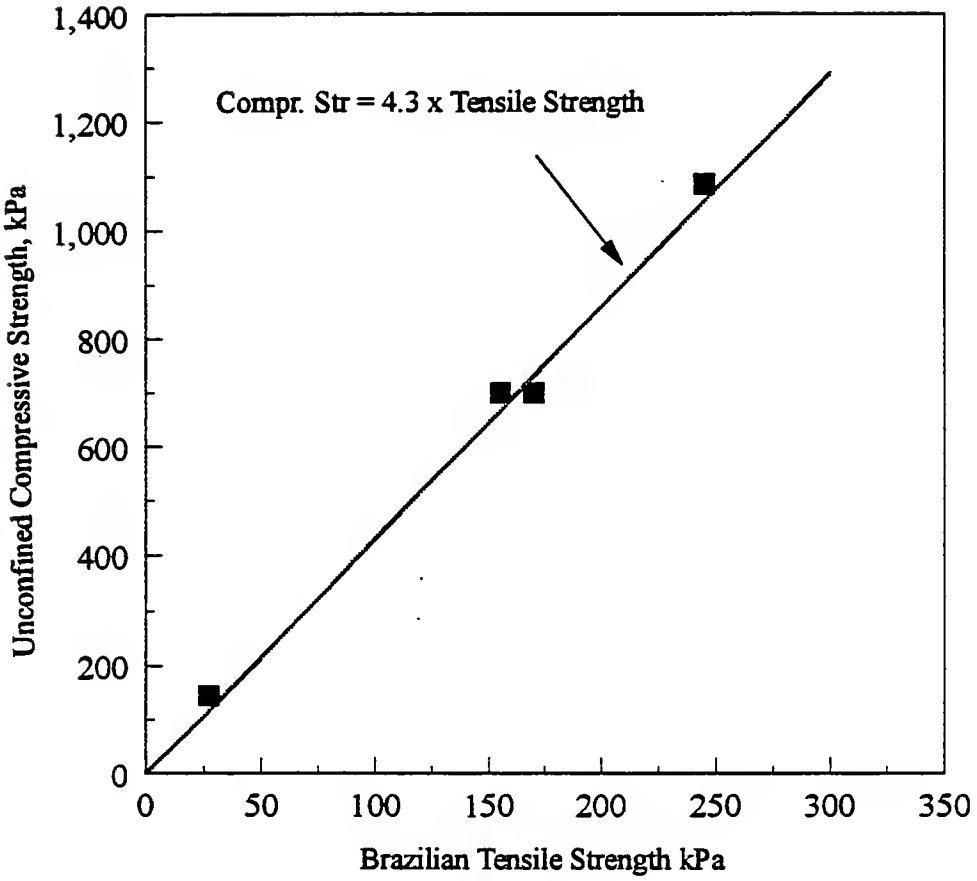


Figure 8.39 Tensile Strength Vs Compressive Strength

## 8.4 Summary

Four mixes were chosen to study the stress-strain-strength behavior of flowable fill. Three mixes contained river sand: Only the cement content was varied in two mixes to see the effect of degree of cementation on stress-strain behavior; the third mix was a high fly ash content mix which contained fly ash more than what is necessary for flow. The fourth mix contained WFS, N. All the mixes contained the same fly ash, GI.

The void ratio of the mixes varied from 0.3 to 0.56. The void ratio mainly depends upon the quantity of the water added to the mix; this quantity, in turn, depends mainly on the properties of the sand, and the proportion of sand and fly ash. The mixes with WFS need more water; therefore, the void ratio was slightly higher. High fly ash content mix also results in higher void ratio. A proper proportioning of sand and fly ash yields a dense material.

The stress-strain curves at different confining pressures indicated that these samples were much less brittle than expected from a cemented material. The stress-strain curves had a broad peak, and a slow rate of strain-softening. The initial linear portion of stress-strain curve is mainly due to the cementation effect. At peak, the friction and dilatancy component of strength were predominant. Increase in cementation caused an increase of both maximum rate of dilation and total amount of dilation. The samples with high fly ash content showed non-dilatant behavior.

Shear strength parameters could be obtained by drawing strength lines. The peak and residual angle of fricton, $\phi'$ was around 36° for the first two mixes with river sand, 33° for the mix with high fly ash content, and around 32° for the mix with WFS. The presence of clay in WFS might have slightly reduced the friction angle. Increasing the cement content increased the cohesion intercept keeping the friction angle approximately constant. Brazilian tensile strength tests indicated that a relation between unconfined compressive strength and tensile strength exists: The unconfined compressive strength was approximately 4.3 times the tensile strength.

In summary, flowable fill is a well-behaved material. It behaves like a granular soil except for the effects of cementation. The stress-strain-strength behavior could be explained within the frame work of soil mechanics concepts.

# CHAPTER 9. RESULTS OF ACCELERATED STRENGTH TESTING

## 9.1 Introduction

The 28-day strength of flowable fill is to be restricted to 1034 kPa (150 psi) to allow for possible future excavation. To make sure that the strength of a particular mix of flowable fill does not exceed this value, the samples are required to be kept for 28 days for strength testing before this mix is used in the field. This can cause major delays in the construction work, and upset the economics of application of this material. This is viewed by many as a major draw back in the application of this material, particularly from the contractors' perspective. These facts motivated the idea of accelerated strength testing to reduce the strength testing time to as short a time as possible. However, use of any complicated technique to achieve this would defeat the whole purpose, because economics is the most important factor; flowable fill has to compete with the soil back fill. A hot water bath technique was used in this research. The basic idea of accelerated strength testing is to speed up the process of hydration of cement in the mix by some means. It is a well known fact that the increase in temperature would accelerate the hydration in cement. Standard ASTM C 684 explains different techniques to accelerate the development of strength for concrete. The Warm Water Method specifies curing the concrete specimens immediately after casting the samples, in water at 35 °C and for 24 hours. The Boiling Water Method involves curing the concrete specimens, one day after casting, in boiling water for 3.5 hours. However, these techniques cannot be applied directly to flowable fill as the amount of cement in flowable fill is very small, and it is a soil-like material.

## 9.2 Experimental Program

### 9.2.1 Mixes

Twenty one mixes were selected for this study, covering two Class F fly ashes, SC and GI, and four sands, river sand, R, and WFSs N, A, and G. The mix proportions and 28-day strengths for these mixes are shown in Table 9.1. The first part of the mix name indicates the source of fly ash, and the letter in the second part indicates the source of sand. The number at the end of the mix name indicates the number of that mix in the series of mixes with that combination of fly ash and sand. The samples were prepared in the regular manner and placed in the humidity chamber until it was ready to be kept in the hot water bath.

### 9.2.2 Accelerated Curing

An electric hot water bath (made by LAB-LINE INSTRUMENTS, Inc) with a thermostat was used in used for accelerated curing. In the first round of testing, three mixes GI-R5, GI-N4 and SC-R1 were tried at 100°C. The samples were removed from the humidity chamber after one day, demolded, and kept immersed in the water bath at 100°C in a metallic tray. The samples disintegrated and collapsed within 3 to 5 minutes. The same thing was tried on these mixes at 2 days and 3 days but with no success. The samples could not withstand the temperature, and disintegrated. To provide protection to the samples from direct contact with boiling water, it was decided to cure them along with the molds. Two types of molds were used- PVC molds and cardboard molds. The samples along with the mold were kept in the hot water for varying length of time: 1 hour, 2 hours, and 3 hours. The samples apparently did not collapse, but after demolding it was observed that several cracks had developed in the sample, and the samples had negligible strength. The molds were capped in the subsequent tests to provide complete protection to the samples. However, this again failed to give any positive results.

Table 9.1 Mix Proportions and 28-day Unconfined Compressive Strength

| Mix Number | Cement | Fly Ash | Sand | Water | 28-day Strength kPa (psi) |
|---|---|---|---|---|---|
| SC-R1 | 30 | 392 | 1474 | 262 | 738(107) |
| SC-N1 | 35 | 257 | 1255 | 376 | 414(60) |
| SC-N2 | 50 | 254 | 1242 | 376 | 834(121) |
| SC-N8 | 30 | 257 | 1256 | 375 | 365(53) |
| SC-N4 | 50 | 122 | 1313 | 386 | 483(70) |
| N3 | 50 | 0 | 1396 | 408 | 338(49) |
| N7 | 60 | 0 | 1387 | 408 | 241(35) |
| SC-G4 | 50 | 254 | 1157 | 409 | 655(95) |
| SC-A3 | 50 | 258 | 1032 | 415 | 683(99) |
| SC-A4 | 50 | 548 | 789 | 402 | 965(140) |
| SC-A1 | 50 | 679 | 679 | 394 | 731(106) |
| SC-A2 | 70 | 669 | 669 | 396 | 1255(182) |
| GI-R5 | 30 | 378 | 1512 | 257 | 621(90) |
| GI-R7 | 35 | 377 | 1508 | 257 | 827(120) |
| GI-R8 | 40 | 376 | 1505 | 257 | 1055(153) |
| GI-R9 | 45 | 375 | 1501 | 258 | 1138(165) |
| GI-N5 | 50 | 161 | 1300 | 381 | 469(68) |
| GI-N7 | 60 | 160 | 1295 | 382 | 517(75) |
| GI-G5 | 50 | 143 | 1284 | 408 | 717(104) |
| GI-A4 | 50 | 361 | 976 | 402 | 545(79) |
| GI-A6 | 60 | 358 | 969 | 402 | 910(132) |

The obvious choice was to reduce the temperature of curing. Twelve samples of each mix were demolded at 3 days, and kept in water bath at $35^0$ C. Apparently the samples did not get damaged at this temperature. Four samples were removed at 24 hours, 48 hours, and 72 hours each time, allowed to cool for one hour, and then tested for compressive strength. Encouraged by the positive results, it was decided to try curing at 1 day age and $50^0$ C, in the hope of further reducing the total time of testing. The samples were tested for strength after 24 hours and 48 hours of curing.

## 9.3 Results

The Figures 9.1 and 9.2 show the photographs of collapsed samples after curing at 100°C. It seems that the high temperature causes an expansion in the flowable fill samples; the material being unable to withstand the stresses caused by this expansion, collapse. The Table 9.2 shows results of the accelerated strength tests. The Figures 9.3 through 9.7 show the accelerated strength plotted against the 28-day strength for different test conditions.

At the age of 3 days and 35°C, after curing for 24 hours ("3 days age-35°C-24 hr. curing"), the correlation between accelerated strength and 28-day strength was fairly good (Figure 9.3). The accelerated strength was approximately 72% of the 28-day compressive strength. The samples attained slightly higher strengths during the "3 days age-35°C-48 hr. curing" tests (Figure 9.4). In two cases, the accelerated strength was equal to the 28-day strength (Mix GI-A4, GI-R7). Continued curing for 72 hours (Figure 9.5) further increased the strength. However, the correlation between the 28-day strength and accelerated strength was poor. In three cases, the accelerated strength far exceeded the 28-day strength (for GI-R7, GI-R8, and GI-N5). Continued curing at this temperature perhaps gets some fly ash to participate in pozzolanic reactions which would not have happened at normal temperature, consequently increasing the accelerated strength to a higher value than the 28-day strength. The samples with river sand, R were more likely to show advantage of the continued curing. The cement content alone was not a factor in influencing the strength gain due to longer period of curing. The cement content for different mixes varied from 30 kg/m$^3$ to 60 kg/m$^3$,

Figure 9.1 Photograph Showing the Collapsed Sample Containing Sand R Sand R and Fly Ash GI After Curing at 100°C

Figure 9.2 Photograph Showing the Collapsed Sample Containing WFS After Curing at 100°C

Table 9.2 Results of Accelerated Strength Tests

| Mix Number | 3-day Strength kPa | 28-day Strength kPa | Accelerated Strength, kPa | | | | |
|---|---|---|---|---|---|---|---|
| | | | Sample Age : 3 days Temperature: 35°C Duration of Curing | | | Sample age: 1 day Temperature: 50°C Duration of Curing | |
| | | | 24 hrs. | 48 hrs. | 72 hrs. | 24 hrs. | 48 hrs. |
| SC-R1 | 131 | 738 | - | - | - | 117 | 345 |
| SC-N1 | 165 | 414 | 352 | - | - | 214 | 317 |
| SC-N2 | 214 | 834 | - | - | - | 558 | 772 |
| SC-N8 | 131 | 365 | 248 | - | - | 186 | 234 |
| SC-N4 | 165 | 483 | 262 | - | - | - | - |
| N3 | 138 | 338 | 193 | - | - | - | - |
| N7 | 103 | 241 | 234 | - | - | - | - |
| SC-G4 | 228 | 655 | 365 | - | - | 379 | 503 |
| SC-A3 | 207 | 683 | 310 | - | - | 262 | 310 |
| SC-A4 | 345 | 965 | 455 | - | - | - | - |
| SC-A1 | 365 | 731 | 600 | - | - | - | - |
| SC-A2 | 490 | 1255 | 993 | - | - | - | - |
| GI-R5 | 276 | 621 | - | - | - | 241 | 338 |
| GI-R7 | 303 | 827 | 793 | 827 | 945 | 448 | 503 |
| GI-R8 | 386 | 1055 | 862 | 958 | 1110 | 510 | 607 |
| GI-R9 | 359 | 1138 | 786 | 896 | 1014 | 772 | 951 |
| GI-N5 | 221 | 469 | 345 | 421 | 607 | 427 | 572 |
| GI-N7 | 255 | 517 | 359 | 462 | 531 | 600 | 903 |
| GI-G5 | 283 | 717 | 427 | 593 | 531 | 462 | 600 |
| GI-A4 | 303 | 545 | 545 | 558 | 552 | 317 | 455 |
| GI-A6 | 352 | 910 | 683 | 689 | 717 | 517 | 696 |

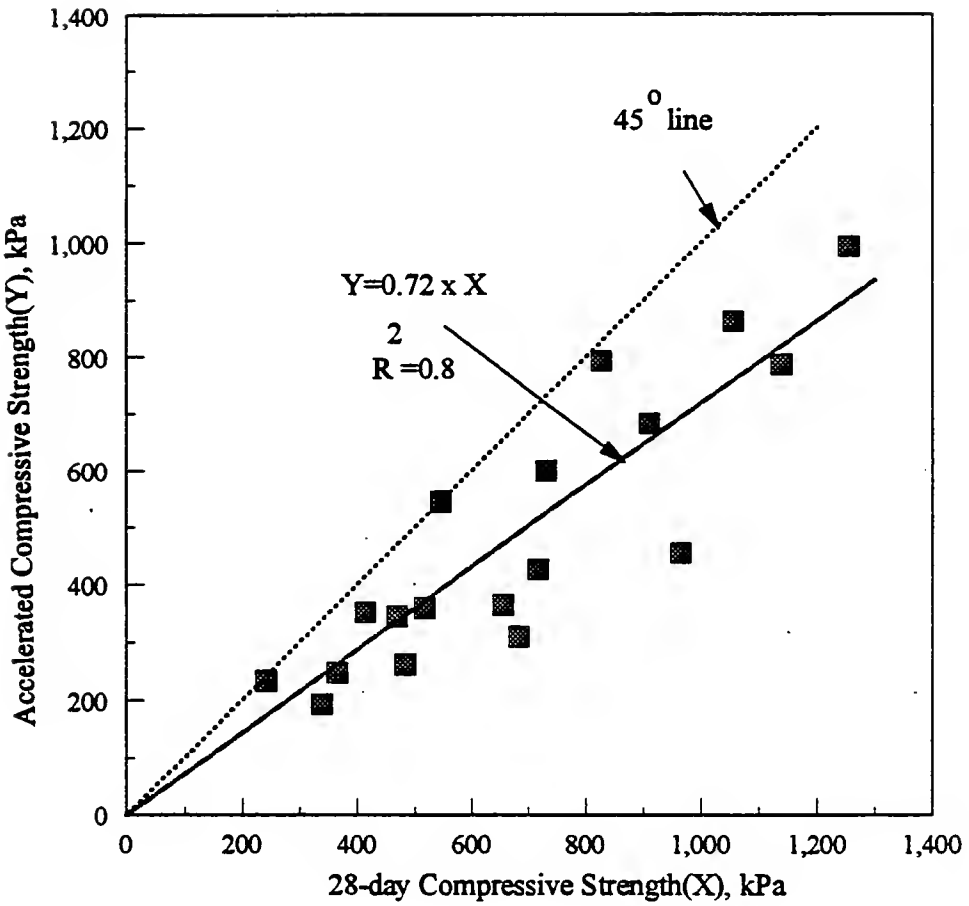


Figure 9.3 Accelerated Strength Test (Age of Samples: 3 days, Temperature: 35°C, Duration of Curing: 24 hours)

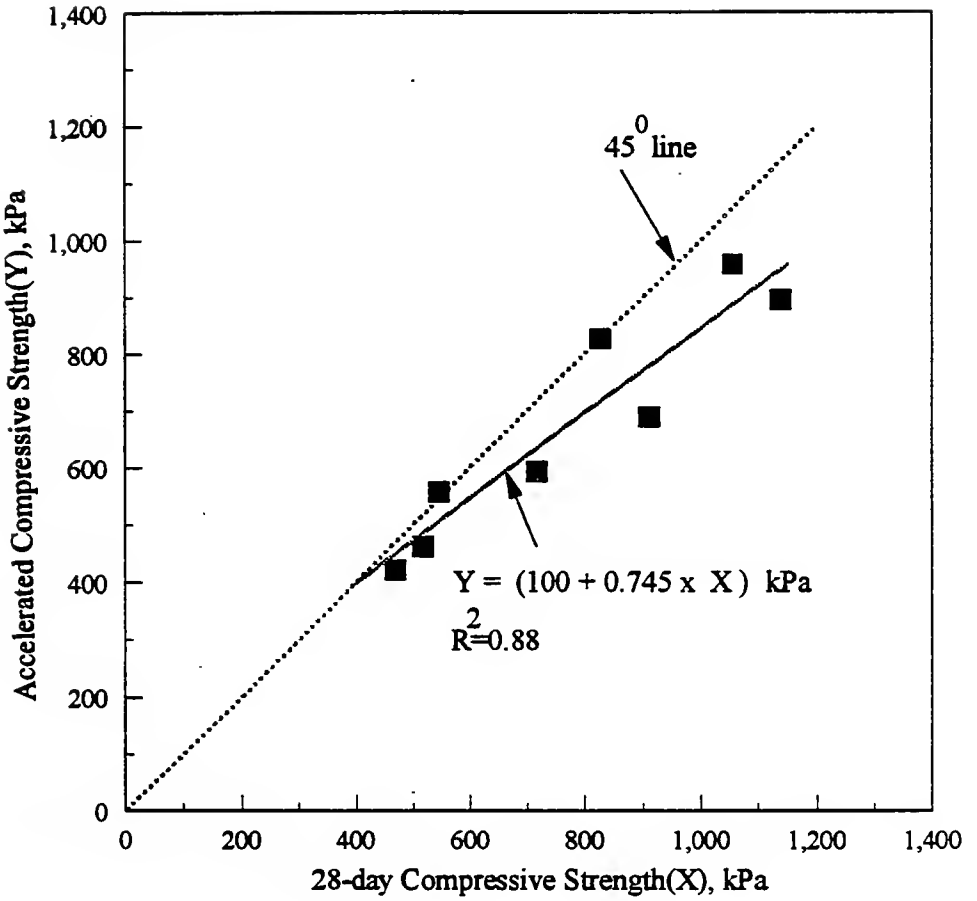


Figure 9.4 Accelerated Strength Test ( Age of Samples: 3 days, Temperature: 35°C, Duration of Curing: 48 hours)

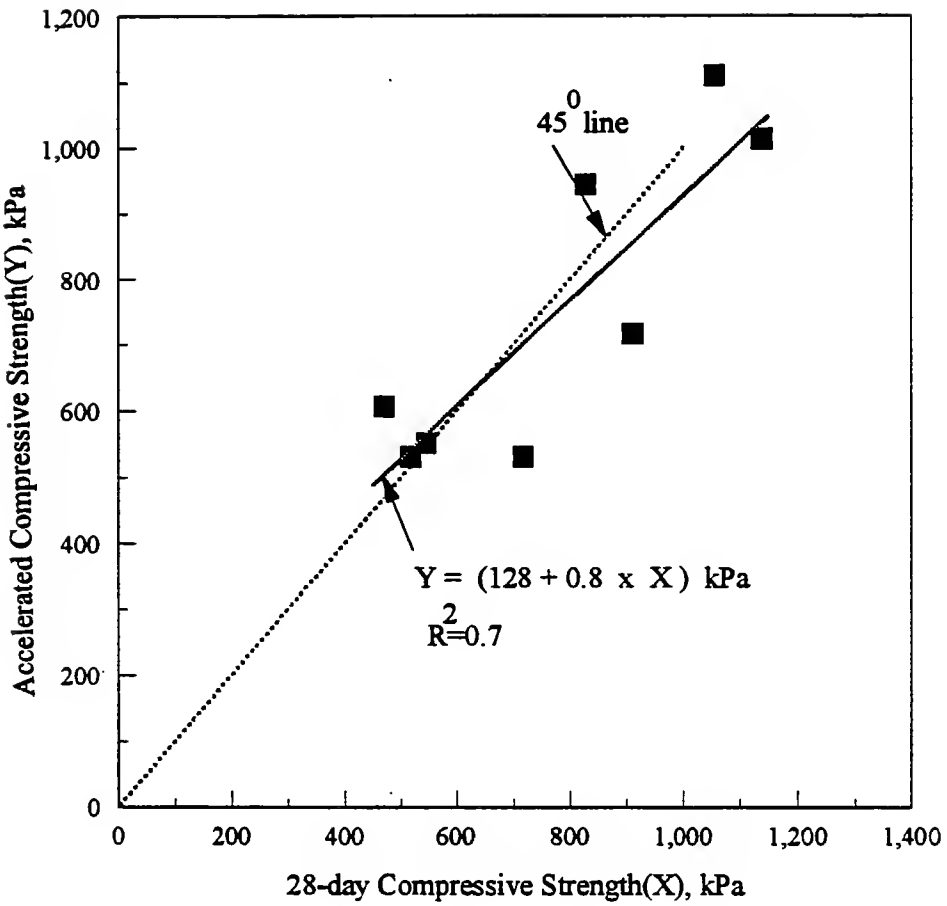


Figure 9.5 Accelerated Strength Test (Age of Samples: 3 days, Temperature: 35°C, Duration of Curing: 72 hours)

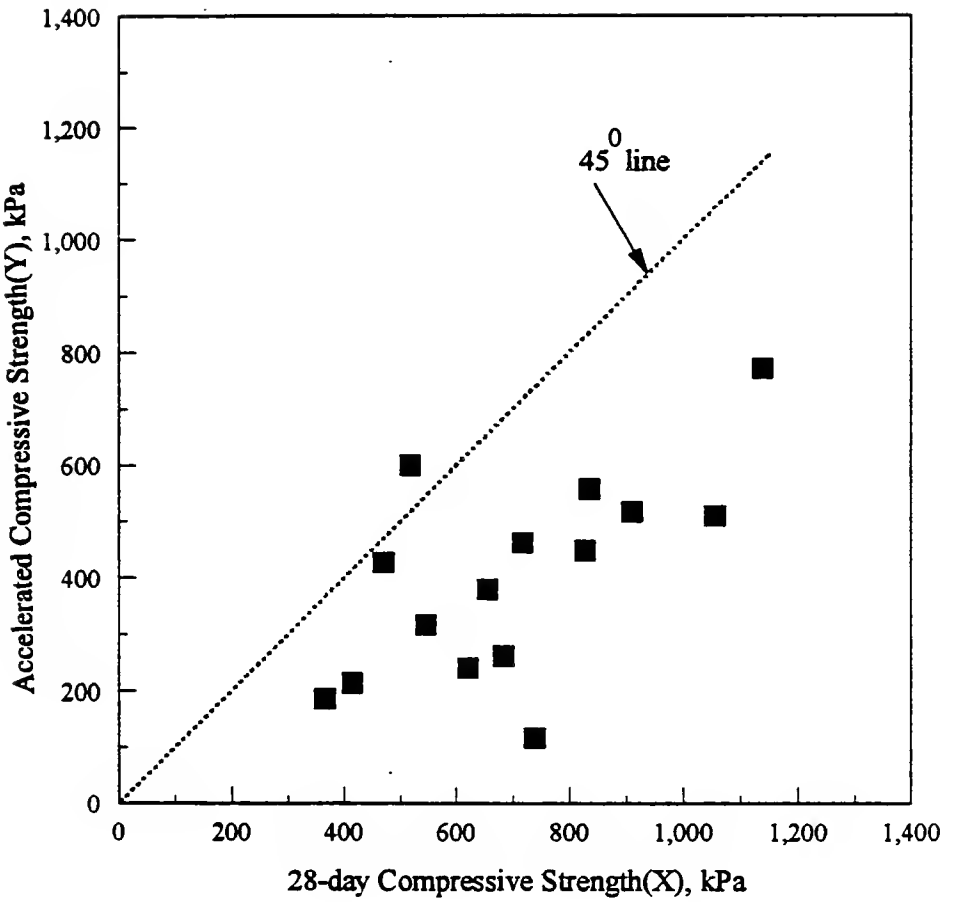


Figure 9.6 Accelerated Strength Test (Age of Samples: 1day, Temperature: 50°C, Duration of Curing: 24 hours)

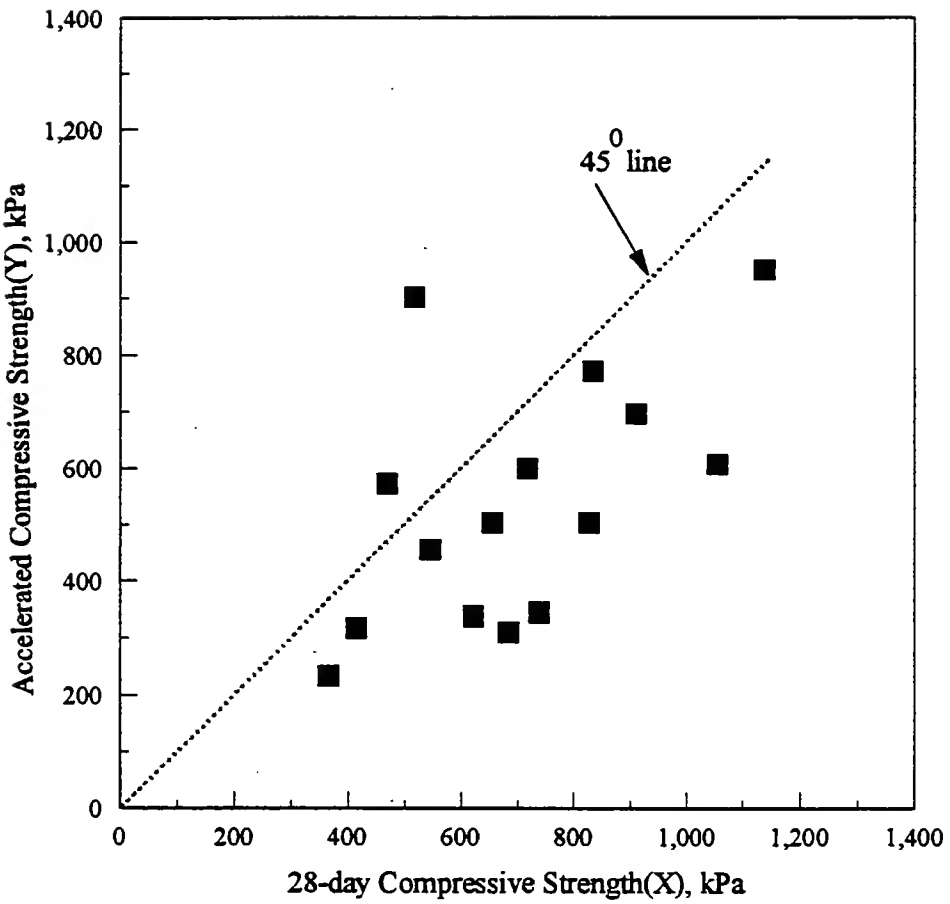


Figure 9.7 Accelerated Strength Test (Age of Samples: 1day, Temperature: 50°C, Duration of Curing: 48 hours)

and did not show any trend with accelerated strength. To see the effect of increasing cement content in the same combination of sand and fly ash, mixes GI-R7, GI-R8, and GI-R9 with cement contents of 35, 40 and 45 kg/m$^3$ respectively were chosen. The increasing cement content did not show any special effect on the accelerated strength.

The "1 day age-50°C-24 hr. curing" and "1 day age-50°C- 48 hr. curing" tests show a lot of scatter (Figures 9.6 and 9.7). One day age seems to be too early to start accelerated curing. Some samples may not be strong enough to withstand demolding and handling stresses. Also, the higher temperature (50°C) might cause some damage to the samples internally.

## 9.4 Summary

The purpose of the accelerated strength test is to reduce the total strength testing time. This is particularly helpful when there is variability in the properties of source materials. The technique for accelerated strength testing should be simple and economical. The hot water bath curing was used in this study.

The flowable fill samples were unable to withstand high temperature at an early age. The samples when cured at 100°C at the age of 3 days, disintegrated and collapsed in the hot water bath within a very short period of time. It seems that the samples did not have sufficient strength to withstand the expansive stresses caused by high temperature.

Curing at 35°C at the age of 3 days gave most encouraging result. The 3 days age-35°C-24 hr. curing tests gave a compressive strength equal to around 72% of 28-day strength. Continued curing for 48 hours and 72 hours slightly increased the strength. However, the data for 72-hour curing were much scattered.

Encouraged by this result, it was decided to increase the temperature to 50°C and reduce the age of samples at the start of curing, from three days to one day. However, the results were not very positive. The correlation between accelerated strength and 28-day strength was very poor. It seems that at one day age, flowable fill samples do not come to a very stable condition internally, and also these samples will have low strength. Subjecting

these samples to higher temperature does not give consistent results. Also the samples might undergo some damage during demolding and handling. So it is the strong opinion of the author that the flowable fill samples should not be disturbed until the age of three days, before doing any accelerated curing.

In summary, by adopting the "3 days age-35°C-24 hr. curing" technique, the total strength testing time can be reduced from 28 days to 4 days. The accelerated strength can be assumed to be 70 to 75% of the 28-day strength for the purpose of predicting the 28-day strength, until a better method of prediction is produced by further research.

# CHAPTER 10. SUMMARY, CONCLUSIONS AND RECOMMENDATIONS

This study focused on utilization of waste foundry sand(WFS) in flowable fill. However, the study addresses much broader perspectives so that a unified and rational approach becomes available to understand and predict the behavior of flowable fill in general. The concepts developed are applicable to any flowable fill containing different types of fine aggregates. It was also attempted to answer some of the questions that need to be answered before flowable fill can be used in many geotechnical applications. Waste foundry sands(WFS) from three sources and class F fly ashes from two sources in the State of Indiana were studied. The WFSs were all green sands. A river sand was also used for the purpose of comparision. The summary and conclusions are summarized in the following paragraphs.

Economy: Since the sand is the major component of flowable fill, replacing clean sand with WFS may be beneficial from both an economical and environmental point of view. The flowable fill using WFS needs more cement compared to the one with clean concrete sands. However, the saving in the cost of sand may outweigh the extra cost of cement. The major cost of WFS arises due to the transportation. The individual foundries may come forward to bear the transportation cost, when hauling to waste disposal sites is more expensive to the foundries.

Flow Behavior: Flowability is an important attribute of flowable fill. Flow curves were developed which help explain the mechanics of flow and help in the design of good mixes. Flow curve represents various proportions of sand, fly ash and water to produce the same flowability, namely, 9 in. spread as measured using a 3 in.× 6 in. open ended cylinder. Two different phenomena control the flow behavior at low fly

ash content and at high fly ash content. At low fly ash content, the fly ash acts as a lubricant, and the spherical shape of the fly ash particles is advantageously used. At high fly ash content, viscous forces dominate the flow, and fly ash particles tend to flocculate, thus losing the advantage due to the spherical shape. There is a transition between these two stages where the water demand to cause the same flow is minimized. This point on the flow curve is named "Point of Minimum Water Demand (PMWD)". The proportions corresponding to the PMWD are expected to produce more dense, less porous, and more economical mixes. The higher the density, the higher will be the contribution due to friction (pure friction plus dilatancy) towards strength. The lower amount of water in the mix reduces overall porosity, thus giving a denser material. It will also reduce the cement requirement because the strength was found to be a function of the water-cement ratio, thus giving an economical mix. At a high fly ash content (above PMWD), the mix becomes highly viscous and sticky, and mixing and handling these mixes in the field might pose some practical problems; on the other hand, at low fly ash content (below PMWD), there is high potential for segregation, because the amount of fly ash may not be sufficient to "hold" the water within the system. Thus, proportions at or around PMWD are ideal for mix design purposes. The WFS needs more water to produce adequate flow, compared to clean sand. The main factor contributing to this is the lower specific gravity of WFS. Lower specific gravity decreases the potential energy of these mixes, which is responsible for producing the flow. Therefore, more water is necessary to produce flow.

Hardening Behavior: After the flowable fill is placed, it starts hardening, and attains most of its strength in about a month. However, the short term strength up to about a day or so is also important, because it determines if the flowable fill can support foot traffic and allow further loading such as placement of pavement courses. The hardening characteristics were evaluated using a mortar penetrometer in conjunction with a soil pocket penetrometer. The results of the soil pocket penetrometer tests

were used to estimate the unconfined compressive strength of flowable fill during the hardening stage. From the unconfined compressive strength, bearing capacity can be estimated using Terzhaghi's bearing capacity equation. The penetration resistance was correlated with the unconfined compressive strength (Equation 10.1).

$$q_u = 0.162 \times P \qquad (10.1)$$

where $q_u$ = unconfined compressive strength

P = penetration resistance as measured by mortar penetrometer

A portable version of the mortar penetrometer is available and can be used in the field. The major factors affecting penetration resistance are found to be the cement content, the nature of fly ash, drainage conditions, and the factors that may accelerate the hydration of cement in the flowable fill. The introduction of a geotextile drainage layer around the sample increased the penetration resistance during the early hardening period. The increase seems to be due to the increase in frictional resistance due to better drainage. The drainage condition in the field depends on the nature of the surrounding soil. The penetration resistance to ensure walkability was determined to be around 448 kPa (65 psi). The time required to achieve this penetration resistance is defined as "walkable time". Comparision of walkable times of different mixes in the laboratory is a useful tool to compare and evaluate the hardening characteristics.

The 28-day Unconfined Compressive Strength: The 28-day unconfined compressive strength is to be restricted to around 1035 kPa(150 psi) to allow for possible future excavation. Several factors affect the strength, the most critical one being water-cement ratio. The relation between 28-day unconfined compressive strength and water-cement ratio was approximated by the Equation 10.2.

$$S_c = 374 + \frac{126905}{(W/C)^3} \qquad (10.2)$$

where $S_c$ = unconfined compressive strength at 28-days in kPa

W/C = water-cement ratio

The concept of W/C ratio in flowable fill should not be confused with that of concrete. In flowable fill, the amount of water affects overall porosity, and thereby, the frictional component of strength (pure friction plus dilatancy). Higher amounts of water decrease the density and decrease the frictional component of strength. The cementation component of strength is directly proportional to the amount of cement in the mix. Thus, W/C ratio works well in predicting strength. The mixes containing WFSs need more water to produce the required flow, and therefore need considerably higher amounts of cement.

Long Term Strength: There is a possibility that the strength gain will continue well beyond 28 days. The strength testing at 90 days indicated that, on an average, a 15-25% increase in strength with respect to 28-day strength may be expected.

Mix Design Procedure: A simple mix design procedure is suggested, using the flow model and strength model explained earlier. The 28-day strength for the final mix is intended to be 690 kPa (100 psi). The procedure involves finding the proportions for two mixes with expected 28-day strengths of 550 kPa (80 psi) and 1035 kPa (150 psi). The W/C ratios ($k_3$) of 9.0 and 5.50 corresponding to the above strengths respectively are chosen based on Equation 10.2. The fly ash content ($k_1$) and water-solid ratio($k_2$) are chosen corresponding to the Point of Minimum Water Demand from the flow curve for a given combination of sand and fly ash. Using $k_1$, $k_2$ and $k_3$ and specific gravities of all components , the weights of cement, fly ash, sand and water for the above two mixes can be computed from the equations in Chapter 6. These two mixes are to be tested for actual 28-day compressive strength. From these two compressive strengths and corresponding cement contents, the cement content necessary for the final mix with a target 28-day compressive strength of 690 kPa (100 psi) is calculated by interpolation. For this cement content, the proportions of fly ash, sand and water for this final mix are again computed in the same way the trial mixes

are designed. In summary, the parameters needed to be determined for mix design are $k_1$ and $k_2$ which can be obtained by experimentally determining the flow curve for a given combination of fly ash and sand, and specific gravities of sand and fly ash.

Pore Size Distribution: The pore structure of flowable fill was studied using mercury intrusion porosimetry technique (MIP). Generally, the MIP data are plotted as pore diameter vs cumulative intruded volume in cc/gm of solid. However, flowable fill contains different components with different specific gravity values. Therefore, a unit dry weight of different mixes would contain different amount of solid volume. Hence, the unit, cc/gm is not an appropriate unit. A new unit, cc/cc solid volume was chosen for cumulative intrusion, which also would incidentally give the cumulative void ratio; and total intruded volume(cc/cc) gives the void ratio. The total intruded volume (cc/cc solid volume) or void ratio mainly depends on the amount of water added to the mix. The mixes with only fly ash had the highest void ratio(around 0.8); the mixes containing river sand had smallest void ratio(around 0.3); and those with WFSs had intermediate void ratios (0.4 to 0.5). The threshold diameter ranged from 3 to 6 microns. The major portion of pore volume was in the diameter range of 0.4 to 3 microns. Proper proportioning of flowable fill can reduce the overall porosity. Increasing the fly ash content does not necessarily reduce the porosity.

Permeability: The permeability for different samples varied from $1.2\times10^{-5}$ cm/sec to $2.6\times10^{-6}$ cm/sec. Both the total porosity and threshold diameter of pores seem to influence permeability. The mixes with river sand had smaller threshold diameter and smaller total intruded volume, and had the lower permeability. The mixes with WFS had comparable permeability values. Though the WFS mixes had much higher porosity due to the high water requirements, the permeability is perhaps partly reduced due to the presence of clay.

pH of Pore Solution: The pH of both bleed water from fresh flowable fill, and expressed pore solution from hardened flowable fill after 28 days of age indicated that

highly alkaline environment exists within the flowable fill (pH was around 11). This was mainly due to the presence of cement. It was also found that the WFSs contain negligible amounts of chlorides. Therefore, the flowable fills containing WFSs can be considered to be non-corrosive.

Bio Assay Toxicity Test: The bio assay tests were conducted on leachates from WFSs alone and also on the expressed pore solution from flowable fills containing WFSs. Some WFSs showed no toxicity. The toxicity values of pore solutions, in some cases, were higher than those of sands alone. The reason for this is not clear.

Stress-Strain-Strength Behavior: Consolidated drained and undrained triaxial tests were conducted up to a maximum confining pressure of 400 kPa on hardened flowable fill samples with unconfined compressive strengths ranging from 145 kPa to 1085 kPa. The void ratio of the mixes varied from 0.3 to 0.56. The stress-strain curves at different confining pressures indicated that flowable fill is much less brittle than expected of a cemented material. The stress-strain curves had a broad peak, and a slow rate of strain-softening. At peak, both cementation and dilatancy components of strength were substantial. The increase in cementation caused an increase in both maximum rates of dilation and total amounts of dilation. Also, the increase in cementation caused an increase in the Mohr Coulomb cohesion intercept with the friction angle remaining constant. The samples with high fly ash content showed non-dilatant behavior. The peak and the residual friction angle were around 36° for the mixes containing river sand, 33° for the high fly ash content mixes, and 32° for the mix with WFS. The presence of clay in WFS may slightly reduce the friction angle in those mixes. The fly ash is seen to be a good frictional material. Brazilian Tensile Strength tests indicated that a relation exists between the tensile strength and unconfined compressive strength; the unconfined compressive strength was approximately 4.3 times the tensile strength. In summary, flowable fill is a well behaved material. It behaves like a cemented granular material.

Accelerated Strength Testing: The purpose of the accelerated strength testing is to reduce the total time for strength prediction. This is particularly helpful when there is a great deal of variability in the properties of the source materials. In such cases, the mixes may have to be tested for strength very frequently. Since each mix has to be kept for 28 days, this might cause undue delays in the construction. A hot water bath curing technique was used in this research. The flowable fill samples disintegrated and collapsed when subjected to high temperature (100°C). It seems that samples did not have sufficient strength to withstand the expansive stresses caused by the high temperatures. The accelerated curing at 35°C for 24 hours at the age of 3 days gave around 72% of the 28-day strength. The total testing time involved in this case is 4 days. The accelerated strength can be assumed to be 70 to 75% of the 28-day strength for the purpose of predicting the 28-day strength, until a better method of prediction is produced by further research.

Recommendations to INDOT : The following recommendations are made to start implementation of the present research. The recommendations are not necessarily limited to the flowable fills containing WFSs, but are applicable to other flowable fills as well.

1. Demonstration projects involving flowable fill using WFS should be arranged. The performance of flowable fill in the field should be closely monitored and compared to the laboratory study carried out in this research. The penetration resistance should be measured during the hardening stage using the field version of the mortar penetrometer.

2. The present specification for flowable fill can be expanded to include WFS as a fine aggregate in flowable fill. Instead of standard mixes, the mix design method suggested in this study should be considered as an alternate. The walkability criteria using penetration resistance should be used instead of the existing rod method.

3. The bioassay test may be used to screen out potentially hazardous WFSs before using them in flowable fill.

Future Research Needs: There are several areas where further research needs to be done.

1. The present research was carried out using only the class F fly ash. Class C fly ashes of marginal marketability should be included in future studies.

2. A great difference exists between the hardening behavior of flowable fill in the laboratory and in the field due to several factors such as drainage conditions, temperature, etc. It is important to be able to simulate the field conditions as closely as possible in order that the laboratory evaluation of hardening behavior be more useful. The use of geosynthetic drainage layer in the present study was found to be very useful in speeding up drainage. However, it is not known how well it simulates the field conditions in different situations. This needs to be further looked into.

3. The strength model suggested in this study may be refined as more strength data become available for flowable fills containing different source materials.

4. Accelerated curing showed promising results. However, more materials should be tested to validate this research. Also, the validity of accelerated curing for flowable fill containing class C fly ash is yet to be determined. Different techniques and different temperatures may also be researched to improve the prediction.

5. Bio assay tests were carried out on the pore solution which was forcefully squeezed out applying very high stresses. It would be more realistic to test leachates from the flowable fill. By doing so, more marginal materials (in terms of toxicity) could be perhaps used in flowable fill.

6. Flowable fill is a relatively new material and has high potential for use in many geotechnical applications. The applications such as landfill liners and seepage cut-off walls should be explored.

# LIST OF REFERENCES

ACI Committee 229 (1994). "Controlled Low Strength Materials (CLSM)." Concrete International, July , pp 55-64.

Adaska, W. S., and Krell, C. W. (1995). "Bibliography on Controlled Low-Strength Materials (CLSM)." Concrete International. Vol. 14, No. 10, pp 42-43.

Bastion, K. C. and Alleman, J. E. (1995). Personal Communication. School of Civil Engineering, Purdue University

Bhat, S. T., Lovell, C. W., Scholer, C. F., and Nantung, T. E. (1995). "Flowable Fill Using Waste Foundry Sand." Proc. Eleventh International Symposium on Use and Management of Coal Combustion By-products (CCBs), EPRI TR-104657, Vol. 2, pp 39-1 to 39-14.

Brakel, J. V., Modry, S., and Svata, M. (1981). "Mercury Porosimetry: State of the Art." Powder Technology, Vol. 29, pp 1-12.

Brewer, W. E. and Hurd, J. O. (1991). "Economical Considerations When Using Controlled Low Strength Material(CLSM-CDF) as Backfill." Transportation Research Record, 1315, pp 28-27.

Bucchi, E. (1972). "A Fast Determination of $\phi$ and $c$ Components of Soil Strength." INARCOS, No. 318.

Das, R. N., Yen, S. C., Puri, V. K., Das, B. M. and Wright, M. A. (1993). "Tensile Stress-Strain Behavior of Lightly Cemented Sands." Int. J. Rockmechanics Mining Sci. Geomech. Abstr. Vol 30, No.7, pp 711-714.

Diamond, S. (1970). "Pore Size Distributions in Clays." Clays and Clay Minerals, Vol. 18, pp 7-23.

Diamond, S. (1971). "Microstructure and Pore Structure of Impact-Compacted Clays." Clays and Clay Minerals, Vol. 19, pp 239-249.

Diamond, S. (1985). " Selection and Use of Fly Ash for Highway Concrete." Joint Highway Research Report, FHWA/IN/JHRP-85/8.

Dolch, W. L. and Diamond, S. (1995). "Durability of Concrete." The Civil Engineering Handbook, Ed. W.F. Chen, CRC Press, Chapter 39.

Emery, J. and Johnston, T. (1986). "Unshrinkable Fill for Utility Cut Restorations." American Concrete Institute, Special Publication 93-10. pp 187-211.

EPA(1980). " Environmental Assessment of Iron Casting." EPA-600/2-80-021, Jan., 157 pp.

Fahnline, D. E. and Regan, R. W. (1995). " Leaching of Metals from Beneficially Used Foundry Residuals into Soils." 50th Industrial Waste Conference, Purdue University, May 8-10.

GAI Consultants (1993). "Use of Coal Combustion By-Products in Highway Construction." Report Prepared for the General Assembly of Indiana and INDOT in Response to House Enrolled Act 1056 and Senate Bill 209.

Good, G. E. (1983). "Turning a Liability into an Asset" Proceedings: Conference on Green Sand Technology-Productivity for the '80s, AFS Technical Center, Des Plaines, Illinois, pp 95-142.

Grinrod, P. (1968). "Application of the Andreasen Pipet Method to the Determination of Particle Size Distribution of Cement and Related Materials." ASTM, SP 473, "Fineness of Cement" pp 45-70.

Ham, R. K., Boyle, W. C. and Kunes, T. P. (1981). "Leachability of Foundry Process Solid Wastes." J. of the Environmental Engineering Division, ASCE, Vol. 107, pp 155-170.

Ham, R. K., Boyle, W. C., Engroff, E. C. and Fero, R. L. (1989). "Determining the Presence of Organic Compounds in Foundry Waste Leachates." Modern Casting, Aug., pp 34-38.

Harris Indiana Industries Directory (1992). Harris Publishing Co., Twinsburg, Ohio, S.I.C. 3321, 3322, 3325, 3365, 3366 and 3369.

Helmuth, R.(1987). Fly Ash in Cement and Concrete. Portland Cement Association, Skokie, Illinois,1987.

Hennis, K. W. and Frishettee, C. W. (1987). "Flash Fill℠. A New Era in Controlled Density Fill." Proceedings: X International Ash Symposium, EPRI TR-101774, Vol 2., pp 53-2 to 53-12.

Indiana Cast Metals Association (1992). "Foundry Survey of 1991", INCMA.

Javed, S. (1994). Use of Waste Foundry Sand in Highway Construction, Ph. D. thesis, School of Civ. Engrg., Purdue University, May , 273 pp.

Kennedy, D. O. and Linne, C. L. (1987). "Environmental and Economical Aspects of Sand Reclamation System." EPRI, Vol. 2, Palo Alto, California, pp 217-228.

Krell, W. C. (1989). "Flowable Fly Ash." Concrete International, Nov. pp 54-58.

Kunes, T. P. and Smith, M. E. (1983). "Waste Disposal Considerations for Green Sand Use in the Foundry Industry." Conference on Green Sand Technology-Productivity for the '80s, AFS Technical Center, Des Plaines, Illinois, pp 143-167.

Larsen, R. L. (1988). "Use of Controlled Low Strength Material in Iowa." Concrete International, July, pp 22-23.

Larsen, R. L. (1990). "Sound Uses of CLSMs in the Environment" Concrete International, July, pp 26-29.

Micromeritics. (1987). Instruction Manual, AutoPore II 9220, Operating Program V1.07, One Micromeritics Drive, Norcross, GA.

Mindes, S. and Young, J. F. (1981). Concrete. Prentice-Hall, Inc., New Jersey.

Naik, T. R., Patel, V. M., Parikh, D. M., and Tharaniyil, M. P.(1994). "Utilization of Used Foundry Sand in Concrete." J. of Materials in Civil Engineering, 6(2), pp 254-263.

Naik, T. R., Tharaniyil, M, P. and Adebayo, O. B. (1994). "Flowable Slurry: Part 1" Report No. REP-178, Center for By-Products Utilization, Dept. of Civil Engineering and Mechanics, The University of Wisconsin, Milwaukee.

Naik, T. R., Ramme, B. W. and Kolbeck, H. J. (1990). "Filling Abandoned Underground Facilities with CLSM Fly Ash Slurry." Concrete International, May, pp 389-398.

Nantung, T. E.(1993). "Design Criteria for Controlled Low Strength Materials." Ph. D. Thesis, School of Civil Engrg., Purdue University, Aug., 344 pp.

Ritter, H. L. And Drake, L. C. (1945). "Pore Size Distribution in Porous Materials- Pressure Porosimeter and Determination of Complete Macropore Size Distribution" Industrial and Engineering Chemistry: Analytical Edition, American Chemical Society, Vol. 17, No. 12, 782-786.

Sitar, N. (1979). Behavior of Slopes in weakly Cemented Soils Under Static and Dynamic Loading." Thesis presented to Stanford University at Stanford, California, in partial fulfillment of the requirements for the degree of Doctor of Philosophy.

Smith, A. (1991). "Controlled Low Strength Material" Concrete Construction, May, pp 389-398.

Sridharan, A., Altschaeffl, A. G., and Diamond, S. (1971). "Pore Size Distribution Studies" J. Soil Mech. Found. Engrg., ASCE, Vol. 97, No. 5, pp 771-787.

Tobin, R. E. (1978). "Flow Cone Sand Tests." ACI Journal, Title No. 75-1, pp 1-12.

Washburn, E. W. (1921). "Note on a Method of Determining the Distribution of Pore Size in a Porous Material." Proc. National Academy of Sciences, Vol. 7, pp 115-116.

Washburn, E. W. (1921). "The Dynamics of Capillary Flow." The Physical Review, Second series, Vol. 17, No. 3, pp 273-283.

Winslow, D. N. (1984). "Advances in Experimental Technique for Mercury Intrusion Porosimetry." Surface and Colloid Science, Vol. 13, Plenum Press, pp 258-282.

# APPENDIX A

# APPENDIX A

## BIOASSAY DETERMINATION OF SPENT FOUNDRY SAND TOXICITY

K. Chad Bastian, Research Assistant
James E. Alleman, Professor
School of Civil Engineering, Purdue University

**ABSTRACT**: In this research, a commercial bacterial bioassay test, Microtox™, has been utilized to examine the effect of spent foundry sands on the environment should the sands be used in INDOT construction projects. Testing to date indicates that sands from many Indiana ferrous foundries could be used without environmental concern, and that the Microtox™ test can be effective in screening suitable sands from those with potential to harm the environment.

**INTRODUCTION**: Recent legislation has caused the Indiana Department of Transportation (INDOT) to examine several industrial solid wastes for possible use as construction materials. One of these materials is spent foundry sand, which is produced in quantities of over 400,000 tons per year in Indiana foundries. The sands' geotechnical properties suggest that they would be useful as substitutes for virgin sand in road base and flowable fill applications. In addition, the sands fulfill existing Indiana environmental requirements to be classified as Type III or Type IV wastes, clearing the way for potential beneficial reuse.

INDOT, in an attempt to gain additional confidence in the sands' harmlessness, arranged for bioassay testing of spent foundry sand samples from around the state. In these bioassays, leachate generated from the sands is exposed to living organisms: the bacteria *Photobacterium phosphorium*. These bacteria, isolated from marine samples, are photoluminescent--they glow. When exposed to a toxicant, however, the light output decreases, and this decrease can be quantified. In this way, the environmental quality of the leachates produced from spent foundry sand can be compared to that of control sands. Qualitative predictions can then be made regarding the long-term effect of spent foundry sand use in INDOT construction projects.

**EXPERIMENTAL METHODS**: The first phase of the testing is leachate generation. A 20 gram sample of foundry sand is placed in a flask, and 80 milliliters of a salt solution (2% NaCl) is added. This salt solution is used because the microorganisms, being marine organisms, require a medium similar to their original environment. The sand suspension is shaken for 18 hours, and then solid-liquid separation is accomplished through centrifugation and filtration. In principle, the actual bioassay phase of the testing is quite simple. The original light output of the bacteria is measured, a small quantity of leachate is added to the sample, and the light output is measured after 5 minutes, and again 15 minutes. The light output measurements are compared with controls, and results are tabulated and analyzed.

# APPENDIX B

# APPENDIX B

## INFORMATION ABOUT NEGATIVES

Information about negatives of the following figures can be obtained from Joint Highway Research Project, Purdue University, West Lafayette, Indiana.

Figure 5.3 Penetration Resistance Test Setup

Figure 5.4 Portable Penetrometer

Figure 5.5 Soil Pocket Penetrometer

Figure 9.1 Photograph Showing the Collapsed Sample Containing Sand R and Fly Ash GI After Curing at 100° C.

Figure 9.2 Photograph Showing the Collapsed Sample Containing Sand WFS After Curing at 100° C.

COVER DESIGN BY ALDO GIORGINI